forests

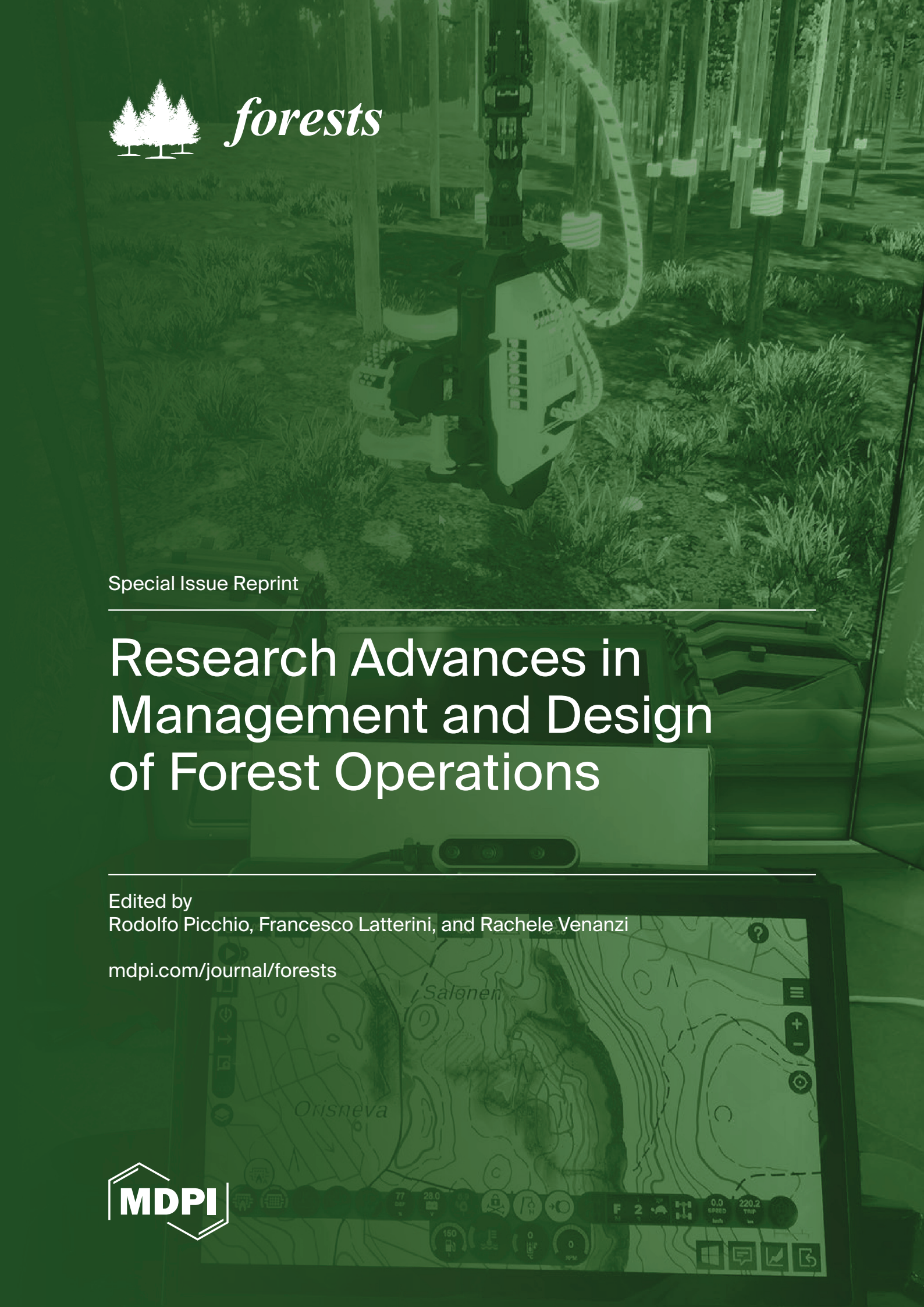

Special Issue Reprint

Research Advances in Management and Design of Forest Operations

Edited by
Rodolfo Picchio, Francesco Latterini, and Rachele Venanzi

mdpi.com/journal/forests

MDPI

Research Advances in Management and Design of Forest Operations

Research Advances in Management and Design of Forest Operations

Guest Editors

Rodolfo Picchio
Francesco Latterini
Rachele Venanzi

MDPI

Basel • Beijing • Wuhan • Barcelona • Belgrade • Novi Sad • Cluj • Manchester

Guest Editors

Rodolfo Picchio
Department of Agricultural and Forest Sciences
University of Tuscia
Viterbo
Italy

Francesco Latterini
Institute of Dendrology
Polish Academy of Sciences
Kórnik
Poland

Rachele Venanzi
Department of Agricultural and Forest Sciences
University of Tuscia
Viterbo
Italy

Editorial Office

MDPI AG
Grosspeteranlage 5
4052 Basel, Switzerland

This is a reprint of the Special Issue, published open access by the journal *Forests* (ISSN 1999-4907), freely accessible at: https://www.mdpi.com/journal/forests/special_issues/G6J8O38XAW.

For citation purposes, cite each article independently as indicated on the article page online and as indicated below:

Lastname, A.A.; Lastname, B.B. Article Title. *Journal Name* **Year**, *Volume Number*, Page Range.

ISBN 978-3-7258-8891-7 (Hbk)
ISBN 978-3-7258-8892-4 (PDF)
https://doi.org/10.3390/books978-3-7258-8892-4

Cover image courtesy of Rodolfo Picchio

© 2026 by the authors. Articles in this reprint are Open Access and distributed under the Creative Commons Attribution (CC BY) license. The reprint as a whole is distributed by MDPI under the terms and conditions of the Creative Commons Attribution-NonCommercial-NoDerivs (CC BY-NC-ND) license (https://creativecommons.org/licenses/by-nc-nd/4.0/).

Contents

About the Editors . . . . . **vii**

Preface . . . . . **ix**

Rachele Venanzi, Rodolfo Picchio, Aurora Bonaudo, Leonardo Assettati, Luca Cozzolino, Eugenia Pauselli, et al.
Evaluating the Reliability of Remote Sensing Techniques for Detecting the Strip Road Network in Boom-Corridor Systems
Reprinted from: *Forests* **2025**, *16*, 1768, https://doi.org/10.3390/f16121768 . . . . . **1**

Matevž Mihelič, Dinko Vusić, Branko Ursić, Antonio Zadro and Raffaele Spinelli
The Effect of Knife Wear and Sharpening Mode on Chipper Productivity and Delays
Reprinted from: *Forests* **2024**, *15*, 1101, https://doi.org/10.3390/f15071101 . . . . . **18**

Mihael Lovrinčević, Ivica Papa, Maja Popović, David Janeš, Tomislav Poršinsky, Tibor Pentek and Andreja Đuka
Methods of Rut Depth Measurements on Forwarder Trails in Lowland Forest
Reprinted from: *Forests* **2024**, *15*, 1021, https://doi.org/10.3390/f15061021 . . . . . **29**

Salvatore F. Papandrea, Stanimir Stoilov, Maria Francesca Cataldo, Krasimir Petkov, Georgi Angelov, Antonio Zumbo and Andrea R. Proto
Evaluation of Productivity and Cost Analysis on a Combined Logging System
Reprinted from: *Forests* **2024**, *15*, 980, https://doi.org/10.3390/f15060980 . . . . . **43**

Valerio Di Stefano, Giorgia Di Domenico, Michele Menta, Elisa Pontuale, Leonardo Bianchini and Andrea Colantoni
Comparison between Different Mechanization Systems: Economic Sustainability of Harvesting Poplar Plantations in Italy
Reprinted from: *Forests* **2024**, *15*, 397, https://doi.org/10.3390/f15030397 . . . . . **57**

Francesco Carbone, Luigi Portoghesi, Manuela Romagnoli, Francesco Barbarese and Teresa Grassi
Production of Chestnut Coppice Biomass in a Framework of Low Mechanization and High Expectations to Combat Climate Change and Other Social Expectations
Reprinted from: *Forests* **2024**, *15*, 412, https://doi.org/10.3390/f15030412 . . . . . **73**

Meghdad Jourgholami, Elahe Alsadat Hosseiniala, Francesco Latterini, Rachele Venanzi and Rodolfo Picchio
The Effects of Soil Compaction on the Growth and Architecture of the Seedlings of Species Commonly Used for Afforestation in Iran
Reprinted from: *Forests* **2024**, *15*, 1090, https://doi.org/10.3390/f15071090 . . . . . **90**

Weiping Hua, Tian Qiu, Xidian Jiang, Junzhong Pan and Baoyin Li
The Estimation of Carbon Storage and Volume in Forest Stands: A Model Incorporating Species Composition and Site Quality
Reprinted from: *Forests* **2025**, *16*, 682, https://doi.org/10.3390/f16040682 . . . . . **102**

Nivaldo S. Martins, Bruno O. Lafetá, Marcio L. R. Oliveira and Reynaldo C. Santana
Maintaining Fertilization Supports Productivity in Second Rotation Eucalypt Plantations
Reprinted from: *Forests* **2025**, *17*, 13, https://doi.org/10.3390/f17010013 . . . . . **119**

About the Editors

Rodolfo Picchio

Rodolfo Picchio (Full Professor) obtained a forest science degree and a PhD degree in forest mechanization at Tuscia University in Viterbo. From 2004 to 2024, he worked as a university researcher and associate professor in forest logging and wood technologies. Since 2004, he has led the 'Forest Utilization Work Group' at Tuscia University (DAFNE). From 2015 to 2017, he served as the president of the master's degree of forest science "Conservation and Restoration of the Forest Environment and Soil Defense" at Tuscia University (DAFNE). He is on the board of the PhD course "Engineering for Energy and Environment" at Tuscia University. His fields of expertise include forest logging, forest mechanization, precision forestry, wood technologies, and the environmental impacts of wood harvesting operations. He has worked as the Italian representative in four EU COST Actions, on silviculture and biomass. Furthermore, he has co-authored 184 peer-reviewed papers in international journals indexed by WoS and Scopus, 30 technical books, and over 200 papers in technical magazines. He also works on the editorial boards of five international scientific journals covering forestry and forest engineering subjects. He is a member of the Italian Society of Silviculture and Forest Ecology.

Francesco Latterini

Francesco Latterini is a researcher at the Institute of Dendrology of the Polish Academy of Sciences, where he has worked since 2022, initially as a Marie Skłodowska-Curie PASIFIC Fellow. He holds a PhD in forest sciences, a master's degree in forest sciences and a bachelor's degree in environmental sciences, all awarded by Tuscia University in Viterbo, Italy. He has also worked as a researcher at the Italian Council for Agricultural Research and Economics and as a visiting scientist at Scion—New Zealand Institute for Forest Research.

His research focuses on sustainable forest operations, forest mechanization, precision forestry, GIS and remote-sensing applications, soil trafficability, and the environmental impacts of timber harvesting. He currently coordinates the international AniLog research project, funded by the VELUX STIFTUNG; and the SOLAR project, funded by the National Science Centre of Poland. He has also led several national and international research activities and participated in numerous European projects.

He has authored or co-authored more than 100 scientific papers indexed in Web of Science and Scopus. He is a member of the Management Committee of COST Action ARiF, representing Poland, and serves on the editorial boards of *Land* and *Discover Forests*. In 2025, he was awarded the Scholarship of the Polish Minister of Science and Higher Education for Outstanding Young Scientists, one of Poland's most prestigious distinctions for early-career researchers.

Rachele Venanzi

Rachele Venanzi (Researcher) obtained degrees in environmental science and the forest science at Tuscia University in Viterbo and a PhD degree in forest mechanization at Padua University. Since 2013, she has worked both as a researcher in forestry and forest logging and wood technologies at Tuscia University, and has been part of the 'Forest Utilization Work Group' at Tuscia University (DAFNE). Her fields of expertise include sustainable forest operations; reduced impact logging; QBS-ar index; sustainable forest management; and forest mechanization. She has worked as the Italian representative in three EU COST Actions on the forestry sector. Furthermore, she has co-authored 118 peer-reviewed papers in international journals indexed by WoS and Scopus, 8

technical books, and over 30 papers in technical magazines. She also works on the editorial boards of international scientific journals covering forestry and forest engineering subjects as a Guest Editor. She is a member of the Italian Society of Silviculture and Forest Ecology.

Preface

This Special Issue focused on the "Research Advances in Management and Design of Forest Operations".

Even if global megatrends and operational challenges drive us to operate more efficiently and sustainably across all sectors, forest management still needs more attention. In particular, one of the most important challenges that forest managers will continue to face concerns the adaptation of forest management and operations to changing climatic conditions. In recent years, the new concept of climate-smart forestry (CSF) has arisen. CSF is a targeted approach or strategy used to increase the climate benefits from forests and the forest sector in a synergistic way. CSF cannot be separated from the sustainable implementation of forest operations. In this context, it is important to consider the new comprehensive research, development and innovation (RDI) studies—improving the cost, energy efficiency and quality of wood-harvesting operations, long-distance transport and forest operations planning. The rapid development of technology, combined with an increase in the demand for wood and reduced access to manpower, is resulting in significant progress in the development of forest machinery. One clear example is Forestry 4.0, which represents the integration of advanced digital technologies—such as artificial intelligence, the Internet of Things, blockchain, and big data analytics—into forest management practices. The main goals of all these recent topics include optimizing resource utilization, reducing waste, improving supply chain management, and enhancing the decision-making process through data-driven insights.

Authors were invited to contribute to this Special Issue with studies from all fields—including experimental studies, monitoring approaches and models—on silviculture and logging activities to contribute to this Special Issue in order to promote knowledge and adaptation strategies for the active management, preservation, and future development of Climate-Smart Forest Operations.

This Special Issue contains nine original papers, some of them reporting the outcomes of long-time experiences, reviewed by international experts in the forestry and forest operations engineering fields.

This Special Issue aimed to increase the knowledge concerning the climate-smart forest operations, with practical implications at the scientific and technical levels.

We are pleased to share these works with the scientific community, forest engineers, private owners, and public managing authorities, hoping that this edition will provide a cognitive base to improve climate-smart forest operations and reduce contrasts between different interests and opinions.

As Guest Editors, we would like to express our gratitude to MDPI, who agreed to publish this book; to the staff of *Forests* and MDPI, for their kindness and professional support; to the reviewers, for improving original texts and clearing little slips; and to the authors, for providing their papers with ethical and scientific rigor.

Guest Editor contributions: The three coeditors contributed equally to organizing the Special Issue, to the editorial work, and to writing this editorial.

Funding: No external funding was obtained for editing this Special Issue and for writing the preface.

Conflicts of Interest: The authors declare no conflicts of interest.

This book collects a representative sample of the most recent papers on the subject, which come from many different countries and cover a variety of subjects, confirming the wide scope covered by the Research Advances in Management and Design of Forest Operations—a topic with broad

development prospects.

This work was supported by the Italian Ministry for education, University and Research

(MIUR) for financial support (Law 232/2016, Italian University Departments of excellence 2023–2027) project "Digitali, Intelligenti, Verdi e Sostenibili (D.I.Ver.So)—UNITUS-DAFNE WP3 and the Agritech National Research Center receiving funding from the European Union Next-GenerationEU (PIANO NAZIONALE DI RIPRESA E RESILIENZA (PNRR)—MISSIONE 4 COMPONENTE 2, INVESTIMENTO

1.4—D.D. 1032 17/06/2022, CN00000022). These papers reflect only the authors' views and opinions, neither the European Union nor the European Commission can be considered responsible for them.

Rodolfo Picchio, Francesco Latterini, and Rachele Venanzi

Guest Editors

forests

MDPI

Article

Evaluating the Reliability of Remote Sensing Techniques for Detecting the Strip Road Network in Boom-Corridor Systems

Rachele Venanzi [1], Rodolfo Picchio [1,*], Aurora Bonaudo [1], Leonardo Assettati [1], Luca Cozzolino [2], Eugenia Pauselli [1], Massimo Cecchini [1], Angela Lo Monaco [1] and Francesco Latterini [3]

[1] Department of Agriculture, Forests, Nature and Energy, Tuscia University, 01100 Viterbo, Italy; venanzi@unitus.it (R.V.); aurora.bonaudo@unitus.it (A.B.); leonardo.assettati@unitus.it (L.A.); eugenia.pauselli@outlook.it (E.P.); cecchini@unitus.it (M.C.); lomonaco@unitus.it (A.L.M.)
[2] Consiglio per la Ricerca in Agricoltura e l'Analisi dell'Economia Agraria, Centro di Ricerca Ingegneria e Trasformazioni Agroalimentari, 00015 Monterotondo, Italy; luca.cozzolino@crea.gov.it
[3] Institute of Dendrology, Polish Academy of Sciences, 62-035 Kórnik, Poland; latterini@man.poznan.pl
* Correspondence: r.picchio@unitus.it

Abstract

Accurate detection of machinery-induced strip roads after forest operations is fundamental for assessing soil disturbance and supporting sustainable forest management. However, in Mediterranean pine forests where canopy openings after boom-corridor thinning are moderate, the effectiveness of different remote sensing techniques remains uncertain. Previous studies have shown that LiDAR-based methods can reliably detect logging trails in different forest stands, but their direct transfer to structurally simpler, even-aged Mediterranean stands has not been validated. This study addresses this gap by testing whether UAV-derived RGB imagery can achieve comparable accuracy to LiDAR-based methods under the canopy conditions of boom-corridor thinning. We compared four approaches for detecting strip roads in a black pine (*Pinus nigra* Arn.) plantation on Mount Amiata (Tuscany, Italy): one based on high-resolution UAV RGB imagery and three based on LiDAR data, namely Hillshading (Hill), Local Relief Model (LRM), and Relative Density Model (RDM). The RDM method was specifically adapted to Mediterranean conditions by redefining its return-density height interval (1–30 cm) to better capture areas of bare soil typical of recently trafficked strip roads. Accuracy was evaluated against a GNSS-derived control map using nine performance metrics and a balanced subsampling framework with bootstrapped confidence intervals and ANOVA-based statistical comparisons. Results confirmed that UAV-RGB imagery provides reliable detection of strip roads under moderate canopy openings (accuracy = 0.64, Kappa = 0.27), while the parameter-tuned RDM achieved the highest accuracy and recall (accuracy = 0.75, Kappa = 0.49). This study demonstrates that RGB-based mapping can serve as a cost-effective solution for operational monitoring, while a properly tuned RDM provides the most robust performance when computational resources are sufficient to work on large point clouds. By adapting the RDM to Mediterranean forest conditions and validating the effectiveness of low-cost UAV-RGB surveys, this study bridges a key methodological gap in post-harvest disturbance mapping, offering forest managers practical, scalable tools to monitor soil impacts and support sustainable mechanized harvesting.

Keywords: LiDAR; UAV; forest operations; forwarder; cut-to-length

1. Introduction

Machinery traffic related to ground-based forest operations primarily affect the soil through compaction, rutting, and displacement [1–3]. Compaction occurs when soil particles are pushed closer together, reducing pore space due to mechanical forces [4–6]. Repeated passes by machinery can deform the soil, especially when the soil water content is high [2,7,8]. Ground-based traffic from forest machinery can negatively impact essential soil functions by increasing soil strength and bulk density [9–11], decreasing water infiltration and saturated hydraulic conductivity [12], and reducing the biodiversity of soil biota [13,14]. These impacts can lead to reduced oxygen availability, increased surface water flow, soil loss, and sedimentation [3]. Ultimately, these adverse effects are likely to hinder tree and root growth [15], negatively affect site productivity [16], and potentially alter soil ecological processes such as litter decomposition rates [17].

Machine traffic while performing forest operation is concentrated along the trails [18–20]. These trails are usually named skid trails when the extraction operation implies the contact of the logs with the ground (skidding), while when using cut-to-length machinery (harvester + forwarder) the term strip roads is used [21,22]. The identification of the skid trail or strip road network established after forest operations is crucial for both monitoring and planning issues [23–25]. Knowing the extent and localization of the trails is the first step to verify if the forest operations were performed in agreement with the regulation requirements [26]. Furthermore, identifying the established trails and mapping them allows for making the skid trail/strip road network fixed, thus making possible to re-use the same trails in the following logging entry and thus limiting the soil surface affected by vehicle movement [18]. Traditionally, the area affected by machine traffic is assessed by post-harvesting field surveys through tracing the visible trails [23]. This method is obviously extremely time and manpower consuming.

Modern technologies in forestry and remote sensing have deeply changed our possibilities to effectively identifying the areas affected by machine traffic [27]. Modern forest machines are equipped with on-board computers, sensors and GNSS (Global Navigation Satellite Systems) which allow for collecting a plethora of information about the forest operations on-time, including the position of the machinery [28]. In this way we can know exactly where the machine trafficked within a given cutting block [29]. However, this applies only when modern machinery is used, which is often not the case in many parts of Europe, including the Mediterranean area [30–33]. Furthermore, in many Countries in Europe including Italy, the major part of the forests is private. Thus, without a dedicated regulatory framework which is currently missing, it is up to the owner if they want to share the data collected by the forest machinery with the controlling entities such as the local forest service for facilitating the post-harvesting monitoring.

To identify the machine trails after harvesting in such cases, we can still rely on remote sensing technologies [25,34,35]. In this context, both Unmanned Aerial Vehicles (UAVs) and aircraft-based platforms (ALS) offer significant advantages, enabling rapid and extensive surveying compared to traditional ground-based methods [36]. These platforms can be equipped with either passive sensors (e.g., RGB cameras) or active sensors (e.g., LiDAR—Light Detection and Ranging), each suited to specific forest conditions for detecting soil disturbance caused by logging machinery. In areas where canopy openings are substantial, such as after clear-cutting or coppicing, passive sensors are generally effective in capturing the trail network, as the visibility of the ground surface is sufficient [37]. Conversely, in cases where canopy cover remains largely intact, such as after thinning or single-tree selection harvesting, active sensors like LiDAR are preferred due to their ability to penetrate the canopy and provide detailed information about the forest floor [38,39].

While airborne laser scanning (ALS) is well suited for large-scale surveys and is typically used to detect major forest road networks [24,40], effective monitoring at the forest-management-unit level, especially shortly after harvesting, requires the use of UAV-based surveys [27]. In any case, the reliability of LiDAR for delineating trail networks is well established, but both the acquisition of LiDAR data (as a consequence of high hardware cost) and their processing are substantially more costly, frequently by an order of magnitude, than surveys relying on passive sensors such as RGB cameras, and they typically require more complex analytical workflows. [41].

In the Mediterranean region, particularly in Central and Southern Italy, there is an extensive area of artificial coniferous plantations [42], predominantly composed of black pine (*Pinus nigra* Arn.), which were established during the first half of the 20th century [43]. Due to the generally low timber quality, partly resulting from the absence of early thinning interventions, wood harvested from these stands is typically suitable only for fuelwood production [44]. In recent years, the introduction of fully mechanized cut-to-length harvesting systems, involving harvesters and forwarders, has significantly increased the efficiency of operations in these pine forests. Additionally, the adoption of alternative thinning approaches, such as boom-corridor thinning, where trees are removed along straight corridors within the reach of the harvester's boom, rather than through selective removal as in traditional thinning from below, has further enhanced harvesting rates and operational productivity [45,46]. Given the large size of the machinery used and the frequent presence of steep terrain, with slopes typically ranging from 30% to 40%, it is essential to monitor soil disturbance caused by forest operations in these pine stands. Addressing this issue requires careful consideration of canopy alterations resulting from the applied silvicultural practices. In particular, the boom-corridor thinning technique produces canopy openings that are less pronounced than those from clear-cutting, but still more distinct than those resulting from conventional selective thinning. This raises the question of whether UAV-based RGB imagery is sufficient for detecting the network of strip roads created during such operations, or if LiDAR-based surveys, with their superior canopy penetration capabilities, are necessary.

To explore this, we conducted a study in a black pine plantation located on Mount Amiata in Tuscany, Italy, following forest operations carried out using the boom-corridor thinning method. We performed both RGB and LiDAR surveys using UAV platforms, and compared the outputs to test the hypothesis UAV-RGB imagery can achieve comparable accuracy to LiDAR-based methods under moderate canopy openings created by boom-corridor thinning.

2. Materials and Methods

2.1. Study Area

The study area (Figure 1), corresponding to one black pine cutting block, is located in the municipality of Arcidosso (Grosseto district, Tuscany, Italy). This logging site was selected because it was highly representative of black pine forests of Central Italy, in terms of biomass stock, topography and applied harvesting system. The surface of the cutting block was 10.65 ha. In the study area the mean annual temperature is 9.3 °C with a mean annual precipitation of 708 mm [47]. The soil is a Cambisol with a loam texture [48]. The elevation of the cutting block ranged from 1119 to 1200 m a.s.l. with a mean elevation of 1150 m a.s.l. Prevalent terrain slope was 28%, but the topography of the cutting block was quite heterogeneous, ranging from almost flat zones to areas at slope higher than 50%.

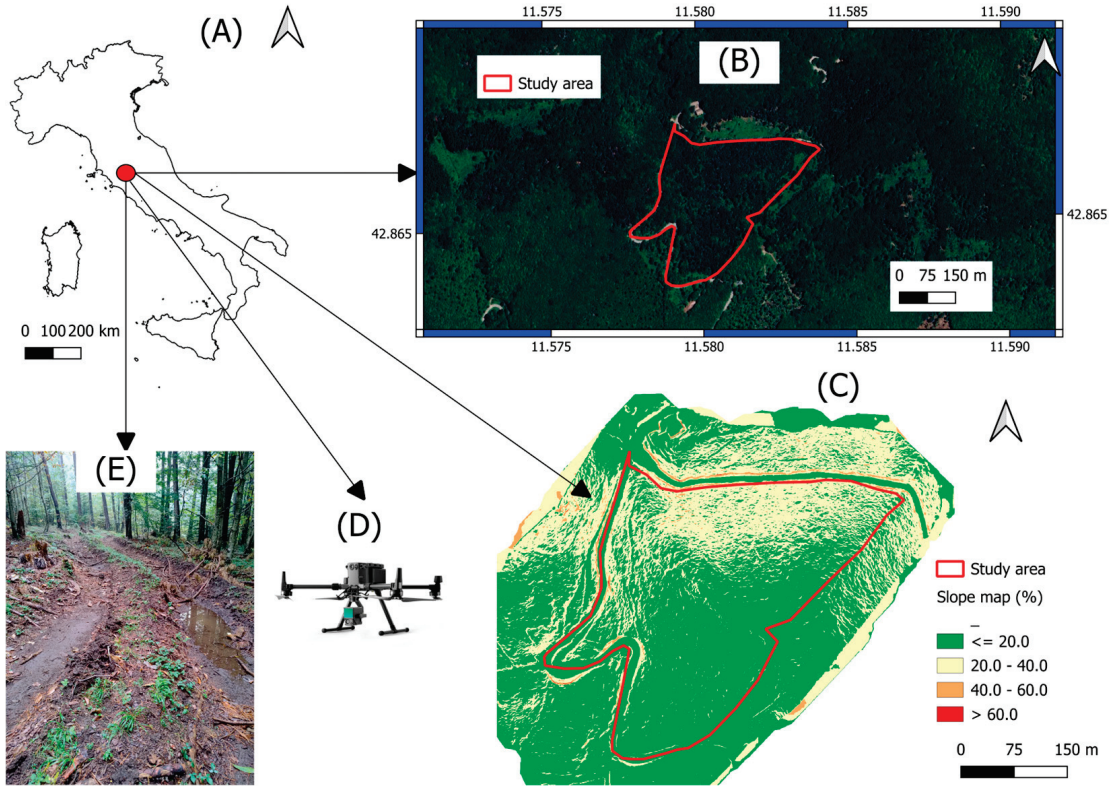

Figure 1. (**A**) Location of the study area within national boundaries. (**B**) Study area overview on ortophotomap acquired in 2024. (**C**) Slope map of the study area, in which the heterogeneous topography of the study area is evident. (**D**) UAV used for LiDAR surveys—DJI Matrice 300 (SZ DJI Technology Co., Ltd., Shenzen, China). (**E**) Vision of a strip road in the study area.

The forest stand consisted of an even-aged black pine forest of about 60 years which was never thinned before. Along with the pines there were spots of chestnut (*Castanea sativa* Mill.) which were not subject to harvesting. Therefore, the actual intervention surface was equal to 7.85 ha. Standing volume before harvesting was 410 m^3 ha^{-1} and the harvested volume was 35% of the standing one (about 140 m^3 ha^{-1}). Forest operations were carried out by the cut-to-length system with an excavator equipped with a processing head for felling and processing, and an 810D forwarder for timber extraction.

2.2. Field and UAV Surveys

Field surveys were carried out at the end of 2024, three months after the end of the forest operations, which were performed in September 2024, where the soil moisture was about 30%–35%. We performed a ground-based survey by a handheld GNSS receiver by tracing and recording all the strip roads established by the forwarder (largely corresponding with those of the felling excavator as usual in cut-to-length operations). This strip roads dataset represented our control strip road network (Figure 2). The GNSS data were collected using a Spectra Precision SP20 handheld receiver (Spectra Geospatial, Westminster, CO, USA) operating in DGPS mode, which applies real-time satellite-based differential corrections (SBAS). Under these conditions, the SP20 provides a typical horizontal positional accuracy of approximately 30–50 cm. No post-processing or RTK corrections were applied.

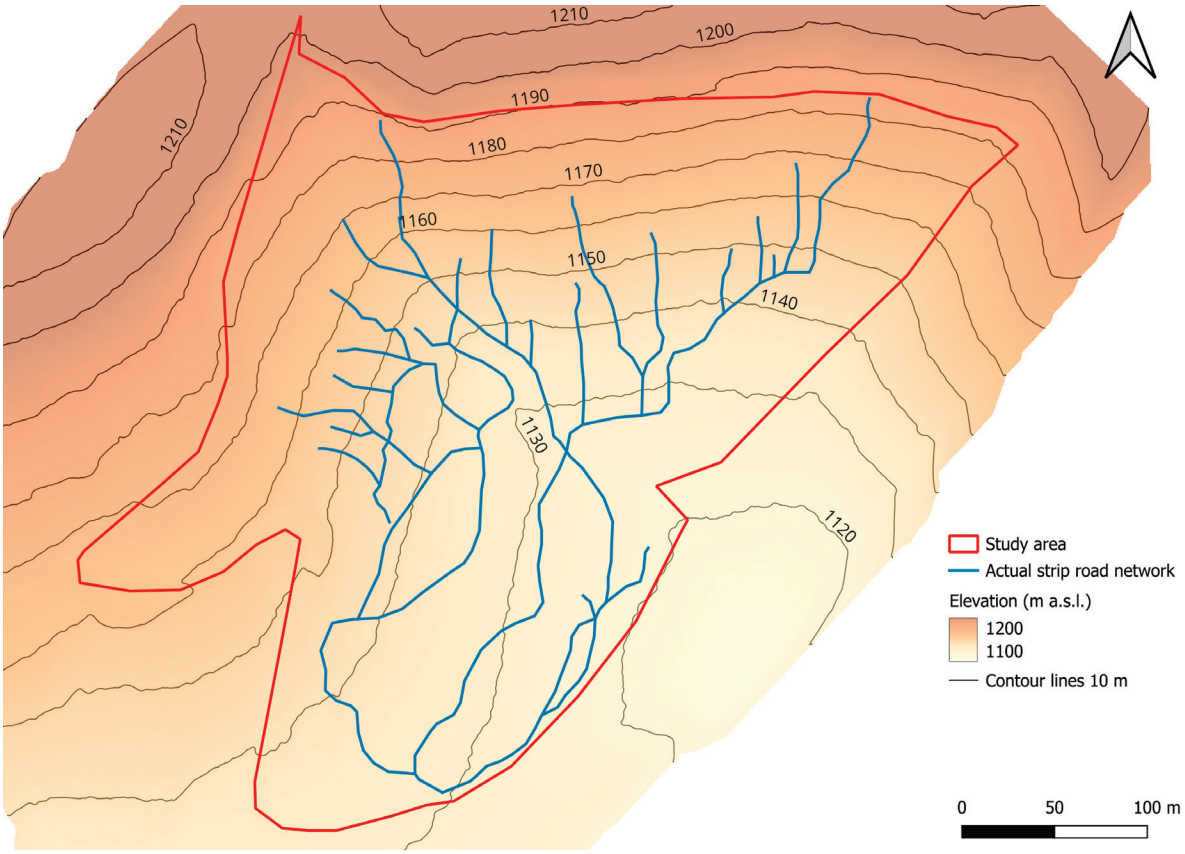

Figure 2. Actual strip road network detected via GNSS survey overlayed to the DTM and related contour lines at 10 m interval.

The day after the GNSS survey, we performed the RGB-UAV survey with a DJI Air 2S (SZ DJI Technology Co., Ltd., Shenzen, China) UAV equipped with a 1" CMOS" image sensor with FOV 88° and 5.4 K resolution. Flight altitude for the UAV-RGB survey was 80 m, with 80% overlap and GSD (Ground Sampling Distance) of 2.3 cm per pixel. One week later we outsourced a professional company to perform a LiDAR-UAV survey by a DJI Matrice 300 equipped with a 5-return LiDAR DJI L2 sensor (SZ DJI Technology Co., Ltd., Shenzen, China). The main flight settings included an altitude of 80 m above ground level, a speed of 6.5 m s^{-1}, a scan angle of ±25° from nadir, a front overlap of about 70%, and a side overlap of about 40%. The density of the obtained LiDAR point cloud was about 600 points per square meter. The percentage of ground points in relation to the total number of points was about 40%. Point cloud density was 686 N m^{-2} in non-strip roads area and 531 N m^{-2} on the strip roads.

2.3. Detection of the Strip Roads

We identified the strip road network using four distinct methods (Figure 3): one based on RGB data and three derived from LiDAR data. Among the LiDAR-based methods, one operates directly on the point cloud, while the other two require the generation of a 0.5 m resolution Digital Elevation Model (DEM) from the point cloud as a preliminary step.

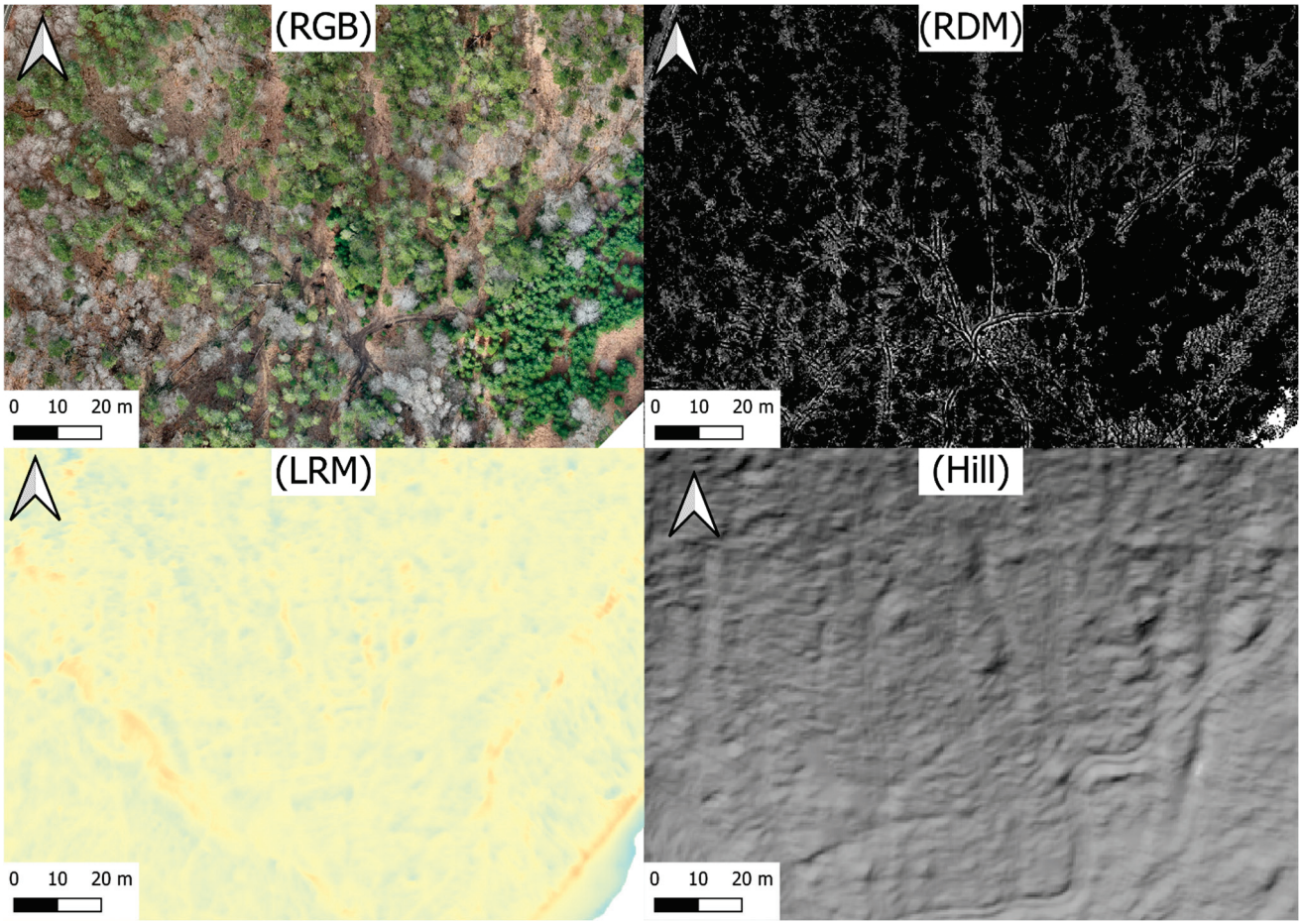

Figure 3. Vision of the same portion of the cutting block according to the four investigated methods for the identification of the strip road network. (**upper left**) RGB, (**upper right**) RDM, (**lower left**) LRM, (**lower right**) Hill.

The method based on passive remote sensing (RGB) involved manually digitizing the strip roads visible in the high-resolution orthophoto produced from the UAV survey. This approach leverages the canopy openings resulting from harvesting activities, which are evident in the RGB imagery, to delineate the trail network.

The first of the LiDAR-based methods is the Hillshading method (Hill). Hillshading enhances terrain visualization by simulating the effects of light and shadow from a defined illumination source [49]. Specifically, The Hillshading technique is a terrain visualization model based on the geometric relationship between light source direction and surface orientation. It simulates illumination across a digital terrain model (DTM) by computing the cosine of the angle between the illumination vector (defined by azimuth and altitude) and the surface normal. The resulting grayscale image enhances relief by representing illuminated slopes as bright and shadowed slopes as dark. In this context, skid trails appear as elongated depressions or flattened surfaces that generate characteristic shading contrasts. Hillshading does not alter elevation values but increases visual interpretability by emphasizing microtopographic variation. This technique, widely available in GIS software (QGIS software version 3.40) under the "hillshade" function, creates a 3D-like effect that accentuates topographic variations. For this method, the DEM is first processed using hillshading, after which the strip roads are manually digitized from the resulting image.

The second method, the Local Relief Model (LRM), enhances the visibility of small-scale terrain features by removing large-scale topographic patterns. The Local Relief Model isolates small-scale topographic variation by removing large-scale terrain trends.

The theoretical foundation of LRM lies in spatial frequency filtering. A low-pass filter (typically Gaussian) is applied to the DTM, acquired after the establishment of the strip roads, to capture broad terrain forms such as ridges and valleys. This smoothed DTM is then subtracted from the original DEM, producing a residual model that highlights local elevation deviations. Positive residuals indicate small elevations (e.g., logs, mounds), while negative ones represent depressions such as strip roads. Thus, LRM enhances subtle geomorphological features that are otherwise obscured by the dominant terrain shape. This technique has proven particularly effective for identifying linear depressions indicative of strip roads [38,50].

The third method, the Relative Density Model (RDM) [51], differs from the previous two by using raw LiDAR point cloud data rather than a DEM. The Relative Density Model is based on the vertical distribution of LiDAR returns within the point cloud. The theoretical assumption is that areas affected by machine traffic exhibit reduced vegetation density and fewer LiDAR returns in the lower height strata. RDM quantifies this by calculating the ratio between the number of LiDAR returns within a specified height range (e.g., 1–5 m) and the total number of returns within each grid cell. Lower RDM values correspond to disturbed zones or bare soil, while higher values indicate undisturbed forest floor or dense understory. The model therefore acts as a proxy for ground-cover continuity and vegetation structural integrity, making it particularly effective for detecting narrow linear disturbances such as strip roads. When visualized as a raster, strip roads appear as narrow, linear features with noticeably low RDM values, distinguishing them from surrounding undisturbed forest.

While the Hillshading method is relatively straightforward and readily applicable, both LRM and RDM required specific adaptations to account for the structural characteristics of Mediterranean forests. For LRM, two key parameters of the Gaussian filter must be carefully chosen: the kernel size and the standard deviation. The kernel size determines the spatial extent of smoothing, while the standard deviation controls its intensity. These parameters must be tailored to suppress large-scale topography (e.g., ridges and gullies) while retaining minor terrain features like strip roads. Based on the scale of the forestry machinery used and the typical dimensions of the resulting trails, we selected a kernel size of 7 m and a standard deviation of 2 m. A comparative view of strip road detection using different kernel sizes and standard deviations is provided in Figure S1 of Supplementary Materials. As shown, the selected parameters enable the most effective identification of the strip roads.

Regarding the RDM, the method was originally developed for tropical rainforests characterized by complex, multi-layered canopies. In those contexts, the commonly used height interval for return density calculation is 1–5 m [51]. However, this range is not appropriate for recently harvested, even-aged Mediterranean pine stands. To select a more suitable interval, we considered the appearance of strip roads in these forests (see Figure 3 RGB). Post-harvest, vegetation is largely absent from the trail surface, and litter cover is significantly reduced. To reflect this, we modified the RDM calculation to assess return density in the 1–30 cm height range (bare soil or only herbaceous cover), aiming to highlight areas of bare soil associated with vehicle tracks. A comparative view of strip road detection using different RDM parameters is provided in Figure S2 of Supplementary Materials. As shown, the chosen parameters proved optimal for achieving clear and reliable identification of the strip roads.

In both the LRM and RDM methods, once the respective rasters were generated, strip roads were manually digitized based on the enhanced visualizations provided by each model. To ensure the robustness and reproducibility of the interpretation, the digitization procedure was independently performed by four different operators. The resulting four

shapefiles were then merged to obtain a consensus strip road pattern. Specifically, the final strip road network was defined by overlaying all individual digitizations and retaining only those trail segments that were identified by at least three out of the four operators. This majority-based approach minimizes subjectivity and operator bias, ensuring that the final map represents the most consistently interpreted features across multiple observers. A vision of the same portion of the cutting block with the rasters obtained with the four methods is given in Figure 3.

2.4. Data Analysis

To assess the accuracy of different methods for identifying strip roads, we compared four classification approaches, RGB, RDM, LRM, and Hill, against a reference dataset obtained through a GNSS survey. The classification results and reference data were represented as binary raster layers obtained from the rasterization of the strip roads shapefile for each method. The shapefile of the strip roads was rasterized with a pixel of 4 m resolution (about the width of the strip roads), where pixel values of 1 indicated the presence of strip roads, and 0 indicated their absence. The entire analysis was performed using QGIS 3.40 [52] for data preprocessing and Rstudio (R version 4.3.3) [53] for accuracy assessment and statistical analysis. Because the number of trail pixels was considerably smaller than the number of background pixels, the dataset exhibited strong class imbalance. To mitigate the bias that such imbalance introduces in global accuracy measures, we adopted a balanced case–control evaluation. For each method, all positive pixels (strip roads pixels identified in the control layer) were retained, while an equal number of background (non-strip roads) pixels were randomly sampled from the logging site area. This balanced subsampling was repeated 1000 times, ensuring robust estimation of performance metrics while maintaining equal representation of classes in each iteration. Each iteration therefore consisted of a balanced dataset composed of all trail pixels and an equal number of randomly sampled background pixels, on which the accuracy metrics were recalculated.

The confusion matrix for each classification method was computed by comparing each method's raster against the control raster. From these confusion matrices, we derived nine accuracy metrics: overall accuracy, precision, recall, Cohen's kappa, Intersection over Union (IoU), Dice Similarity Coefficient (DSC), true positive rate (TPR), false positive rate (FPR), and specificity.

Each metric (all dimensionless) was calculated as follows:

- Overall Accuracy = (TP + TN)/(TP + TN + FP + FN). Represents the overall proportion of correctly classified pixels (both strip roads and non-strip roads). It gives a general sense of model performance but can be misleading when classes are imbalanced.
- Precision = TP/(TP + FP). Indicates how many of the pixels predicted as strip roads were actually strip roads. High precision means fewer false positives (non-strip roads areas wrongly classified as strip roads).
- Recall (Sensitivity, TPR) = TP/(TP + FN). Measures the proportion of actual strip roads pixels that were correctly identified. High recall means fewer false negatives (missed strip roads pixels).
- Cohen's Kappa = (Observed Accuracy − Expected Accuracy)/(1 − Expected Accuracy). A statistic that adjusts accuracy for agreement that occurs by chance. Values range from −1 (complete disagreement) to 1 (perfect agreement). A value of 0 implies random classification.
- Intersection over Union (IoU) = TP/(TP + FP + FN). Indicates the overlap between predicted and actual strip roads areas. A higher IoU means a greater spatial match between method output and control.

- Dice Similarity Coefficient (DSC) = (2 × TP)/(2 × TP + FP + FN). Another measure of spatial overlap. Dice is more sensitive to small overlaps and often used in image segmentation tasks.
- False Positive Rate (FPR) = FP/(FP + TN). Represents the proportion of non-strip roads areas incorrectly predicted as strip roads. Lower FPR values indicate better performance.
- Specificity = TN/(TN + FP). Reflects the ability of a method to correctly identify non-strip roads areas. High specificity complements recall by ensuring that the background (non-strip roads) areas are not falsely marked.

The raster values were extracted and compared using logical operations to derive true positives (TP), false positives (FP), false negatives (FN), and true negatives (TN). Each of these metrics captures a different aspect of classification performance. While accuracy provides a general view, precision and recall offer insight into the balance between omission and commission errors. Cohen's Kappa ensures that agreement is not due to chance, and spatial metrics like IoU and DSC quantify the geometric match of trail shapes between prediction and reference.

To quantify variability and assess statistical differences among methods, we applied a non-parametric bootstrap procedure based on the balanced subsampling results. Each of the 1000 balanced iterations yielded a value for each accuracy metric, forming a bootstrap distribution per method and per metric. For each distribution, we computed the mean and 95% confidence intervals (CIs) using the 2.5th and 97.5th percentiles. To test for statistically significant differences among methods, a one-way ANOVA was performed separately for each metric, followed by Tukey's Honest Significant Difference (HSD) post hoc test.

The computations were carried out in R version 4.4.3 using the terra [54], ggplot2 [55], and reshape2 [56] packages.

3. Results

The length of the identified strip road network and the related percentage of soil surface affected by machine traffic per each investigated method is reported in Table 1, while the visual representation of the strip roads detected with the various methods is available in Figures S3–S6 in Supplementary Materials. Only the RDM method estimated an impacted surface similar to the actual one, while the other three methods strongly underestimated the actual surface affected by machine traffic.

Table 1. Identified strip road network per each method and control dataset. Percentage of impacted surface calculated considering the actual harvested surface of 7.85 ha and an average strip road width of 3.8 m.

Method	Strip Road Network Length (m)	Impacted Surface (%)
Control	2981	14.43
RGB	1552	7.51
RDM	2621	12.68
LRM	1636	7.91
Hill	1056	5.11

Below, Table 2 presents the considered accuracy metrics, including overall accuracy, precision, recall, and Cohen's Kappa, Intersection over Union (IoU), Dice Score, True Positive Rate (TPR), False Positive Rate (FPR), and Specificity.

Table 2. Accuracy metrics and results of the statistical comparison. Abbreviations: CI: confidence interval; IoU: Intersection over Union; DSC: Dice Score; TPR: True Positive Rate; FPR: False Positive Rate. Different lowercase letters in the column "Tukey group" indicate statistically significant differences at $p < 0.05$.

Metric	Method	Mean	CI_Low	CI_High	Tukey Group
Accuracy	RDM	0.746	0.744	0.747	a
	RGB	0.636	0.634	0.636	b
	LRM	0.635	0.633	0.636	c
	Hill	0.609	0.608	0.609	d
Kappa	RDM	0.491	0.488	0.493	a
	RGB	0.271	0.267	0.273	b
	LRM	0.270	0.266	0.271	c
	Hill	0.217	0.215	0.218	d
Precision	RDM	0.996	0.989	1.000	b
	RGB	0.994	0.981	1.000	c
	LRM	0.994	0.981	1.000	c
	Hill	0.997	0.988	1.000	a
Recall	RDM	0.493	0.493	0.493	a
	RGB	0.273	0.273	0.273	b
	LRM	0.271	0.271	0.271	c
	Hill	0.218	0.218	0.218	d
IoU	RDM	0.492	0.491	0.493	a
	RGB	0.272	0.271	0.273	b
	LRM	0.271	0.270	0.271	c
	Hill	0.218	0.218	0.218	d
DSC	RDM	0.660	0.658	0.661	b
	RGB	0.428	0.427	0.428	c
	LRM	0.426	0.425	0.427	a
	Hill	0.358	0.357	0.358	d
TPR	RDM	0.493	0.493	0.493	a
	RGB	0.273	0.273	0.273	b
	LRM	0.271	0.271	0.271	c
	Hill	0.218	0.218	0.218	d
FPR	RDM	0.002	0.000	0.005	a
	RGB	0.002	0.000	0.005	a
	LRM	0.002	0.000	0.005	a
	Hill	0.001	0.000	0.003	b
Specificity	RDM	0.998	0.995	1.000	c
	RGB	0.998	0.995	1.000	a
	LRM	0.998	0.995	1.000	a
	Hill	0.999	0.997	1.000	a

The RDM method demonstrated the highest overall accuracy (0.746) and Kappa coefficient (0.491), indicating a strong agreement with the reference strip roads. The RGB method (0.636 accuracy, 0.271 Kappa) followed as the best-performing approach, showing lower agreement with the control data. The LRM method (0.635 accuracy, 0.270 Kappa) performed slightly lower, while the Hill method (0.609 accuracy, 0.217 Kappa) exhibited the weakest agreement with the reference strip roads. The results show that RGB outperformed both LRM (slightly) and Hill in all classical accuracy metrics, demonstrating that high-resolution drone imagery can be a viable alternative to LiDAR for detecting strip roads. However, RGB was still less accurate than RDM, which had the highest overall agreement with the control data.

Precision, which measures how many of the identified strip roads are actually correct, was relatively high for RGB (0.994), indicating that it avoided excessive false detections. However, its recall (0.273) was significantly lower than RDM (0.493), suggesting that it failed to detect a considerable portion of the actual strip roads. Compared to the LiDAR methods, RGB performed better than LRM and Hill in recall, indicating a greater ability to identify strip roads. However, RDM had the best balance of high recall and high precision, making it the most robust method overall.

The Intersection over Union (IoU) and Dice Score (DSC) provide insight into the spatial agreement between the detected and actual strip roads. Again, RDM had the highest IoU (0.492) and DSC (0.660), while RGB showed moderate performance with an IoU of 0.272 and DSC of 0.428. Notably, RGB outperformed LRM (IoU = 0.271, DSC = 0.426) and Hill (IoU = 0.218, DSC = 0.358), reinforcing its effectiveness compared to these LiDAR-derived methods.

The False Positive Rate (FPR) measures the percentage of areas mistakenly classified as strip roads. The RGB method had an FPR of 0.002, meaning it produced a very low level of false detections, similar to LRM and RDM, and slightly higher than Hill (0.001). Specificity, which measures the ability to correctly identify non-strip roads areas, was highest for Hill (0.999), followed by the other three methods with a value of 0.998. This suggests that RGB effectively avoided misclassifying non-strip roads areas while still achieving a reasonable level of recall.

4. Discussion

From an ecological perspective, both the underestimation and overestimation of machinery-induced disturbance can have significant implications for forest management and impact assessment [57]. Underestimating disturbance may lead to an incomplete understanding of the spatial extent and severity of soil compaction and rutting [58]. This, in turn, could result in an underappreciation of long-term effects on soil structure, hydrological processes, and nutrient cycling, ultimately compromising the sustainability of repeated mechanized operations in the same stands [59]. Conversely, overestimating disturbance may artificially inflate the perceived ecological footprint of forest operations, leading to overly restrictive management responses or misinformed policy decisions regarding allowable harvesting intensity or machine types. Both biases therefore affect the accuracy of post-harvest monitoring and the ability to evaluate compliance with sustainable forest management standards. By improving the precision of disturbance mapping, forest managers can more reliably assess the real extent of soil and understory disturbance, enabling adaptive practices that balance operational efficiency with ecological protection. Our study was conducted to specifically address this important topic in the framework of sustainable forest operations.

The results of this study confirmed the initial hypothesis that high-resolution RGB imagery acquired via UAV is effective in detecting strip roads established by boom-corridor thinning in Mediterranean pine forests. Among the methods tested, the RGB-based approach demonstrated good performance across a variety of accuracy metrics, particularly considering the simplicity and accessibility of the method (Table 2). These findings are particularly relevant in forest contexts where the canopy opening is moderate, as in boom-corridor thinning, and where rapid, cost-effective monitoring tools are needed.

Nonetheless, the Relative Density Model (RDM) emerged as the most accurate method overall, showing superior values for nearly all statistical metrics, including precision, recall, and intersection-over-union (IoU) (Table 2). Our findings reinforce the robustness of the RDM method and mirror results obtained in tropical forest studies, where the approach was initially applied to identify skid trails after selective logging. In those cases, reported

percentage of detected trails generally fell within the 65%–70% range [34,51,60,61]. Furthermore, the RDM method was also individuated as the most performing in previous research in the Mediterranean context, where it achieved Cohen's Kappa up to 0.50 in various forest types [36]. By properly adjusting the parameters, especially the height interval used to capture the reduction in vegetation within strip roads, it effectively identified disturbed areas in even-aged Mediterranean pine plantations. This adaptability reinforces the potential for broader application of RDM across forest types when parameterized appropriately.

However, it is important to highlight the practical limitations of the RDM method. Unlike the other techniques, RDM is computed directly from the LiDAR point cloud, rather than from a Digital Elevation Model (DEM), which makes it considerably more demanding in terms of computational resources. Effective use of RDM, particularly when relying on graphical software such as CloudCompare 2.14 beta, requires high-performance hardware with significant RAM, processing power, and graphic card capacity. This makes it less suitable for practitioners working with standard computing resources. To provide a practical reference, the analysis was performed on a workstation equipped with 64 GB of RAM and an Intel Core i9 processor; under these conditions, the computation required approximately five minutes and utilized up to 80% of the available memory. When the same procedure was attempted on a standard user-grade laptop (8 GB RAM, Intel Core i5 processor), the system failed to complete the operation due to insufficient computational capacity.

In comparison, the hillshading (Hill) method—despite its ease of use and wide availability in standard GIS software—showed the lowest performance. This is consistent with the findings of Affek et al. [49], who also noted the limitations of hillshade visualization for subtle terrain features in forested environments with less than 40% of actual machinery trails detected. Its reliance on visual contrast derived from artificial lighting angles renders it less reliable for consistent identification of strip roads. However, it is worth highlighting that this was the method with the highest specificity, highlighting that when the Hill method detects a strip road, we can be almost sure that the strip roads actually exist.

The Local Relief Model (LRM), while showing intermediate results, offered a good compromise between simplicity and accuracy. As demonstrated in previous studies [38,62], local relief filtering can successfully isolate microtopographic features like strip roads, particularly when parameters are carefully tailored to the size and depth of the disturbances. However, it requires careful adjustment of Gaussian smoothing filters to effectively eliminate broader terrain forms while preserving the smaller depressions associated with trail formation.

However, while RDM and RGB showed high accuracy, the future of such methodologies likely lies in their integration with automated classification techniques. Machine learning offers the potential to greatly enhance efficiency by removing the need for manual digitization. That said, such approaches require large, annotated datasets for training, resources that are often unavailable in small-scale, fragmented forest ownerships like those typical of Central Italy and much of the Mediterranean region. Moreover, the recent literature shows that the accuracy levels achieved through machine learning methods for trail detection are comparable to those obtained in this study using RDM and even RGB, with higher overall accuracy (0.846) achieved only under optimal conditions (even-aged young stands of coniferous species) [63]. Thus, while automation is a clear benefit, it does not yet translate into superior precision.

It is also necessary to acknowledge some limitations of the present study. The first one consists of using manual digitalization, which implies a certain level of subjectivity depending on the operator. The application of machine learning (ML), as previously stated, could be a possible solution to make strip road identification more objective and faster when working on large areas. However, although machine learning (ML) methods rep-

resent an increasingly powerful tool for automated feature extraction in remote sensing, their application was not pursued in this study for several reasons. First, the extent of the study area (approximately 8 ha, corresponding to about 3 km of strip roads) results in a dataset that is too limited to train data-intensive models such as convolutional neural networks, which typically require large numbers of labeled examples to achieve reliable generalization [64–66]. In addition, the operational scale considered here, namely the forest management unit, does not justify the use of complex ML workflows, as manual digitization proved to be highly efficient, requiring only 10–15 min per method to delineate all strip roads. At this scale, ML would not meaningfully reduce processing time or improve practical usability. Furthermore, the purpose of the study is to offer forest managers solutions that are directly applicable within routine monitoring practices; introducing more elaborate ML procedures would increase technical complexity without delivering proportional benefits. While ML techniques could play a valuable role in large-area applications, such as regional- or management-plan–level disturbance mapping where airborne laser scanning would serve as the primary data source, these scenarios fall outside the scope of the present work.

A second limitation arises from the fact that the analysis was carried out in only one study area, which, while highly representative of Mediterranean even-aged pine forests undergoing mechanized thinning, does not capture the full variability of forest structures or terrain conditions that may affect method performance. Nevertheless, the chosen site provides a suitable and relevant context for testing our hypothesis and drawing meaningful conclusions. A further potential limitation of this study concerns the transferability of the results to other forest types and terrain conditions. The analyses were conducted in a relatively homogeneous black pine stand located on moderate to steep slopes typical of Mediterranean mountain forests. While the selected site is representative of many artificial coniferous stands in Central and Southern Italy, the structural characteristics and understory development may differ substantially in other forest ecosystems. Similarly, steeper or more heterogeneous terrain could affect both UAV data quality and the performance of terrain-based LiDAR derivatives such as LRM and RDM [36]. Consequently, the accuracy levels and method rankings reported here should be viewed as context-dependent, and further validation across different species compositions, canopy densities, and slope gradients is needed to confirm the robustness of these findings under broader environmental conditions.

5. Conclusions

This study addressed the challenge of detecting machinery-induced strip roads in Mediterranean pine forests following boom-corridor thinning operations. Given the need for sustainable forest management of these widely distributed stands, the ability to monitor soil disturbance accurately and efficiently is essential. We compared four different methods for identifying strip roads—one based on UAV-derived RGB imagery and three based on LiDAR data, including Hillshading, the Local Relief Model (LRM), and the Relative Density Model (RDM).

Our results confirm that RGB method, despite its reliance on passive sensors, can effectively detect the strip road network under the moderate canopy openings characteristic of boom-corridor thinning. This finding supports our initial hypothesis and highlights the operational value of low-cost UAV-RGB surveys in such forestry contexts. Among the LiDAR-based approaches, the RDM method proved to be the most accurate and reliable, even when applied in a temperate Mediterranean conifer forest—significantly different from the tropical environments where it was originally developed. However, the RDM method is also the most computationally intensive, requiring high-performing hardware and careful parameter tuning.

From a practical standpoint, these findings provide clear guidance for forest managers and practitioners. Specifically, the RDM approach delivered the highest performance, but UAV-based RGB surveys, thanks to their lower cost, satisfactory accuracy, and user-friendly implementation, represent a highly suitable option for identifying the strip road network after boom-corridor thinning in coniferous stands.

Nevertheless, the generalizability of the results remains limited by the characteristics of the study area, a single, relatively homogeneous black pine stand on moderately steep terrain. Further research should validate the findings across a wider range of forest types, canopy structures, and slope gradients to confirm their applicability in more diverse contexts. Looking forward, the integration of automation and machine learning offers promising directions for future work. Approaches based on convolutional neural networks (CNNs), deep learning segmentation of point clouds, or hybrid optical–LiDAR feature extraction could greatly reduce operator dependency and increase processing scalability. Such advances would allow continuous, near-real-time monitoring of forest disturbance over larger areas while maintaining the precision required for sustainable forest management.

Supplementary Materials: The following supporting information can be downloaded at: https://www.mdpi.com/article/10.3390/f16121768/s1.

Author Contributions: Conceptualization, R.P. and F.L.; Data curation, R.P., A.B. and F.L.; Formal analysis, R.V., R.P., A.B., L.C., E.P. and F.L.; Investigation, R.P., L.A., L.C. and E.P.; Methodology, R.V., R.P., L.A., L.C., E.P. and F.L.; Software, A.B., L.A., E.P. and F.L.; Supervision, R.V., R.P., A.L.M. and F.L.; Validation, R.P., M.C. and A.L.M.; Writing—original draft, R.V. and F.L.; Writing—review & editing, R.V., R.P., M.C. and A.L.M. All authors have read and agreed to the published version of the manuscript.

Funding: This research received no external funding.

Data Availability Statement: The data supporting this research are available at https://doi.org/10.5281/zenodo.17590891.

Acknowledgments: This study was carried out in cooperation with the Agritech National Research Center–WP 4.1–Task 4.1.4 and received funding from the European Union Next-GenerationEU (PIANO NAZIONALE DI RIPRESA E RESILIENZA (PNRR)–MISSIONE 4 COMPONENTE 2, INVESTIMENTO 1.4–D.D. 1032 17/06/2022, CN00000022). This paper reflects only the authors' views and opinions, neither the European Union nor the European Commission can be considered responsible for them. The study was further supported by the Statutory Research Fund of the Institute of Dendrology, Polish Academy of Sciences. The authors would like to thank Dario Gattafoni and Francesco Ingino from Multicoopter Drone (Perugia, Italy) for providing the UAV-LiDAR surveys.

Conflicts of Interest: The authors declare no conflicts of interest.

References

1. Grünberg, J.; Ghaffariyan, M.R.; Jourgholami, M.; Labelle, E.R.; Kaakkurivaara, N.; Robert, R.C.G.; Kühmaier, M. Criteria for Assessing the Sustainability of Logging Operations—A Systematic Review. *Curr. For. Rep.* **2023**, *9*, 350–369. [CrossRef]
2. Grünberg, J.; Holzleitner, F.; Behringer, M.; Gollob, C.; Kanzian, C.; Katzensteiner, K.; Kühmaier, M. Impacts of a Fully Mechanized Timber Harvesting System on Soil Physical Properties after a Pronounced Dry Period. *Soil. Tillage Res.* **2025**, *251*, 106551. [CrossRef]
3. Behringer, M.; Grünberg, J.; Katzensteiner, K.; Kitzler, B.; Kohl, B.; Lechner, V.; Malli, A.; Markart, G.; Meißl, G.; Scheidl, C. Comparison of the Effect of Winch-Assisted Timber Harvesting Systems and Cable Yarding on Soil Water Retention and Surface Runoff in a Temperate Deciduous Forest. *J. Hydrol.* **2025**, *658*, 133183. [CrossRef]
4. Ring, E.; Andersson, M.; Hansson, L.; Jansson, G.; Högbom, L. Logging Mats and Logging Residue as Ground Protection during Forwarder Traffic along till Hillslopes. *Croat. J. For. Eng.* **2021**, *42*, 445–462. [CrossRef]
5. Hemmat, A.; Adamchuk, V.I. Sensor Systems for Measuring Soil Compaction: Review and Analysis. *Comput. Electron. Agric.* **2008**, *63*, 89–103. [CrossRef]

6. Frey, B.; Kremer, J.; Rüdt, A.; Sciacca, S.; Matthies, D.; Lüscher, P. Compaction of Forest Soils with Heavy Logging Machinery Affects Soil Bacterial Community Structure. *Eur. J. Soil. Biol.* **2009**, *45*, 312–320. [CrossRef]
7. Mohtashami, S.; Hansson, L.; Eliasson, L. Estimating Soil Strength Using GIS-Based Maps—A Case Study in Sweden. *Eur. J. For. Eng.* **2023**, *9*, 70–79. [CrossRef]
8. Mohtashami, S.; Eliasson, L.; Jansson, G.; Sonesson, J. Influence of Soil Type, Cartographic Depth-to-Water, Road Reinforcement and Traffic Intensity on Rut Formation in Logging Operations: A Survey Study in Sweden. *Silva Fenn.* **2017**, *51*, 1–14. [CrossRef]
9. Nazari, M.; Arthur, E.; Lamandé, M.; Keller, T.; Bilyera, N.; Bickel, S. A Meta-Analysis of Soil Susceptibility to Machinery-Induced Compaction in Forest Ecosystems Across Global Climatic Zones. *Curr. For. Rep.* **2023**, *9*, 370–381. [CrossRef]
10. Vega-Nieva, D.J.; Murphy, P.N.C.; Castonguay, M.; Ogilvie, J.; Arp, P.A. A Modular Terrain Model for Daily Variations in Machine-Specific Forest Soil Trafficability. *Can. J. Soil. Sci.* **2009**, *89*, 93–109. [CrossRef]
11. Pastén, H.R.; Contreras, S.M.; Thiers, E.Ó. Impacts Caused by the Traffic of Ground-Based Forest Harvesting Machinery: State of the Art and Future Guidelines for Chile. *Geoderma Reg.* **2025**, *40*, e00939. [CrossRef]
12. Hansson, L.; Šimůnek, J.; Ring, E.; Bishop, K.; Gärdenäs, A.I. Soil Compaction Effects on Root-zone Hydrology and Vegetation in Boreal Forest Clearcuts. *Soil. Sci. Soc. Am. J.* **2019**, *83*, S105–S115. [CrossRef]
13. Latterini, F.; Horodecki, P.; Dyderski, M.K.; Scarfone, A.; Venanzi, R.; Picchio, R.; Proto, A.R.; Jagodziński, A.M. Mediterranean Beech Forests: Thinning and Ground-Based Skidding Are Found to Alter Microarthropod Biodiversity with No Effect on Litter Decomposition Rate. *For. Ecol. Manag.* **2024**, *569*, 122160. [CrossRef]
14. Klein-Raufhake, T.; Hölzel, N.; Schaper, J.J.; Hortmann, A.; Elmer, M.; Fornfeist, M.; Linnemann, B.; Meyer, M.; Rentemeister, K.; Santora, L.; et al. Severity of Topsoil Compaction Controls the Impact of Skid Trails on Soil Ecological Processes. *J. Appl. Ecol.* **2024**, *61*, 1817–1828. [CrossRef]
15. Schäffer, J.; von Wilpert, K.; Kublin, E. Analysis of Fine Rooting below Skid Trails Using Linear and Generalized Additive Models. *Can. J. For. Res.* **2009**, *39*, 2047–2058. [CrossRef]
16. Labelle, E.R.; Kammermeier, M. Above- and Belowground Growth Response of Picea Abies Seedlings Exposed to Varying Levels of Soil Relative Bulk Density. *Eur. J. For. Res.* **2019**, *138*, 705–722. [CrossRef]
17. Enez, K.; Aricak, B.; Sariyildiz, T. Effects of Forest Harvesting Activities on Litter Decomposition Rates of Scots Pine, Trojan Fir and Sweet Chestnut. *Sumar. List.* **2015**, *139*, 361–367.
18. Werder, M.; Bont, L.G.; Schweier, J.; Thees, O. A Comprehensive Analysis of Time Investment in Skid Trail Planning for Forest Access. *PLoS ONE* **2025**, *20*, e0317963. [CrossRef]
19. Latterini, F.; Camarretta, N.; Janiszewska-Latterini, D.; Pasquini, D.; Moss, J.; Watt, M.S. Soil Trafficability Maps: A Geospatial Tool for Reducing Soil Damage and Supporting Sustainable Forest Management in New Zealand. *Land Degrad. Dev.* **2025**, *36*, 5602–5612. [CrossRef]
20. DeArmond, D.; Ferraz, J.B.S.; Lima, A.J.N.; Higuchi, N. Surface Soil Recovery Occurs within 25 Years for Skid Trails in the Brazilian Amazon. *Catena* **2024**, *234*, 107568. [CrossRef]
21. Contreras, M.A.; Parrott, D.L.; Chung, W. Designing Skid-Trail Networks to Reduce Skidding Cost and Soil Disturbance for Ground-Based Timber Harvesting Operations. *For. Sci.* **2016**, *62*, 48–58. [CrossRef]
22. Stempski, W.; Jabłoński, K.; Jakubowski, J. Effects of Strip Roads on Volume Increment of Edge Trees. *Drewno* **2021**, *64*, 5–15. [CrossRef]
23. Contreras, M.; Parra, C.; Cárdenas, C.; Hermosilla, C.; Pastén, R.; Aedo, D. Skid Trail Network Visualizer: A Computational Tool to Generate Skid Trails Created by Ground-Based Timber Harvesting Machines and Facilitate Soil Disturbance Monitoring. *Comput. Electron. Agric.* **2024**, *225*, 109282. [CrossRef]
24. Roussel, J.-R.; Bourdon, J.-F.; Morley, I.D.; Coops, N.C.; Achim, A. Correction, Update, and Enhancement of Vectorial Forestry Road Maps Using ALS Data, a Pathfinder, and Seven Metrics. *Int. J. Appl. Earth Obs. Geoinf.* **2022**, *114*, 103020. [CrossRef]
25. Waga, K.; Tompalski, P.; Coops, N.C.; White, J.C.; Wulder, M.A.; Malinen, J.; Tokola, T. Forest Road Status Assessment Using Airborne Laser Scanning. *For. Sci.* **2020**, *66*, 501–508. [CrossRef]
26. Sterenczak, K.; Moskalik, T. Use of LIDAR-Based Digital Terrain Model and Single Tree Segmentation Data for Optimal Forest Skid Trail Network. *IForest* **2014**, *8*, 661–667. [CrossRef]
27. Latterini, F.; Camarretta, N.; Watt, M.S. Remote Sensing for Planning Harvesting Operations and Monitoring Their Effects on the Forest Ecosystem: State of the Art and Future Perspectives. *For. Ecol. Manag.* **2025**, *597*, 123175. [CrossRef]
28. Becker, R.M.; Keefe, R.F.; Anderson, N.M. Use of Real-Time GNSS-RF Data to Characterize the Swing Movements of Forestry Equipment. *Forests* **2017**, *8*, 44. [CrossRef]
29. Salmivaara, A.; Holmström, E.; Kulju, S.; Ala-Ilomäki, J.; Virjonen, P.; Nevalainen, P.; Heikkonen, J.; Launiainen, S. High-Resolution Harvester Data for Estimating Rolling Resistance and Forest Trafficability. *Eur. J. For. Res.* **2024**, *143*, 1641–1656. [CrossRef]
30. Spinelli, R.; Magagnotti, N.; Lombardini, C. Performance, Capability and Costs of Small-Scale Cable Yarding Technology. *Small-Scale For.* **2010**, *9*, 123–135. [CrossRef]

31. Manzone, M.; Spinelli, R. Efficiency of Small-Scale Firewood Processing Operations in Southern Europe. *Fuel Process. Technol.* **2014**, *122*, 58–63. [CrossRef]
32. Del Giudice, A.; Scarfone, A.; Santangelo, E.; Latterini, F.; Stefanoni, W. Modelling the Productivity and Economic Feasibility for Bioenergy Production in a Mediterranean Oak Coppice. *Drewno Pr. Nauk. Doniesienia Komun. Wood Res. Pap. Rep. Announc.* **2024**, *67*, 00026. [CrossRef]
33. Macrì, G.; De Rossi, A.; Papandrea, S.; Micalizzi, F.; Russo, D.; Settineri, G. Evaluation of Soil Compaction Caused by Passages of Farm Tractor in a Forest in Southern Italy. *Agron. Res.* **2017**, *15*, 478–489.
34. Wedeux, B.; Dalponte, M.; Schlund, M.; Hagen, S.; Cochrane, M.; Graham, L.; Usup, A.; Thomas, A.; Coomes, D. Dynamics of a Human-Modified Tropical Peat Swamp Forest Revealed by Repeat Lidar Surveys. *Glob. Change Biol.* **2020**, *26*, 3947–3964. [CrossRef]
35. Craven, M.; Wing, M.G. Applying Airborne LiDAR for Forested Road Geomatics. *Scand. J. For. Res.* **2014**, *29*, 174–182. [CrossRef]
36. Latterini, F.; Dyderski, M.K.; Picchio, R.; Venanzi, R.; Spinelli, R.; Magagnotti, N.; Schweier, J.; Kushwaha, S.K.P.; Camarretta, N.; Watt, M.S. Mapping Skid Trails and Evaluating Soil Disturbance From UAV-Based LiDAR Surveys in Mediterranean Forests. *Land Degrad. Dev.* 2025; *early view*. [CrossRef]
37. Siafali, E.; Tsioras, P.A. An Innovative Approach to Surface Deformation Estimation in Forest Road and Trail Networks Using Unmanned Aerial Vehicle Real-Time Kinematic-Derived Data for Monitoring and Maintenance. *Forests* **2024**, *15*, 212. [CrossRef]
38. Mohieddinne, H.; Brasseur, B.; Gallet-Moron, E.; Lenoir, J.; Spicher, F.; Kobaissi, A.; Horen, H. Assessment of Soil Compaction and Rutting in Managed Forests through an Airborne LiDAR Technique. *Land Degrad. Dev.* **2022**, *34*, 1558–1569. [CrossRef]
39. Görgens, E.B.; Mund, J.P.; Cremer, T.; de Conto, T.; Krause, S.; Valbuena, R.; Rodriguez, L.C.E. Automated Operational Logging Plan Considering Multi-Criteria Optimization. *Comput. Electron. Agric.* **2020**, *170*, 105253. [CrossRef]
40. Morley, I.D.; Coops, N.C.; Roussel, J.-R.; Achim, A.; Dech, J.; Meecham, D.; McCartney, G.; Reid, D.E.B.; McPherson, S.; Quist, L.; et al. Updating Forest Road Networks Using Single Photon LiDAR in Northern Forest Environments. *For. Int. J. For. Res.* **2024**, *97*, 38–47. [CrossRef]
41. Pecho, P.; Škvareková, I.; Ažaltovič, V.; Bugaj, M. UAV Usage in the Process of Creating 3D Maps by RGB Spectrum. *Transp. Res. Procedia* **2019**, *43*, 328–333. [CrossRef]
42. Di Marzio, N. An Overview of Forest Cover and Management in Italy. *Nova Meh. Sumar.* **2020**, *41*, 63–71. [CrossRef]
43. Cantiani, P.; Marchi, M. A Spatial Dataset of Forest Mensuration Collected in Black Pine Plantations in Central Italy. *Ann. For. Sci.* **2017**, *74*, 50. [CrossRef]
44. Magagnotti, N.; Pari, L.; Spinelli, R. Re-Engineering Firewood Extraction in Traditional Mediterranean Coppice Stands. *Ecol. Eng.* **2012**, *38*, 45–50. [CrossRef]
45. Bergström, D.; Fernandez-Lacruz, R.; de la Fuente, T.; Höök, C.; Krajnc, N.; Malinen, J.; Nuutinen, Y.; Triplat, M.; Nordfjell, T. Effects of Boom-Corridor Thinning on Harvester Productivity and Residual Stand Structure. *Int. J. For. Eng.* **2022**, *33*, 226–242. [CrossRef]
46. de la Fuente, T.; Bergström, D.; Fernandez-Lacruz, R.; Hujala, T.; Krajnc, N.; Laina, R.; Nordfjell, T.; Triplat, M.; Tolosana, E. Environmental Impacts of Boom-Corridor and Selectively Thinned Small-Diameter-Tree Forests. *Sustainability* **2022**, *14*, 6075. [CrossRef]
47. Fick, S.E.; Hijmans, R.J. WorldClim 2: New 1-km Spatial Resolution Climate Surfaces for Global Land Areas. *Int. J. Climatol.* **2017**, *37*, 4302–4315. [CrossRef]
48. Poggio, L.; de Sousa, L.M.; Batjes, N.H.; Heuvelink, G.B.M.; Kempen, B.; Ribeiro, E.; Rossiter, D. SoilGrids 2.0: Producing Soil Information for the Globe with Quantified Spatial Uncertainty. *Soil.* **2021**, *7*, 217–240. [CrossRef]
49. Affek, A.N.; Zachwatowicz, M.; Sosnowska, A.; Gerlée, A.; Kiszka, K. Impacts of Modern Mechanised Skidding on the Natural and Cultural Heritage of the Polish Carpathian Mountains. *For. Ecol. Manag.* **2017**, *405*, 391–403. [CrossRef]
50. Hesse, R. LiDAR-derived Local Relief Models—A New Tool for Archaeological Prospection. *Archaeol. Prospect.* **2010**, *17*, 67–72. [CrossRef]
51. D'oliveira, M.V.N.; Reutebuch, S.E.; McGaughey, R.J.; Andersen, H.-E. Estimating Forest Biomass and Identifying Low-Intensity Logging Areas Using Airborne Scanning Lidar in Antimary State Forest, Acre State, Western Brazilian Amazon. *Remote Sens. Environ.* **2012**, *124*, 479–491. [CrossRef]
52. QGIS Development Team. *QGIS Geographic Information System*, version 3.40; Open Source Geospatial Foundation: Beaverton, OR, USA, 2024.
53. R Core Team. *R: A Language and Environment for Statistical Computing*, version 4.4.3; R Foundation for Statistical Computing: Vienna, Austria, 2024.
54. Hijmans, R.J.; Bivand, R.; Forner, K.; Ooms, J.; Pebesma, E.; Sumner, M.D. *Package 'Terra.'*; R Foundation for Statistical Computing: Vienna, Austria, 2022; p. 384.
55. Wickham, H.; Chang, W.; Wickham, M.H. *Package 'Ggplot2.': Create Elegant Data Visualisations Using the Grammar of Graphics*, version 2; R Foundation for Statistical Computing: Vienna, Austria, 2016; pp. 1–189.

56. Wickham, H.; Wickham, M.H. Package 'Reshape'. 2022. Available online: https://cran.rproject.org/web/packages/reshape2/reshape2.pdf (accessed on 19 September 2020).
57. Labelle, E.R.; Hansson, L.; Högbom, L.; Jourgholami, M.; Laschi, A. Strategies to Mitigate the Effects of Soil Physical Disturbances Caused by Forest Machinery: A Comprehensive Review. *Curr. For. Rep.* **2022**, *8*, 20–37. [CrossRef]
58. Haas, J.; Ellhöft, K.H.; Schack-Kirchner, H.; Lang, F. Using Photogrammetry to Assess Rutting Caused by a Forwarder—A Comparison of Different Tires and Bogie Tracks. *Soil. Tillage Res.* **2016**, *163*, 14–20. [CrossRef]
59. Latterini, F.; Horodecki, P.; Dyderski, M.K.; Kamczyc, J.; Witkowski, R.; Venanzi, R.; Jagodziński, A.M. Insufficient Logging Intervals Impede Upper Soil Recovery in Temperate Beech Forests: Insights from Two Case-Studies in Poland. *Ecol. Evol.* **2025**, *15*, e72302. [CrossRef] [PubMed]
60. Ellis, P.; Griscom, B.; Walker, W.; Gonçalves, F.; Cormier, T. Mapping Selective Logging Impacts in Borneo with GPS and Airborne Lidar. *For. Ecol. Manag.* **2016**, *365*, 184–196. [CrossRef]
61. Melendy, L.; Hagen, S.C.; Sullivan, F.B.; Pearson, T.R.H.; Walker, S.M.; Ellis, P.; Kustiyo; Sambodo, A.K.; Roswintiarti, O.; Hanson, M.A.; et al. Automated Method for Measuring the Extent of Selective Logging Damage with Airborne LiDAR Data. *ISPRS J. Photogramm. Remote Sens.* **2018**, *139*, 228–240. [CrossRef]
62. Mohieddinne, H.; Brasseur, B.; Spicher, F.; Gallet-Moron, E.; Buridant, J.; Kobaissi, A.; Horen, H. Physical Recovery of Forest Soil after Compaction by Heavy Machines, Revealed by Penetration Resistance over Multiple Decades. *For. Ecol. Manag.* **2019**, *449*, 117472. [CrossRef]
63. Abdi, O.; Uusitalo, J.; Kivinen, V.P. Logging Trail Segmentation via a Novel U-Net Convolutional Neural Network and High-Density Laser Scanning Data. *Remote Sens.* **2022**, *14*, 349. [CrossRef]
64. Hamedianfar, A.; Mohamedou, C.; Kangas, A.; Vauhkonen, J. Deep Learning for Forest Inventory and Planning: A Critical Review on the Remote Sensing Approaches so Far and Prospects for Further Applications. *For. Int. J. For. Res.* **2022**, *95*, 451–465. [CrossRef]
65. Wang, Y.; Zhang, W.; Gao, R.; Jin, Z.; Wang, X. Recent Advances in the Application of Deep Learning Methods to Forestry. *Wood Sci. Technol.* **2021**, *55*, 1171–1202. [CrossRef]
66. Holzinger, A.; Schweier, J.; Gollob, C.; Nothdurft, A.; Hasenauer, H.; Kirisits, T.; Häggström, C.; Visser, R.; Cavalli, R.; Spinelli, R.; et al. From Industry 5.0 to Forestry 5.0: Bridging the Gap with Human-Centered Artificial Intelligence. *Curr. For. Rep.* **2024**, *10*, 442–455. [CrossRef] [PubMed]

Disclaimer/Publisher's Note: The statements, opinions and data contained in all publications are solely those of the individual author(s) and contributor(s) and not of MDPI and/or the editor(s). MDPI and/or the editor(s) disclaim responsibility for any injury to people or property resulting from any ideas, methods, instructions or products referred to in the content.

forests

MDPI

Article

The Effect of Knife Wear and Sharpening Mode on Chipper Productivity and Delays

Matevž Mihelič [1], Dinko Vusić [2,*], Branko Ursić [2], Antonio Zadro [3] and Raffaele Spinelli [4]

[1] Department of Forestry and Renewable Forest Resources, Biotechnical Faculty, University of Ljubljana, Jamnikarjeva ul. 101, 1000 Ljubljana, Slovenia; matevz.mihelic@bf.uni-lj.si
[2] Faculty of Forestry and Wood Technology, University of Zagreb, Svetošimunska cesta 23, 10000 Zagreb, Croatia; bursic@sumfak.unizg.hr
[3] Matije Gupca Odvojak 2 7, 32254 Vrbanja, Croatia; azadro94@gmail.com
[4] CNR IBE, Via Madonna del Piano 10, I-50019 Sesto Fiorentino, Italy; spinelli@ivalsa.cnr.it
* Correspondence: dvusic@sumfak.unizg.hr

Abstract: The production of wood chips can be achieved using different types of wood chippers whose productivity can be influenced by many factors including proper knife management. Research was conducted to determine the productivity of the new Diamant chipper in chipping air-dried tops stacked at a roadside landing and to compare the efficiency of dry sharpening and wet sharpening in restoring chipper productivity, the time required by dry sharpening with that of knife replacement, and the cost of dry sharpening to knife change in real-life conditions. To clearly define the influence of knife management, a model of the effect of knife wear on chipper productivity was produced. Analysis of variance was used to check the significance of any differences in chipping and total time consumption per cycle. Multiple regression was used to express the relationship between chipping time consumption per cycle and the cumulated mass processed by a set of knives—the latter taken as an indicator of knife wear. The study lasted 10 full workdays, included a total of 136 truckloads or 3560 t of fresh wood chips (or green tons = gt), and resulted in the average productivity of 59.0 gt per productive chipping hour (excluding all delays) or 39.4 gt per machine scheduled hour (including all delays). Delays represented 37% of total worksite time. Knife management (dry sharpening or change) accounted for 30% of the total delay time due to raw material contamination. Dry sharpening took 30% less time than a full knife change. As wear accumulated and knives lost their edge, the chipping time per cycle increased from 25 in the first cycle (full truck load) to 38 min in the third cycle. The presented study offers robust productivity figures, together with a reliable estimate of the productivity losses caused by knife wear, and could help improve knife management in order to increase chipper productivity as well as reduce unnecessary delays.

Keywords: dry sharpening; wet sharpening; delay time

1. Introduction

In order to reduce greenhouse gas emissions in the atmosphere, the European Union has set ambitious targets in its strategies, a part of which is biomass use. In the European Union, forestry accounts for more than 60% of domestic biomass supplied for energy purposes [1]. The rising trend of energy use from renewable energy sources has boosted the demand for wood fuel [2], although wood fuel prices remain relatively low, which makes biomass supply a risky business, where production costs can easily exceed market prices [3]. To mitigate such risk, there is a constant need to optimize wood fuel supply chains. Therein, the most expensive production step in terms of energy and cost is wood comminution [4]. That is why a considerable amount of research is devoted to improving logistics [5,6], chipper selection [6,7], and machine configuration [8,9]. It is uneconomical to modify the overall chipper characteristics like engine power; therefore, the choice of the appropriate machine for the extent of operations and logistics is paramount; however, it has

been demonstrated that it is possible to maximize the efficiency of comminution equipment. When chippers are used, knife maintenance and overall conditions are paramount [10,11] and can tip the balance of the economy of operations with higher productivity and better product quality [12] and thus higher product value. Therefore, knife wear has a dominant effect on fuel consumption, chipper productivity, and product quality [12–16], and this effect is generally stronger than the effect of tree species or chipper configuration [14].

Chipper knife wear is the result of a complex combination of mechanical, thermal, electrical, and chemical processes [17], which leads to an increase in the blade front angle and a consequent loss of efficiency in its shearing action [18]. Chipper knives are generally made of high-grade cold working alloy steel of different types and are normally hardened to between 55 and 60 HRC (Rockwell scale) [10]; thus, wear is slow but still inevitable. The only remedy to knives becoming blunt is to restore their blade angle through periodic sharpening. This requires removing part of the knife through abrasion, which leads to progressive material loss until the integrity and functionality of the knife can no longer be guaranteed, and replacement takes place. Normal wear caused by contact with wood can be compounded by accelerated wear due to the presence of contaminants in the feedstock, such as dirt, stones, or metal. Chipper knives are designed to cut wood—not minerals—and the presence of the latter generally results in fast wear or sudden damage. Decision on the optimal time for knife change or sharpening is usually based on the subjective feeling of the machine operator [19].

The problem of blade wear can be tackled with two different approaches. One is to use cheap disposable knives, which removes the need for sharpening and reduces the cost of a premature write-off [20]. The other is to use conventional re-usable knives, which are regularly sharpened when they become dull. This latter approach is the dominant one and is adopted by most operators. In that case, blunt knives are removed from the chipper and replaced with a set of new knives, for later sharpening with a wet sharpener. A sharpener is a precision tool that grinds the blade surface at a set angle to restore proper shape. Water is poured over the blade during sharpening to prevent heating damage to the metal. Wet sharpening is very effective but requires a dedicated piece of equipment and can only be performed after removing the knives from the chipper—generally at a workshop. Otherwise, knives can be honed manually on the fly with portable electric grinders, without removing them from the chipper (dry sharpening). The result is not as good as with a wet sharpener because manual grinding is not accurate enough and it cannot restore a proper front angle; thus, dry sharpening is not intended to replace wet sharpening, but rather to complement it [10], making use of the time available during interaction delays in the field and extending the time between wet sharpening sessions. Regardless of the approach adopted in each case, all operators are faced with the opposing needs of extending the time between knife replacement (and eventual resharpening) and minimizing the efficiency losses derived from gradual knife blunting.

Therefore, the goals of this study were:

(1) To determine the productivity of the new Diamant chipper;
(2) To model the effect of knife wear on chipper productivity;
(3) To compare the efficiency of dry sharpening and wet sharpening in restoring chipper productivity;
(4) To compare the time required by dry sharpening with that of knife replacement (for taking the knives to the workshop and wet sharpening them);
(5) To compare the cost of dry sharpening and wet sharpening.

2. Materials and Methods

2.1. Materials

Research was conducted at two chipping sites, both located in the lowland forests of the Spačva basin, east Croatia (Table 1). In the period of chipping, the average temperature was 22.5 °C, average monthly precipitation was 71 mm, and average humidity was 70%. At both chipping sites, the raw material consisted of air-dried tops stacked at a roadside

landing as a result of a common practice in Croatian lowland forests in which forwarders are used for primary transport [21,22] and a management method in which logging residue is completely removed from the regeneration stand after felling [23] to be chipped after seasoning at the roadside, as is common in most supply chains in European countries [24] and stated as the most cost-efficient [25]. The tops had been forwarded to the roadside after roundwood transport in two preparatory cuts conducted in hardwood stands in the last quarter of 2018 (chipping site B) and between the end of 2018 and the first quarter of 2019 (chipping site A). Visual observation indicated that the stacked tops had been contaminated with dirt during handling and transport and that contamination seemed more severe at chipping site A.

Table 1. Chipping sites data.

Chipping Site	A	B
Forest office	Strošinci	Vrbanja
Management unit	Debrinja	Vrbanjske šume
Coordinates	44°57′08.6″ N 19°06′15.0″ E	45°00′36.4″ N 18°58′04.2″ E
Raw material	Tops	Tops
Species	65% hedge maple (*Acer campestre* L.) 35% narrow-leaved ash (*Fraxinus angustifolia* Vahl), European hornbeam (*Carpinus betulus* L.), pedunculate oak (*Quercus robur* L.), and other hard broadleaves	40% European hornbeam 31% narrow-leaved ash 14% hedge maple 15% other hard broadleaves, common linden (*Tilia cordata* Mill.), pedunculate oak, and white poplar (*Populus alba* L.)
Moisture content	39.5 ± 3.4%	28.7 ± 3.7%

At both sites (Figure 1), chipping was conducted with the same Albach Diamant 2000 (ALBACH Maschinenbau AG, D-85088 Menning, Germany) self-propelled industrial chipper, which discharged the chips directly into chip vans (semitrailer trucks) (Table 2). Chipping site B offered better work conditions than chipping site A, since the landing was located along the main forest road and offered enough space for the trucks to maneuver. In contrast, the landing at chipping site A was placed along a secondary forest road that did not offer enough space for maneuvering. Therefore, empty chip trucks had to drive to a suitable space some 750 m further ahead in order to turn around and come back to the landing facing the way out. In this case, each truck change required the chipper to travel to the nearest suitable passing area.



(**a**) (**b**)

Figure 1. (**a**) Chipping site A; (**b**) chipping site B.

Table 2. Chipper specifications.

Make and Model	Albach Diamant 2000
Power, kW	565
Length, m	10.34
Width, m	2.55
Height (lifted cabin), m	3.95 (4.80)
Weight, t	32
Tires	650/65R 42
Intake width, mm	1230
Intake height, mm	980
Rotor speed, r/min	420
Number of blades	6, 8, 12
Crane type	Forwarder crane Epsilon, S110F
Crane max. range, m	10.1
Crane max. load at 10.1 m, t	1

The chipper featured the new, seventh-generation drum, with 6 staggered knives (Figure 2). Seventh-generation drums have an open design and carry replaceable knife mounts and brackets, which enable the fine-tuning of cut length to the target chip size. In particular, chip length can be changed from 15 to 60 mm. However, the unit used for the experiment was equipped with short knives (200 mm) and small brackets that did not enable significant knife adjustments. Therefore, the same cut length (38 mm) and screen (80 mm × 80 mm mesh size) were used for the entire duration of the experiment.

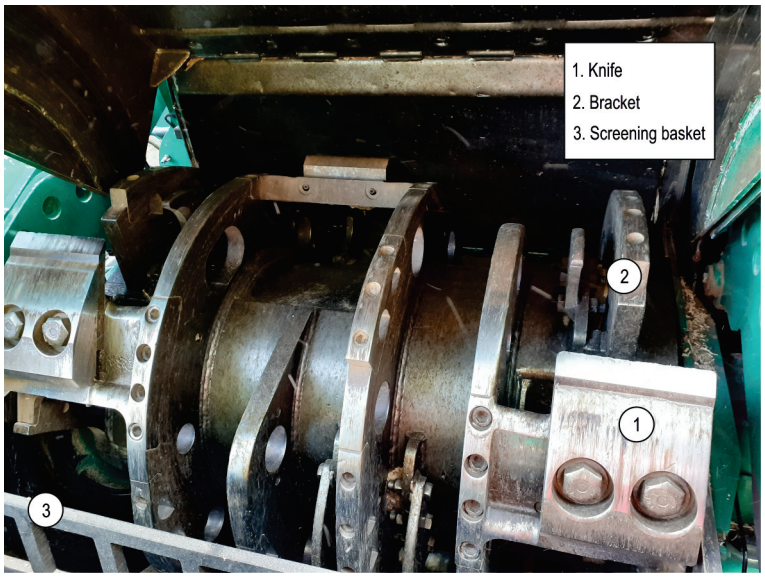

Figure 2. The seventh-generation open drum with 6 knives.

In the trial, both wet and dry sharpening were used—the former for knives that were severely degraded, the latter for a quick refresh of knives on the fly. Wet sharpening required taking the worn-out knives off of their brackets and replacing them with sharp knives, while dry sharpening was applied to slightly worn knives and was performed manually with a portable electric grinder, without removing the knives from the chipper. This task was entirely manual, without the metal bevel guides designed for this purpose. Therefore, the quality of dry sharpening was heavily dependent on variable operator competence, experience, and care. However, dry sharpening was an established practice within the company, and one would expect it to be performed with sufficient competence. The producer of the knives used during the test uses 1.2360 steel for the production of knives. The steel has a hardness of 56 to 59 HRC (Rockwell scale). The same type of knives

are still regularly used by the contractor. The cutting edge was wet sharpened to a 30° angle. Wet sharpening was performed by Winter Hobelmesser Schleifmaschine Grinder 1700 Auto Magnetic machine (Henrik WINTER, HOLZTECHNIK GmbH, D-04159 Leipzig-Stahmeln, Germany) using the standard method. The thickness of the removed material depended on the severity of knife damage, but on normally damaged knives, the grinder was set to remove 2 mm of the knife edge.

2.2. Methods

Time studies were conducted to determine chipping time and delays at both chipping sites [26]. When recording the delays, the reason for each event was recorded along with its duration. Later on, the delays were grouped into functional categories. All recorded delays were included in the productivity model. A single chipping cycle was represented by the truckload, and all recorded time consumption (in minutes) was associated with the truckload mass, as determined at the factory weighbridge. Chip moisture content (m.c.) was determined with a Schaller BLL humimeter randomly sampling 3 to 4 truckloads per day.

Cycles during which knife sharpening or change took place (at the end of the cycles) were highlighted in the original database. The total mass of chips processed by a set of knives before change (or dry sharpening) was obtained by summing the mass of all trucks between two change or sharpening events.

Statistical analyses were performed with the Statistica TIBCO Software Inc. (2020) Data Science Workbench, version 14. Analysis of variance was performed to check the significance of any differences in chipping and total time consumption per cycle, as well as truckload mass between the chipping sites. Multiple regression was used to express the relationship between chipping time consumption per cycle and the cumulated mass processed by a set of knives—the latter taken as an indicator of knife wear. Non-parametric tests (Mann–Whitney and chi-square) were used to compare sample means, as the tests are robust and widely used in the literature. Significant differences in the intensity and duration of the knife sharpening/change between the chipping sites were tested using the non-parametric Kolmogorov–Smirnov test, as normality of data is not required. Statistical significance was accepted for $\alpha < 0.05$.

All figures reported in this study refer to fresh hardwood chips, with a water mass fraction between 28% and 40%.

3. Results

The study lasted 10 full workdays and included a total of 136 truckloads, or 3560 t of fresh wood chips (or green tons = gt). A total of 71 cycles were recorded at chipping site A over five workdays (1844 gt) and 65 cycles were recorded at chipping site B, also over five workdays (1716 gt). On average, 27.4 $\pm$ 4.0 min/cycle of chipping time (43.7 $\pm$ 11.9 min/cycle of total time) was needed for the production of 26.0 $\pm$ 1.7 gt/cycle at chipping site A. At chipping site B, the corresponding figures were: 26.9 $\pm$ 4.5 min/cycle chipping time (42.2 $\pm$ 12.5 min/cycle of total time) and 26.4 $\pm$ 1.8 gt/cycle. The grand average for productivity was 59.0 gt per productive chipping hour (excluding all delays) or 39.4 gt per machine scheduled hour (including all delays).

The analysis of variance found no statistically significant differences between work sites in terms of chipping time per cycle (F = 0.385, p = 0.535), total time per cycle (F = 0.497, p = 0.482), and truckload mass (F = 1.998, p = 0.159). Therefore, the data from the two sites were amalgamated and used as a single database.

Delays represented 37% of total worksite time, for a delay factor (delay time/productive time) of 0.58. Detailed analysis of the delays recorded at the different chipping sites (Table 3) indicated that the more favorable conditions encountered at site B did result in a reduction of those delays that were associated with truck swapping, to the benefit of shorter turnout time. However, that benefit was eroded by a longer transportation distance and the

inadequate availability of trucks; eventually, shorter truck changing times were offset by longer waiting times, compared with site A.

Table 3. Structure of recorded time (worksite time).

Chipping Site	A	B	Total
Total worksite time, min	3104	2746	5850
Productive (chipping) time, min	1944	1750	3694
Delays, min	1160	996	2156
Knife sharpening, min (%)	166 (14.3)	136 (13.7)	302 (14.0)
Knife change, min (%)	215 (18.5)	129 (13.0)	344 (16.0)
Other mechanical delays, min (%)	115 (9.9)	84 (8.4)	199 (9.2)
Truck change, min (%)	531 (45.8)	329 (33.0)	860 (39.9)
Truck waiting, min (%)	14 (1.2)	183 (18.4)	197 (9.1)
Moving and bunching, min (%)	9 (0.8)	15 (1.5)	24 (1.1)
Break, min (%)	60 (5.2)	65 (6.5)	125 (5.8)
Talk, min (%)	50 (4.3)	55 (5.5)	105 (4.9)

Knife management (dry sharpening or change) accounted for 30% of the total delay time due to raw material contamination. Knife management amounted to 12.3% and 9.7% of the total time at site A and site B, respectively. The average knife management time per cycle was 5.4 ± 10.9 min and 4.1 ± 8.9 min respectively for site A and site B, without any significant differences according to the Kolmogorov–Smirnov test ($p > 0.1$). Therefore, a single average knife management delay time was estimated for each of the two sharpening modes.

As wear accumulated and the knives lost their edge, chipping time per cycle increased from 25.0 min to 25.6 min between the first and the second cycle, up to 38.0 min after chipping 79 t in the third cycle. After that, the knives were dry sharpened or changed. Despite the low coefficient of determination ($R^2 = 0.2298$), productivity clearly decreased with the cumulated mass processed by a set of knives (Figure 3) with a slightly steeper trend for dry-sharpened knives. Statistical significance was demonstrated through multiple regression analysis. The results of the analysis are shown in Table 4, which proves the highly significant and inverse relationship between productivity and the amount of chips processed by a set of knives. Although highly significant, this function has a relatively low explanatory value (23% of the overall variability) due to the expected large background noise derived from the erratic presence of contaminants in the chipped material. A few small stones can cause instant damage to the blades, thus dramatically impairing their performance. The same wood pile can contain material with variable levels of contamination, and therefore, knives may need to be changed after 2, 3, or more than 6 loads, depending on chance. When a pocket of particularly contaminated material is engaged, performance will drop more rapidly than for the rest of the pile. The same regression analysis showed no significant differences between wet- and dry-sharpened knives.

Table 4. Results of the multiple regression analysis for the effect of knife wear on productivity.

Chipping Productivity gt PMH^{-1} = a + b sum gt + c Wet + d Wet sum gt R^2 adj. = 0.239, n = 136, RMS = 7.484				
	Coeff	**SE**	**T-Value**	***p*-Value**
a	68.572	2.477	27.685	<0.0001
b	−0.136	0.036	−3.731	0.0003
c	−2.011	3.096	−0.650	0.5171
d	0.012	0.044	0.270	0.7879

Notes: gt = green tons; PMH = productive machine hours, excluding all delays; sum gt = total mass (gt) chipped by a set of knives since they were sharpened (i.e., indicator of wear); Wet = indicator variable for the wet sharpening treatment: 0 = dry-sharpened knives; 1 = wet-sharpened knives; n = number of observations; RMS = root mean square; SE = standard error.

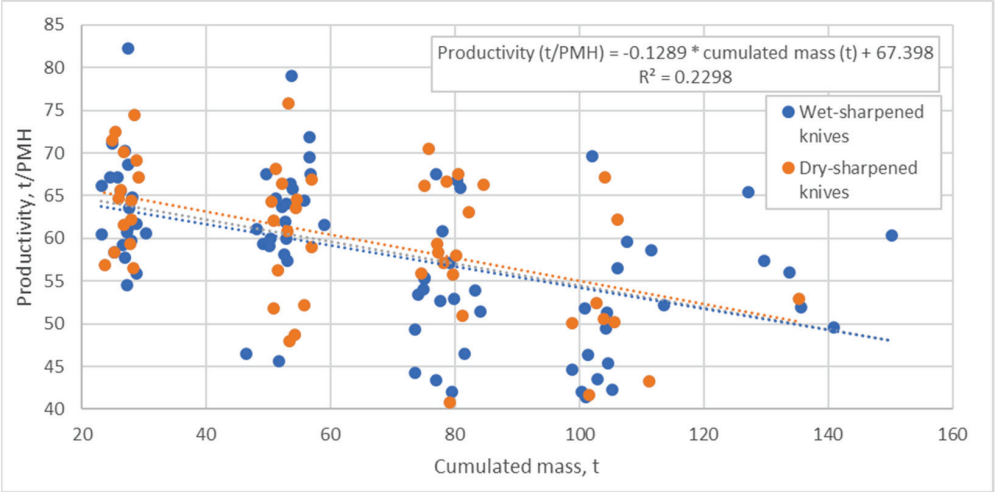

Figure 3. Chipping productivity as a function of the mass of chips processed by a set of knives, for wet- and dry-sharpened knives.

Furthermore, decompositional analysis of the time series indicated a substantial decline in productivity after the second cycle regardless of knife maintenance mode (dry sharpening of the older knives or replacement with new wet-sharpened knives). For the first cycle, median chipping productivity after dry sharpening was not significantly (p = 0.3087) higher than median productivity immediately after wet sharpening, with 65.6 t/h vs. 63.5 t/h.

The maximum number of loads chipped with a set of knives was six for wet-sharpened knives and five for dry-sharpened knives. Excluding the data of the last knife set (that was probably not fully used up), the average number of loads per knife set was 4, regardless of the sharpening treatment. The median mass of chips produced before a fresh set of knives needed new sharpening was 104.5 gt for wet-sharpened knives and 105.4 gt for dry-sharpened knives. The actual difference was therefore small and had no statistical significance (p = 0.71), possibly because the number of samples was too small to dampen the large variability caused by the erratic presence of contaminants in the chipped wood.

Finally, the study offered conclusive evidence that dry sharpening took much less time (−30%) than a full knife change (i.e., removing the worn-out knives and installing new ones). In this study, the average dry sharpening session took about 20 min (SD = 13 min), while the average full knife change took 29 min (SD = 29 min). The difference was not just large but also highly significant (p = 0.00163). Furthermore, one should not forget that knife change does not only carry the cost and the time of the change but also that of wet sharpening in the workshop. The price requested by the local workshop for sharpening a set of knives amounted to EUR 15. Therefore, the average knife change costs EUR 15 plus 29 min of chipper operator time. If the latter is costed at 50 EUR/h, then the total cost of wet sharpening is EUR 39. In contrast, dry sharpening only takes 20 min of operator time or EUR 17. Wet sharpening is then 2.3 times more expensive than dry sharpening. If one also spreads that cost over the larger amount of chips processed after dry sharpening (i.e., 105.4 gt vs. 104.5 gt), the impact of dry sharpening over the produced ton of chips is 0.16 EUR/gt, while that of wet sharpening is 0.37 EUR/gt, which is quite a dramatic difference.

4. Discussion

The present study offers valuable insights into the chipping process, and the information it has produced can be considered quite robust, thanks to the extended observation time (two entire weeks) and the large amount of work performed during that time (136 truckloads). On the other hand, the observational character of the study makes that

information lacking in some details, which suggests caution when drawing conclusions from it.

In general, the results of the study are plausible, and they are corroborated by the figures reported in the existing literature. The productivity levels reported herein are comparable with those obtained for the previous models of the same chipper [27] or for similar chipper models that have recently appeared on the market [28]. More in general, those figures are fully within the ranges reported by Bergström and Di Fulvio [29] for a larger array of industrial chippers. The same corroboration is obtained for delay time: the ~40% delay factor reported in this study matches the figures presented by Spinelli and Visser [30], Belbo and Vivestad [31], and Mihelič et al. [32] quite well—with the latter two studies specifically addressing the case of roadside landings with various degrees of accessibility.

The good representation of delay time is not surprising for a study that extended over two full weeks. This time span was likely long enough to catch most of the delay occurrences and to offer a balanced perspective, where the impact of erratic events was suitably dampened. Concerning delays, it is interesting to see how different categories tend to balance each other; if the truck changing time is shortened, then the truck waiting time increases, eventually denying the benefit of better landing accessibility. This seems to reflect the apparent general rule of delay compensation, already observed by Spinelli and Magagnotti [14] who described how a reduction in waiting time was offset by an increase in rest time. In fact, no general rule covers compensation for delays; if such compensation is often observed, that is because opportunities for improvement are missed with alarming frequency. Essentially, if the truck terminal time is reduced, then one should integrate an additional truck into the transportation task and profit from the longer time available to the chipper for filling up trucks. Otherwise, it is inevitable that the time saved through quicker maneuvering will be occupied by an increase in waiting time. It is just that simple. Most rationalization efforts covering just one step in a chain are doomed to fail, and that is indeed a general rule.

Eventually, what the study says with a strong voice is that the Diamant 2000 is a very productive machine but that its large potential is limited by organizational factors that expand delay time. The data show that quite clearly, and we believe there can be very few objections to that statement. The same could be said for its corollary, namely, if you have a very productive machine, you need to create the conditions for that machine to unleash its full potential. But therein, the issue becomes somewhat more complex. Several operators have found out that it is easier to use very productive machines to compensate for the difficulty of precision management. Besides being expedient, compensation through exuberant productivity is the only rational solution when management is fragmented between different contractors—typically one for chipping and the other for transportation. In that case, precision management of the entire chain becomes a real challenge, and deploying extra capacity is the only alternative.

Despite the large variability observed for the effect of knife wear, the study also offers plausible figures for performance reduction consequent to knife wear and the overall duration of the knives. It indicates that productivity decreased between 15% and 28% after chipping between 100 and 115 gt of wood, which would match the 15% decrease reported by Nati et al. 2010 [11] after processing between 115 and 280 gt of chips or the 32% decrease reported by Spinelli and Magagnotti [14] after processing 120 gt of chips. The figures are all quite close, even if those studies were conducted under different conditions and with different machines. However, all machines were industrial drum chippers in the >300 kW class, working at landings and fed with hardwood material.

What is missing from this study is an assessment of fuel consumption and chip particle size and of their variation with blade wear. This is a consequence of its observational character, which does not deny the fundamental validity of the study but advises against trying to infer too much from it. In particular, the absence of fuel use data makes it difficult to develop a minimum cost curve for the frequency of knife change. Such a curve would

represent only part of the reality because it would be based on productivity alone, and it would disregard the important contribution of varying fuel efficiency. Similarly, the absence of particle size data denies information about the criteria used by the operator for deciding when to sharpen the chipper knives. Anecdotal evidence indicates that most operators make the decision based on the excessive decay in chip quality [19], but the absence of any such figures from this study makes it difficult to determine how consistent the operator was with his knife-sharpening decisions. In fact, the inherently subjective knife sharpening criteria adopted by all operators make it inevitable that observational blade wear studies are confounded by very large variability. Nevertheless, most have returned comparable results, which bear a clear witness to the important role of operator competence and experience.

Finally, some interesting inferences can be drawn from the knife sharpening vs. knife change time study. The knife change time reported in this study is aligned with that indicated by other chipper delay studies [30] but almost twice as long as reported by Spinelli and Magagnotti [14]. The latter study indicated a mean knife change time between 13 and 16 min, depending on whether a power wrench was available or not. In the worst case, the knife change time required a maximum of 26 min. The shorter time reported in that study may depend on better work conditions (a workshop) and/or better operator worker and competence. However, another highly suggestive explanation is that the chipper in that study used two full-length knives, whereas that in the present study was equipped with six knives. It stands to reason that it would take less time to replace two knives instead of six, however longer and heavier the two full-length knives are. Therefore, one possible inference from that result is that dry sharpening may represent a faster knife-restoring option compared to changing, especially with those chippers that are equipped with many staggered knives and less so with those chippers that are equipped with fewer conventional full-length knives.

5. Conclusions

The study presented in this paper produces a wealth of interesting new information about chipping performance: it offers robust productivity figures, together with a reliable estimate of the productivity losses caused by knife wear; it generates useful suggestions for delay time control; and it raises a number of interesting questions and yields many good insights about chipper knife management. The productivity of the new Albach Diamant 2000 wood chipper ranged from 26.9 $\pm$ 4.5 min/cycle (site B) to 27.4 $\pm$ 4.0 min/cycle (site A) chipping time. The used model of the effect of knife wear on chipper productivity showed a significant impact of total chipped mass per set of knives on chipper productivity. Regarding the fact that wet-sharpened knives lasted a maximum of six loads and dry-sharpened knives lasted a maximum of five loads, it may be concluded that the edge of wet-sharpened knives can last longer. Considering the costs of knife management (dry sharpening and wet sharpening), dry sharpening required less time and equipment which resulted in 2.3 times lower expenses than wet sharpening, which can have a significant influence on the economy of the operation. On one side, frequent downtime of the chipper can be utilized for knife sharpening, thus increasing the efficiency of the operation, and on the other side, savings could occur due to less time spent in the workshop wet sharpening the knives. Future research should include the quality determination of produced wood chips, e.g., particle size distribution, which can provide more information to make more concise conclusions and find the best chipper settings in order to improve productivity without negatively influencing wood chips parameters. All things considered, the study is a witness to the fact that a properly planned and conducted observational study still offers considerable benefits, even when it lacks the advantages and the power of a controlled experiment.

Author Contributions: Conceptualization, M.M. and D.V.; methodology, D.V.; validation, R.S., M.M. and D.V.; formal analysis, R.S., D.V., M.M. and B.U.; investigation, A.Z.; writing—original draft preparation, D.V. and M.M.; writing—review and editing, R.S., D.V., M.M. and B.U.; visualization, D.V., B.U. and M.M.; supervision, R.S. All authors have read and agreed to the published version of the manuscript.

Funding: This research received no external funding.

Data Availability Statement: The original data set is not publicly available, but it can be requested from the authors.

Conflicts of Interest: The authors declare no conflicts of interest.

References

1. Brief on Biomass for Energy in the European Union. Available online: https://op.europa.eu/en/publication-detail/-/publication/7931acc2-1ec5-11e9-8d04-01aa75ed71a1/language-en (accessed on 18 April 2024).
2. Krausmann, F.; Erb, K.H.; Gingrich, S.; Lauk, C.; Haberl, H. Global patterns of socioeconomic biomass flows in the year 2000: A comprehensive assessment of supply, consumption and constraints. *Ecol. Econ.* **2008**, *65*, 471–487. [CrossRef]
3. Palander, T.; Voutilainen, J. Modelling fuel terminals for supplying a combined heat and power (CHP) plant with forest biomass in Finland. *Biosyst. Eng.* **2013**, *114*, 135–145. [CrossRef]
4. Talbot, B.; Suadicani, K. Analysis of two simulated in-field chipping and extraction systems in spruce thinnings. *Biosyst. Eng.* **2005**, *91*, 283–292. [CrossRef]
5. Volk, T.A.; Eisenbies, M.H.; Hallen, K. The development of harvesting systems in woody biomass supply chains: A case study of short rotation woody crops. In *Sustainable Biorefining of Woody Biomass to Biofuels and Biochemicals*; Kumar, D., Kumar, S., Rajendran, K., Ray, R.C., Eds.; Woodhead Publishing: Cambridge, UK, 2024; pp. 43–63.
6. Piqueiro, H.; Gomes, R.; Santos, R.; de Sousa, J.P. Managing Disruptions in a Biomass Supply Chain: A Decision Support System Based on Simulation/Optimisation. *Sustainability* **2023**, *15*, 7650. [CrossRef]
7. Stolarski, J.; Wierzbicki, S.; Nitkiewicz, S.; Stolarski, M.J. Wood Chip Production Efficiency Depending on Chipper Type. *Energies* **2023**, *16*, 4894. [CrossRef]
8. Nogueira, D.F.B.; Fiedler, N.C.; Vidaurre, G.B.; Lopes, E.D.; Pelissari, C.K.R.; Ramalho, A.H.C.; Robert, R.C.G.; Maffioletti, F.D. Quality of eucalyptus wood chips for bioenergy as a function of drying time and horizontal chipper settings. *Heliyon* **2024**, *10*, e25991. [CrossRef] [PubMed]
9. Fiorineschi, L.; Cascini, G.; Rotini, F.; Tonarelli, A. Versatile grinder technology for the production of wood biofuels. *Fuel Process. Technol.* **2020**, *197*, 106217. [CrossRef]
10. Spinelli, R.; Marchi, E. Trends and Perspectives in the Design of Mobile Wood Chippers. *Croat. J. For. Eng.* **2021**, *42*, 25–38. [CrossRef]
11. Nati, C.; Spinelli, R.; Fabbri, P.G. Wood chips size distribution in relation to blade wear and screen use. *Biomass Bioenergy* **2010**, *34*, 583–587. [CrossRef]
12. Kuptz, D.; Hartmann, H. Influence of tree species and machine settings on chip quality and specific energy consumption of a stationary drum chipper. *Biomass Bioenergy* **2021**, *155*, 106305. [CrossRef]
13. Krilek, J.; Čabalová, I.; Výbohová, E.; Mamoňová, M.; Ťavodová, M.; Melicherčík, J.; Gendek, A.; Aniszewska, M.; Todaro, L.; Giudice, V.L. Assessment of the chipping process of beech (*Fagus sylvatica* L.) wood: Knives wear, chemical and microscopic analysis of wood. *Wood Mater. Sci. Eng.* **2024**, *19*, 473–484. [CrossRef]
14. Spinelli, R.; Magagnotti, N. The effect of raw material, cut length, and chip discharge on the performance of an industrial chipper. *For. Prod. J.* **2012**, *62*, 584–589. [CrossRef]
15. Kuptz, D.; Hartmann, H. The effect of raw material and machine setting on chipping performance and fuel quality—A German case study. *Int. J. For. Eng.* **2015**, *26*, 60–70. [CrossRef]
16. Kuptz, D.; Hartmann, H. Evaluation of Fuel Quality, Throughput Rate and Energy Consumption During Non-Industrial Wood Chip Production with Three PTO Driven Chippers. *Croat. J. For. Eng.* **2022**, *43*, 109–122. [CrossRef]
17. Moiseev, A. Wear resistance of wood cutting tools. *Lesn. Promyshlennost* **1981**, 110.
18. Obreshkov, P. *Wood Processing Machines*; Wood Research Institute: Sofia, Bulgaria, 1996; p. 192.
19. Spinelli, R.; Hartsough, B. A survey of Italian chipping operations. *Biomass Bioenergy* **2001**, *21*, 433–444. [CrossRef]
20. Spinelli, R.; Magagnotti, N. Using disposable chipper knives to decrease wood fuel processing cost. *Fuel Process. Technol.* **2014**, *126*, 415–419. [CrossRef]
21. Mederski, P.S.; Borz, S.A.; Đuka, A.; Lazdinš, A. Challenges in Forestry and Forest Engineering–Case Studies from Four Countries in East Europe. *Croat. J. For. Eng.* **2021**, *42*, 117–134. [CrossRef]
22. Bumber, Z.; Đuka, A.; Popović, M.; Poršinsky, T. Soil Characteristics in Oak Lowland Stand—A Case Study of a 6 Wheeled Forwarder's Impact on Forest Soil. *Croat. J. For. Eng.* **2024**, *45*, 85–95. [CrossRef]

23. Vucelja, M.; Borz, S.A.; Bjedov, L.; Tomljanović, K.; Kranjec Orlović, J.; Boljfetić, M.; Matijević, M.; Margaletić, J. Forest Residue Management Impact on Rodent (Rodentia: Murinae, Arvicolinae) Damage in Pedunculate Oak (*Quercus robur* L.) Forests in Croatia. *Croat. J. For. Eng.* **2023**, *44*, 121–135. [CrossRef]
24. Moskalik, T.; Gendek, A. Production of Chips from Logging Residues and Their Quality for Energy: A Review of European Literature. *Forests* **2019**, *10*, 262. [CrossRef]
25. Belbo, H.; Talbot, B. Systems Analysis of Ten Supply Chains for Whole Tree Chips. *Forests* **2014**, *5*, 2084–2105. [CrossRef]
26. Björheden, R.; Thompson, M.; Rickards, J. *Forest Work Study Nomenclature, WP 3.04.02. Test Edition Valid 1995–2000*; International Union of Forestry Research Organisations (IUFRO), Department of Operational Efficiency, Swedish University of Agricultural Sciences: Garpenberg, Sweden, 1995; 16p.
27. Mihelič, M.; Spinelli, R.; Magagnotti, N.; Poje, A. Performance of a new industrial chipper for rural contractors. *Biomass Bioenergy* **2015**, *83*, 152–158. [CrossRef]
28. Magagnotti, N.; Spinelli, R.; De Francesco, F.; Lombardini, C. A Versatile Terrain and Roadside Chipper for Energy Wood Production in Plantation Forestry. *Balt. For.* **2016**, *22*, 107–115.
29. Bergström, D.; Di Fulvio, F. Review of efficiencies in comminuting forest fuels. *Int. J. For. Eng.* **2019**, *30*, 45–55. [CrossRef]
30. Spinelli, R.; Visser, R. Analyzing and estimating delays in wood chipping operations. *Biomass Bioenergy* **2009**, *33*, 429–433. [CrossRef]
31. Belbo, H.; Vivestad, H. Predicting delay factors when chipping wood at forest roadside landings. *Int. J. For. Eng.* **2018**, *29*, 128–137. [CrossRef]
32. Mihelič, M.; Spinelli, R.; Poje, A. Production of wood chips from logging residue under space-constrained conditions. *Croat. J. For. Eng.* **2018**, *39*, 223–232.

Disclaimer/Publisher's Note: The statements, opinions and data contained in all publications are solely those of the individual author(s) and contributor(s) and not of MDPI and/or the editor(s). MDPI and/or the editor(s) disclaim responsibility for any injury to people or property resulting from any ideas, methods, instructions or products referred to in the content.

forests

MDPI

Article

Methods of Rut Depth Measurements on Forwarder Trails in Lowland Forest

Mihael Lovrinčević [1], Ivica Papa [1,*], Maja Popović [1], David Janeš [2], Tomislav Poršinsky [1], Tibor Pentek [1] and Andreja Đuka [1]

[1] University of Zagreb, Faculty of Forestry and Wood Technology, Svetošimunska cesta 23, 10000 Zagreb, Croatia; mlovrin@sumfak.unizg.hr (M.L.); mpopovic@sumfak.unizg.hr (M.P.); tporsinsky@sumfak.unizg.hr (T.P.); tpentek@sumfak.unizg.hr (T.P.); aduka@sumfak.unizg.hr (A.Đ.)
[2] Croatian Forests Ltd., Forest Administration Office Delnice, Supilova 32, 51300 Delnice, Croatia; david.janes@hrsume.hr
* Correspondence: ipapa@sumfak.unizg.hr

Abstract: Rutting measurements are a significant part of scientific research on the impact of forest vehicles on the forest soils and damage to the forest transport infrastructure. Although photogrammetric methods of measurement or measurements based on LiDAR (light detection and ranging) data are increasingly being used for rutting measurements, the previous research conducted using these methods indicated the challenge of recording water-filled ruts. For this reason, it is necessary to define a reliable method of rutting field measurement in lowland forest stands characterized by a high level of groundwater that fills the ruts shortly after the passage of forest vehicles. This research analyzed the measurement accuracy using a total station and a GNSS RTK device with a CROPOS correction base in relation to the measuring rod that represented the reference method. Based on recorded and processed data, ruts are displayed in two ways: as net and as gross value of rut depth. The analysis of net rutting revealed a statistically significant difference between the calculated rut depths based on measurements with a GNSS RTK device and other methods. On average, the net rutting measured by the GNSS RTK device was 2.86 cm smaller than that of the reference method. When calculating the gross rutting, which consisted of the net rut depth and the bulge height, no statistically significant difference was found between the measurement methods used. Based on this result, the bulge height was also analyzed, and showed a statistically significant difference between the data recorded by the GNSS RTK device and other methods. It can be concluded that measuring the depth of ruts with a total station gives accurate data and represents the optimal modern field measurement method for the same or similar terrain conditions. In contrast, the GNSS RTK device, which constantly gives higher elevation points, can be used to measure gross rutting.

Keywords: GNSS RTK; total station; measure rod; soil damage; flooded forests; rutting

1. Introduction

In today's modern, technologically based, eco-efficient, and sustainable forestry, transport infrastructure is one of the key elements of maintaining and improving forest management [1,2]. Forest transport infrastructure, therefore, serves as the basis for the functioning of the entire forest management system. Timber transport is the core of transport in forestry, and there is a constant need to build an optimal forest transport infrastructure network. Timber transport is divided into primary and secondary transport [3]. Primary transport is conducted on a secondary forest traffic infrastructure network from the forest stand to a landing site. Secondary (long-distance) transport continues using forest roads, public roads, railways, or navigable waterways to the end user. Secondary forest traffic infrastructure in the Republic of Croatia is divided into skid roads, skid or forwarder trails, and cable lines. Different timber harvesting systems use skid roads or skid trails (forwarder trails) depending on the terrain where the timber extraction is performed. Skid roads are

constructed on sloped terrains with pronounced surface obstacles and heavier construction categories of materials, while skid trails (forwarder trails) are peculiar for flatter terrains without pronounced surface obstacles and lighter construction categories of materials [4]. Forwarder trails represent temporary forest transport infrastructure created by driving a route through the forest and the successive passage of a forest vehicle along that route; they are characteristic of lowland forests and the chainsaw/harvester and forwarder timber harvesting system.

It is a known fact that the continuous passage of vehicles on the forest floor causes damage to the soil [5,6] and, depending on the soil type, on the root system [7]. Soil compaction, or the formation of ruts due to soil compaction, represents forest vehicles' most significant and obvious impact on the soil. The soil on which the appearance of ruts has been recorded is characterized by reduced water and air capacity due to the loss of micro and macro pores, mixing of soil layers, loss of organic layer, and increased amount of CO_2 [6,8,9]. Regeneration of such damaged soil can last for several decades [10–12]. Because of the above, almost every scientific study of the impact of forest vehicles on the forest soil and environmentally acceptable technologies contains rutting measurements. Unfortunately, the methodology of measuring on the ground (terrestrial measurements) using simple measuring instruments, such as a meter, is often insufficiently explained [13–15].

Based on the review of the available literature, it can be concluded that the manual measurement of ruts, using a measuring stick or similar, is still the most often used method [16,17]. As an alternative to the measuring rod, Toivio et al. [18] use a self-leveling construction laser device, a leveling rod, and a laser beam detector to monitor the change in the depth of the rut, and the authors have no objections to the system used. One possible alternative is using GNSS (Global Navigation Satellite System) RTK (real-time kinematic) devices to measure the rut depths. GNSS RTK devices or systems enable the measurement with centimeter accuracy [19,20]. However, the precision of GNSS devices in forest conditions and the applicability of such systems depend on several factors: (1) the canopy structure and its density; (2) the type of trees; (3) the terrain of the area; and (4) the season of field measurements [21–24]. While investigating adequate soil protection from compaction resulting from timber extraction operations, Ring et al. [15] also measured the depth of ruts using a GNSS RTK device (Topcon GRS-1) and a switch meter. Rutting measurements were not the primary goal of the research, and the methodology itself was not described in detail. The estimated error of the GNSS RTK device was 4 cm, and, based on this, the authors concluded that the GNSS RTK method of field measurement of rut depth represents a valuable substitute for the classic measurement method. At the same time, the authors reported that certain illogicalities were recorded during the measurement of the rut depth with the GNSS RTK device, which was manifested by a decrease in the value of the rut depth between two passes of the machine. The authors also highlighted the unresolved issue of determining the ground's reference zero/initial state when calculating the rut depth.

With the advancement of technology, it is possible to measure the depth of ruts using photogrammetry or LiDAR (light detection and ranging) systems [25–27]. The measurement of the rut depths based on photogrammetric methods, especially based on aerial photographs taken by an unmanned aerial vehicle, enables an accurate representation of the terrain and the calculation of rutting that do not differ statistically significantly compared to the reference methods used [28,29]. Photogrammetric processing and depth analysis of ruts are related not only to unmanned aerial vehicles but also to using a camera on a pole. Pierzchała et al. [30] compared different software tools for photo processing. The authors emphasized that the photogrammetric method of measuring the depth of ruts is as accurate as manual measurement. Salmivaara et al. [31] investigated the applicability of the 2D LiDAR system when measuring ruts and determined that the average error of this system is 3.5 cm. Water in the ruts makes it difficult to use photogrammetric methods and LiDAR technology and is a prominent problem in the studies mentioned and others [32–34]. Depending on the water depth, the error can be up to 15 cm [28]. One of the characteristics of lowland forests is the high water level, occasionally flooded land, along

with stagnant water that usually remains throughout the winter and spring periods [35]. For this reason, it is necessary to use other methods that guarantee accurate measurement of rutting, especially in lowland forests with high water levels.

Depending on the authors, the constituent parts of the ruts and their calculations are performed in several ways. Haas et al. [36] divided rutting or deepening into net-deepening and gross-deepening. Gross-deepening is made up of bulge height and net-deepening. Meek [37] and Poršinsky [8] measured the rut depth as the difference between the original ground surface and the ground surface after the vehicle has passed, not including the bulge height in the calculation.

This research describes the method of measuring and calculating ruts in detail. The hypothesis is that the depth of ruts on forwarder trails in lowland forests can be accurately measured using a GNSS RTK device with a CROPOS (CROatian POsitioning System) correction base and a total station.

2. Materials and Methods

2.1. Research Area

The research was conducted in January 2022 in a 58-year-old ash forest stand (*Leucojo aestivi-Fraxinetum angustifoliae* Glavač 1959) (45°36′10.812″ (N), 16°14′48.150″ (E)) (Figure 1). The forest stand of the researched area is managed by Croatian Forests Ltd., the Forest Administration Zagreb, Forest Office (FO) Velika Gorica, Management Unit (MU) Turopoljski lug, subcompartment 137a. According to the forest management plan, the stand's structure is characterized as dense, and the soil as amphigley. The altitude of the research area is 98 m a.s.l. The researched forest stand represents the Republic of Croatia's characteristic lowland flood forest. Narrow-leaved ash (*Fraxinus angustifolia* Vahl) habitats in the Republic of Croatia are strongly influenced by geomorphological and hydrological processes, which affect the formation and development of soil. Hydrological processes manifest in occasional flooding of habitats, water stagnation in winter and spring, and a high groundwater level during the growing season [35]. All the mentioned processes result in a microrelief with characteristic ridges and depressions.

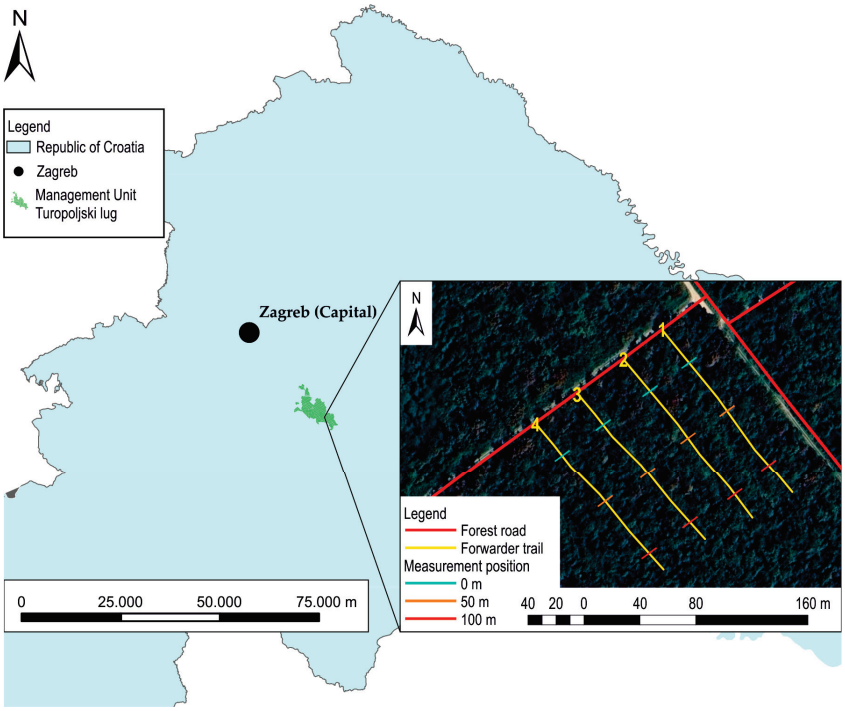

Figure 1. Research area in MU Turopoljski lug, subcompartment 137a, FO Velika Gorica.

The daily temperature during the research ranged from −11 °C to +8 °C, while the soil temperature at a depth of 10 cm was from 0 °C to +2 °C and only the humus layer was frozen. The current moisture of the surface soil layer ranged from 55% to 70%. A digital penetrometer Eijkelkamp Penetrologger (Giesbeek, The Netherlands) was used to measure penetration with a cone surface range of 2 cm^2 and the angle of cone at 30°. The soil cone index (*CI*) at a soil depth of 15 cm (CI_{15}) was 515 ± 160 kPa, with a range of 200 to 900 kPa, while at a depth of 5 to 25 cm ($CI_{5–25}$) it was 516 ± 179 kPa, with a range from 100 to 1100 kPa. The shear strength of the soil was measured with the Eijkelkamp—Field Inspection Vane Tester with 20 × 40 mm wing dimension, a measuring range of 0 to 130 kP, and a reading accuracy of 2 kPa. On the surface the shear strength was 9 ± 6 kPa, and 19 ± 8 kPa at a soil depth of 15 cm. The measurements of the soil's bearing capacity confirmed that it is an amphigley soil—soft soil with limited bearing capacity.

2.2. Rut Formation

The rut formation occurred as a result of the consecutive passage of a Komatsu 875 eight-wheeled forwarder along the same track. As mentioned, the research was carried out in January, as medium–heavy and heavy forwarders, like Komatsu 875, in the Republic of Croatia are mostly used for forwarding timber in the winter time [38].

The net weight of the forwarder is 21,385 kg and it has a declared load capacity of 16,000 kg. The width of the forwarder used in the research was 2.98 m. Based on the width of the forwarder and the average width of the forwarder trail in the Republic of Croatia (3.5–4 m) [39], the width of the measuring position was defined, which is explained in detail in Section 2.3. *Route measurement*. During the passage on forwarder trails (FTs), the forwarder exported 34 logs of narrow-leaved ash with a total volume of 14,079 m^3 (gross), or 11,628 kg. The wheels of the front and rear axles were equipped with tires of the same dimensions, 710/45-26.5 20 PR (Ply Rating) (Nokian Forest King TRS 2), which, depending on the forwarder trail on which they were moving, were fitted with additional traction aid: (FT1) tracks on the front and rear axle; (FT2) tracks on the rear axle and chains on the front axle; (FT3) without mounted tracks or chains; and (FT4) tracks on the rear axle. Depending on the equipment used, the total weight of the forwarder with the load was between 33,013 kg and 36,503 kg (Figure 2). The measurement of the mass characteristics of the forwarder was performed under the ISO 13860 (2016) standard [40].

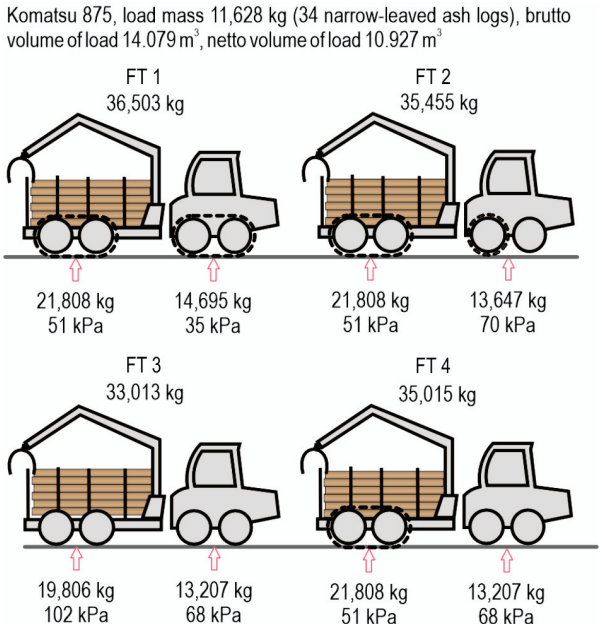

Figure 2. Mass characteristics of Komatsu 875 forwarder with different traction aid.

On FT1, FT2, and FT4, the forwarder made 10 passes as planned, while on FT3, due to 100% slipping, the forwarder could not make more than 6 passes. The total length of each of the forwarder trails was longer than 115 m.

2.3. Rut Measurement

Permanent measuring positions (MPs) where the rut depth was measured were located at the beginning (0 m) (MP 1), at the fiftieth meter (MP 2), and at the hundredth meter of the FT (MP 3). Before the initial (0 m) and final MPs, a certain length of the FT was left for the forwarder to reach operational speed and prevent soil damage due to movement from the MPs. The layout of the measurement site used in this research was based on the measurement method used by Meek [37] and Poršinsky [8]. The measuring positions were placed perpendicular to the direction of the forwarder movement, had a total width of 4.5 m, and consisted of two vertical posts on which there was a horizontal bar with marked measurement points. In contrast to the characteristic measurement points used by Meek [37], fixed measurement points were used during this research. The distance between the fixed measurement points was 20 cm (a total of 21 measurement points per MP) (Figure 3). The ruts were measured using three devices: measuring (geodetic) rod; total station STONEX TS R35WINCE (StoneX Group, New York, NY, USA); and RTK GNSS STONEX S900A terrestrial receiver with correction base CROPOS, whose characteristics are shown in Table 1. This research used the measuring rod as a reference measurement method. On each trail, two points necessary for georeferencing the total station were recorded; one point represented the position of the total station, while the other point represented back sight reading. The coordinates of the points were measured by the arithmetic mean of three 10 s independent measurements using the GNSS RTK method [41]. The recording on each measuring position started with the recording of the point with the total station, then the GNSS RTK device was placed on the same position, and then the measuring rod (leveling, geodetic rod) was also placed in the same position. To enable the recording of the same positions in the field, the recording was performed by 5 people (the total station operator, the person who carried the prism, the operator of the GNSS RTK device, the person who took the readings with the leveling bar, and the person who entered the results from the leveling bar in the prepared form). Later data processing was performed only for the measuring rod method in the manner described in Figure 3.

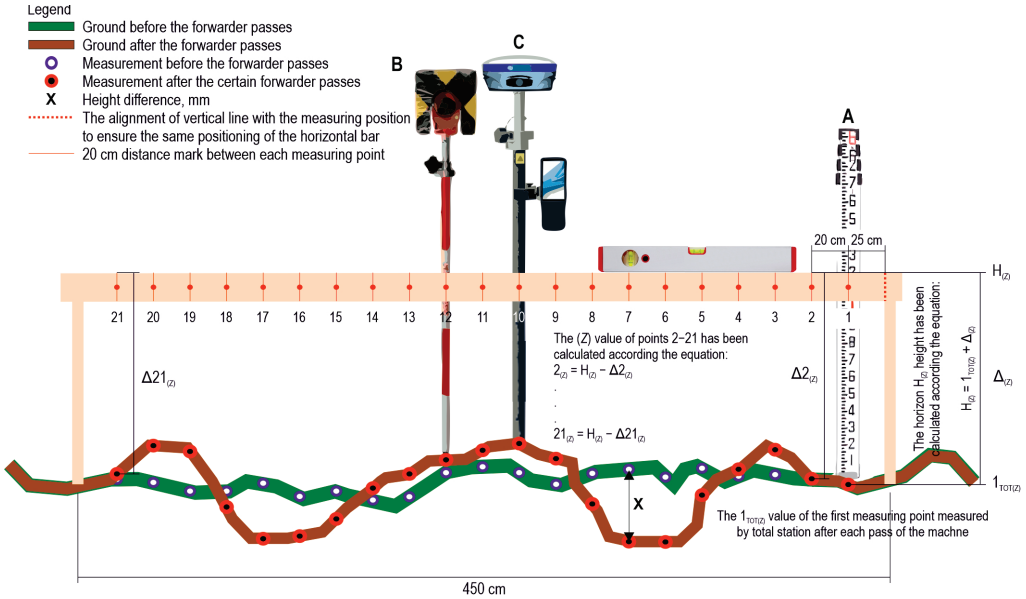

Figure 3. Graphic representation of measurement position and measuring equipment used: (**A**) measuring rod; (**B**) prism (part of the total station STONEX TS R35WINCE); (**C**) GNSS RTK.

Table 1. Technical specification of equipment used.

Total Station Stonex R35		**RTK GNSS Receiver Stonex S900A**	
ANGLE MEASUREMENT (angle units)	DEG 360° /GON 400/MIL 6.400	**RECEIVER (satellite tracked)**	GPS: L1 C/A, L1C, L1P, L2C, L2P, L5
			GLONASS: L1 C/A, L1P, L2C, L2P
			BEIDOU: B1, B2, B3
			GALILEO: E1, E5a, E5b
			QZSS: L1 C/A, L1C, L2C, L5
			SBAS: L1, L5
DISTANCE MEASUREMENT RANGE	Standard mode prism 3.000 m	**INTERNAL RADIO (range)**	3–4 Km in urban environment Up to 10 Km with optimal conditions
	Long mode prism 5.000 m		
DISTANCE MEASUREMENT ACCURACY	Standard mode prism 2 mm + 2 ppm	**POSITIONING (real time kinematic)**	Fixed RTK Horizontal (8 mm + 1 ppm RMS)
	Long mode prism 2 mm + 2.5 ppm		Fixed RTK Vertical (15 mm + 1 ppm RMS)
LASER PLUMMET (laser type)	635 nm semiconductor laser	**COMMUNICATION (Bluetooth)**	2.1 + EDR, V4.0
POWER SUPPLY (battery)	7.4 V/3.400 mAh Li-ion	**POWER SUPPLY (battery)**	2 rechargeable and replaceable 7.2 V—3400 mAh Intelligent lithium batteries
POWER SUPPLY (working time (angle + distance meas.))	Up to 5 h	**POWER SUPPLY (working time)**	Up to 12 h (2 batteries hot swap)
PHYSICAL SPECIFICATION (dimensions)	206 × 203 × 360 mm	**PHYSICAL SPECIFICATION (dimensions)**	Φ 157 mm × 76 mm
PHYSICAL SPECIFICATION (weight including battery and tribrach)	6.1 kg	**PHYSICAL SPECIFICATION (weight)**	1.19 kg (with one battery) 1.30 kg (with two batteries)

The field measurement was performed before the passage of the forwarder (undamaged ground), and after the 1st, 5th, and 10th passes for FT1, FT2, and FT4, and after the 1st and 5th passes for FT3 due to vehicle slippage.

In order to reduce potential human errors to a minimum, during the conducted research, the total station was positioned in a fixed place around the middle of each researched FT, the height of the prism was not changed, and care was taken to keep the prism upright, which was achieved by using a central spirit level installed on the prism.

The used correction base of the GNSS RTK device CROPOS represents a system of 57 permanent reference GNSS stations located at 70 km from each other. Reference stations collect satellite measurement data and calculate correction parameters available to field users via mobile Internet (GPRS (General Packet Radio Service)/GSM (Global Systems for Mobile)) [42].

2.4. Data Analysis

A database was formed in Microsoft Excel 2021 (Microsoft Corporation, Redmond, WA, USA) by transferring data collected by a total station and GNSS RTK device and by entering data collected by a measuring rod (Figure 4). For the purposes of this research, net rutting (N) and gross rutting (G) were analyzed. Net rutting represents the difference between the soil terrain's elevation before the vehicle passage and the compacted soil terrain's elevation (after vehicle pass) while gross rutting represents the sum of the bulge height (B) and value of net rutting. Bulge height describes the difference between the elevation of the soil ejected from each side of the rut and the elevation of the terrain before the vehicle passes. To calculate the gross rutting, bulge height value was calculated as the average height of the ejected soil on both sides of the rut.

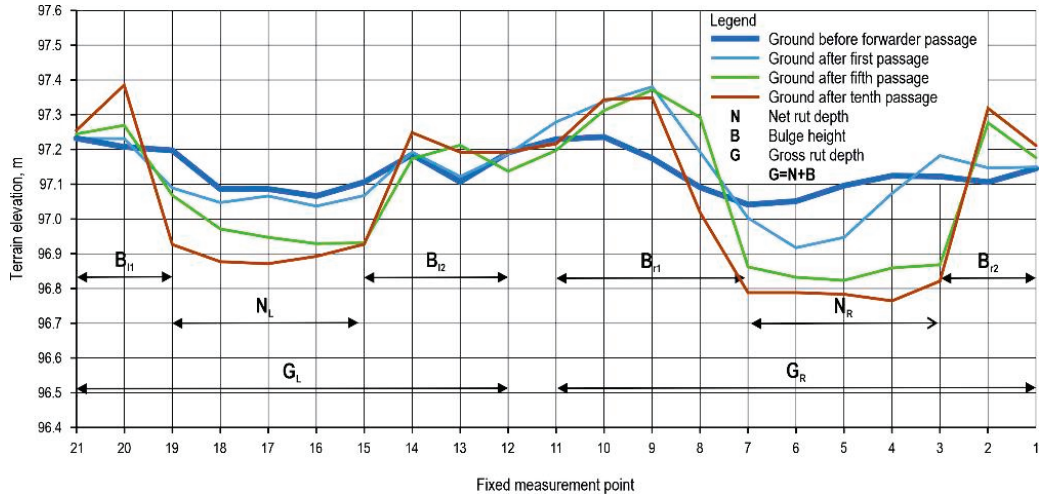

Figure 4. Example of a rut graphic display. Marked on the graphic display are the measurements used for calculating net rutting (**N**), bulge height (**B**), and gross rutting (**G**).

After calculating ruts according to each method, further statistical data processing was carried out in the program Statistica v. 14.0.0.15. (TIBCO software Inc. Palo Alto, CA, USA): data normality testing (Kolmogorov–Smirnov and Lilliefors tests); descriptive statistical analysis; *t*-test for determining differences between data and calculating the statistical significance of differences in mean values. One-way analysis of variance (ANOVA) followed by the Tukey post hoc test was used to determine differences between all 3 used measuring methods and the relationship between calculated rut depths and other independent variables, while factorial ANOVA was used to determine the relation between measuring methods and forwarder trails for rut depth (net rutting) and rut depth increase between passages.

3. Results

A total of 945 field measurements were recorded for each method, a total of 2835. Regardless of the calculation method, the data were normally distributed. Due to the specific microrelief on which the rut measurements were carried out, the rut values, measured with a measuring rod as a reference method, ranged between 0 and 59.13 cm.

3.1. Net Rutting

A total of 288 measurements per method were used to calculate the net rutting. The total station measured the deepest average net rut depth (12.12 cm), while the measurement using the GNSS RTK device gave the lowest average depth (8.77 cm). The average value of the ruts measured by the reference method (measuring rod) was 11.63 cm. The largest calculated rut depth was 49.8 cm and was measured using a GNSS RTK device. It was observed that the depth of the ruts between different vehicle passages (for example,

between the 5th and 10th passages) decreased, and in some readings, the depth showed a positive sign, which would mean that there was an uplift of the ground after the passage compared to the zero state. This phenomenon occurred in the same places and passages regardless of the measurement method, and an error during measurement can be ruled out as the reason for this phenomenon.

ANOVA followed by post hoc Tukey HSD (honestly significant difference) test indicated statistically significant differences for net rutting between measuring methods. No statistically significant difference was found between the reference method and the total station, while they were found when comparing GNSS RTK measurements with the ones from the other methods (Figure 5).

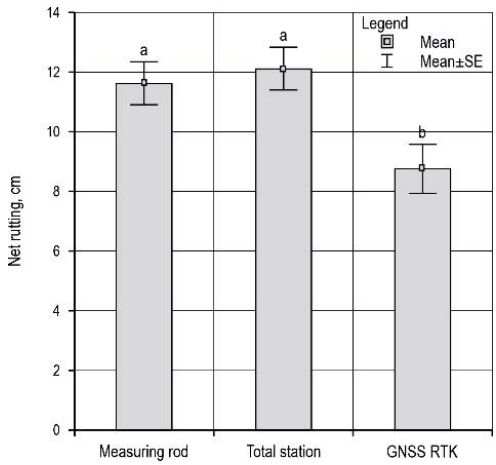

Figure 5. Difference in net rutting by measuring methods. Data are presented as mean ± SE (standard error). Letters denote statistical difference between measuring methods (Tukey HSD), respectively, at $p < 0.05$.

Although the factorial ANOVA showed no statistical significance between interaction of measuring method and FT for rut depth, the biggest deviation of the GNSS RTK device can be clearly seen on the FT1 (Figure 6). The FT1 (tracks on front and rear tires) had the smallest rut depth with an average depth of 5.90 cm measured by the reference method. The average rut depth measured by the GNSS RTK device was 1.30 cm on FT1. The GNSS RTK device underestimated the rut depth values on all forwarder trails except FT2 (tracks on the rear axle and chains on the front axle).

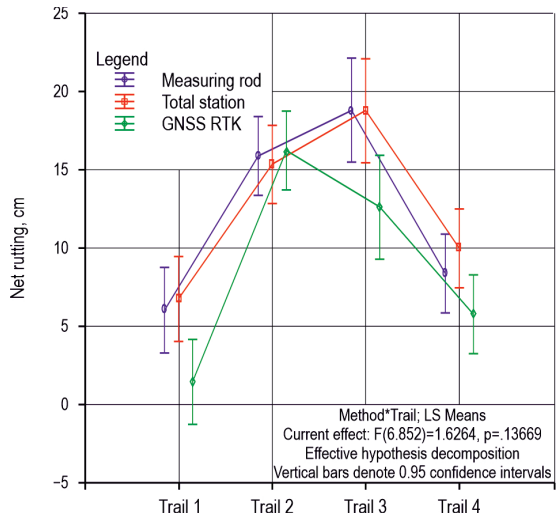

Figure 6. Difference in net rutting depth by measuring methods (method), forwarder trails, and combination of both (method * trail).

3.2. Gross Rutting

The calculated gross rutting gave statistically insignificant differences between the methods used in relation to the calculated net rutting. The average gross rutting measured by the GNSS RTK device was 21.82 cm and, as with the net ruts, it was smaller compared to the total depth of the ruts measured by the measuring bar and the total station, 22.33 cm and 22.21 cm, respectively (Table 2). The GNSS RTK device underestimated the rut depth values on all forwarder trails except for FT2, where the highest depth values were calculated compared to other methods. Positive values of the gross rutting (the height after the passage is higher than the height of the ground before the first passage) were observed again, but they were smaller compared to the net ruts. The reason for the lower values is the method of calculation where the height of the ejected soil is added to the net depth of the rut.

Table 2. Gross and net rutting by methods.

Rutting Values	Measuring Rod	Total Station	GNSS RTK
Max. net rutting	38.76 cm	42.82 cm	37.19 cm
St. Dev. net rutting	12.24 cm	12.21 cm	13.97 cm
Mean net rutting	11.63 cm	12.12 cm	8.77 cm
Max. gross rutting	57.79 cm	59.13 cm	55.23 cm
St. Dev. gross rutting	13.80 cm	14.07 cm	14.39 cm
Mean gross rutting	22.33 cm	22.21 cm	21.82 cm

ANOVA followed by post hoc Tukey HSD test did not show statistically significant differences for gross rutting between measuring methods.

3.3. Bulge Height

The absence of a statistically significant difference between the gross rutting measured by the GNSS RTK device and other methods, while it was determined in the case of net rutting, indicates that the bulge height influenced the reduction in the difference between the methods used. For this reason, the measured bulge heights were further analyzed. As expected, the heights measured by the GNSS RTK device were the highest, on average higher by 2.89 cm, compared to the reference method. The heights measured by the total station were the smallest on average. The average height of the ejected soil was 10.43 cm. ANOVA followed by a post hoc Tukey HSD test showed a statistically significant difference in the measured heights of the ejected soil between GNSS RTK devices and other measurement methods (Figure 7).

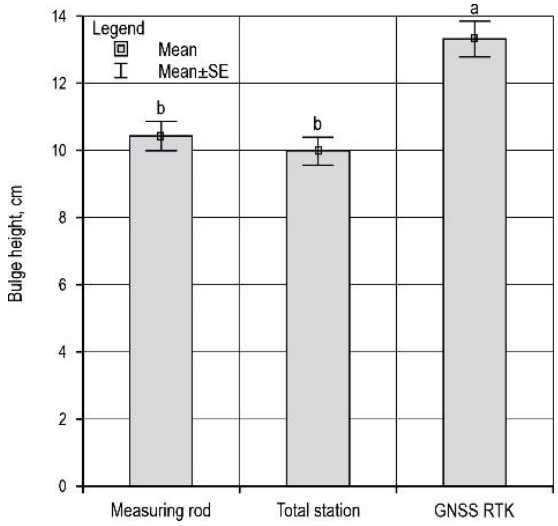

Figure 7. Difference in bulge height by measuring methods. Data are presented as mean ± SE. Letters denote statistical differences between measuring methods (Tukey HSD), respectively, at $p < 0.05$.

The most significant differences in the bulge height between the GNSS RTK device and other measurement methods were recorded on the FT1 and FT3, i.e., forwarder trails, where the GNSS RTK device most underestimated the rut depths when calculating the net rutting. The smallest differences between measurements were recorded on FT2.

3.4. Rut Depth Increase

Finally, the influence of the number of vehicle passes on net and gross rutting was analyzed based on the calculated values. The obtained results point to the fact that, regardless of the measurement method, the greatest increase in the value of the net rut depth occurred between the first and fifth passes of the forwarder and amounted to field measurement: with a measuring bar (85.19% of the gross rut value); total station (86.28% of the gross rut value); or GNSS RTK device (86.42% of the gross rut value). Similar results, but with a slightly lower percentage, were also observed in the analysis of the gross value of ruts. The largest increase in the value of the gross rutting occurred between the first and fifth passes of the forwarder and amounted to field measurement: with a measuring bar (83.66% of the gross rut value); total station (82.99% of the gross value of the rut depth); or GNSS RTK device (81.48% of the gross value of the rut depth) (Figure 8).

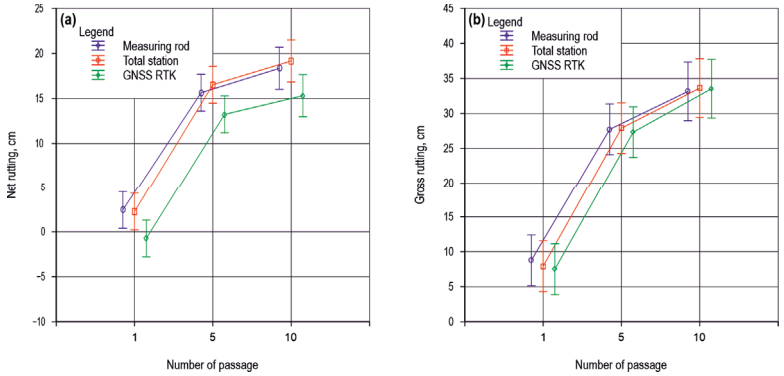

Figure 8. Rut depth increase between passages: (**a**) net rutting; (**b**) gross rutting.

The correlation coefficient (r) between the net rut depth and the error in relation to the reference measurement method was 0.45 with $p = 0.00021$, indicating a weak connection between the tested variables. The data equalization curve is GNSS RTK measuring error = $-5.062 + 0.21955 \times$ GNSS RTK rutting, with a determination coefficient (r^2) of 0.20 (Figure 9). The described curve has an upward trend.

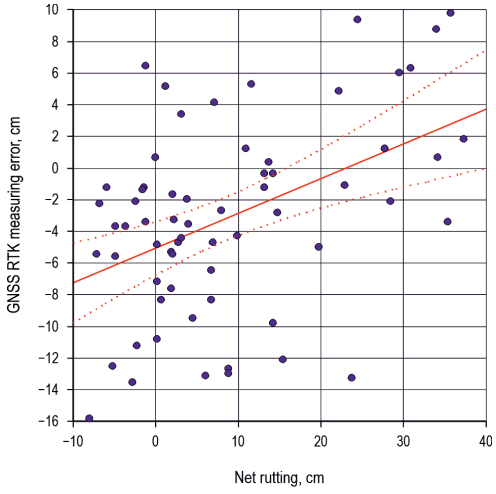

Figure 9. Impact of net rut depth on measuring error.

4. Discussion

This research analyzed the accuracy of the different rut measurements using a total station and a GNSS RTK device with a CROPOS correction base in relation to the measuring rod that represented the reference method. A total of 2835 measurements were performed. The analysis of net rutting (ground elevation before vehicle passage–ground elevation after each measured passage) indicated that the total station underestimated the depth of ruts by 0.49 cm on average, which represents a satisfactory accuracy and a statistically insignificant error. During the research, minor deflections were noticed in the central spirit level due to the passage of the forwarder near the total station. We believe that moving the total station to a place further away from the passage of a forest vehicle would give more accurate results. However, in that case, it would be necessary to have higher visibility from the total station to the prism in a wider area, which could not be recommended because of further reduction in the productive area of the forest stand. In addition, it was determined that the width of the measuring area along the forwarder trail of 4.5 m may be insufficient. It was observed that because of the successive passage of the forwarder and the widening of the ruts, the poles that marked the first and the last place of measurement slightly moved. The widening of the ruts and the ejection of a large amount of soil was caused by the high current moisture of the surface layer of the soil, which ranged from 55% to 70%, and the soil had a limited bearing capacity. Košir [43] stated that as a result of the repeated passage of vehicles, the tread width of the ground expands by 0.5 m in each direction. The forwarder used during this research was 2980 mm wide, so the gate width of 4.5 m is the limiting value. For future research, it is recommended to use a measuring site width of 5 m, as already applied in some research [8,44], if this width would not significantly affect the stand. The GNSS RTK device made an average error of 2.86 cm when measuring net depths. Similar results were found in the study by Ring et al. [15], who reported an error of 4 cm, although it is unclear what rut depth they measured. Considering that rut depths of up to 10 cm are environmentally acceptable, as recommended by the EcoWood protocol and Bavarian State Institute of Forestry for effective wood harvesting on sensitive forest soils [45], measurement errors in the amount of 2.86 cm can be the reason for stopping timber harvesting operation if they are not necessary. The GNSS RTK device underestimated the rut depth values on all forwarder trails except FT2. Weather and other conditions did not change during the research, and the settings of the device itself were the same on all investigated forwarder trails; unfortunately, the reason for the smallest errors of the GNSS RTK device on FT2 cannot be concluded. The calculated gross rutting did not differ statistically significantly between the depth measurement methods used. Based on this result, a statistical analysis of the bulge height was performed, which showed a statistically significant difference between the GNSS RTK device and other methods. The GNSS RTK device gave an average of 2.89 cm higher values of the height of the ejected soil. From this, we can conclude that the GNSS RTK device constantly measured the higher altitude of all recorded points. Due to the method of calculating the net rutting and bulge height, the sum of which constitutes the gross rut value, no statistically significant difference was observed between the gross rut depths of the analyzed methods. For this reason, we believe that the use of GNSS RTK devices is possible in operational forestry for measuring gross rutting. This way of measuring gross ruts would enable the forestry profession to measure gross rutting daily, quickly, and accurately enough. The smallest differences between measurement methods, during the calculation of all components of the analysis of this research, were observed on FT2. The reason for this could not be determined from the collected data. The weak correlation between the measured net rutting of the GNSS RTK device and the error concerning the depth measured by the measuring rod indicates that the error does not depend, or depends only slightly, on the rut depth; that is, the greater the depth of the rut, the greater the error. Influence of the number of vehicle passes on net and gross rutting was also analyzed and it indicated that the greatest increase in the value of rutting was between the first and fifth passes, which is in accordance with the research of other authors [46–48]. The obtained smaller rut values

between two passes and the positive value of the rut depth, as in Ring et al. [15], can be explained by the pressing of the soil under the wheels due to the pronounced microrelief full of depressions and humps. Also, it should be noted that the research was conducted in winter, when the canopies of the trees in the research area were without leaves, and for this reason, the visibility of the GNSS RTK device to a sufficient number of satellites was not questionable. According to [22,23], the canopy structure would affect the accuracy and time effect during data collection, and in our opinion, the vegetation period measurements with the RTK device would not be possible, that is, this should be determined by further research. Measuring with a measuring rod, although accurate, is time-consuming, both in the field and during field data entry into a personal computer with a higher probability of a human error. Regardless of the method of measurement and calculation of net and gross rut depth, it was determined that the change in rut depth is the greatest during the first five passes of a forwarder along the same track.

5. Conclusions

Finally, we can conclude that the total station as a measuring instrument is reliable and accurate for measuring ruts, be it net or gross rutting. Time consumption during fieldwork with this instrument is identical to that with a measuring rod, with less possibility of an error when reading measurements and much faster and easier data transfer to a personal computer. Moving the instrument away from where the forest vehicle is passing and ensuring a stable base is a critical phase of the measurements. The GNSS RTK device, if used for measuring gross rutting, represents a sufficiently accurate method that is as time-consuming as the other methods used. However, the use of the GNSS RTK device requires one operator, while the other methods require at least two people. The observed constant overestimation of the altitude of the measured points makes it impossible to accurately measure net rutting. In addition to the impossibility of accurate measurement of net rutting, the use of GNSS RTK devices is limited to the winter period when the canopy is without leaves [21–24]. On the other hand, the canopy does not represent a limitation in the operation of the total station. However, an accurate method, such as a tape measure, measuring rod, or manual measurement, is subject to human error. As stated in the introduction, water inside the ruts is challenging when measuring with photogrammetry or LiDAR sensors. Based on all the above, the analysis of the obtained data, and the review of the available literature, we believe that the total station represents the optimal field measurement method for determining gross or net ruts in lowland flooded forests.

Author Contributions: Conceptualization, I.P. and M.L.; methodology, I.P.; software, M.P. and M.L.; validation, A.Đ., T.P. (Tomislav Poršinskyand), D.J. and T.P. (Tibor Pentek); formal analysis, I.P.; investigation, M.L. and D.J.; resources, A.Đ. and T.P. (Tibor Pentek); data curation, M.P.; writing—original draft preparation, M.L. and I.P.; writing—review and editing, I.P. and A.Đ.; visualization, I.P., M.P. and M.L.; supervision, T.P. (Tomislav Poršinskyand); project administration, T.P. (Tibor Pentek); funding acquisition, A.Đ. All authors have read and agreed to the published version of the manuscript.

Funding: The research was carried out as a part of the project "Conservation of narrow-leaved ash stands (*Fraxinus angustifolia* Vahl) in the Republic of Croatia with an emphasis on harmful biotic factors" funded by the Ministry of Agriculture of the Republic of Croatia from the Funds for The Multifunctional Role of Forests: A part of this research was also funded by the Croatian Science Foundation under the project "Quantity and structure of fir and spruce biomass in changed climatic conditions" (UIP-2019-04-7766).

Data Availability Statement: Data is contained within the article.

Acknowledgments: The authors wish to thank the University of Zagreb Faculty of Forestry and Wood Technology for the support during the research.

Conflicts of Interest: David Janeš is now employed by the company Croatian Forests, Ltd. The remaining authors declare that the research was conducted in the absence of any commercial or financial relationships that could be construed as a potential conflict of interest.

References

1. Pentek, T.; Poršinsky, T. Forest Transportation Systems as a Key Factor in Quality Management of Forest Ecosystems. In *Forest Ecosystems—More than Just Trees*, 1st ed.; Blanco, J.A., Ed.; InTech: London, UK, 2012; pp. 433–464.
2. Bumber, Z. Primjena GIS-a Pri Analizi Otvorenosti GJ Šiljakovačka Dubrava II Kroz Strukturu Prihoda Drva u Prostoru i Vremenu. Master's Thesis, Šumarski Fakultet, Sveučilište u Zagrebu, Zagreb, Croatia, 2011.
3. Greulich, F. Transportation Networks in Forest Harvesting: Early Development of the Theory. In Proceedings of the International Seminar on New Roles of Plantation Forestry Requiring Appropriate Tending and Harvesting Opreations, Tokyo, Japan, 29 September–5 October 2002.
4. Pentek, T.; Nevečerel, H.; Ecimović, T.; Lepoglavec, K.; Papa, I.; Tomašić, Ž. Strategijsko planiranje šumskih prometnica u Republici Hrvatskoj–raščlamba postojećega stanja kao podloga za buduće aktivnosti. *Nova Meh. Sumar.* **2014**, *35*, 63–78.
5. Picchio, R.; Mederski, P.S.; Tavankar, F. How and how much, do harvesting activities affect forest soil, regeneration and stands? *Curr. For. Rep.* **2020**, *6*, 115–128. [CrossRef]
6. Cambi, M.; Certini, G.; Neri, F.; Marchi, E. The impact of heavy traffic on forest soils: A review. *For. Ecol. Manag.* **2015**, *338*, 124–138. [CrossRef]
7. Nadezhdina, N.; Prax, A.; Čermák, J.; Nadezhdin, V.; Ulrich, R.; Neruda, J.; Schlaghamersky, A. Spruce roots under heavy machinery loading in two different soil types. *For. Ecol. Manag.* **2012**, *282*, 46–52. [CrossRef]
8. Poršinsky, T. Djelotvornost i Ekološka Pogodnost Forvardera Timberjack 1710 pri Izvoženju Oblovine iz Nizinskih Šuma Hrvatske. Ph.D. Thesis, Šumarski Fakultet, Sveučilište u Zagrebu, Zagreb, Croatia, 2005; pp. 1–170.
9. Latterini, F.; Venanzi, R.; Picchio, R.; Jagodziński, A.M. Short-term physicochemical and biological impacts on soil after forest logging in Mediterranean broadleaf forests: 15 years of field studies summarized by a data synthesis under the meta-analytic framework. *Forestry* **2023**, *96*, 547–560. [CrossRef]
10. Mohieddinne, H.; Brasseur, B.; Spicher, F.; Gallet-Moron, E.; Buridant, J.; Kobaissi, A.; Horen, H. Physical recovery of forest soil after compaction by heavy machines, revealed by penetration resistance over multiple decades. *For. Ecol. Manag.* **2019**, *449*, 117472. [CrossRef]
11. Sohrabi, H.; Jourgholami, M.; Jafari, M.; Shabanian, N.; Venanzi, R.; Tavankar, F.; Picchio, R. Soil recovery assessment after timber harvesting based on the Sustainable Forest Operation (SFO) perspective in Iranian temperate forests. *Sustainability* **2020**, *12*, 2874. [CrossRef]
12. Labelle, E.R.; Hansson, L.; Högbom, L.; Jourgholami, M.; Laschi, A. Strategies to mitigate the effects of soil physical disturbances caused by forest machinery: A comprehensive review. *Curr. For. Rep.* **2022**, *8*, 20–37. [CrossRef]
13. Edlund, J.; Bergsten, U.; Löfgren, B. Effects of two different forwarder steering and transmission drive systems on rut dimensions. *J. Terramech.* **2012**, *49*, 291–297. [CrossRef]
14. Gerasimov, Y.; Katarov, V. Effect of bogie track and slash reinforcement on sinkage and soil compaction in soft terrains. *Croat. J. For. Eng.* **2010**, *31*, 35–45.
15. Ring, E.; Andersson, M.; Hansson, L.; Jansson, G.; Högbom, L. Logging mats and logging residue as ground protection during forwarder traffic along till hillslopes. *Croat. J. For. Eng.* **2021**, *42*, 445–462. [CrossRef]
16. Sirén, M.; Salmivaara, A.; Ala-Ilomäki, J.; Launiainen, S.; Lindeman, H.; Uusitalo, J.; Sutinen, R.; Hänninen, P. Predicting forwarder rut formation on fine-grained mineral soils. *Scand. J. For. Res.* **2019**, *34*, 145–154. [CrossRef]
17. Ilintsev, A.; Bogdanov, A.; Nakvasina, E.; Amosova, I.; Koptev, S.; Tretyakov, S. The natural recovery of disturbed soil, plant cover and trees after clear-cutting in the boreal forests, Russia. *IFOREST J.* **2020**, *13*, 531. [CrossRef]
18. Toivio, J.; Helmisaari, H.-S.; Palviainen, M.; Lindeman, H.; Ala-Ilomäki, J.; Sirén, M.; Uusitalo, J. Impacts of timber forwarding on physical properties of forest soils in southern Finland. *For. Ecol. Manag.* **2017**, *405*, 22–30. [CrossRef]
19. Feng, Y.; Wang, J. GPS RTK performance characteristics and analysis. *Positioning* **2008**, *7*, 1–8. [CrossRef]
20. Luo, X.; Schaufler, S.; Branzanti, M.; Chen, J. Assessing the benefits of Galileo to high-precision GNSS positioning–RTK, PPP and post-processing. *Adv. Space Res.* **2021**, *68*, 4916–4931. [CrossRef]
21. Brach, M.; Zasada, M. The effect of mounting height on gnss receiver positioning accuracy in forest conditions. *Croat. J. For. Eng.* **2014**, *35*, 245.
22. Andreas, H.; Abidin, H.Z.; Sarsito, D.A.; Pradipta, D. Study the capabilities of RTK Multi GNSS under forest canopy in regions of Indonesia. *E3S Web Conf.* **2019**, *94*, 01021. [CrossRef]
23. Feng, T.; Chen, S.; Feng, Z.; Shen, C.; Tian, Y. Effects of canopy and multi-epoch observations on single-point positioning errors of a GNSS in coniferous and broadleaved forests. *Remote Sens.* **2021**, *13*, 2325. [CrossRef]
24. Abdi, O.; Uusitalo, J.; Pietarinen, J.; Lajunen, A. Evaluation of Forest Features Determining GNSS Positioning Accuracy of a Novel Low-Cost, Mobile RTK System Using LiDAR and TreeNet. *Remote Sens.* **2022**, *14*, 2856. [CrossRef]
25. Talbot, B.; Pierzchała, M.; Astrup, R. Applications of remote and proximal sensing for improved precision in forest operations. *Croat. J. For. Eng.* **2017**, *38*, 327–336.
26. Heppelmann, J.B.; Talbot, B.; Antón Fernandéz, C.; Astrup, R. Depth-to-water maps as predictors of rut severity in fully mechanized harvesting operations. *Int. J. Eng.* **2022**, *33*, 108–118. [CrossRef]
27. Palander, T.; Kärhä, K. Utilization of image, LiDAR and gamma-ray information to Improve environmental sustainability of cut-to-length wood harvesting operations in peatlands: A management systems perspective. *ISPRS Int. J. Geo-Inf.* **2021**, *10*, 273. [CrossRef]

28. Marra, E.; Wictorsson, R.; Bohlin, J.; Marchi, E.; Nordfjell, T. Remote measuring of the depth of wheel ruts in forest terrain using a drone. *IJFE* **2021**, *32*, 224–234. [CrossRef]
29. Talbot, B.; Nowell, T.; Berg, S.; Astrup, R.; Routa, J.; Väätäinen, K.; Ala-Ilomäki, J.; Lindeman, H.; Prinz, R. Continuous surface assessments of wheel rutting compared to discrete point measurements—do the benefits justify the efforts? In Proceedings of the Nordic Baltic Conference on Forest Operations for the Future, Elsinore, Denmark, 22–24 September 2020.
30. Pierzchała, M.; Talbot, B.; Astrup, R. Measuring wheel ruts with close-range photogrammetry. *Forestry* **2016**, *89*, 383–391. [CrossRef]
31. Salmivaara, A.; Miettinen, M.; Finér, L.; Launiainen, S.; Korpunen, H.; Tuominen, S.; Uusitalo, J. Wheel rut measurements by forest machine-mounted LiDAR sensors–accuracy and potential for operational applications? *IJFE* **2018**, *29*, 41–52. [CrossRef]
32. Marra, E.; Cambi, M.; Fernandez-Lacruz, R.; Giannetti, F.; Marchi, E.; Nordfjell, T. Photogrammetric estimation of wheel rut dimensions and soil compaction after increasing numbers of forwarder passes. *Scand. J. For. Res.* **2018**, *33*, 613–620. [CrossRef]
33. Ferenčík, M.; Dudáková, Z.; Kardoš, M.; Sivák, M.; Merganičová, K.; Merganič, J. Measuring Soil Surface Changes after Traffic of Various Wheeled Skidders with Close-Range Photogrammetry. *Forests* **2022**, *13*, 976. [CrossRef]
34. Gülci, S.; Şireli, S. The evaluation of SfM technique in the determination of surface deformation on skidding roads following timber harvesting. *Eur. J. For. Eng.* **2019**, *5*, 52–60. [CrossRef]
35. Pernar, N.; Bakšić, D.; Perković, I.; Vrbek, B. Soil properties of narrow-leaved ash sites in Croatia. In *Narrow-Leaved Ash in Croatia*, 1st ed.; Anić, I., Ed.; Academy of Forestry Sciences: Zagreb, Croatia, 2022; pp. 179–222.
36. Haas, J.; Ellhöft, K.H.; Schack-Kirchner, H.; Lang, F. Using photogrammetry to assess rutting caused by a forwarder—A comparison of different tires and bogie tracks. *Soil. Tillage Res.* **2016**, *163*, 14–20. [CrossRef]
37. Meek, P. An evaluation of four methods for procesessing timber at the stump. *For. Eng. Res. Inst. Can. (FERIC) Pointe-Claire Que. Tech.* **1993**, 1–8.
38. Pandur, Z.; Đuka, A.; Šušnjar, M.; Bačić, M.; Ostović, K.; Lepoglavec, K. Analiza gaženja tla prilikom strojne sječe, izrade i izvoženja drva u prorednoj sastojini listača. *Nova Meh. Sumar.* **2018**, *39*, 1–12.
39. Poršinsky, T.; Pandur, Z.; Bumber, Z.; Lovrinčević, M.; Ursić, B.; Đuka, A. Dimenzijske i masene značajke forvardera. *Šumar. List* **2022**, *146*, 387–401.
40. *ISO 13860*; Machinery for Forestry—Forwarders—Terms, Definitions and Commercial Specifications. International Standard Organization: Geneva, Switzerland, 2016.
41. Mihelič, J.; Robek, R.; Kobal, M. Determining bulk factors for three subsoils used in forest engineering in Slovenia. *Croat. J. For. Eng.* **2022**, *43*, 303–311.
42. CROPOS—Državna Mreža Referentnih Stanica Republike Hrvatske. Available online: https://www.cropos.hr/ (accessed on 8 December 2023).
43. Košir, B. Vpliv strojne sečnje na sestoj in gozdna tla. In Proceedings of the Strojna Sečnja v Sloveniji, Ljubljana, Slovenia, October 2002; pp. 66–82.
44. Solgi, A.; Zenner, E.K.; Naghdi, R.; Masumian, A.; Shoja, R.; Behjou, F.K. Evaluating the Effectiveness of Mulching for Reducing Soil Erosion in Skid Trail Switchbacks. *Croat. J. For. Eng.* **2022**, *43*, 339–353. [CrossRef]
45. Kremer, J.; Wolf, B.; Matthies, D.; Borchert, H. *Bodenschutz beim Forstmaschineneinsatz*, 3rd ed.; Bosch, T., Ed.; LWF: Freising, Germany, 2012.
46. Eliasson, L.; Wästerlund, I. Effects of slash reinforcement of strip roads on rutting and soil compaction on a moist fine-grained soil. *For. Ecol. Manag.* **2007**, *252*, 118–123. [CrossRef]
47. Han, H.S.; Page-Dumroese, D.; Han, S.K.; Tirocke, J. Effects of slash, machine passes, and soil moisture on penetration resistance in a cut-to-length harvesting. *IJFE* **2006**, *17*, 11–24. [CrossRef]
48. Prinz, R.; Mola-Yudego, B.; Ala-Ilomäki, J.; Väätäinen, K.; Lindeman, H.; Talbot, B.; Routa, J. Soil, driving speed and driving intensity affect fuel consumption of forwarders Croat. *J. For. Eng.* **2023**, *44*, 31–43.

Disclaimer/Publisher's Note: The statements, opinions and data contained in all publications are solely those of the individual author(s) and contributor(s) and not of MDPI and/or the editor(s). MDPI and/or the editor(s) disclaim responsibility for any injury to people or property resulting from any ideas, methods, instructions or products referred to in the content.

forests

MDPI

Article

Evaluation of Productivity and Cost Analysis on a Combined Logging System

Salvatore F. Papandrea [1], Stanimir Stoilov [2], Maria Francesca Cataldo [1], Krasimir Petkov [2], Georgi Angelov [2], Antonio Zumbo [1,*] and Andrea R. Proto [1]

[1] Department of AGRARIA, Mediterranean University of Reggio Calabria, Feo di Vito snc, 89122 Reggio Calabria, Italy; salvatore.papandrea@unirc.it (S.F.P.); maria.cataldo@unirc.it (M.F.C.); andrea.proto@unirc.it (A.R.P.)

[2] Department of Technologies and Mechanization of Forestry, University of Forestry, 10, Kliment Ohridski Blvd., 1797 Sofia, Bulgaria; stoilovs@ltu.bg (S.S.); petkowb5029@abv.bg (K.P.); ggangelov@ltu.bg (G.A.)

* Correspondence: antonio.zumbo@unirc.it

Abstract: The efficient planning and control of timber harvesting operations is crucial to growth productivity and reducing costs, and different systems or methods are applied to obtain elevated performance. In particular, cable yarding is a highly appreciated and very efficient wood extraction method in areas that are difficult to access with ground-based extraction machines. Combined logging systems are not diffuse and not often implemented. For this reason, the use and the application of innovative methods are limited. However, some combinations have recently been observed in forest operations. This study, conducted in a deciduous stand in Bulgaria, paid attention to the combination of a tractor-mounted tower yarder (Valentini V400) with a clambunk skidder (Timberjack 1010D), aiming to examine the viability and develop the operational efficiency of the two-stage extraction system and to define the time, log volume extracted per unit by the yarder and the clambunk, and the yarding and skidding costs. The researchers carried out a time-motion study and performed a regression analysis to identify those variables that are most likely to affect the duration of work elements and productivity. For cost analysis, the COST model was used. The mean productivity of the tower yarder was 10.34 m^3/PMH and 8.11 m^3/SMH, while for the clambunk skidder, the productivity was 6.23 m^3/PMH and 4.93 m^3/SMH. The net costs for the combined logging system were calculated as 120.87 €/PMH and 14.93 €/m^3. This study adds new data about the correct use of both machines, supporting their application in beech forests.

Keywords: forest operations; skidding; yarding; performances; deciduous stands

1. Introduction

Cable yarders are an important system of skidding and transporting timber and their use in the mountainous regions of Europe is widespread [1,2].

During the last ten years, the use of all-terrain mobile tower cable cranes has been increasing due to their adaptability in operating both in uphill as well as in downhill configurations. However, modern cable yarding technology fills this gap, and productivity models can assist users in their work, to maximize the performance of their machines [3]. On difficult terrain, cable cranes represent a cost-effective alternative system compared to ground-based logging, and results in a much lower site impact too [4,5]. Over the past two decades, forest operations have been developing timber harvesting guidelines to mitigate the environmental impacts of tree felling and transport. Efficient forest management is essential for the resilience of these ecosystems. The use of this combined logging system helps reduce the effect of timber harvesting [6]. Cable yarders are used mainly for timber harvest using parallel or fan-shaped schemes [7], and new double-hitch carriages have been applied for full suspension. This different method requires longer to load up but permits a similar performance [8].

Worldwide, the principal use of these machines is in coniferous stands and rarely in deciduous stands [9]. Cable yarding in hardwood is widespread in the Appalachians in the Northeast of the US [10–14], southern Germany [1], southern Italy [15,16], Bulgaria [9,17], and Turkey [18]. In Bulgaria the quota of deciduous tree species is 71%, while the quota of total assets growing is 55.5% [19,20]. Therefore, the use of these machines is important in the Bulgarian logging industry. In one example, a cable logging team of three workers tested a yarder for single-span layouts, while a different team of four members worked using both a yarder and skidder [21,22]. In the Northeast US, Huyler and LeDoux [13] found that yarding delays were approximately 35% of the total cycle time for operational, mechanical, and non-productive time descriptions on steep slopes. The delays are separate from the delay-free times used to estimate the total cycle time [13].

To raise the performance of cable yarding worked in European beech (*Fagus sylvatica* L.) stands in the Ograzhden Mountains (southwest Bulgaria), Dimitrov [17] showed that productive times for bunching (28%), extraction (21%), and carriage unloading (13%) should be decreased. In the mentioned paper, the performance of the yarder was defined as moderate (3.22 m^3/PMH). This productivity is comparable with other research carried out in a mixture of Oriental spruce (*Picea orientalis* (L.) Link.), Normann fir (*Abies nordmanniana* (Stev.) Mattf.), and Scots pine (*Pinus sylvestris* (L.) forests in Turkey (6.6 $m^3 \cdot h^{-1}$, 5.5 $m^3 \cdot h^{-1}$, and 5.0 $m^3 \cdot h^{-1}$) [23]. In Italy, Zimbalatti and Proto [15] showed that three cable cranes extracted inferior volumes of timber compared to their load potential; in fact, the average extracted volume was inferior compared to the load capacity of the carriage. Melemez et al. [18] showed that for a slope of terrain greater than 50%, the most efficient extraction occurs by the use of a skyline. The study carried out by Stoilov [9] in a deciduous stand of European beech (90%) and European hornbeam (10%) in the Sredna Gora Mountains, Central Bulgaria, showed that the mean productivity of a truck-mounted tower yarder was close to the maximum for that type (9.12 $m^3 \cdot PMH^{-1}$ and 8.41 $m^3 \cdot SMH^{-1}$). The gross costs for yarding uphill a whole tree by the studied tower yarder were estimated at 146.52 € per PMH and 13.02 € per m^3. Fixed costs (26.84%) and variable costs (29.86%) were higher than labor costs (21.44%).

Most operations may be considered economically skillful if the costs of operations are determined carefully, taking into account all factors in a high-yield stand [10]. Schweier [1] showed that the harvesting costs of two different systems in flat terrains are similar, determining the cost of using a Koller K507 at 33 € $\cdot m^{-3}$, while that of a Valentini V400 cable crane was 36 € $\cdot m^{-3}$. Between the two systems, the Koller K507 was more cost-efficient in processing timber of large dimensions.

Combining a tower yarder with other extraction machines, although known for a long time, is not often implemented [24]. However, such combinations have recently been observed, such as with a clambunk skidder.

The clambunk skidder lends to replacing or being used together with skidders, feller–bunchers, and processors [25]. Stokes and Schilling [26] have demonstrated that clambunk skidders mitigate the adverse effects of operations on conventional and challenging sites, while also enhancing the efficacy of the harvesting system. The use of this machine is more advantageous as the extraction distance and number of passes over the site increase, reducing road construction. On a clambunk skidder, the load is positioned on an integrally mounted loader and it is held by top-opening jaws [27]. In South Africa, Oberholz [28] has obtained a productivity of 5.7 m^3/PMH to 50 m^3/PMH in pine stands using a clambunk skidder with a capacity of 18 t, with uphill slopes 0%–25%, downhill slopes 0%–40%, and skidding distances of 50–1000 m. The variable, fixed, and administration costs were the most significant for cost analysis. Clambunk production costs differed with skidding distance because this variable involved travelling times. In Brazil, Dos Santos et al. [29] have studied the average harvesting cost of a clambunk skidder in a stand of eucalyptus. It was equal to 1.7 € $\cdot m^{-3}$, for an average distance of extraction of 241.23 m with a volume average of 0.39 $m^3 \cdot tree^{-1}$. This cost ranged from R$3.14 to R$6.93 m^{-3} (around 1.10 to 2.40 € $\cdot m^{-3}$) for extraction distances of 106 m and 366 m, respectively [29]. In a study, Ghaffariyan [30]

reported an average productivity varying from 9.3 m^3/PMH to 78.0 m^3/PMH in coniferous forests and plantations. The type of machine, the volume of logs, the slope of the terrain, and the skidding distance affect the performance of the skidder.

The aim of this present study was to examine the viability and to improve the use and operational efficiency of the two-stage extraction system, consisting of a tractor-mounted tower yarder and clambunk skidder in deciduous stands, and to analyze the time consumption, harvesting productivity, and costs for both machines. The adoption of these machines is useful for improving the economic and environmental performance of wood harvesting in deciduous forests, also involved in the Natura 2000 network.

2. Materials and Methods

2.1. The Study Site

This research was conducted in the Vitinya State Hunting Range (Figure 1), sited in the Western Balkan Mountains, Sofia Province (Table 1). This study focused on the Valentini V400 (Valentini srl, Cles, Italy) tractor-based tower yarder and Timberjack 1010D (Deere & Company, Moline, IL, USA) single-drum cable + clambunk skidder shown in Figures 2 and 3.

Table 1. Technical data of research area.

Location	Subcompartment 91-v N 42°49′9.788″; E 23°43′7.0468″
Elevation	1300 m asl
Forest tree	European beech (*Fagus sylvatica*, L.) 100%
Stand age	90 years
Silvicultural system	High natural forest
Total area	12.0 ha
Cutting area	10.0 ha
Silvicultural intervention	Thinning, removal intensity 15%
Average tree height	21 m
Average DBH of tree	30 cm
Average slope	29° (55%)
Volume site	3580 m^3 (334 $m^3 \cdot ha^{-1}$)
Extraction direction	Uphill

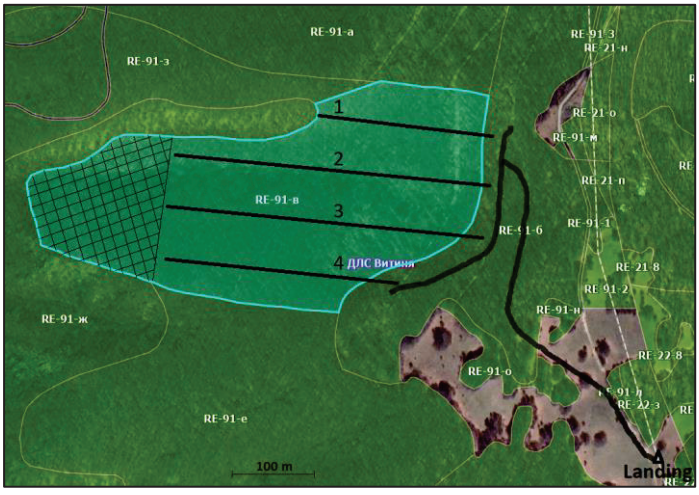

Figure 1. Location of case study (—skidding road; —tower yarder skyline; Δ—landing). ДЛС Витиня means Vitinya State Hunting Range.



Figure 2. Valentini V 400 tractor-based tower yarder.



Figure 3. Timberjack 1010D clambunk skidder.

2.2. Description of the Machines, Work Team, and Time Study

To start with harvesting operations, trees were felled, delimbed, and crosscut into stems and stem sections. Wood materials in the stems and logs were extracted initially by the Valentini V400 tractor-mounted tower yarder to the skidding road and from there transported semi-suspended by the Timberjack-1010D clambunk skidder to the landing. To avoid the yarded stems sliding back into the cutting area, they were hauled by the clambunk skidder with its built-in single drum winch and then loaded at their thick ends into the clambunk using the hydraulic crane. The personnel of both machines consisted of 3 workers: a tower yarder operator, choker-setter, and clambunk skidder operator. All had more than 5 years of experience and were aged 40–50. Technical data of the studied machines are shown in Tables 2 and 3. As shown in Figure 1, four parallel-shaped corridors were created with the following lengths and slopes: Corridor 1—220 m, 14° (25%); Corridor 2—400 m, 19° (34%); Corridor 3—400 m, 19° (34%); and Corridor 4—320 m, 17° (31%). For each corridor, 30 cycle times were monitored, and 120 turns were collected during forest operations. A single-span uphill configuration was monitored in each detailed phase. The longitudinal slope of the skidding road in the section from Corridor 4 to midway between Corridor 2 and Corridor 1 at the tower yarder averages 11° (19%) uphill. In the section to the landing it is 3° (5%), also uphill, which, however, is not much slope resistance to the operation of the dedicated clambunk skidder.

Table 2. Technical data of Valentini V400 tractor mounted tower yarder.

Parameter	Value
Skyline	
Length/cable diameter	400 m/16–17 mm
Pulling force	67 kN
Mainline	
Length/cable diameter	400 m/10 mm
Pulling force	21–28 kN
Pulling speed	3–4.5 m/s (10.8–16.2 km/h)
Guylines	4(5) × 60 m, Ø14 mm
Tower height	10 m
Base machine	Belarus 1221.3 farm tractor (96 kW)
Diesel engine power	Minimum 89 kW (120 hp)
Weight of tower yarder (incl. cables)	3800 kg

Table 3. Technical data of Timberjack 1010D clambunk skidder.

Parameter	Value
Engine type:	John Deere 4045 HTJ76
Rated power	86 kW at 2000 min^{-1}
Maximum net torque	498 Nm at 1400 min^{-1}
Transmission	Hydrostatic-mechanical transmission with low and high range
Travel speeds forward and reverse	High: 0–22 km/h; Low: 0–8 km/h
Max. tractive effort	140 kN
Sizes:	
Length	9.05 m
Width	2.70 m
Transport height	3.70 m
Ground clearance	605 mm
Wheelbase	4.80 m
Load capacity	11,000 kg
Operating weight	12,700–13,700 kg
Max. load rating	10,000 kg
Crane:	CF5
Gross lifting torque	102 kNm
Winch	One-drum
Cable length	65 m
Nominal pulling force of winch	50 kN

The tower yarder work cycle was divided into several elements [31–34]. Six work elements were separated and considered to estimate the work cycle time [13]; they were like those described by Proto and Zimbalatti [16]:

- Carriage outhaul (CO);
- Lateral outhaul and hook (LOH);
- Lateral inhaul (LI);
- Carriage inhaul (CI);
- Unhook (U);
- Delay time (D).

The work phase of the clambunk skidder has been divided into the following 8 elements:

- Travel unloaded (TU);
- Maneuvering (M);
- Winching (W);
- Loading (LOAD);
- Travel loaded (TL);
- Unloading (UNLOAD);
- Sorting and piling (SP);

- Delays (DS).

2.3. Costs Analysis

Machine costs for the extraction of 1 m^3 of wood materials were calculated according to the COST model [35] based on the parameters as follows: number of operators, operator costs per hour, and productive machine hours (PMHs) (without delays). Hourly machine costs are given in both PMHs and scheduled machine hours (SMHs), including delays. Purchase costs and operator wages were sourced from catalogs and accounting documents [33]. Fuel costs were determined with the refilling fuel tank method provided before operations and accounting for the fuel used by topping up at the end of the workday. The costs of the tested machines were based on assuming that companies in the logging industry work on average 150 days per year, distributed on 20–21 working days per month, an average of 5–6 actual working hours per day, not considering the time needed for day meals. Therefore, the machines work 910–1050 scheduled hours within a year at a use coefficient of 70% [36,37].

2.4. Data Analysis

A time and motion study is carried out to find the duration of work items and productivity. Thus, those variables that are most likely to influence them are determined. Each phase is timed with a stopwatch and the effective time is separated from the delay time. Yarding and skidding distance were counted by a GPS. Winching distances and terrain slopes were measured with a professional laser range finder with a built-in clinometer. The volume of the single skidded logs was assessed using the Huber formula. Regression analysis of the experimental data was performed to obtain equations for predicting the dependent variables of duty cycle time and machine productivity. The independent variables that were used to model the yarder were as follows: yarding distance L_{TY}, lateral yarding distance l_Y, load volume per cycle V_{TY}, terrain slope angle i, and the load's number of trees n_{TY}. Information on the independent variables skid distance L_{CS} as well as number n_{CS} and stem volume V_{CS} were used to model skidder performance.

Descriptive statistics of the variables were found and stepwise backward regression was used to model the variability of duty cycle time and machine productivity based on independent variables. The normal distribution of the experimental data values was established using the Kolmogorov–Smirnov (K–S test) and Shapiro–Wilk tests.

A confidence level of 95% ($\alpha = 0.05$) and an assumed probability of $p < 0.05$ were used for regression analysis. Independent variables are significant at $p < 0.05$, i.e., a strong presumption against the null hypothesis. Statistica 8 software (StatSoft Inc., Tulsa, OK, USA) was used to process the experimental data.

3. Results and Discussion

The summary of the experimental data from 120 yarding and 30 clambunk skidder cycles for each of the selected variables used in the cycle time and production equations is shown in Table 4.

Table 4. Average field data collected.

Variables	Cycle Time, Minutes			Distance, m		
	Mean Value ± St. dev.	Min	Max	Mean Value ± St. Dev.	Min	Max
Yarding						
Carriage outhaul (CO)	0.72 ± 0.089	0.60	0.90	123.83 ± 17.47	90	150
Lateral outhaul and hook (LOH)	3.49 ± 0.54	2.20	4.60	12.84 ± 3.29	6	22
Lateral inhaul (LI)	0.36 ± 0.047	0.25	0.43	12.84 ± 3.29	6	22
Carriage inhaul (CI)	0.86 ± 0.11	0.70	1.08	123.83 ± 17.47	90	150
Unhook (U)	0.40 ± 0.087	0.25	0.50			
Delays (DY)	7.72 ± 13.16	0.33	33.22			

Table 4. *Cont.*

Variables	Cycle Time, Minutes			Distance, m		
	Mean Value ± St. dev.	Min	Max	Mean Value ± St. Dev.	Min	Max
Total cycle time (T_{TY})	13.68 ± 13.62	5.07	39.15			
Delay-free cycle time ($T_{net,TY}$)	6.04 ± 0.71	4.63	7.55			
Load volume per cycle (turn), m^3	1.01 ± 0.33	0.75	1.91			
Productivity, m^3 per PMH	10.34 ± 2.07	7.20	17.63			
Productivity, m^3 per SMH	8.11 ± 3.83	1.17	15.15			
Number of stems per cycle	1.43 ± 0.50	1	2			
Skyline slope, deg	17.25 ± 2.05	14	19			
Number of cycles per SMH	7.66 ± 3.53	1.53	11.84			
Skidding						
Travel unloaded (TU)	6.08 ± 1.37	3.88	7.50	693.03 ± 180.38	467	870
Maneuvering (M)	0.35 ± 0.12	0.17	0.58			
Winching (W)	22.61 ± 6.72	6.73	38.50			
Loading (LOAD)	2.55 ± 0.15	2.32	305			
Travel loaded (TL)	12.46 ± 2.29	8.67	15.00	693.03 ± 180.38	467	870
Unloading (UNLOAD)	2.32 ± 0.08	2.15	2.50			
Sorting and piling (SP)	2.23 ± 0.12	2.00	2.40			
Delays (DS)	12.51 ± 1.43	10.33	16.47			
Total cycle time (T_{CS})	61.11 ± 7.63	46.97	79.27			
Delay-free cycle time ($T_{net,CS}$)	48.60 ± 8.00	32.02	68.27			
Productivity, m^3 per PMH	6.23 ± 1.35	3.85	10.23			
Productivity, m^3 per SMH	4.93 ± 1.11	2.77	8.37			
Number of stems per cycle	6.63 ± 1.22	3	9			
Number of cycles per SMH	1.00 ± 0.13	0.76	1.28			
Speed loaded, $km \cdot h^{-1}$	3.30 ± 0.38	2.56	3.82			
Speed unloaded, $km \cdot h^{-1}$	6. 82 ± 0.58	4.42	7.45			
Mean speed, $km \cdot h^{-1}$	4.44 ± 0.43	3.63	5.02			

3.1. Duration of Work Cycle Elements—Tower Yarder Unit

The work phases of the tower yarder (Figure 4) were subdivided into the following times (including delays): lateral outhaul and hook (LOH) occupied 26% of the time, followed by carriage inhaul (CI) 6%, carriage outhaul (CO) 6%, unhook (U) 3%, and lateral inhaul (LI) 3%, respectively. The percentages of times excluding delays were as follows: LOH occupied 60% of the time, CI 14%, CO 13%, U 7%, and LI 6%, respectively. The predominant part of the cycle time (Figure 1), excluding and including delays, was dedicated to the lateral outhaul and hooking (LOH) of the tree (60% and 26%, respectively), followed by carriage inhaul (14% and 6%, respectively) and carriage outhaul (13% and 6%). The other phases had approximately similar proportions: unhook (7% and 3%, respectively) and lateral inhaul (6% and 3%, respectively), excluding and including delays. Delays accounted for 56% of the total phase time and could be divided into operational and mechanical delays, respectively, for 52% and 4% of the total phase time of the studied cable yarder machine. Operational delays, 92% of all delays of the tower yarder, were predominantly due to the clambunk work phase (travel loaded to landing, unloading, sorting and piling, and travel unloaded). Within this time, the tower yarder can only make one phase (turn), waiting for the clambunk skidder to winch the extracted stems, due to the danger of them sliding back to the cutting area. A total of 66% of the work phase time, without delays, involved operations of lateral yarding (29% including delays). These operations include the lateral pull of the main line and the extraction of the load. In these conditions, the machine works at a moderate and low level of carriage payload capacity usage, with an average yarding distance of 123.83 m from nominal length, an average lateral yarding distance of 12.84 m, and an average slope of 17.25°. To estimate the yarding phase time (with and without delays), a regression analysis on time data was performed to create a prediction equation, using the independent factors in Table 4. The delay-free cycle time

(Equation (1)) and the cycle time with delays regression models (Equation (3)) obtained for cable extraction with significant factors are displayed in Table 5. In Equation (1), the minimum values of $T_{net,TY}$ may reach for this eventuality lower rates of yarding distance L_{TY} and terrain slope angle *i*. The total cycle time of the tower yarder (Equation (3)) will decrease as the yarding distance L_{TY} is decreased and the lateral yarding distance *l* and the number of load stems n_{TY} are increased.

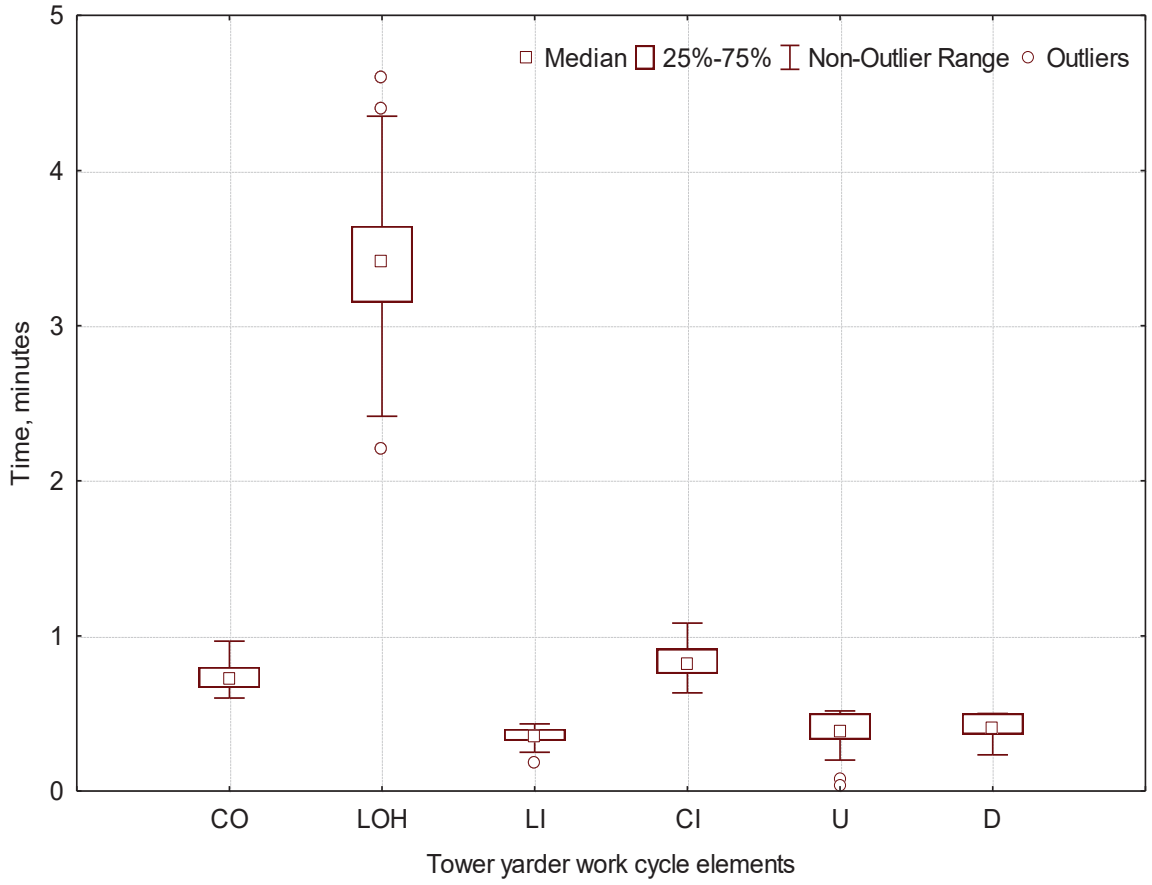

Figure 4. Elemental time consumption of tower yarder unit. Note: CO—carriage outhaul, LOH—lateral outhaul and hook, LI—lateral inhaul, CI—carriage inhaul, U—unhook, D—delays.

Table 5. Work cycle time prediction models.

Equations	*F*	R^2	R^2_{adj}	SE	*p*-Value
$T_{net,TY} = 1.88 + 0.026 \cdot L_{TY} + 0.053 \cdot i$. (1)	36.01	0.38	0.37	0.59	<0.05
$T_{net,CS} = 26.84 + 0.028 \cdot L_{CS} + 3.15\, n_{CS}$. (2)	18.11	0.57	0.54	5.21	<0.05
$T_{TY} = 0.26 \cdot L_{TY} - 1.44 \cdot l - 6.08 \cdot n_{TY}$. (3)	10.50	0.21	0.19	32.32	<0.05
$T_{CS} = 0.29 \cdot L_{CS} + 3.64 \cdot V_{CS}$. (4)	21.04	0.61	0.58	5.30	<0.05

Note: $T_{net,TY}$—delay-free cycle time, tower yarder; L_{TY}—yarding distance, tower yarder; *i*—terrain slope angle; $T_{net,CS}$—delay-free cycle time, clambunk skidder; L_{CS}—skidding distance; n_{CS}—number of stems; T_{TY}—total cycle time, tower yarder; *l*—lateral yarding distance; n_{TY}—load's number of trees; T_{CS}—total cycle time, clambunk skidder; V_{CS}—load volume per phase, clambunk skidder.

3.2. Duration of Work Cycle Elements—Clambunk Skidder

The clambunk skidder work cycles (Figure 5) were subdivided into the following (including delays): winching (W) occupied 36% of the time, followed by travel loaded (TL) 22%, travel unloaded (TU) 11%, loading (LOAD) 4%, unloading (UNLOAD) 3%, sorting and piling (SP) 3%, and maneuvering (M) 1%, respectively. The percentages of time excluding delays were as follows: W occupied 45% of time, TL 27%, TU 14%, LOAD

5%, UNLOAD 4%, SP 4%, and M 1%, respectively. The delays accounted for 19% of the total cycle time and are divided into operational and mechanical delays, respectively, for 16% and 3% of the total cycle time of the clambunk skidder. The operational efficiency obtained during the study of the Timberjack 1710 clambunk skidder extracting whole eucalyptus trees for chipping was 78.30%, while mechanical availability was 87.38% [29]. From Table 5, the delay-free clambunk skidder cycle time $T_{net,CS}$ regression model (2) shows that a reduction can be achieved by reducing the number of stems n_{CS} in the payload. The same conclusion applies to the total cycle time of the clambunk skidder T_{CS} given by Equation (4). Within the subdivision of operations of the clambunk skidder (excluding delays), winching (36%), and movement (34%) took up the most time, followed by loading and unloading (7%) and sorting and piling at landing (3%). The mean speed of the studied clambunk skidder was 4.25 km·h^{-1}. The clambunk skidder with a load had an average speed of 3.23 km·h^{-1}, and an average of 6.28 km·h^{-1} without a load. The difference is 3.05 km·h^{-1}—almost double the unloaded weight since the skidding resistance forces of the rear parts of the stems do not act when moving without a load.

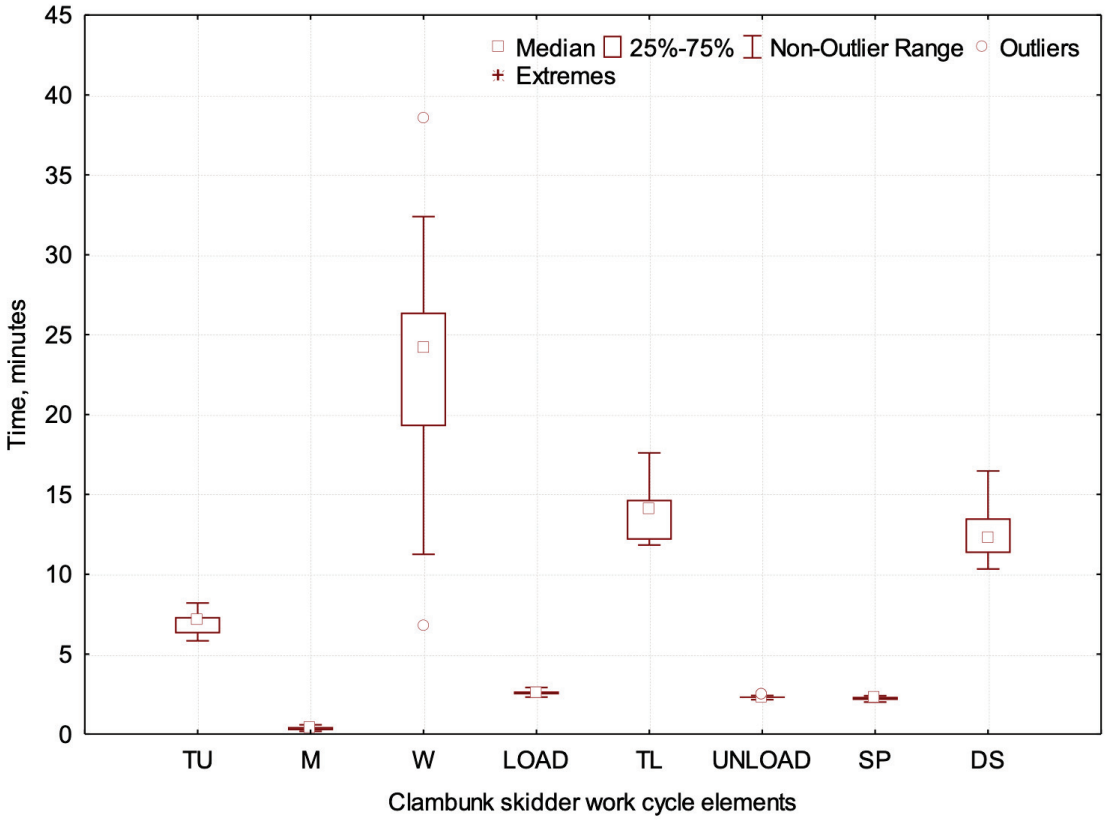

Figure 5. Elemental time consumption of clambunk skidder. Note: TU—travel unloaded, M—maneuvering, W—winching, LOAD—loading, TL—travel loaded, UNLOAD—unloading, SP—sorting and piling, DS—delays.

Orlovský et al. [38], for an LKT 81 ILT cable skidder with knuckle-boom, stated an average speed of 3.75 km·h^{-1} with load, and an average speed of 4.45 km·h^{-1} without load, i.e., lower than the values we found. However, Spinelli and Magagnotti [39] reported an average speed of 8.1 km·h^{-1} without load and an average speed of 7.3 km·h^{-1} loaded travel, for a 96 kW agricultural tractor, significantly higher than this study. Also, for a John Deere 548H, the average speed was 8.60 km·h^{-1} and 6.00 km·h^{-1}, respectively, for travel loaded and unloaded [38]. To reduce movement time, the clambunk skidder should increase its travel speed. Unfortunately, the terrain conditions do not afford a significant increase in speed.

3.3. Productivity Analysis

The productivity of the studied machines was described by the regression equations (Table 6). The tower yarder productivity (without delays), described by Equation (5) in Table 6, can be increased by reducing distance and skyline slope and increasing load volume. The same can be said for tower yarder productivity including delays (Equation (6)) by reducing lateral yarding distance. Another option is a truck-based yarder with a hydraulic crane with a grapple to place the yarded stems on the road. If the hydraulic crane is equipped with a processor head, crosscutting and subsequent forwarding of assortments (logs) is possible. In these two cases, one will move from a serial to a parallel production system.

Table 6. Productivity prediction models.

Equations	F	R^2	R^2_{adj}	Std. Error	p-Value
$P_{PMH,TY} = 7.63 - 0.041 \cdot L_{TY} - 0.11 \cdot i + 9.67 \cdot V_{TY}$, $m^3 \cdot h^{-1}$ (5)	110.48	0.74	0.73	1.07	$p < 0.05$
$P_{SMH,TY} = 9.11 - 0.084 \cdot L_{TY} + 0.36 \cdot l + 3.39 \cdot n_{TY}$, $m^3 \cdot h^{-1}$ (6)	22.50	0.37	0.35	3.08	$p < 0.05$
$P_{PMH,CS} = 4.42 - 0.0036 \cdot L_{CS} + 0.84 \cdot V_{CS}$, $m^3 \cdot h^{-1}$ (7)	63.27	0.91	0.81	0.61	$p < 0.05$
$P_{SMH,CS} = 2.35 - 0.0021 \cdot L_{CS} + 0.79 \cdot V_{CS}$, $m^3 \cdot h^{-1}$ (8)	106.40	0.89	0.88	0.40	$p < 0.05$

Note: $P_{PMH,TY}$—productivity machine hours, tower yarder; L_{TY}—yarding distance, tower yarder; i—terrain slope angle; V_{TY}—load volume per phase, tower yarder; $P_{SMH,TY}$—scheduled machine hours, tower yarder; l—lateral yarding distance; n_{TY}—load's number of trees; $P_{PMH,CS}$—productivity machine hours, clambunk skidder; L_{CS}—skidding distance; V_{CS}—load volume per phase, clambunk skidder; $P_{SMH,CS}$—scheduled machine hours, clambunk skidder.

From Equation (7), to increase the clambunk skidder delay-free productivity, the load volume per phase V_{CS} should be increased, whereas the skidding distance L_{CS} in it should be decreased. The clambunk skidder productivity including delays is calculated by Equation (8) in Table 6, and the opportunities for increase are the same as for delay-free productivity.

Consequently, the productivity models indicate skidding distance and load volume extracted per phase (turn) as the most important factors affecting the skidding productivity of the studied clambunk skidder in the conditions of thinning in European beech forests. Of course, further studies could evaluate the influence of other variables to compare productivity in several stands.

The average productivity, obtained at an average skidding distance of 693 m, average load volume per cycle of 5.02 m^3, and mean 6.6 stems per phase (turn), is 6.23 $m^3 \cdot PMH^{-1}$ and 4.93 $m^3 \cdot SMH^{-1}$ respectively.

These productivity rates are close to those reported by Orlovský et al. [38] for the LKT 81 ILT with knuckle-boom loader, which, at an average skidding distance of 316 m and mean load volume per phase of 8.00 m^3, are 6.31 $m^3 \cdot PMH^{-1}$ and 4.20 $m^3 \cdot SMH^{-1}$, respectively. Borz et al. [40] determined a higher value of productivity in terms of PMH and SMH (4.40 $m^3 \cdot h^{-1}$ and 3.10 $m^3 \cdot h^{-1}$, respectively) testing a TAF 690 skidder covering an average distance of 1700 m. The mean productivity for a TAF 690 PE in similar terrain conditions and a shelterwood system obtained by Stoilov et al. [24] was 16.0 $m^3 \cdot PMH^{-1}$ and 14.00 $m^3 \cdot SMH^{-1}$, respectively, for an average distance of 264 m (2.6 shorter than that in this present study), mean load volume of 3.94 m^3 (1.3 lower than that in this present study), and mean 2.2 logs per travel.

For the John Deere 548H skidder, Proto et al. [37] registered a harvesting performance of 30.5 m^3 per PMH and 25 m^3 per SMH in conditions of an average seven logs extracted per turn, at a mean extraction distance of 275 m, average and maximum winching distances, respectively, of 35 and 65 m, and a mean volume skidded per cycle of 3.90 m^3.

The tower yarder and clambunk skidder present a serial production system. In the serial system the production processes are performed individually in sequence [41], since after the stems are extracted by the tower yarder, the skidding process starts.

The use of the serial production system for timber extraction allows both machines to be used more rationally and thoroughly, and, consequently, increases their productivity, improves the technical maintenance of equipment and current repairs, ensures the possible full compliance of forestry equipment with natural production conditions, and, ultimately, increases the efficiency of logging production. For a serial production system of machines to be effective in specific terrain and production conditions, it must be designed in such a way that their productivity must be equal or multiple and efficient for a given volume of production. This study ensures the full rate of utilization of equipment, reduces production costs, and allows for reducing manual labor in the forest stand to the minimum possible, i.e., only until felling, delimbing, pulling, and hooking the stems to the yarder mainline. The majority of operations are carried out at convenient workplaces near forest roads and landings, which reduces the risk of occupational injuries. In addition, the use of the forwarder crane supports the bucking, sorting and piling of the received assortments on the landing.

Therefore, by equating the delay-free productivity models of the two machines, parameter values can be determined. The effect of the yarding distance L_{TY} on the skidding distance L_{CS} for a skyline slope of 17° and carriage payload of 1 m^3 is shown in Figure 6a.

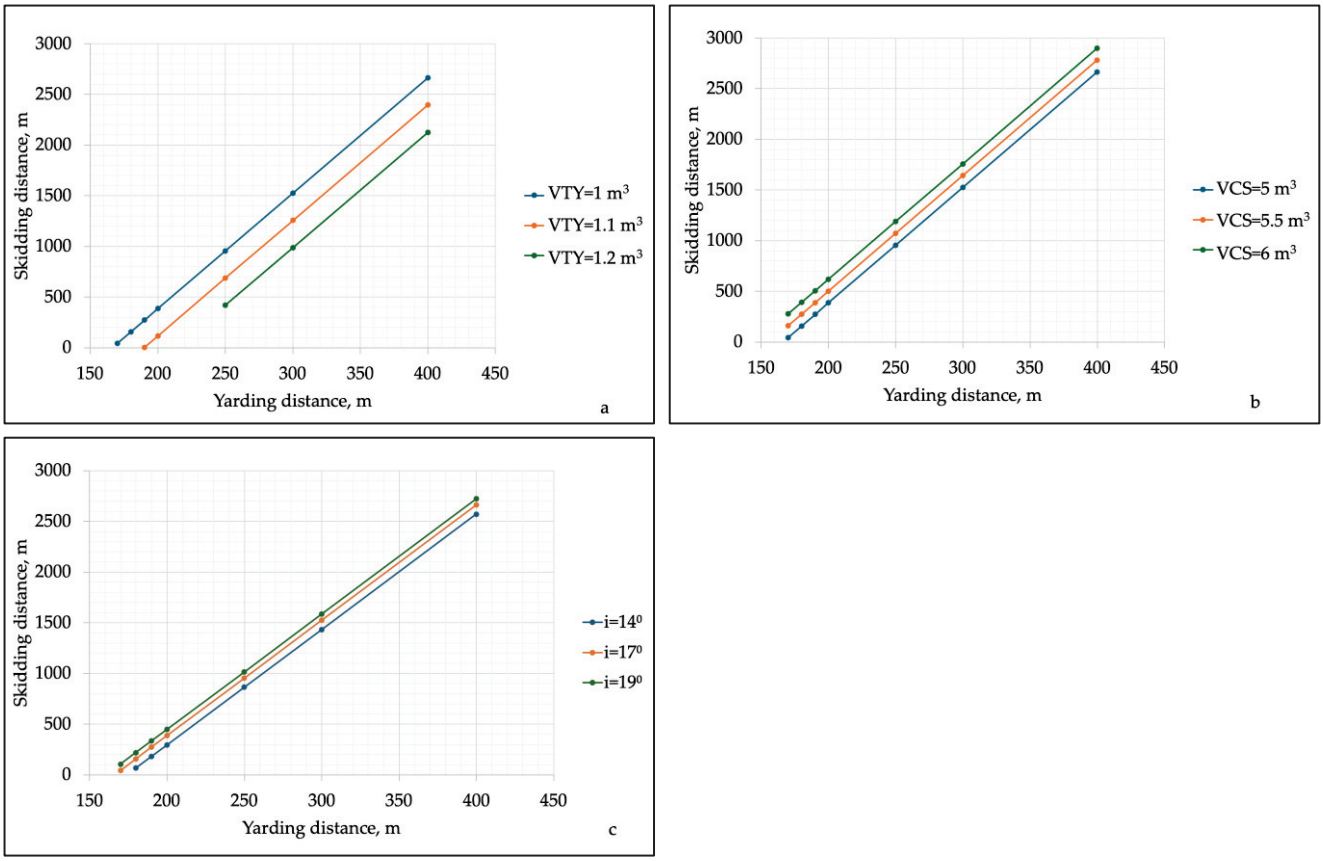

Figure 6. (**a**–**c**) Different parameters influenced by yarding distance and skyline slope. Note: VTY—load volume per phase, tower yarder; VCS—load volume per phase, clambunk skidder, *i*—terrain slope angle.

An increase in yarding distance and skidder payload results in an increase in skidding distance where delay-free productivity is equal. An increase in carriage payload has a similar effect on the skidding distance at constant values of skyline slope of 17° and skidder payload of 5 m^3 (Figure 6b). The influence of skyline slope with other parameters constant is shown in Figure 6c. Increasing the skyline slope, other parameters being constant, leads

to a decrease in delay-free yarding productivity, but an increase in the corresponding skidding distance.

3.4. Costs

The extraction net costs of the studied production system for stem yarding and skidding in a beech stand were calculated at 120.87 € PMH and the harvesting costs at 14.93 €/m^3 (Table 7). The gross extraction costs of a Koller K501 for cutting trees in a predominantly beech stand were calculated at 13 €/m^3 [9], slightly lower than that of the tower yarder and clambunk skidder studied here. The net extraction costs of a Timberjack 1010D combi–forwarder in similar production and terrain conditions were estimated at 4.1 €/m^3 [20], which is three times lower.

Table 7. Extraction costs.

Classification of Costs	Costs per Hour, € h^{-1}		
	Valentini V400	Timberjack 1010D	Production System
Purchase price	130,000	25,000	155,000
Total fixed costs:	21.08	10.79	31.27
Depreciation	5.85	7.50	13.35
Interest	3.93	0	3.93
Insurance	9.67	0.74	10.41
Garaging	0.74	0.74	1.48
Taxes	0.15	0.07	0.23
Machine transfer	0.74	0.74	1.48
Total variable costs:	23.63	25.66	49.29
Fuel and lubricants	15.53	15.53	31.06
Tires and tracks	0.60	2.64	3.24
Maintenance and repair	4.55	7	11.55
Winch cables and choker cables	2.95	0.49	3.44
Labor costs	26.66	13.2	39.86
Net costs	71.37	49.5	120.87
Net costs, € per m^3	6.90	8.03	14.93

Note: The purchase price of the Valentini V400 includes the price of the tractor.

In comparison, Proto et al. have determined that the costs of skidding for a John Deere 548H skidder in chestnut stands in South Italy were between 3.6 and 5.8 €·m^{-3} (for an average distance reaching between 266 and 276 m, an average load between 3.88 and 4.01 m^3, and an average slope of 27%) [37]. In Kardzhali Province (Bulgaria), Stoilov et al. [42] reported an extraction cost of an HSM 805 ZL double-drum cable skidder equal to 14.24 €·m^{-3} in a stand of conifers (for an average distance of 69 m, an average load 4.06 m^3, and an average slope of 34%).

In general, these costs are slightly above the extraction costs reported with other machines in this region. This is probably due to the lower performance of the studied extraction system, due to longer delays.

4. Conclusions

The studied extraction system has many advantages. Very often, on steep terrains, in the absence of sufficient landing space, logs which were obtained in a cutting area under difficult working conditions are yarded. The yarder's unloading area must be cleared after each turn for new carriage loads. In the case studied, the yarded stems are pulled with the winch of the skidder. Otherwise, they will inevitably fall back into the clearing. It is also possible to pull the stems with an additional winch or tractor, even with animal power.

The studied system allows for the extraction of stems or stem sections, which reduces operations in clearing, felling, and delimbing, and the remaining operations of crosscutting, sorting, and piling are performed after skidding on the landing under more convenient working conditions.

A disadvantage of the studied extraction system is the long delays due to the skidder waiting for a sufficient load to be collected, and subsequently, during skidding, the yarder waits with the extracted load on the carriage for the skidder to return to pull the load onto the skid road.

Author Contributions: Conceptualization, S.F.P., S.S. and A.R.P.; methodology, S.F.P., S.S., G.A., A.Z. and K.P.; software, S.S. and G.A.; validation, S.S. and A.R.P.; resources, A.R.P.; data curation, S.S. and A.R.P.; writing—original draft preparation, S.F.P., S.S., M.F.C., A.Z. and A.R.P.; writing—review and editing, S.F.P., S.S. and A.R.P. All authors have read and agreed to the published version of the manuscript.

Funding: This research received no external funding.

Data Availability Statement: Data are contained within the article.

Acknowledgments: This work was supported by the inter-institutional agreement between the University of Forestry (Bulgaria) and the Mediterranean University of Reggio Calabria (Italy) and by the PhD course "Agricultural, Food and Forestry Science" of the Mediterranean University of Reggio Calabria (Italy)—XXXIX cycle.

Conflicts of Interest: The authors declare no conflicts of interest.

References

1. Schweier, J.; Klein, M.L.; Kirsten, H.; Jaeger, D.; Brieger, F.; Sauter, U.H. Productivity and cost analysis of tower yarder systems using the Koller 507 and the Valentini 400 in southwest Germany. *Int. J. For. Eng.* **2020**, *31*, 172–183. [CrossRef]
2. Stoilov, S.; Proto, A.R.; Angelov, G.; Papandrea, S.F.; Borz, S.A. Evaluation of salvage logging productivity and costs in sensitive forests of Bulgaria. *Forests* **2021**, *12*, 309. [CrossRef]
3. Stoilov, S.; Angelov, G.; Panicharova, T.; Mederski, P.S.; Proto, A.R. Modeling productivity and estimating costs of processor tower yarder in shelterwood cutting of pine stand. *Forests* **2023**, *14*, 195. [CrossRef]
4. LeDoux, C.B.; Huyler, N.K. *Cost Comparisons for Three Harvesting Systems Operating in Northern Hardwood Stands*; Research Paper NE-715; U.S. Department of Agriculture, Forest Service, Northeastern Research Station: Newtown Square, PA, USA, 2000; 4p. [CrossRef]
5. Spinelli, R.; Magagnotti, N.; Lombardini, C. Performance, capability and costs of small-scale cable yarding technology. *Small-Scale For.* **2010**, *9*, 123–135. [CrossRef]
6. Tampekis, S.; Kantartzis, A.; Arabatzis, G.; Sakellariou, S.; Kolkos, G.; Malesios, C. Conceptualizing Forest Operations Planning and Management Using Principles of Functional Complex Systems Science to Increase the Forest's Ability to Withstand Climate Change. *Land* **2024**, *13*, 217. [CrossRef]
7. Peters, P.A.; LeDoux, C.B. *Stream Protection with Small Cable Yarding Systems*; Northeastern Forest Experiment Station, USDA Forest Service: Morgantown, WV, USA, 1984; 17p.
8. Spinelli, R.; Magagnotti, N.; Cosola, G.; Labelle, E.; Visser, R.; Erber, G. The Effect of Yarding Technique on Yarding Productivity and Cost: Conventional Single-Hitch Suspension vs. Horizontal Double-Hitch Suspension. *Croat. J. For. Eng.* **2021**, *43*, 369–380. [CrossRef]
9. Stoilov, S. Productivity and costs of cable yarding in group shelterwood system in deciduous forests. *For. Ideas* **2021**, *27*, 331–342.
10. LeDoux, C.B. *Stump-to-Mill Timber Production Cost Equations for Cable Logging Eastern Hardwoods*; USDA Forest Service, Research Paper NE-566; U.S. Department of Agriculture, Forest Service, Northeastern Forest Experiment Station: Broomall, PA, USA, 1985; 6p. [CrossRef]
11. LeDoux, C.B. When is Hardwood Cable Logging Economical? *J. For.* **1985**, *83*, 295–298. [CrossRef]
12. Huyler, N.K.; LeDoux, C.B. *Cycle-Time Equation for the Koller K300 Cable Yarder Operating on Steep Slopes in the Northeast*; Research Paper NE-705; U.S. Department of Agriculture, Forest Service, Northeastern Forest Experiment Station: Radnor, PA, USA, 1997; 4p. [CrossRef]
13. Huyler, N.K.; LeDoux, C.B. Yarding cost for the Koller K300 cable yarder: Results from field trials and simulations. *North. J. Appl. For.* **1997**, *14*, 5–9. [CrossRef]
14. Visser, R.; Shawn, B.; Hank, S. *Cable Logging Opportunities in the Appalachian Mountains*; US Forest Service: Washington, DC, USA, 2001.
15. Zimbalatti, G.; Proto, A.R. Cable logging opportunities for firewood in Calabrian forests. *Biosyst. Eng.* **2009**, *102*, 63–68. [CrossRef]

16. Proto, A.R.; Zimbalatti, G. Firewood cable extraction in the southern Mediterranean area of Italy. *For. Sci. Technol.* **2016**, *12*, 16–23. [CrossRef]
17. Dimitrov, D. Investigation on work time and productivity of forest skyline Koller K 300 in Ograzhden Mountain. *For. Ideas* **2012**, *18*, 92–96.
18. Melemez, K.; Tunay, M.; Emir, T. A comparison of productivity in five small-scale harvesting systems. *Small-Scale For.* **2014**, *13*, 35–45. [CrossRef]
19. EFA. *Annual Report of Executive Forest Agency*; Executive Forest Agency (EFA), Ministry of Agriculture: Sofia, Bulgaria, 2022; 80p.
20. Stoilov, S.; Proto, A.R.; Oslekov, D.; Angelov, G.; Papandrea, S.F. Forest operations using a combi–forwarder in deciduous forests. *Small-Scale For.* **2023**, *23*, 25–40. [CrossRef]
21. Kellogg, L.D. *Machines and Techniques for Skyline Yarding of Smallwood*; Research Bulletin 36; Forest Research Laboratory, School of Forestry, Oregon State University: Corvallis, OR, USA, 1981; 17p.
22. Kellogg, L.D.; Olsen, E.D. *Increasing the Productivity of a Small Yarder: Crew Size, Skidder Swinging, Hot Thinning*; Research Bulletin 46; Forest Research Laboratory, School of Forestry, Oregon State University: Corvallis, OR, USA, 1984; 45p.
23. Senturk, N.; Özturk, T.; Demir, M. Productivity and costs in the course of timber transportation with the Koller K300 cable system in Turkey. *Build. Environ.* **2007**, *42*, 2107–2113. [CrossRef]
24. Stoilov, S.; Papandrea, S.F.; Angelov, G.; Oslekov, D.; Zimbalatti, G.; Proto, A.R. Productivity analysis and costs of wheel cable skidder during salvage logging in European beech stand. *J. Agric. Eng.* **2023**, *54*, 2. [CrossRef]
25. LeDoux, C.B. *Mechanized Systems for Harvesting Eastern Hardwoods*; Gen. Tech. Rep. NRS-69; U.S. Department of Agriculture, Forest Service, Northern Research Station: Newtown Square, PA, USA, 2010; 13p. [CrossRef]
26. Stokes, B.J. Schilling, Improved harvesting systems for wet sites. *For. Ecol. Manag.* **1997**, *90*, 155–160. [CrossRef]
27. Stokes, B.J.; Ashmore, C.; Rawlins, C.L.; Sirois, D.L. *Glossary of Terms Used in Timber Harvesting and Forest Engineering*; General Technical Report SO—73; U.S. Department of Agriculture, Forest Service, Southern Forest Experiment Station: New Orleans, LA, USA, 1989; 33p. [CrossRef]
28. Oberholz, F. Articulated skidders. Forest Engineering South Africa. 2002. Technical Note 1/5-2002. 7p. Available online: https://forestry.co.za/ (accessed on 7 May 2024).
29. Dos Santos, P.H.A.; de Souza, A.P.; da Cunha Marzano, F.L.; Minette, L.J. Produtividade e custos de extração de madeira de Eucalipto com clambunk skidder (Productivity and costs of eucalyptus wood extraction with Clambunk skidder). *Rev. Árvore Viçosa-MG* **2013**, *37*, 511–518. [CrossRef]
30. Ghaffariyan, M.R. Reviewing productivity studies of skidders working in coniferous forests and plantations. *Silva Balc.* **2020**, *21*, 83–98. [CrossRef]
31. Kellogg, L.D.; Milota, G.V.; Miller, J.R.M. A Comparison of Skyline Harvesting Costs for Alternative Commercial Thinning Prescriptions. *J. For. Eng.* **1996**, *7*, 7–23. [CrossRef]
32. Olsen, E.D.; Hossain, M.M.; Miller, M.E. *Statistical Comparison of Methods Used in Harvesting Work Studies*; College of Forestry, Forest Research Laboratory: Corvallis, OR, USA, 1998.
33. Proto, A.R.; Skoupy, A.; Macrì, G.; Zimbalatti, G. Time consumption and productivity of a medium size mobile tower yarder in downhill and uphill configurations: A case study in Czech Republic. *J. Agric. Eng.* **2016**, *47*, 216–221. [CrossRef]
34. Munteanu, C.; Ignea, G.H.; Akay, A.E.; Borz, S.A. Yarding pre-bunched stems in thinning operations: Estimates on time consumption. *Bull. Transilv. Univ. Bras. Ser. II For. Wood Ind. Agric. Food Eng.* **2017**, *10*, 43–54.
35. Ackerman, P.; Belbo, H.; Eliasson, L.; De Jong, A.; Lazdins, A.; Lyons, J. The COST model for calculation of forest operations costs. *Int. J. For. Eng.* **2014**, *25*, 75–81. [CrossRef]
36. Spinelli, R.; Magagnotti, N. The effects of introducing modern technology on the financial, labour and energy performance of forest operations in the Italian Alps. *Forest Policy Econ.* **2011**, *13*, 520–524. [CrossRef]
37. Proto, A.R.; Macrì, G.; Visser, R.; Russo, D.; Zimbalatti, G. Comparison of Timber extraction Productivity between Winch and Grapple Skidding: A Case Study in Southern Italian Forests. *Forests* **2018**, *9*, 61. [CrossRef]
38. Orlovský, L.; Messingerová, V.; Danihelová, Z. Analysis of the time efficiency of skidding technology based on the skidders. *Cent. Eur. For. J.* **2020**, *66*, 177–187. [CrossRef]
39. Spinelli, R.; Magagnotti, N. Wood extraction with farm tractor and sulky: Estimating productivity; cost and energy consumption. *Small-Scale For.* **2012**, *11*, 73–85. [CrossRef]
40. Borz, S.A.; Ignea, G.; Popa, B.; Spârchez, G.; Iordache, E. Estimating time consumption and productivity of roundwood skidding in group shelterwood system—A case study in a broadleaved mixed stand located in reduced accessibility conditions. *Croat. J. For. Eng. J. Theory Appl. For. Eng.* **2015**, *36*, 137–146.
41. Yoshimura, T.; Suzuki, Y.; Sato, N. Assessing the Productivity of Forest Harvesting Systems Using a Combination of Forestry Machines in Steep Terrain. *Forests* **2023**, *14*, 1430. [CrossRef]
42. Stoilov, S.; Angelov, G.; Aladzhov, S.; Nichev, P. Productivity models and costs of combined skidder-Harvester in coniferous forests. *For. Ideas* **2021**, *27*, 169–181.

Disclaimer/Publisher's Note: The statements, opinions and data contained in all publications are solely those of the individual author(s) and contributor(s) and not of MDPI and/or the editor(s). MDPI and/or the editor(s) disclaim responsibility for any injury to people or property resulting from any ideas, methods, instructions or products referred to in the content.

forests

MDPI

Review

Comparison between Different Mechanization Systems: Economic Sustainability of Harvesting Poplar Plantations in Italy

Valerio Di Stefano [1,2], Giorgia Di Domenico [1,2,*], Michele Menta [1], Elisa Pontuale [2], Leonardo Bianchini [1] and Andrea Colantoni [1]

[1] Department of Agriculture and Forest Sciences (DAFNE), University of Tuscia, Via S. Camillo de Lellis snc, 01100 Viterbo, Italy; valerio.distefano@crea.gov.it (V.D.S.); l.bianchini@unitus.it (L.B.); colantoni@unitus.it (A.C.)

[2] Council for Agricultural Research and Economics, Research Centre for Forestry and Wood, Via Valle della Quistione, 27, 00166 Rome, Italy

* Correspondence: giorgia.didomenico@crea.gov.it; Tel.: +39-06-47836241

Abstract: After a period of significant development, poplar cultivation in Italy has been in rapid decline since the 1980s. Because of its marked ductility, poplar is valuable for both wood furniture and energy production. Production could be increased through mechanization, because innovative machinery and equipment can reduce the exposure of forest workers to common risk factors, ensure greater and better productivity, increase the efficiency of operations, and reduce costs. There are various systems for the mechanization of poplar production (from traditional to advanced and pushed mechanization). We describe the range of possibilities (in terms of both the techniques adopted and the machines used) for planting, harvesting, and chopping poplar. Based on our analysis of operating costs, we conclude that mechanized poplar production could reduce the average cost per ton of wood chips (EUR/t) by 23% and the average gross cost per hectare of wood chips produced (EUR/ha) by 37%.

Keywords: poplar cultivation; mechanization; harvesting systems; economic sustainability

1. Introduction

In Italy, the management of forest stands of natural origin is increasingly oriented towards the promotion of functions of a non-speculative nature and of public environmental interest. In this context, the sustainable production of wood from poplar trees plays a significant role in storing carbon dioxide from the atmosphere, sequestering it in long-term works (such as furniture, building materials, etc.). This practice contributes to the pursuit of collective well-being, promoting climate change mitigation and environmental and landscape improvement in rural areas.

While, on the one hand, the environmental functions can be entrusted more with the natural forest heritage, on the other hand, the economic productive function is increasingly delegated to arboriculture plants. These plants provide a positive response to the needs of accelerated production (with increases not reachable in the forest), the possibility of better planning, and the search for consistency and homogeneity of the dimensions and technological characteristics of the assortments obtainable [1], while carrying out in part the environmental functions delegated to the natural forest patrimony. In this regard, the common agricultural policy (CAP) provides economic incentives for the cultivation of more environmentally sustainable poplar hybrids (MSA), at the suggestion of the "From Farm to Fork" strategy [2], with the aim of contributing to carbon neutrality by 2050 [3].

The poplar cultivation sector in Italy is undergoing an important evolution, both in technical and economic terms: from 2018 to today, the price per ton of poplar wood has increased by 50% from EUR 45 to 50 per ton to the current EUR 100–110 per ton.

The reasons for this evolution are many, and the most important is certainly the ductility of poplar wood: soft, whitish and light, it lends itself well to being worked, glued, and painted. It can be used in various economic and production sectors such as carpentry (packaging, scaffolding elements, wood wool, plywood, chipboard, matches, and occasionally furniture) and in the paper industry [4]. For outdoor use, poplar wood is usually heat-treated. Moreover, poplar is a renewable energy source; it is among the most efficient tree species, as—more than others—it optimizes the production yield of biomass that is used to produce thermal and electrical energy.

However, a careful analysis of the state of poplar cultivation is difficult today due to the progressive reduction in the information base, not only on the extent of cultivated areas, production, and the number of operators, but also economic variables directly linked to production (timber prices, costs of cultivation operations, concession fees, etc.). It is true, however, that the growing increase in labor costs in recent years has not been fully offset by an increase in the market value of the timber product, and for the entrepreneur to maintain their business, they are necessarily forced to keep costs as low as possible. The costs derived from crop production contribute significantly to the final cost of the biomass [5,6] and there are many aspects of the agronomic process that could be optimized through applying science and innovation. Therefore, it is necessary to identify these aspects correctly as a first step to finding alternative solutions [7,8]. To increase the economic sustainability of poplar weights, productivity, and therefore the competitiveness of the material on the market, it is certainly necessary to strengthen and improve the level of mechanization by encouraging the use of more innovative machines [9].

The benefits of mechanization development from the 1980s to the present are evident [10]: an increase in the level of mechanization offers advantages to wood workers not only in reducing costs and increasing the productivity of the yard [10], but also in ensuring greater worker safety [11–13]. In the present work, three possible levels of mechanization to be used in the different phases of the forest worksite (felling/staging, harvesting, shredding, and loading) are distinguished and analyzed: (i) traditional, (ii) advanced, and (iii) pushed.

While at the traditional level, the use of a chainsaw is mainly expected, at the advanced one, the abatement occurs with a head of abatement (e.g., pliers with clamping arms and cutting device at the base, mounted on a hydraulic articulated arm of a machine with sufficient power, normally >80 kw), thus leaving the staging phase to the chainsaw. The integration of mechanical means takes place in heavy mechanization in which a series of combined saws called combined harvesters (both for felling and for setting up) are used.

For the harvesting phase, more traditional means, such as the use of a tractor with the addition of a winch (traditional and advanced mechanization) [14], have been replaced by more advanced means, such as by a forwarder or an articulated trolley and a skidder or an articulated tractor equipped with pliers and/or winch.

The aim of this work is to analyze the main mechanization techniques present in the field of poplar cultivation, deepening the multitude of machines used in forestry processing and devoting ample space to the analysis of the operating costs of equipment in a comparative perspective with respect to the most effective and sustainable level of mechanization.

The following techniques were used for this review of the scientific literature: the main search engine used was the Scopus and Science Direct database. Keywords such as forestry mechanization, poplar cultivation, short rotation coppice, harvesting systems, and operating costs were used for the research. There was also bibliographical research at the library of the Council for Research in Agriculture and Economics (CREA) in Rome and Casale Monferrato (AL). The selection criteria for the articles for this review focus on the year of publication, preferring the most recent scientific publications except for the issue of operating costs, as there is no recent literature on this subject, and on the consistency with the main species under analysis, namely poplar. Articles with a similar type of cultivation of forest species and category of use of final biomass were also considered.

2. Poplar Cultivation in Italy

The poplar cultivation in Italy is a sector of excellence to produce wood for industrial and energy use [4]. Wood arboriculture occupies about 100,000 ha [15] and the sector is dominated by poplar cultivation that, compared to the total forest area, provides half of the annual harvests of wood [16]. Covering less than 1% of the national forest area, 46,125 ha in total, it supplies about 1 million m^3 of round wood per year, equal to 45% of the domestic round wood [17]. The production area is located for 94% in the Po Valley with prevalence in Lombardy and Piedmont (70%) for a total of over 32,000 ha of poplar. More than 50% of the area falls in floodplain areas, just under 30% in Special Protection Areas (SPAs), while the remaining 20% is in Sites of Community Interest (SCI) and in park areas [4].

It should be noted that since the period 1950–1970, there has been a phase of great development of Italian poplar cultivation, the extension of which has reached over 170,000 ha of plantations. However, since the 1980s, poplar plantations have experienced a period of marked and constant decline until they reached less than half of the initial values, or about 83,000 ha [18].

According to the last National Forest Inventory [19], the Italian area of artificial poplar in 2015 is equal to 51,592 hectares with a total surface loss of 14,678 ha compared to 2005. According to [4], other estimates made on a sample basis in 2018 with reference to poplar weights of a surface equal to or greater than 5000 m^2, excluding polycyclic poplar plantations, reported that the total area of poplar trees in Italy is equal to 46,125 ha. Considering the above, the estimates underline the already known phase of decline with a loss of about 40,000 ha compared to the beginning of the year 2000. The following histogram (Figure 1) shows the estimated regional area (ha) for poplar cultivation in Italy in 2015 and 2018.

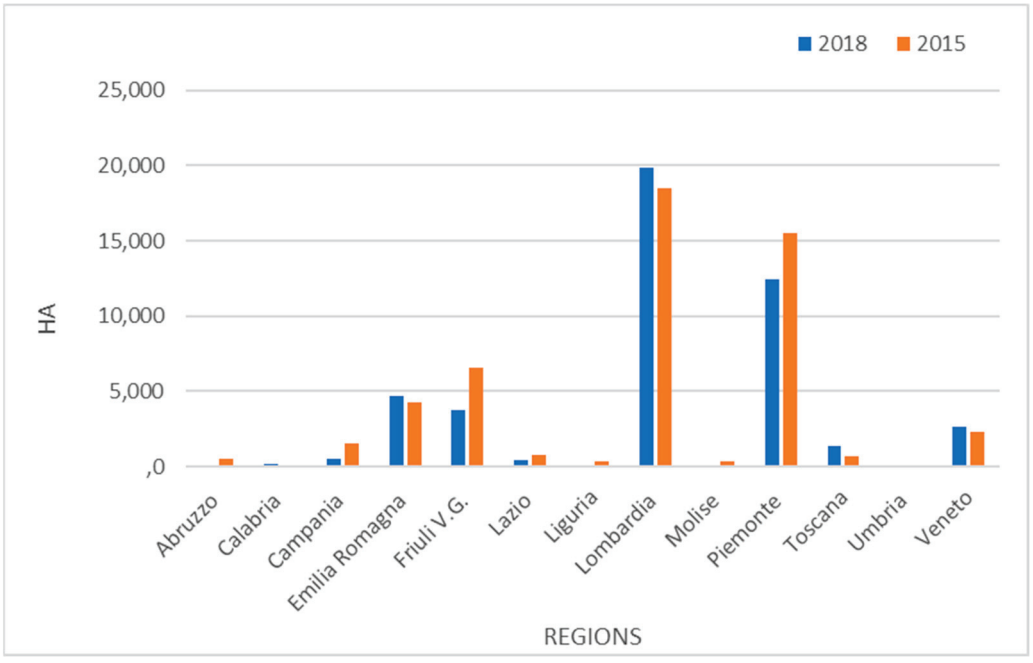

Figure 1. Regional estimated area (ha) for poplar cultivation in Italy in 2015 [19]–2018 [4]. The histogram shows only those regions with poplar cultivation with an extension of more than 50 ha in the years considered.

3. Mechanization in Plant Systems

The short rotation coppice (SRC) is a cultivation system that has been adopted for about thirty years in Italy for fast-growing species [20] such as poplar. It is used, generally, to produce biomass (wood chips for energy uses or as industrial material). This model provides a high level of density (5000–10,000 plants per hectare) and yield shifts every

2–3 years [21–25]. By applying longer shifts (5–7 years), the model is also referred to as medium rotation coppice (MRC) [20,26]. In the latter case, the density is about 1600/ha plants and the aim is the production of biofuel [27].

Finally, the traditional planting system provides for 8–12-year shifts and cultivation densities of 280–300 plants per hectare, and the final product is good-quality wood for industry and to produce products such as paper, sawn timber, and panels [28].

The economic viability of the plant depends mainly on minimizing the cost of production of the final product, especially in the case of SRC and MRC, taking into account the low commercial value of wood chips and the competition that this has on the market (there are much cheaper materials such as sawmill waste). This reduction in the cost of production can only be achieved through the complete and efficient mechanization of field operations; among these, the most expensive are certainly harvesting and planting [14,29,30].

Starting from the plant phase, there are different models of machines that differ in the type of transplant organs, the type of feed, or the type of plant material used. In the case of the SRC, and therefore of a cultivation system characterized by a sixth of the "dense" plant, the best propagation material is the cutting, while for a sixth of the "sparse" plant, generally used in the MRC or in a traditional plant, the rod is used (pegs of about 2 m) [31].

For the planting of the cuttings, it is possible to mechanize the whole process using machines capable of operating a mechanized burial. The machines to be used are: Rotor planter and Spapperi discs transplanter (Figures 2 and 3).



Figure 2. *New Holland* TD5050 crawler *Rotor* planter in experimental farm "Ovile" in Rome.



Figure 3. *Spapperi* hydraulic cuttings transplanter.

The first machine consists of a metal track with meshes fixed inside another cylinder, through which a piston operates. Thanks to the traction of the engine, this piston slides down, allowing for the insertion of the cutting into the cylinder. This system allows us to progressively insert the cutting vertically into the ground, whereby the planting takes place without the opening of a groove and without the air remaining around it. The *Rotor* is brought with a three-point linkage of tractors of at least 40 kW of power (55 HP) and for its operation, it requires three operators. The working speed is about 0.8–0.9 km/h with a labor requirement of 11.5 h/ha. The working capacity is 0.25 ha/h, with a productivity of about 1250/1500 cuttings/ha/employee.

The second is equipped with clamp injectors that carry out the transplantation, arranged radially and equidistant from each other on a large metal wheel that moves due to the drag caused by the movement of the tractor [32]. With the rotation of the wheel, when an injector element is found in a vertical position and perpendicular to the ground, a special proximity switch, through a solenoid valve, controls the extension of a hydraulic jack that, in turn, pushing the injector element down, inserts the cutting into the soil. The machine must be coupled to a tractor of at least 90 kW and its operation requires two operators. The working speed is about 1.4–1.6 km/h with a labor requirement of 3.5 h/ha. The working capacity is 0.87 ha/h, with a productivity of about 1750–1800 cuttings/ha/employee.

The rotor transplanter inflicts the cuttings vertically, while the disc transplant performs less accurate work, but is also able to mulch along the row with a plastic film with the dedicated module.

In the case of bolts, the cutting of the ground is carried out by means of a drill; the planting is performed manually by two operators; and the recoating is carried out by means of inclined ridgers (spreader) and compacting rollers. Now, there are only prototypes that are not yet on the market, such as the "R-Innova 500P", a machine developed on behalf of R-Innova by the agro-mechanical services company situated in Stagnati di Ostiano (Italy). These vehicles are also equipped with a platform for the transport of the material and an acoustic or light signal, electrically controlled by a device, indicating the transplantation distance [33].

In light of the above, the use of a semi-automatic cuttings transplanter, compared to the traditional manual or mechanization techniques of the first level, guarantees a significantly reduced working time and a limited use of labor [32].

4. Mechanization in Harvesting Systems

Harvesting systems are an essential component of woody biomass supply chains [34] and represent one of the most expensive processes along the entire production chain [35,36]. Poplar harvesting systems can be distinguished based on different parameters such as the density of the plant, the size of the trees, the space for handling the machines, the cultivation system, as well as the production purpose and the level of mechanization.

Generally, in the European Union's poplar yard, mechanization follows the custom-made harvesting model, in which the trees are taken in commercial lengths per log (cut-to-length—CTL). This is a fast and productive cutting method [37,38] that involves the use of a harvester that fells and prepares the logs in lengths generally of 2 m or 4 m, and then these are transported to the forest landing, through a forwarder. The use of CTL technology offers several advantages, in particular, an accurate evaluation and measurement of individual trees directly on the felling field, which is reflected in a better quality of the timber in terms of reducing the contamination of the logs, quality of uprooting, and recovered value [27,39,40].

At the same time, however, the CTL is relatively expensive and designed for processing single trees, which does not fit well with the limits imposed by plantations of small trees [40]. An alternative method is the harvesting system of the whole tree (whole-tree harvesting—WTH) [41], which consists of: (i) felling of whole trees, (ii) dragged by a skidder grapple on the landing, and (iii) transformed into trunks [27,39,42].

As can be seen, the WTH method requires three steps instead of the two required by the CTL method; however, the workflow is sustained at higher speeds, and the processing of trees, once on the ground, minimizes the influence of trunk size on extraction efficiency [27,43]. The WTH method, already particularly appreciated in the USA, is much more effective in terms of productivity in the felling and extraction operation, especially in the presence of constraints due to the reduced size of the trees, where the previous CTL method is unfavorable.

From an economic point of view, the WTH system provides a 10% higher productivity than the CTL system and a cost reduction of around 15 EUR/t [39]. However, the two methods shown are poorly specialized harvesting systems for medium-shift-coppice crops [44–46].

Two other harvesting systems exist and are widely diffused in the poplar trees of North America: system-to-peripheral accumulations and system-to-centralized accumulation.

The first involves felling and setting up by a dedicated machine characterized by a shear head; then the material is transported with a wheel loader to the landing where the woodchipper–root–debarker unit (CSS) is located. The centralized storage system, instead, provides the transportation of the felled plants to the storage area through a disc head mounted on a dedicated forestry tractor. Subsequently, they are transported with a forwarder to the roadside and divided according to the type of retractable assortment, sawn timber or discarded selvedges and/or small plants, whereby the latter are chipped through the CSS. Both work systems can produce more than 400 tons of biomass per day, with a total cost of EUR 12–24 per ton of biomass [46].

For the harvesting of young plantations, the only economically sustainable solution is multi-shaft handling (MTH), where more than one tree is collected per work cycle, compensating for small volumes of material [12,41]. In this case, the felling is made with a mini-crawler blast chiller characterized by a head equipped with a disc saw and accumulation arm, able to break down and accumulate two plants per work cycle, and concentrating six rows of plants on a single swath. This system is efficient and economical, having the advantage of using inexpensive and extremely mobile vehicles [46].

5. Mechanization in Chopping Systems

In recent years, the increasing use of alternative energy sources as opposed to fossil fuels and the consequent creation of power plants or small plants for the production of thermal energy has diversified the use of wood waste products. This is also in light of the main European policies and legislative acts enacted by the European Union itself, the European Green Deal and REPowerEU, which are also regarded as incentives for the use of renewable energy sources for greater environmental and energy sustainability [22,31]. The biomass produced by the chipping of short-rotation woody crops (SRWCs) is considered one of the most interesting options to generate renewable energy [47]. The production of wood chips also ensures the recovery of an average of 20–30% of biomass, which would otherwise be a residue of utilization [46]. With the chipper, it is possible to reduce the size of the original woody biomass up to a size of 2 × 2 cm; the larger the original product, the harder the machine will work, and it will take longer to chip. The poplar, due to the small size of its trunk and branches, is one of the forest species most suitable for chipping [48].

The lack of knowledge on harvesting [49] and the uncertainties regarding the expected costs and profits [50,51] are the main reasons why farmers hesitate to establish SRWCs [52].

In general, two different chopping systems are used for SRWCs: cut-and-store and cut-and-chip [36], as shown below (Figure 4).

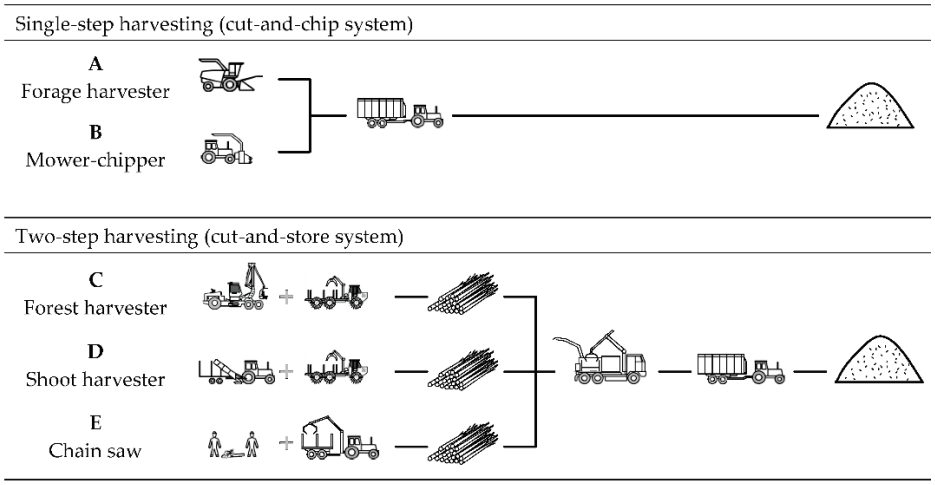

Figure 4. Cut-and-chip system (**A**,**B**) and cut-and-store system (**C**–**E**) [53].

The first system is realized in two phases that take place physically and are temporarily separated [26]: (i) harvesting and (ii) hauling and chipping the cut stems [54]. The harvesting systems, discussed in the previous paragraph, can be performed in a manual [55] or mechanical way. The manual harvesting is not interesting unless there are conditions for which the mechanized system cannot be used (e.g., reduced size of the plant) [36]. Mechanized harvesting operations are performed by using a specialized harvesting head attached to an agricultural vehicle that allows for the harvesting and transport in the storage place such as a dedicated site to intervene later [56] or within the plantation itself (swath) [26].

According to a study conducted in Belgium on the harvesting of a short-rotation poplar plantation [36], it was found that in the cut-and-store system, the manual harvesting is performed much more slowly than the mechanized one (0.01 vs. 0.37 ha h^{-1}), resulting in lower productivity (0.15 vs. 8.84 t h^{-1}) and higher costs (8688 vs. 779 EUR ha^{-1}).

In the cut-and-chip system, instead, felling and chipping occur simultaneously by using mower-feeders that directly unload the wood chips in special trailers, thus facilitating transport. According to [36], the cut-and-chip harvesting system is intermediate in terms of performance and productivity compared to the cut-and-store system: the hourly cost is lower for the manual cut-and-store system than that which is mechanized (440 vs. 674 EUR h^{-1}), and this does not compensate for the higher cost per hectare and ton (10.142 vs. 2232 EUR ha^{-1} and EUR 426 vs. 94 EUR t^{-1}). For clarity, it is specified that the values considered for manual harvesting are 0.01 hah^{-1} and 0.15 th^{-1}, while for mechanized harvesting, they are 0.37 hah^{-1} and 8.84 th^{-1}.

Upon evaluating the relevant Italian literature [30,57–60], some harvest parameters calculated on short-rotation poplar plantations have been synthesized and are shown in Table 1 under both the mechanized cut-and-store system and cut-and-chip harvesting system. The mechanized cut-and-store chipping system (using a Jenz Hem 561) shows an average productivity of 13.90 th^{-1} and an average cost per hectare of 1594.5 (EUR ha^{-1}); the cut-and-chip system instead shows an average productivity of 15.98 (th^{-1}) and an average cost per hectare of 475.08 (EUR ha^{-1}). For the latter case, the self-propelled forage harvesters (SPFHs), commonly called self-propelled mulchers, that is, vehicles equipped with a very specific cutting head, are Valmet 921 + 840 and Jenz HEM 561, GBE-1 e GBE-2, Claas HS-2, and HTM 1500 e Biopoplar, among which the most important versions were developed by Italian companies [26,52,57].

Table 1. Literature survey of harvesting operations of poplar cultivations in short rotation. Relevant parameters of the mechanized cut-and-store and cut-and-chip harvesting systems are presented. Data were collected from various studies reported in the literature [36].

System	Plant Density (ha^{-1})	Above-Ground Age (y)	Stocking Biomass (tha^{-1})	Performance (hah^{-1})	Productivity (th^{-1})	Cost per Hour (EUR h^{-1})	Cost per Hectare (EUR ha^{-1})	Cost per Ton (EUR t^{-1})	Machine	Reference
Cut and Store—Hauling			51.33	0.23	5.64	70	304	12	Valmet 840	[61]
Cut and Store—Chipping			25.49	0.22	13.63	340	1531	25	JENZ HEM 561	[60]
			31.15	0.20	14.09	340	1681	24	JENZ HEM 561	
			25.85	0.20	12.37	340	1704	27	JENZ HEM 561	
			30.01	0.23	15.54	340	1462	22	JENZ HEM 561	
Cut and Chip	1670	5	91.00	6.03	7.87	110	664	14	Valmet 921 + 840 and Jenz HEM 561	[60]
	1670	5	81.50	5.51	9.22	110	606	12	Valmet 921 + 840 and Jenz HEM 561	
	1670	5	91.00	6.37	8.26	110	700	13	Valmet 921 + 840 and Jenz HEM 561	
	1670	5	81.50	5.97	8.83	110	656	12	Valmet 921 + 840 and Jenz HEM 561	
	14,100	2	21.90	1.30	16.86	322	418	19	GBE-2	[57]
	7100	2	16.70	0.60	27.86	552	330	20	GBE-2	
	10,000	1	8.58	0.90	7.68	203	227	26	Claas HS-2	[59]
	6000	2	19.60	0.82	16.08	234	285	15	GBE-1	
	9000	3	24.30	0.46	11.14	270	589	24	HTM 1500	
	6000	3	30.20	0.66	19.96	210	318	11	Biopoplar	
	6000	3	24.00	0.79	18.86	210	267	11	Biopoplar	
	6000	2	27.70	0.53	14.55	210	400	14	Biopoplar	
	6000	2	32.20	0.28	8.88	210	716	24	Biopoplar	
	5550	2	20.90	0.93	22.57				GBE-2	[57]
	5550	2	33.70	1.20	27.97				GBE-2	
	9520	2	31.00	1.06	29.14				GBE-2	

The following cost analysis refers only to a chipper on forwarders and therefore to a cut-and-chip harvesting system.

6. Economic Analysis of the Construction Forest Site

Below is a reworking of costs (EUR/h) made by the authors to estimate the operating costs of the machines at present. Unfortunately, it has not been possible to calculate the productivity of the machines (ton/ha), but for completeness, these data were taken from references, as presented in the previous paragraphs.

The economic evaluation is aimed at quantifying the hourly costs of the equipment and machines considered in a hypothetical traditional cultivation system and in an SRC system.

The mechanization levels examined are as follows:

(1) Traditional mechanization;
(2) Advanced/pushed mechanization.

In the first case, the following equipment/machines are considered: GS 630 standard 2T chainsaw (felling and equipment), in the case of traditional mechanization, tractor "Fendt 600 Vario" with drum winch (wood), and an 88 kW self-propelled loader (load).

In the second case, i.e., for the SRC and therefore with extensive mechanization, the following equipment/machines are considered: the harvester "Timberjak 1270 C Advance" (felling and preparation of the material), the forwarder "Komatsu 845" (logging), the "Erjo" chipper mounted on the forwarder (shredding) and, finally, for stacking, an 88 kW self-propelled loader.

The following table (Table 2) lists all the technical and economic elements used to calculate the hourly cost of using the machines. The technical values (nominal power, useful life, annual use) and the economic values (e.g., new value) were extrapolated from the data sheets of each machine operator. For the other estimated elements, the calculation equation used in the last column of the following table was inserted. In regard to average fuel costs, 1.89 EUR/L was considered for petrol and 1.45 EUR/L for agricultural fuel. Please note that the table below also shows the costs of using a Feller buncher with the wheel loader "Komatsu WA80M-8" for advanced mechanization, but that this has not been considered for the subsequent estimates of effectiveness and productivity of the system.

The elaboration of the operating cost of the machines (values in EUR/hour, Table 3) was carried out by proposing some technical coefficients deemed more suitable [62] and by applying an analytical methodology that distinguishes fixed and variable costs [62,63] as well as by applying mathematical formulas found in the main calculation methodologies proposed by different authors [64–67]. Relative to the cost of the labor, it has been considered that a single gross tariff correlates to 15 EUR/hour, inclusive of all the insurance and provident and assistance burdens previewed by the Italian legislation [18].

For greater clarity in the assessment of the economic sustainability of the machines, the productivity values given in reference [13] were considered. Based on the average gross labor productivity (th^{-1}) for individual operations, the authors have elaborated and estimated the average cost per ton of wood chips produced (EUR/t). The values are shown in the table below (Table 4).

However, having considered hypothetical cultivation systems, the present review is limited to resume the productivity reported in the literature [13]. Considering the application of traditional mechanization (chainsaw, winch, chipper pulled by tractor, and loader), the average gross time range for the felling/staging phase varies from 145.9 h/ha to 72.9 h/ha, for extraction from 19 h/ha to 12.7 h/ha, and for loading 12.9–9.6 h/ha for a total amount of hours ranging from 177.8 h/ha to 95.2 h/ha. Instead, in the case of an advanced mechanization level (harvester, forwarder, chipper on forwarder and loader), the average gross utilization time is considerably reduced: during the felling/staging phase, the hours per hectare per worker vary from 14.5 to 6.6 h/ha, for the extraction from 7.8 to 6.2 h/ha, and finally for the load from 6.7 to 4.9 h/ha for a total range from 29 to 17.7 h/ha.

Table 2. Technical and economic elements adopted for the calculation of the hourly cost of machines according to the phases of use and the level of mechanization adopted.

		Felling/Staging			Skidding		Shredding		Load	
Level of Mechanization		**Traditional (T)**	**Advanced (A)**	**Pushed (P)**	**T/A**	**P**	**T/A**	**A/P**	**T/A/P**	
Technical and Economic Elements	**Symbols**	**Chainsaw**	**Feller Buncher**	**Harvester**	**Tractor with Winch**	**Forwarder**	**Chipper Pulled by Tractor**	**Chipper on Forwarder**	**Charger**	**Equations or Values**
New value (EUR)	V_0	946	100.000	380.000	50.000	220.000	100.000	520.000	80.000	
Recovery value (EUR)	V_n	601.71	22.130	84.094	11.065	48.686	22.130	115.076	17.704	V_0*0.86 ^{Y}
Useful life (years)	Y	3	10	10	10	10	10	10	10	
Annual use (h)	H	700	1000	1000	1000	1000	800	800	800	
Nominal power (kW)	P	3.5	75	173	113	140	360	404	88	
Interest rate (%)	i	4	4	4	4	4	4	4	4	
Average fuel cost (EUR/L)	Cfu	1.89	1.45	1.45	1.45	1.45	1.45	1.45	1.45	
Fuel density (kg/L)	Fd	0.7	0.86	0.86	0.86	0.86	0.86	0.86	0.86	
Average lubricant cost (EUR/L)	Clu	4.5	9	9	9	9	9	9	9	
Hourly fuel consumption (L/h)	Chf	0.68	9.59	22.12	14.45	17.9	46.05	51.67	11.25	
Hourly lubricant consumption (L/h)	Chl	0.32	0.32	0.73	0.26	0.55	1.4	1.7	0.26	
Storage space (m^2)	Ss	0.6	25.6	48.4	28.2	32.9	30	41.9	18.4	le*wi*1.5 (*)
Shelter construction cost (EUR/m^2)	Ccs	500	500	500	500	500	500	500	500	
Coeff. miscellaneous expenses	C.me	0.001	0.005	0.01	0.003	0.005	0.005	0.01	0.001	0.001–0.01
Coeff. insurance	C.i	0.02	0.02	0.02	0.02	0.02	0.02	0.02	0.02	0.01–0.03
Coeff. overheads	C.o	0.001	0.005	0.005	0.005	0.005	0.005	0.005	0.001	0.001–0.01
Coeff. storage costs	C.cs	0.02	0.05	0.05	0.05	0.05	0.05	0.05	0.05	0.02–0.05

(*) le and wi indicate the length and width of the machine, respectively [62].

Table 3. Hourly operating costs of machines (including labor) at different stages of use of the poplar weight, considering different levels of mechanization.

		Felling/Staging			Skidding		Shredding		Load	
Level of Mechanization		**Traditional (T)**	**Advanced (A)**	**Pushed (P)**	**T/A**	**P**	**T/A**	**A/P**	**T/A/P**	
Cost Items	**Symbols**	**Chainsaw**	**Feller Buncher**	**Harvester**	**Tractor with Winch**	**Forwarder**	**Chipper Pulled by Tractor**	**Chipper on Forwarder**	**Charger**	**Equations Used**
VARIABLE COSTS (VCh)										
Maintenance	MA	0.5	6.0	22.8	3.0	13.2	6.0	31.2	4.8	$V_0 \times \mu$ (*)
Fuel cost	FC	1.29	13.91	32.07	20.95	25.96	66.77	74.92	16.31	Cfu × Chf
Lubricant cost	LC	0.26	2.78	6.41	4.19	5.19	12.6	14.98	3.26	Clu × Chl

Table 3. *Cont.*

Level of Mechanization		Felling/Staging			Skidding		Shredding		Load	
		Traditional (T)	Advanced (A)	Pushed (P)	T/A	P	T/A	A/P	T/A/P	
Cost Items	**Symbols**	**Chainsaw**	**Feller Buncher**	**Harvester**	**Tractor with Winch**	**Forwarder**	**Chipper Pulled by Tractor**	**Chipper on Forwarder**	**Charger**	**Equations Used**
Miscellaneous expenses	MIE	0.01	0.1	0.38	0.05	0.22	0.06	0.65	0.1	$V_0/(Y \times H) \times C.me$
Labor	LA	15	15	15	15	15	15	15	15	
Total VCh		17.1	37.8	76.7	43.2	59.6	100.43	136.8	39.5	MA + FC + LC + MIE + LA
FIXED COSTS (FCh)										
Amortization	AM	0.16	7.79	29.59	3.89	17.13	24.33	50.62	7.79	$(V_0 - Vn)/(A \times H)$
Insurance	INS	0.03	2.0	7.6	1.0	4.4	2.5	13.0	2.0	$(V_0 \times C.i)/H$
Storage	STO	0.01	0.64	1.21	0.71	0.82	0.09	1.31	0.57	$(Ccs \times Ss \times C.me)/H$
Interest	IN	0.04	2.44	9.28	1.22	5.37	3.05	15.88	2.44	$[((V_0 + V_n)/(2 \times H)) \times i]/100$
Overhead	OH	0.001	0.06	0.24	0.03	0.14	0.15	0.40	0.01	$(AM + INS + STO + IN) \times C.o$
Total FCh		0.60	12.93	47.92	6.85	27.86	30.12	81.21	12.81	AM + INS + STO + IN + OH
TOTAL COSTS (EUR/h)		**17.62**	**50.72**	**124.58**	**50.05**	**87.43**	**130.55 ***	**217.96**	**52.29**	

(*) Maintenance costs are estimated as a percentage of the new value. The maintenance coefficients (μ) are between 0.00005 and 0.00006. * To the cost of chipper pulled by tractor must be added the operating cost of the tractor, which has been estimated at 50 (EUR/h).

Table 4. Average cost per ton of wood chips (EUR/t) at different stages of use of the poplar weight, considering different levels of mechanization.

Level of Mechanization	Felling/Staging		Skidding		Shredding		Load
	Traditional (T)	Pushed (P)	T/A	P	T/A	A/P	T/A/P
	Chainsaw	**Harvester**	**Tractor with Winch**	**Forwarder**	**Chipper Pulled by Tractor**	**Chipper on Forwarder**	**Charger**
TOTAL COSTS (EUR/h)	17.62	124.58	50.05	87.43	130.55 *	217.96	52.29
PRODUCTIVITY (t/h)	1.2–2.5	12.4–27.1	9.8–14.2	23–29	10.4–14	14–18	10.4–20.1
TOTAL COSTS * (EUR/t)	**9.52**	**6.30**	**4.17**	**3.36**	**14.80**	**13.62**	**5.03–2.60**

* Average of productivity values given in reference [13].

The cost analysis for the final product, in relation to the degree of mechanization, reveals that the implementation of a higher level of mechanization entails a significant reduction in the overall costs of the yard.

Based on the analyses carried out, the adoption of a high level of mechanization leads to a reduction in operating costs per ton from 33.52 EUR/t to 25.88 EUR/t; similarly, the costs per hectare increase from an amount of 4518.8 EUR/ha to 2850.8 EUR/ha.

In addition, it should be considered that the estimates are based on an annual use of the machines at a maximum power of around 800–1000 h; less use would entail considerable cost increases compared to those reported.

According to [4], a team that adopts a push mechanization can use up to 100 ha per year against about 12–15 ha of those who work with traditional yard methods. Therefore, a level of mechanization push is feasible and advantageous only if the technical, logistic, and commercial organization of the enterprise allows us to optimize the potentiality of the means available that must work with continuity over the whole day and the year.

A higher level of mechanization also shows great advantages in terms of productivity. The high degree of mechanization allows for a high level of work organization and an increase in the productivity of the site.

The use of the harvester gives the yard a daily productivity of up to 35 tons per worker compared to 12 tons in the traditional system [4,68]. When compared with a more traditional working methodology, there is a reduction in working time of 117 h per worker, which in terms of productivity, corresponds to 6.86 t/ha per worker as opposed to 1.26 t/ha [69].

These economic and work organization advantages translate into greater company efficiency, including at the budgetary level, as well as an improved psychophysical well-being of workers—well-being which, in turn, results in an increased working capacity and improved productivity [70,71].

Economic and production efficiency, as analyzed in paragraph 4, can be further increased using new innovative machines and new technologies [72,73]. Precision forestry, autonomous and assisted driving, as well as the latest generation of remote sensing, offer significant benefits for forest production and operator safety [71].

It is fair to point out that, for a complete and comparative analysis of the two systems, it would be appropriate to quantify the revenues from the final products (quality wood for industry, in the case of the traditional and wood chip systems in the case of SRC) [74,75].

7. Conclusions

From the work carried out, it has been understood how mechanization in the forestry sector and, in particular, in that of poplar cultivation can help to increase economic efficiency to improve productivity and reduce worker accidents, as well as increase the psychophysical well-being of workers.

From the analysis of the data carried out, it can be noted that, given the high initial investment, the implementation of a high level of mechanization entails a significant reduction in the overall costs of the yard, as well as a higher plant productivity and therefore higher profits.

In fact, based on the calculation of the operating costs of the machines implemented by the authors, it seems that the use of a strong mechanization involves a percentage reduction of the average cost per ton of wood chips produced (EUR/t) of 23%, from 33.52 EUR/t to 25.88 EUR/t and a percentage reduction of the average gross cost per hectare of wood chips produced (EUR/ha) of 37%, from an amount of 4518.8 EUR/ha to 2850.8 EUR/ha.

Economic and production efficiency, analyzed in Section 4, can be further enhanced by using innovative new machines and new technologies such as autonomous and assisted driving and latest-generation remote sensing, which offer significant benefits for forest production and operator safety. By using these innovative machines, it is possible to have higher-quality final products, thus guaranteeing broad protection for the consumer who

will be less averse to purchasing and will contribute to increasing the turnover of the market for new renewable energies deriving from woody biomass.

Of course, the European and national institutions must play a key role in encouraging the generational replacement of obsolete agricultural and forestry machinery and in encouraging the use of the latest technologies.

Author Contributions: Conceptualization, V.D.S., G.D.D. and A.C.; Data analysis, G.D.D. and V.D.S.; Methodology, V.D.S., G.D.D. and A.C.; Writing original draft, V.D.S. and G.D.D.; Review and editing, E.P., M.M., L.B. and A.C. All authors have read and agreed to the published version of the manuscript.

Funding: This research received no external funding.

Data Availability Statement: Not applicable.

Acknowledgments: This research was carried out within the framework of the Ministry for Education, University, and Research (MIUR) initiative, the "Department of Excellence" (Law 232/2016) DAFNE Project 2023-27, "Digital, Intelligent, Green and Sustainable (acronym: D.I. Ver.So)" and under the General Agreement between Council for Agricultural Research and Economics and University of Tuscia.

Conflicts of Interest: The authors declare no conflicts of interest.

References

1. Castro, G.; Fragnelli, G.; Zanuttini, R. *La Pioppicoltura e Il Compensato Di Pioppo Dell'Industria Italiana*; Edizioni Lampi di Stampa: Vignate, Italy, 2014; ISBN 978-88-488-1580-2.
2. European Commission. *2020 A Farm to Fork Strategy for a Fair, Healthy and Environmentally-Friendly Food System*; European Commission: Brussels, Belgium, 2020.
3. Livingstone, D.; Smyth, B.M.; Cassidy, R.; Murray, S.T.; Lyons, G.A.; Foley, A.M.; Johnston, C.R. Reducing the Time-Dependent Climate Impact of Intensive Agriculture with Strategically Positioned Short Rotation Coppice Willow. *J. Clean. Prod.* **2023**, *419*, 137936. [CrossRef]
4. Corona, P.; Bergante, S.; Castro, G.; Chiarabaglio, P.M.; Coaloa, D.; Facciotto, G.; Gennaro, M.; Giorcelli, A.; Rosso, L.; Vietto, L.; et al. *Linee Di Indirizzo per Una Pioppicoltura Sostenibile Linee Guida*; Rete Rurale Nazionale: Rome, Italy, 2018.
5. de Wit, M.; Faaij, A. European Biomass Resource Potential and Costs. *Biomass Bioenergy* **2010**, *34*, 188–202. [CrossRef]
6. Gasol, C.M.; Brun, F.; Mosso, A.; Rieradevall, J.; Gabarrell, X. Economic Assessment and Comparison of Acacia Energy Crop with Annual Traditional Crops in Southern Europe. *Energy Policy* **2010**, *38*, 592–597. [CrossRef]
7. Fuertes, A.; Oliveira, N.; Cañellas, I.; Sixto, H.; Rodríguez-Soalleiro, R. An Economic Overview of Populus Spp. in Short Rotation Coppice Systems under Mediterranean Conditions: An Assessment Tool for Decision-Making. *Renew. Sustain. Energy Rev.* **2021**, *151*, 111577. [CrossRef]
8. Vincenti, B.; Proto, A.R.; Paris, E.; Palma, A.; Carnevale, M.; Guerriero, E.; Bernardini, F.; Tonolo, A.; Di Stefano, V.; Gallucci, F. Chemical and Physical Characterization of Pellet Composed of Biomass of Different Essences. In Proceedings of the European Biomass Conference and Exhibition Proceedings, Marseille, France, 6–9 July 2020; pp. 124–127.
9. Sgroi, F. Precision Agriculture and Competitive Advantage: Economic Efficiency of the Mechanized Harvesting of Chardonnay and Nero d'Avola Grapes. *J. Agric. Food Res.* **2023**, *14*, 100774. [CrossRef]
10. Verani, S.; Sperandio, G. Meccanizzazione Spinta in Pioppeto. *Sherwood* **2007**, *137*, 29–33.
11. Sperandio, G.; Acampora, A.; Del Giudice, A.; Civitarese, V. Models for the Evaluation of Productivity and Costs of Mechanized Felling on Poplar Short Rotation Coppice in Italy. *Forests* **2021**, *12*, 954. [CrossRef]
12. Spinelli, R.; Hartsough, B.R.; Owende, P.M.O.; Ward, S.M. Productivity and Cost of Mechanized Whole-Tree Harvesting of Fast-Growing Eucalypt Stands. *Int. J. For. Eng.* **2002**, *13*, 49–60. [CrossRef]
13. Verani, S.; Sperandio, G.; Civitarese, V.; Spinelli, R. Harvesting Mechanization in Plantations for Wood Production: Working Productivity and Costs. *For. Riv. Selvic. Ecol. For.* **2017**, *14*, 237–246. [CrossRef]
14. Tavankar, F.; Picchio, R.; Nikooy, M.; Jourgholami, M.; Latterini, F.; Venanzi, R. Effect of Soil Moisture on Soil Compaction during Skidding Operations in Poplar Plantation. *Int. J. For. Eng.* **2021**, *32*, 128–139. [CrossRef]
15. Mattioli, W.; Puletti, N.; Coaloa, D.; Rosso, L.; Chianucci, F.; Grotti, M.; Corona, P. INARBO:IT: Inventario Degli Impianti Di Arboricoltura Da Legno in Italia. *Sherwood For. Alberi Oggi* **2019**, *239*, 7–10.
16. Coaloa, D.; Chiarabaglio, P.M.; Bergante, S.; Rosso, L. Gestione Assicurativa Dei Rischi in Pioppicoltura. *L'Italia For. Mont.* **2021**, *76*, 109–120. [CrossRef]
17. Coaloa, D.; Chiarabaglio, P.; Giorcelli, A.; Pelleri, F.; Plutino, M.; Rosso, L.; Corona, P. Redditività Di Pioppeti Ad Alto Fusto e Di Piantagioni Di Latifoglie a Legname Pregiato in Italia. *For. J. Silvic. For. Ecol.* **2020**, *17*, 101–108.
18. Corona, P.; Di Stefano, V.; Mariano, A. Knowledge Gaps and Research Opportunities in the Light of the European Union Regulation on Deforestation-Free Products. *Ann. Silvic. Res.* **2023**, *48*, 87–89. [CrossRef]

19. Gasparini, P.; Di Cosmo, L.; Floris, A.; De Laurentis Editors, D. *Springer Tracts in Civil Engineering*; Springer: Berlin/Heidelberg, Germany, 2015.
20. Pignatti, G.; Verani, S.; Sperandio, G. Produzione Di Legna Da Ardere Da Cedui Di Eucalipto a Turno Breve: Produttività Di Lavoro e Costi. *L'Italia For. E Mont.* **2019**, *74*, 217–226. [CrossRef]
21. Civitarese, V.; Faugno, S.; Picchio, R.; Assirelli, A.; Sperandio, G.; Saulino, L.; Crimaldi, M.; Sannino, M. Production of Selected Short-Rotation Wood Crop Species and Quality of Obtained Biomass. *Eur. J. For. Res.* **2018**, *137*, 541–552. [CrossRef]
22. Imbrenda, V.; Coluzzi, R.; Di Stefano, V.; Egidi, G.; Salvati, L.; Samela, C.; Simoniello, T.; Lanfredi, M. Modeling Spatio-Temporal Divergence in Land Vulnerability to Desertification with Local Regressions. *Sustainability* **2022**, *14*, 10906. [CrossRef]
23. Palma, A.; Gallucci, F.; Papandrea, S.; Carnevale, M.; Paris, E.; Vincenti, B.; Salerno, M.; Di Stefano, V.; Proto, A.R. Experimental Study of the Combustion of and Emissions from Olive and Citrus Pellets in a Small Boiler. *Fire* **2023**, *6*, 288. [CrossRef]
24. Paris, E.; Vincenti, B.; Palma, A.; Carnevale, M.; Salerno, M.; Proto, A.R.; Papandrea, S.F.; Di Stefano, V.; Serafini, L.; Gallucci, F. Monitoring of atmospheric markers emitted by the combustion of biomass: Comparison between citrus and olive. In Proceedings of the European Biomass Conference and Exhibition Proceedings, Bologna, Italy, 5–8 June 2023; pp. 726–728.
25. Verani, S.; Sperandio, G.; Picchio, R.; Marchi, E.; Costa, C. Sustainability Assessment of a Self-Consumption Wood-Energy Chain on Small Scale for Heat Generation in Central Italy. *Energies* **2015**, *8*, 5182–5197. [CrossRef]
26. Santangelo, E.; Scarfone, A.; Del Giudice, A.; Acampora, A.; Alfano, V.; Suardi, A.; Pari, L. Harvesting Systems for Poplar Short Rotation Coppice. *Ind. Crops Prod.* **2015**, *75*, 85–92. [CrossRef]
27. Spinelli, R.; Magagnotti, N.; Kovacs, B.; Heger, P.; Mihelic, M. Productivity and Cost Assessment of Two Harvesting Methods for Medium-Rotation Poplar Plantations. *Scand. J. For. Res.* **2023**, *38*, 79–86. [CrossRef]
28. Di Matteo, G.; Nardi, P.; Verani, S.; Sperandio, G. Physiological Adaptability of Poplar Clones Selected for Bioenergy Purposes under Non-Irrigated and Suboptimal Site Conditions: A Case Study in Central Italy. *Biomass Bioenergy* **2015**, *81*, 183–189. [CrossRef]
29. Cielo, P.; Zanuttini, R. Utilizzazione Del Pioppeto Con Harvester. Due Cantieri a Confronto. *Sherwood For. Alberi Oggi* **2007**, *133*, 37–42.
30. Spinelli, R.; Magagnotti, N.; Picchi, G.; Lombardini, C.; Nati, C. Upsized Harvesting Technology for Coping with the New Trends in Short-Rotation Coppice. *Appl. Eng. Agric.* **2011**, *27*, 551–557. [CrossRef]
31. Bianchini, L.; Marucci, A.; Sateriano, A.; Di Stefano, V.; Alemanno, R.; Colantoni, A. Urbanization and Long-Term Forest Dynamics in a Metropolitan Region of Southern Europe (1936–2018). *Sustainability* **2021**, *13*, 12164. [CrossRef]
32. Bianchini, L.; Alemanno, R.; Di Stefano, V.; Cecchini, M.; Colantoni, A. Soil Compaction in Harvesting Operations of *Phalaris Arundinacea* L. *Land* **2022**, *11*, 1031. [CrossRef]
33. Saracino, A.; Cona, F.; Guida, G.; Saulino, L.; Spina, C.; Teobaldelli, M.; Allevato, E.; Todaro, L. *Manuale Tecnico Di Innovazioni Nella Filiera Corta per La Produzione, Raccolta Ed Uso Di Legna Da Boschi Cedui e Piantagioni a Breve Rotazione a Fini Energetici*; Academia: San Francisco, CA, USA, 2014; ISBN 978-88-7853-349-3.
34. Volk, T.A.; Eisenbies, M.H.; Hallen, K. The Development of Harvesting Systems in Woody Biomass Supply Chains: A Case Study of Short Rotation Woody Crops. In *Sustainable Biorefining of Woody Biomass to Biofuels and Biochemicals*; Woodhead Publishing: Cambridge, UK, 2024; pp. 43–63. [CrossRef]
35. Pecenka, R.; Ehlert, D.; Lenz, H. Efficient Harvest Lines for Short Rotation Coppices (SRC) in Agriculture and Agroforestry. *Agron. Res.* **2014**, *12*, 151–160.
36. Vanbeveren, S.P.P.; Schweier, J.; Berhongaray, G.; Ceulemans, R. Operational Short Rotation Woody Crop Plantations: Manual or Mechanised Harvesting? *Biomass Bioenergy* **2015**, *72*, 8–18. [CrossRef]
37. Lundbäck, M.; Häggström, C.; Nordfell, T. Worldwide Trends in the Methods and Systems for Harvesting, Extraction and Transportation of Roundwood. In Proceedings of the 6th International Forest Engineering Conference, Rotorua, New Zealand, 16–19 April 2018.
38. Lundbäck, M.; Häggström, C.; Nordfjell, T. Worldwide Trends in Methods for Harvesting and Extracting Industrial Roundwood. *Int. J. Engl. Lit.* **2021**, *32*, 202–215. [CrossRef]
39. De Francesco, F.; Magagnotti, N.; Kováč, B.; Heger, P.; Heilig, D.; Heil, B.; Kovács, G.; Zemánek, T.; Spinelli, R. Integrated Harvesting of Medium Rotation Hybrid Poplar Plantations: Systems Compared. *Forests* **2022**, *13*, 1873. [CrossRef]
40. Magagnotti, N.; Spinelli, R.; Kärhä, K.; Mederski, P.S. Multi-Tree Cut-to-Length Harvesting of Short-Rotation Poplar Plantations. *Eur. J. For. Res.* **2021**, *140*, 345–354. [CrossRef]
41. Spinelli, R.; Magagnotti, N.; Lombardini, C. Low-Investment Fully Mechanized Harvesting of Short-Rotation Poplar (*Populus* Spp.) Plantations. *Forests* **2020**, *11*, 502. [CrossRef]
42. Grove, P.M.; Conrad, J.L.; Dahlen, J. Volume and Value Recovery Com- Parison of Processor and Conventional Systems in Pine Stands of the U.S. *Int. J. Engl. Lit.* **2020**, *31*, 29–36.
43. Premer, M.I.; Froese, R.E.; Vance, E.D. Whole-Tree Harvest and Residue Recovery in Commercial Aspen: Implications to Forest Growth and Soil Productivity across a Rotation. *For. Ecol. Manag.* **2019**, *447*, 130–138. [CrossRef]
44. Ghezehei, S.B.; Wright, J.; Zalesny, R.S.; Nichols, E.G.; Hazel, D.W. Matching Site-Suitable Poplars to Rotation Length for Optimized Productivity. *For. Ecol. Manag.* **2020**, *457*, 117670. [CrossRef]
45. Picchio, R.; Verani, S.; Sperandio, G.; Spina, R.; Marchi, E. Stump Grinding on a Poplar Plantation: Working Time, Productivity, and Economic and Energetic Inputs. *Ecol. Eng.* **2012**, *40*, 117–120. [CrossRef]

46. Verani, S.; Sperandio, G.; Picchio, R.; Spinelli, R.; Picchi, G. *La Raccolta Meccanizzata Del Pioppo. Iniziativa Finanziata Dal Programma Di Sviluppo Rurale per Il Veneto 2007–2013 Organismo Responsabile Dell'informazione: Veneto Agricoltura Autorità Di Gestione: Regione Del Veneto-Dipartimento Agricoltura e Sviluppo Rurale Organizzazione Delle Nazioni Unite per L'alimentazione e L'agricoltura*; Veneto Agricoltura: Mestre Venezia, Italy, 2014.
47. Commission of the European Community Renewable Energy Road Map. *Renewable Energies in the 21th Century: Building a More Sustainable Future. Communication from the Commission to the European Council and the European Parliament (2006/848)*; Commission of the European Community Renewable Energy Road Map: Brussels, Belgium, 2007.
48. Sperandio, G.; Verani, S.; Tarchi, M. Pioppo a Rotazione Triennale, Più Biomassa Con l'irrigazione. *Terra Vita* **2015**, *13*, 38–41.
49. Sherrington, C.; Bartley, J.; Moran, D. Farm-Level Constraints on the Domestic Supply of Perennial Energy Crops in the UK. *Energy Policy* **2008**, *36*, 2504–2512. [CrossRef]
50. El Kasmioui, O.; Ceulemans, R. Financial Analysis of the Cultivation of Poplar and Willow for Bioenergy. *Biomass Bioenergy* **2012**, *43*, 52–64. [CrossRef]
51. El Kasmioui, O.; Ceulemans, R. Financial Analysis of the Cultivation of Short Rotation Woody Crops for Bioenergy in Belgium: Barriers and Opportunities. *Bioenergy Res.* **2013**, *6*, 336–350. [CrossRef]
52. Schweier, J.; Becker, G. Harvesting of Short Rotation Coppice-Harvesting Trials with a Cut and Storage System in Germany. *Silva Fenn.* **2012**, *46*, 287–299. [CrossRef]
53. Pecenka, R.; Lenz, H.; Jekayinfa, S.O.; Hoffmann, T. Influence of Tree Species, Harvesting Method and Storage on Energy Demand and Wood Chip Quality When Chipping Poplar, Willow and Black Locust. *Agriculture* **2020**, *10*, 116. [CrossRef]
54. Eriksson, L.; Gustavsson, L. Comparative Analysis of Wood Chips and Bundles-Costs, Carbon Dioxide Emissions, Dry-Matter Losses and Allergic Reactions. *Biomass Bioenergy* **2010**, *34*, 82–90. [CrossRef]
55. Marogel-Popa, T.; Cheţa, M.; Marcu, M.V.; Duţă, C.I.; Ioraş, F.; Borz, S.A. Manual Cultivation Operations in Poplar Stands: A Characterization of Job Difficulty and Risks of Health Impairment. *Int. J. Environ. Res. Public. Health* **2019**, *16*, 1911. [CrossRef]
56. Berhongaray, G.; El Kasmioui, O.; Ceulemans, R. Comparative Analysis of Harvesting Machines on an Operational High-Density Short Rotation Woody Crop (SRWC) Culture: One-Process versus Two-Process Harvest Operation. *Biomass Bioenergy* **2013**, *58*, 333–342. [CrossRef]
57. Fiala, M.; Bacenetti, J. Economic, Energetic and Environmental Impact in Short Rotation Coppice Harvesting Operations. *Biomass Bioenergy* **2012**, *42*, 107–113. [CrossRef]
58. Manzone, M.; Balsari, P. Poplar Woodchip Storage in Small and Medium Piles with Different Forms, Densities and Volumes. *Biomass Bioenergy* **2016**, *87*, 162–168. [CrossRef]
59. Spinelli, R.; Nati, C.; Magagnotti, N. Using Modified Foragers to Harvest Short-Rotation Poplar Plantations. *Biomass Bioenergy* **2009**, *33*, 817–821. [CrossRef]
60. Spinelli, R.; Schweier, J.; De Francesco, F. Harvesting Techniques for Non-Industrial Biomass Plantations. *Biosyst. Eng.* **2012**, *113*, 319–324. [CrossRef]
61. Nahm, M.; Brodbeck, F.; Sauter, U.H. *Verschiedene Erntemethoden Für Kurzumtriebsplantagen. Ergebnisse aus der Praxis*; Forstliche Versuchs-und Forschungsanstalt Baden-Württemberg: Freiburg, Germany, 2012.
62. Sperandio, G. Ceduo Di Eucalipto per Produzione Di Cippato. Sostenibilità Economica Di Un Cantiere a Meccanizzazione Spinta. *Sherwood* **2010**, *167*, 39–44.
63. Carbone, F. Costi Di Esercizio Delle Macchine, Delle Operazioni e Degli Interventi Selvicolturali. *L'Italia For. Mont.* **2008**, *63*, 333–350. [CrossRef]
64. Baraldi, G.; Capelli, G. *Elementi Tecnici per Il Calcolo Del Costo Di Esercizio Delle Macchine Agricole*; Genio Rurale; Edagricole: Bologna, Italy, 1973; Volume 9, pp. 37–76.
65. Biondi, P. *Meccanica Agraria. Le Macchine Agricole*; UTET: Torino, Italy, 1999.
66. Hippoliti, G. *Appunti Di Meccanizzazione Forestale*; S.E. Fiorentino: Firenze, Italy, 1997.
67. Ribaudo, F. Il Costo Di Esercizio Delle Macchine Agricole. *Macch. E Mot. Agric.* **1977**, *101*, 101–116.
68. Cielo, P.; Zanuttini, R. La Raccolta Del Legno Nei Pioppeti. *Ital. For. Mont.* **2004**, *6*, 467–482.
69. Verani, S.; Sperandio, G.; Matteo, G. Di Analisi Del Lavoro Della Claas Jaguar 880 Con Testata GBE-1 Nella Raccolta Di Un Pioppeto Da Biomassa. *For. Riv. Selvic. Ecol. For.* **2010**, *7*, 22–27. [CrossRef]
70. Colantoni, A. Different Pellet Mixtures Obtained from Spent Coffee Grounds: Energetic Characterization. 2020, pp. 357–359. Available online: https://www.researchgate.net/profile/Leonardo-Bianchini/publication/349771136_DIFFERENT_PELLET_MIXTURES_OBTAINED_FROM_SPENT_COFFEE_GROUNDS_ENERGETIC_CHARACTERIZATION/links/60410a23299bf1e07856e1c4/DIFFERENT-PELLET-MIXTURES-OBTAINED-FROM-SPENT-COFFEE-GROUNDS-ENERGETIC-CHARACTERIZATION.pdf (accessed on 15 February 2024).
71. Di Stefano, V.; Bianchini, L.; Alemanno, R.; Colantoni, A. *New Technologies and Safety in Agriculture: SAFETY AR*; Springer Nature: Cham, Switzerland, 2023; Lecture Notes in Civil Engineering; Volume 337, pp. 517–522. ISBN 9783031303289.
72. Colantoni, A.; Villarini, M.; Monarca, D.; Carlini, M.; Mosconi, E.M.; Bocci, E.; Rajabi Hamedani, S. Economic Analysis and Risk Assessment of Biomass Gasification CHP Systems of Different Sizes through Monte Carlo Simulation. *Energy Rep.* **2021**, *7*, 1954–1961. [CrossRef]
73. Colantoni, A.; Allegrini, E.; Boubaker, K.; Longo, L.; Di Giacinto, S.; Biondi, P. New insights for renewable energy hybrid photovoltaic/wind installations in Tunisia through a mathematical model. *Energy Convers. Manag.* **2013**, *75*, 398–401. [CrossRef]

74. Poponi, S.; Colantoni, A.; Cividino, S.R.S.; Mosconi, E.M. The Stakeholders' perspective within the B corp certification for a circular approach. *Sustainability* **2019**, *11*, 1584. [CrossRef]
75. Monarca, D.; Cecchini, M.; Guerrieri, M.; Colantoni, A. Conventional and alternative use of biomasses derivated by hazelnut cultivation and processing. *Acta Hortic* **2009**, *845*, 627–634. [CrossRef]

Disclaimer/Publisher's Note: The statements, opinions and data contained in all publications are solely those of the individual author(s) and contributor(s) and not of MDPI and/or the editor(s). MDPI and/or the editor(s) disclaim responsibility for any injury to people or property resulting from any ideas, methods, instructions or products referred to in the content.

forests

MDPI

Article

Production of Chestnut Coppice Biomass in a Framework of Low Mechanization and High Expectations to Combat Climate Change and Other Social Expectations

Francesco Carbone [1,*], Luigi Portoghesi [1], Manuela Romagnoli [1], Francesco Barbarese [1] and Teresa Grassi [2]

[1] Department for Innovation in Biological, Agro-Food and Forest Systems (DIBAF), University of Tuscia, Via San Camillo de Lellis snc, 01100 Viterbo, Italy; lporto@unitus.it (L.P.); mroma@unitus.it (M.R.); francesco.barbarese@unitus.it (F.B.)

[2] Department of Agriculture and Forest Sciences (DAFNE), University of Tuscia, Via San Camillo de Lellis snc, 01100 Viterbo, Italy; teresa.grassi@studenti.unitus.it

* Correspondence: fcarbone@unitus.it; Tel.: +39-0761-357748

Abstract: Climate change has become one of the most critical problems facing modern society. Sustainable forest management can be an important solution to counter the increasing concentration of carbon dioxide in the atmosphere. In particular, management of the chestnut forest could prove to be an effective strategy to absorb carbon dioxide as this species is characterized by sustained growth, so it has a high capacity to store carbon, and through the use of wood products, it is possible to sequester it for a considerable period. Chestnut (*Castanea sativa* Mill.) forests cover an area of about 800,000 ha in Italy, most of which is managed as coppice. It plays a central role in the Latium Region where its productive function is very important, as it provides timber of excellent quality. The purpose of this paper is to verify whether the current management of chestnut is efficient, as well as whether retractable wood products can contribute to the fight against climate change. The chestnut coppice located in the municipality of Tolfa (Lazio region, Italy) produces timber for 352 m^3/ha and stores about 390,000 kg of CO_2. Wood residues and losses during woodworking, together with emissions for the use of machineries, generate emissions of 368,000 kg of CO_2. The chestnut semi-finished products, with long-term use prospects, retain a net volume of 22,000 kg of CO_2. Although this is good for combating climate change, the amount of CO_2 stored is very low, less than 6% of the CO_2 stored by functional unit. Chestnut wood has a high versatility of use, so it could replace several products generated by fossil raw materials. Moreover, the implementation of precision forestry, the adoption of forest management more oriented to favor larger plants, the development of local economies and the reduction in the carbon footprint of the wood supply chain through the use of sustainable technologies would increase the capacity for climate change mitigation and increase the added value of its products.

Keywords: *Castanea sativa* Mill.; ecological footprint; carbon sink; climate change; climate-smart forestry

1. Introduction

The growth of industrialization has significantly altered the global carbon cycle. The level of greenhouse gases in the atmosphere has increased considerably, with major effects on the weather–climate system. An increase of 1.0 °C (±0.2) compared to the pre-industrial level has been estimated [1,2]. The impact of this evolution on natural systems and humanity induces the adoption of effective mitigation and countermeasures [3].

The ecological footprint is one of the tools available to monitor human pressure on ecosystems. While on the one hand it records resource consumption, on the other hand, it recognizes the existence of the ecological surplus that expresses the amount of greenhouse gases absorbed [4–7]. Forest ecosystems, whose ability to absorb atmospheric

CO_2 contributes to combating climate change, are part of this framework. This is an ecosystem service widely recognized and documented in the scientific literature [8–10].

Forest ecosystems are recognized for their capacity to absorb CO_2 and fix it in woody tissues and soil. Referring to the role of plants, in the growth phase, there is the accumulation of CO_2 that remains in the wood for the complete life cycle, depending on the type of use [11–13]. In the successive phases of processing and use, however, there are energy-consuming processes that both physically and figuratively reduce the stored ecological surplus. The contribution to combating climate change is therefore a direct consequence of the following:

- Wood density, a parameter that depends on the species;
- Forest management approaches;
- Working processes in forests;
- Timber handling;
- Working processes in the sawmill.

It is known that tree growth responds to biological laws and requires appropriate climatic and soil conditions. In productive forests, thinning is the most effective strategy in terms of the trees' dimensional and structural characteristics to be felled during the final cut, with positive effects in terms of carbon sequestration [14]. Considering that the wood yielded from these trees is suitable for long-term use, timber is a meritorious commodity, even if the working processes to satisfy the standards for use generate emissions. Thus, there is great interest in developing an approach to account for the absorptions and emissions of CO_2 using the Life Cycle Assessment (LCA) methodology [15], recently updated [16]. The approach consists of evaluating all phases of the production cycle, starting from the CO_2 stored in the wood at the time of felling (functional unit), tracking all inputs and outputs related to the transformation process and their emissions, to arriving at final product associated with ecological surplus [17–19]. In this specific case, the objective is to determine the formal contribution of the net carbon dioxide surplus eligible for climate change mitigation purposes [20,21].

Many studies in this field have utilized LCA. Specifically, for chestnut, Martinez-Alonso and Berdasco [20] determined the carbon footprint of wood products from sweet chestnut (*Castanea sativa* Mill.) forests in northern Spain. Carbone et al. [21] assessed the net carbon dioxide surplus (Net-CDS) in coppiced chestnut forests in a volcanic area in central Italy.

The chestnut (*Castanea sativa* Mill.) is a tree species that is widespread in Europe and the Middle East (Figure 1). In Italy, it covers an area of approximately 770,000 ha [22,23], most of which are managed as coppices with standards [24]. This form of management is considered the oldest form of sustainable forest management in the Mediterranean area, focusing on rapidly producing woody biomass and environmental benefits [25–27]. The Lazio region is notable for having chestnut coppice forests with high average annual growth rates and high-quality physical–mechanical characteristics [28–32].

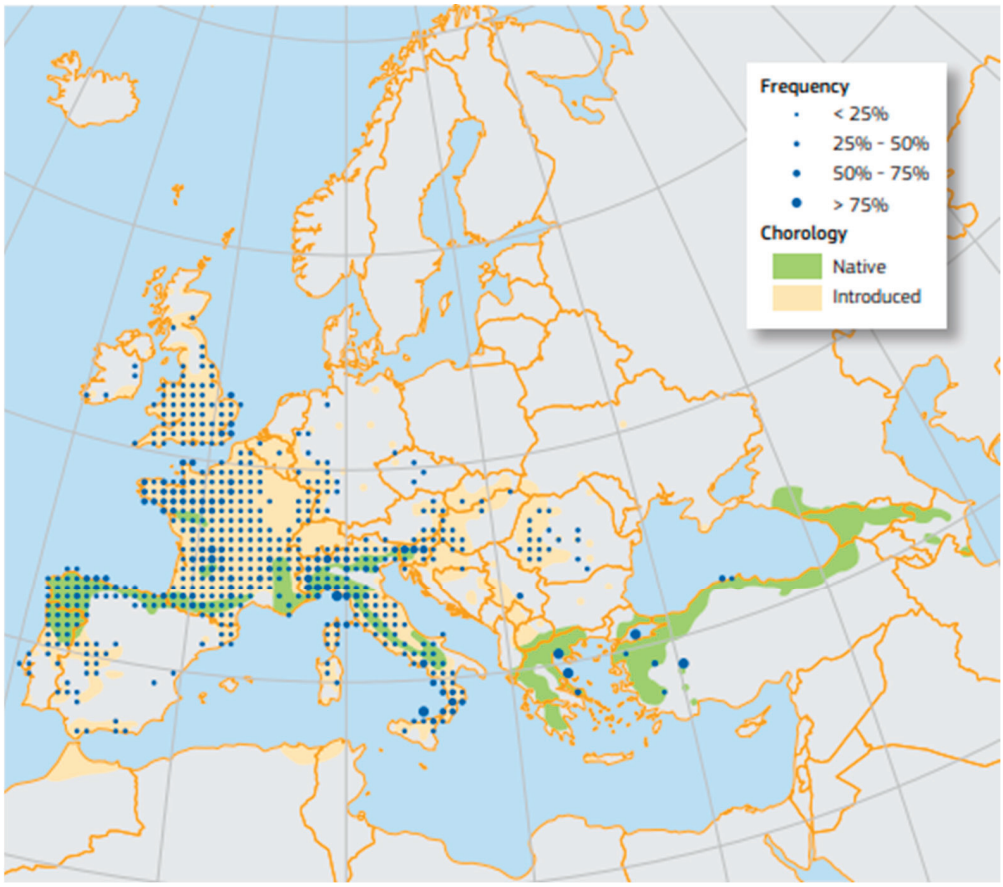

Figure 1. Geographical distribution of chestnut in Europe and the Middle East [33].

This study is part of a larger research project aimed at enhancing the tangible and intangible characteristics of chestnut coppice and chestnut wood. The hypothesis is to verify whether chestnut coppices can increase their performance both in woody production and in the provision of ecosystem services. In technical terms, this would mean a more efficient management of these semi-natural forest ecosystems, making a greater contribution both to combating climate change and to satisfying the community expectations (climate-smart forestry) [34].

It involves the first segments of the forest–wood chain, from forest management to sawmill. In order to implement forest management, forest farming involves the logging company. The use of tools, instruments, machines and machineries, both in the forest and in the sawmill, generates emissions that are offset by the CO_2 stored in the wood.

Using LCA with a multi-gate approach, the CO_2 balance was constructed, distinguishing the wood production destined for immediate use from that destined for long-term use. Only the latter part is effective for combating climate change.

2. Materials and Methods

2.1. The Study Area

2.1.1. Context

The study area is located within the territory owned by the local authorities of Tolfa that covers approximately 8000 ha, with a forested area of 2400 ha, mostly covered by coppiced stands of oak (*Quercus cerris* L.). It is included within the sites of the Natura 2000 network, identified as ZPS IT 6030005 Comprensorio Tolfetano Cerite Manziate, SIC IT 6030004 Valle di Rio Fiume, part of SIC IT 6030003 Boschi Mesofili di Allu- miere and part of SIC IT 6030001 Fiume Mignone (mid-course).

2.1.2. Tree Composition

The chestnut coppice area is situated to the northeast of the Lazio region (Figure 2) on the Tolfa mountains, in low relieves (400–800 m a.s.l.) of volcanic origin. The area covered by chestnut coppice is approximately 85 ha, which represents 4% of the entire forest property (2400 ha). In the area identified for the measurements, the predominant species is chestnut (83%), while the other species are present in small numbers (Figure 3).



Figure 2. Location of the chestnut coppice in the Tolfa area (Geoportale Regione Lazio, 2018) [35].

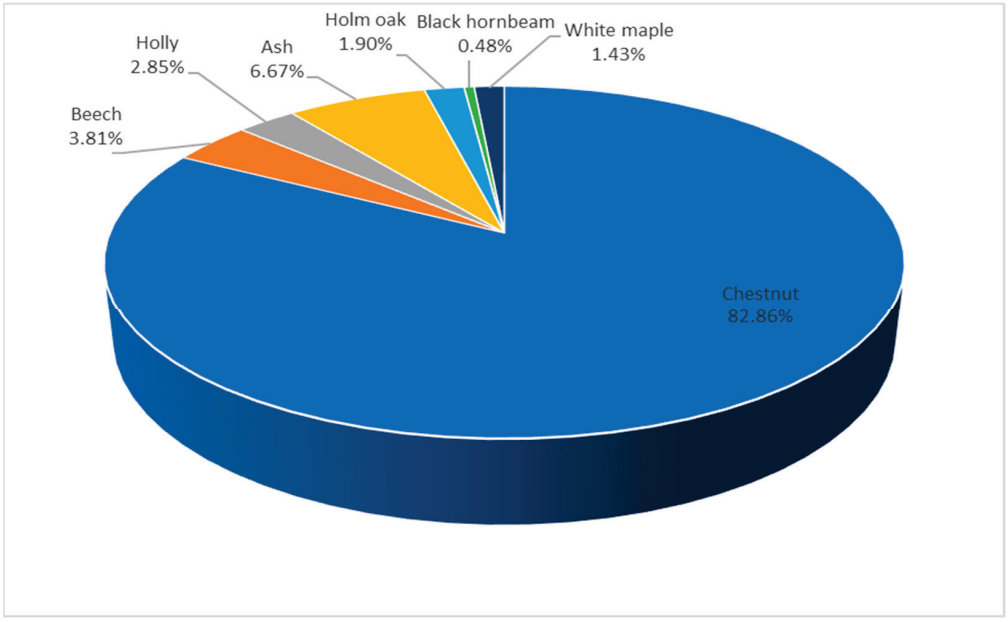

Figure 3. Tree composition.

2.1.3. Management

Traditionally, the management of chestnut wood was aimed at the production of fencing poles. The current Forest Management Plan, which will expire in 2028, adopted the conventional approach based on an essential silvicultural module. The plan suggests, eventually, a thinning between the age of 10 and 15 years, which in this rotation has not been implemented, while providing a final cutting at the age of 21 years and the release of 70 standards per hectare at the time of harvesting. After 21 years, the expected average of

chestnut wood production is 164 m^3/ha. The prevision of the Forest Management Plan is very coherent to the data registered at the final cutting (Table 1).

Table 1. Main parameters of chestnut coppice according to the Forest Management Plan, implemented since 2013, and the current situation (2023).

Parameters	U of M	Expected Parameters in 2023	Parameters Registered in 2023
Age		28–31	28–31
Average diameter	cm	11.28	15.62
Average height	m	13.00	15.78
Average basal area	m^2/ha	25.38	26.83
Stand density	tree/ha	2815	2660
Expected average production	m^3/ha	164.00	169.23 (1)

(1) These data exclude the dead chestnut wood (150.35 m^3/ha) and wood from other species (33.22 m^3/ha). Including the 169.23 m^3/ha of chestnut wood for operational use, the total production of wood is 352.80 m^3/ha.

2.1.4. Forest Management and the Quantification of Standing Volume

The forest stand was subjected to final cutting during the 2022/2023 harvesting season. Prior to the work, an inspection was carried out to identify a plot that was representative of the entire forest in which to carry out the measurement operations. The circular plot has a radius of 10.38 m. All trees, except those left standing after the cut as standards, were sequentially numbered, and for each tree, the species and the diameter at breast height were recorded.

After felling and stacking of trees in a temporary storage area, the following measurements were taken for all chestnut plants:

- Total height;
- Height of stem until the diameter is 8 cm;
- Diameter of stem at 8 m in height.

It was considered useful to take these two additional measurements for the comparative volume analysis. For the other hardwood species (17%), the diameter and height parameters were measured using conventional methods.

2.2. Wood Productions and Use

The total volume of the sample plot was determined using the following method:

- For tree stems with prospects of long-term use, volume tables of the species "Chestnut", under category "Volume stem and large branches (dm^3)", was used [36];
- For dead trees, parts of trees, suppressed trees or other species, the diameter at 1.30 m was measured, heights were recorded with the Vertex instrument and the taper coefficient was acquired using the Forest Management Plan.

The total overall volume felled per unit area, the net of released plants, has been estimated at 352.80 m^3/ha (Figure 4), which represents the functional unit under study expressed in volume. The wood is distributed as follows:

- Chestnut wood for operational use covers 169.23 m^3/ha, of which 135.38 m^3/ha are destined for the sawmill, 20.31 m^3/ha for energy purposes and 13.54 m^3/ha released for natural decomposition;
- Dead chestnut wood, with a volume of 150.35 m^3/ha, has been allocated for energy purposes at 120.28 m^3/ha and 30.07 m^3/ha for natural decomposition;
- Wood from other species covers 33.22 m^3/ha, of which 23.25 m^3/ha is for energy purposes and 9.96 m^3/ha is released for natural decomposition.

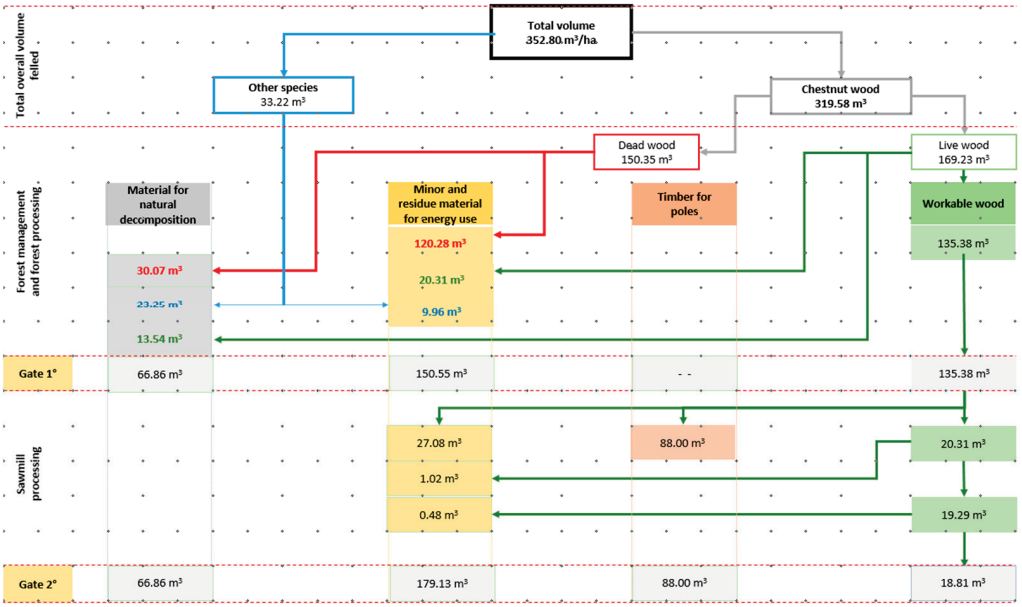

Figure 4. Reduction in the total overall volume and distribution of wood by category.

At gate 1, the destination categories are divided as follows: operational timber, 135.38 m^3/ha, which, following processing, has been allocated as follows:

- Workable wood, 20.31 m^3;
- Timber for poles, 88.00 m^3;
- Minor and residue material for energy use, 27.08 m^3.

The workable wood is first reduced to the required thickness and after drying for 3–4 years, undergoes final planning. At the end of this process, the volume introduced into the timber market (gate 2) amounts to 18.81 m^3. Given the initial volume, the allocation at gate 2 for the product categories is shown in Figure 5.

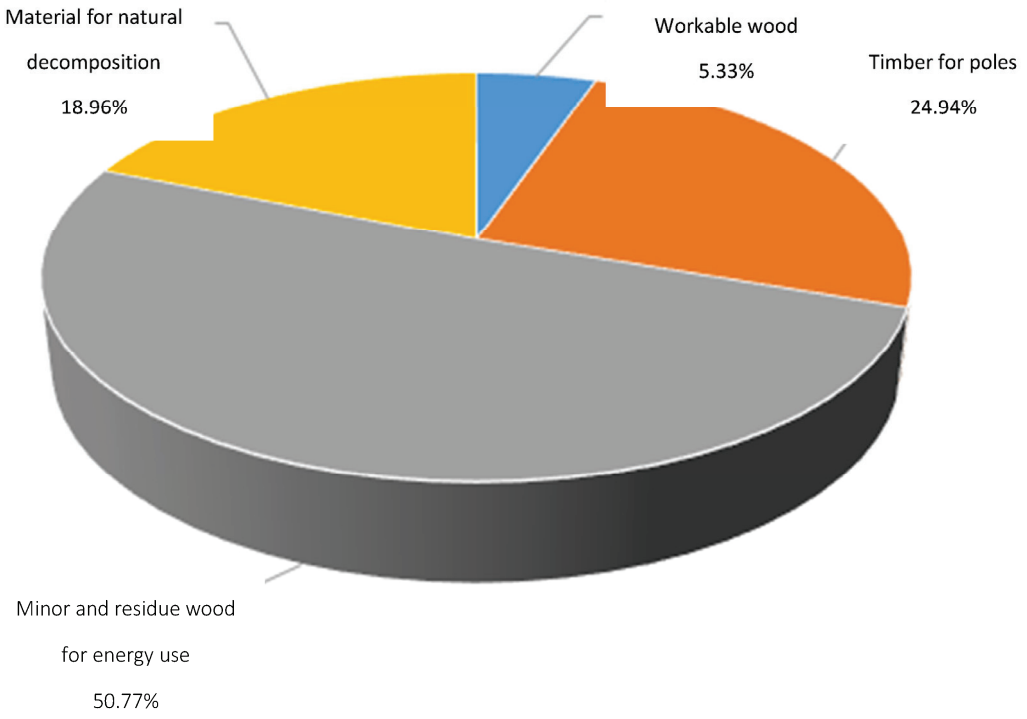

Figure 5. Distribution of the total overall volume by product category.

2.3. Wood Processing

The logging operation was carried out by a local forestry company that annually processes approximately 25,000 m^3/year of raw timber, mainly chestnut. The main equipment in the forest consists of chainsaws, a tractor with a winch and an excavator with a clamp. The felled trees were subsequently processed at the company's own sawmill, which is equipped with essential machinery, including a log saw and a band saw with a semi-automatic carriage and a thickness planer, in addition to other tools for material handling.

2.3.1. Forest Management

Forest felling was carried out by qualified workers using chainsaws. The felling operations involved chestnut and plants of other species, live, dead and/or dominated. After felling, branches were removed from the chestnut and other species. This waste material was released into the forest for natural decomposition. The timber of interest to the markets was extracted with a winch mounted on a tractor and was stacked in a temporary storage area. In chestnut trees, the plants are limbed, sectioned and the tops and damaged or curved parts are removed. The logs obtained were subsequently loaded onto the truck using an excavator with a clamp and then transported to the sawmill on a truck with a maximum capacity of 1.20 tons. The branches, curved tops and woody material from other species were loaded and taken to the company for appropriate processing, intended for their entry into the wood market for energy purposes.

2.3.2. Sawmill Processing

Upon arrival at the sawmill, the logs were unloaded in the temporary storage area. A qualified operator proceeded to qualify the individual logs on the basis of their dimensional characteristics and appearance, seeking the best possible end-use destination among the following categories:

- Workable wood: larger-sized logs, reduced to planks and subjected to natural seasoning. This material is stacked in special areas, and after 3–4 years of natural seasoning, it is processed using a band saw and thickness planer to obtain sharp-edged planks.
- Poles: a wide range of products that differ in diameter and height (Table 2) and are widely used outdoors. The name of the products are specific to the local area.
- Residual wood: this category includes wood residues obtained in the first selection in the forest (defective topping, etc.) as well as waste (defective wood, etc.) obtained from the processing of stems and branches in the sawmill, with a prospective allocation on the wood market for energy use.

Table 2. Range of products made of the chestnut coppice for category of timber for poles.

	Height m	**Diameter cm**
Min	1.50	5.00
Max	4.50	16.00

2.4. CO_2 Dynamics

2.4.1. Calculation of Absorptions

The following formula proposed from the IPCC [37] was adopted for the determination of CO_2 stored in wood:

$$V(CO_2) = \left[ML \times CC \times \left(\frac{PA_{(CO_2)}}{PA_{(C)}} \right) \right] \quad (1)$$

where:

1. ML is the wood density;
2. CC is the carbon content in chestnut wood;
3. PA (CO_2) is the molar mass of CO_2;
4. PA (C) is the molar mass of C.

The specific weights of the different forest species present in the area are shown in Table 3. As regards chestnut wood, cross-sections were extracted from some of the felled plants in the plot area. The density was 607.11 kg/m^3, significantly higher than the conventional wood density for this tree species [38]. For the other species, the density was obtained from technical manuals, determining the average value given the specified value ranges for each species. Only for holly was it quantified as the average value among the companion species. The volume of CO_2 stored by the various species ranges from 1069.48 to 1564.74 kg CO_2/m^3.

Table 3. The specific weight of the different forest species.

Species	Density		CO_2 Absorbed
	Range of Density kg/m^3	Compute Density kg/m^3	CO_2 kg
Chestnut (1)	430–580	607.11 (1)	1069.48
Holm oak	710–1070	890	1564.74
Holly (2)	700–850	775	1362.55
Beech	680–970	825	1450.46
Ash	700–850	775	1362.55
Black hornbeam	620–820	720	1265.86
White maple	530–800	665	1169.16

Legend: (1) value determined by the Wood Technology Laboratory for Industry and Cultural Heritage, Department for the Innovation of Biological, Agro-food and Forestry Systems of the University of Tuscia, Viterbo. (2) Average value of accompanying species. Source: Peso Specifico Legno. Wiki-Fisica. Accessed on 11 October 2023.

2.4.2. Calculation of Emissions

The raw wood material is introduced into the forest–wood supply chain, undergoing processing first in the forest and then in the sawmill. These processes favor the re-emission of part of the stored CO_2 into the atmosphere, occurring through the following pathways:

- Indirect means, as a consequence of wood losses.
- Direct means, as a consequence of wood processing.

Indirect emissions are the result of processing raw wood, both in the forest and at the sawmill, to obtain assortments for long-term use. The overall resulting wood material (branches, curved tops, chips, sawdust, etc.) is generally classified as wood for energy purposes, thus destined for short-term to very short-term uses with the consequent re-emission of absorbed CO_2. In the case under study, the forestry company releases part of the residual material into the forest for natural decomposition. In both cases, the specific balance of the net emissions from processing is neutral.

Direct emissions are those released by fossil-fueled capital equipment which, in the Tolfa area, is traditional. These emissions are distinguished between the following:

(i) Actions: (a) forest management; (b) raw material management; (c) workable material management; (d) timber for pole management; (e) woody residue management; (f) monitoring, control and surveillance; (g) operation of the forestry company and sawmill.

(ii) Sources, which are distinguished between capital equipment such as (h) forestry equipment; (i) transportation equipment; (j) equipment for internal wood handling; (k) monitoring equipment, as well as other capital equipment, such as (l) permanently invested assets; (m) emissions generated for the production of instrumental assets.

For the purposes of calculation, the actions referred to in (a), (b), (c), (d) and (e), are as follows:

- Direct emissions, i.e., those generated by the use of instrumental assets for activities in the forest and at the sawmill. They are quantified as a product of the following variables:
  - ➢ Technical parameters [PT] (productivity, time of use, distances, etc.).
  - ➢ Energy [E].
  - ➢ CO_2 conversion coefficient [$CCCO_2$].
- Collateral emissions, meaning emissions generated by the monitoring, control and surveillance activities in the forest (letter f) (which depend on the kilometers travelled), as well as the energy used for administrative, accounting and commercial activities in the operation of the forestry company and sawmill (letter g) (quantified in terms of a percentage, equal to 0.8%).
- Remote emissions, i.e., emissions related to the CO_2 emitted when the structures were built where wood processing takes place (permanently invested assets), as well as when the tools used in the processes (instrumental assets) were produced, both by the forestry company and sawmill. For both types of assets, the quantification of emissions can be determined assuming that the emissions for the production of structural capital are known [CS], and these must be related to the years of their working life [Y] and the average annual volume worked [VML], obtaining the percentage of emissions per unit of worked volume [E(%)]. Formally, it is calculated by the following equation:

$$E(\%) = \frac{E(100\%)}{[Y] \times [VML]} \quad (2)$$

which in this case amounts to 16.71%.

Commonly, machines (chainsaw, truck, etc.) are powered by conventional fuel, while machinery is powered by electricity, which is made available from conventional power plants. The emission coefficients and specific unit emissions of machines and machinery are shown in Table 4.

Table 4. Specific unit emissions of CO_2.

	Action	Machines and Machinery	Power	Hourly Consumption [(1)] (Liters)	Distances (km)	Conversion Coefficient [(2)] CO_2 eq	Emissions CO_2 eq/Hour
Forest processing	Felling	Chainsaw	Fuel	1.25		2.66	3.3
	Sectioning	Chainsaw	Fuel	1.25		2.66	3.3
	Wood extraction	Tractor with winch	Fuel	5.62		2.66	14.9
	Loading logs	Excavator with clamp	Fuel	5.0		2.66	13.3
	Loading waste material	Excavator with clamp	Fuel	5.0		2.66	13.3
	Transportation	Truck	Fuel		52	2.66	
Sawmill processing	Unloading	Crane with hydraulic clamp	Fuel	5.0		2.66	13.3
	Internal handling	Crane with hydraulic clamp	Fuel	5.0		2.66	13.3
	Sectioning workable wood	Log saw	Electricity			0.55	
	Handling workable wood	Forklift	Fuel	5.0		2.66	13.3
	Stacking for seasoning of workable wood	Forklift	Fuel	5.0		2.66	13.3
	Handling seasoned workable wood	Forklift	Fuel	5.0		2.66	13.3
	Stacking workable wood	Forklift	Fuel	5.0		2.66	13.3
	Handling timber for poles	Forklift	Fuel	5.0		2.66	13.3
	Stacking timber for poles	Forklift	Fuel	5.0		2.66	13.3
	Handling residual wood	Crane with hydraulic clamp	Fuel	5.0		2.66	13.3
	Sectioning residual wood	Semi-automatic saw	Electricity			0.55	
	Stacking residual wood	Crane with hydraulic clamp	Fuel	5.0		2.66	13.3

Sources: [(1)] Data produced from experts; [(2)] UK Emissions Trading Scheme, Department for Environment, Food and Rural Affairs, UKETS (01)05rev2.

3. Results

3.1. Balance Sheet of CO_2

The construction of the balance sheet is based on the traditional framework that juxtaposes the assets with the liabilities, which in this case are the absorptions and emissions of greenhouse gases.

3.1.1. Balance Sheet—Active Section

The first item listed on the active side of the balance sheet is the functional unit, which is the initial endowment potentially available for climate change mitigation. It is represented by the amount of CO_2 absorbed by the coppice in the Tolfa area, predominantly chestnut, over 21 years of growth. The functional unit amounts to 389,746 kg CO_2/ha. Of this, 88% is attributed to chestnut wood, with approximately 41% unfortunately being dead standing wood due to the lack of thinning over time. Additionally, there is absorption from other species (12%) (Figure 6).

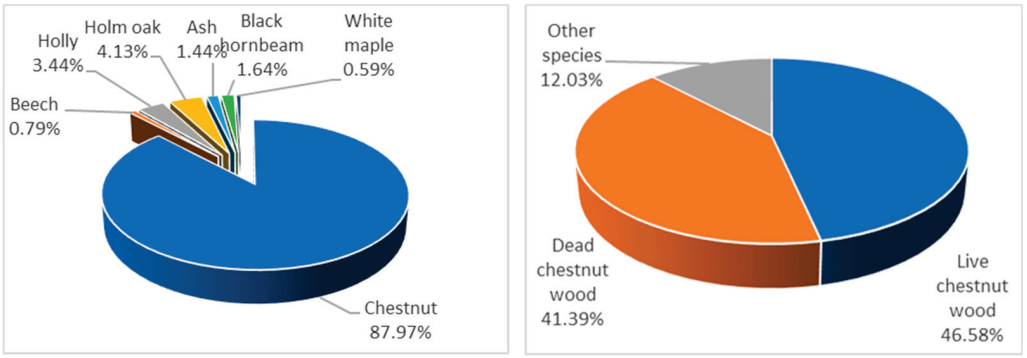

(**a**) (**b**)

Figure 6. Contribution of forest species to the determination of the functional unit: (**a**) percentage contribution of each forest species; (**b**) percentage contribution of dead chestnut wood, live chestnut wood and other species.

3.1.2. Balance Sheet—Passive Section

The passive section, instead, is divided into two parts: (i) the loss of timber and (ii) the climate-changing emissions.

The Loss of Timber

In this section, the reduction in the useful timber volume along the processing chain is quantified in order to acquire the appropriate physical dimension characteristics for providing long-term services. The partial balance of the discarded timber, the net emissions due to the use of instrumental assets, is at a neutral balance because in the short term, the CO_2 stored during their growth is re-released into the atmosphere. In the context of climate change mitigation, the discarded volumes represent unaccountable losses. The objective of this section is therefore to estimate the fraction of CO_2 from the functional unit re-emitted into the atmosphere, both for the forest and sawmill processing.

The processing of felled raw timber in the forest is distinguished between that of live chestnut trees at the time of the operation, as well as other minor species, along with dead standing chestnut trees. Live chestnut trees, including shoots and standards, are reduced to transportable logs. This is achieved by removing the branches on the felling site and by trimming and eliminating the curved basal stubs. Other species and dead chestnut trees are processed on the felling site, removing the branches while also preserving the stems and branches (up to 5 cm in diameter) that can be sold on the energy market. In the sawmill, the chestnut logs are cut and directed to the following production lines: workable wood, timber for poles and timber for energy purposes. The quantification of woody volume losses is 333.99 m^3, while the quantification of losses in terms of CO_2 is 363,625 kg (Table 5).

Table 5. Analysis of losses by processing area and product category (data in kg of CO_2).

Gate		Description	Passive
	Forest	Branches	79,056
		Wood for energy use	163,997
1	Sub-total		243,053
	Sawmill	Timber for poles	93,928
		Wood for energy use (waste)	21,676
		Wood for energy use (trimmings)	4969
2	Sub-total		120,572
Total			363,625

Climate-Changing Emissions

The construction of the passive section involves the analysis of the actions and instrumental capital (sources) employed. Actions that generate direct emissions in the forest include the following

(a) Forest management, which is based on the felling of the stand, excluding standards to be left as part of the forest;
(b) Management of raw material, through the following:
    (b1) Clearing branches of all species, with the difference that for chestnut destined for construction timber, all branches are removed, while for other species and dead chestnut, stems and branches (hereafter referred to as FBR) of interest to the energy market are saved;
    (b2) Wood extraction is carried out using a tractor equipped with a winch, while for the FBR of other species and dead chestnut trees, they are first sectioned on the felling site and then harvested using a tractor with cages;
    (b3) Sectioning of only the logs at the storage area, with the removal of the curved basal stump and trimming to a length suitable for transportation;
(c) Loading of logs and FBR onto the truck;
(d) Transportation to the sawmill.

Upon arrival of the timber at the sawmill, the process continues with the following:

(e) Timber management, which involves the following:
    (e1) Unloading and allocating the timber to the two dedicated temporary storage areas for logs and other materials;
    (e2) From the temporary storage area, logs are moved to the processing area;
    (e3) Trimming and selection for the three production lines:
        (e3a) workable wood;
        (e3b) timber for poles;
        (e3c) timber for energy use.

The timber processing line (e3a) involves (i) trimming and thickness cutting; ii) formation of stacks; (iii) allocation of stacks in drying areas; (iv) after approximately 3–4 years, the timber is brought back to the processing area for thickness planning; (v) placement of semi-finished chestnut products on the market. The timber line for poles (e3b) involves (i) the sawing of poles to a defined length; (ii) formation of stacks by standard size classes; (iii) allocation of the poles to the market. Finally, in the timber processing line for energy use (e3c), waste and residual materials from forest operations are collected, excluding branches, while from sawmill processing waste, wood chips, sawdust, etc., are collected.

The other actions that generate collateral emissions include (a) monitoring and control, involving periodic inspections and minor maintenance interventions; (b) the operational activities of the company's administration and the sawmill.

Regarding emissions due to the use of instrumental capital, these include (a) forestry tools, especially the chainsaw, used for stand management, the processing of raw material, and the selection and trimming of logs; (b) machinery and equipment, such as the

excavator with a hydraulic clamp for the loading and unloading of timber, the band saw, the thickness planer, as well as the machine for testing and controlling management activities; (c) transport and handling equipment, such as trucks and forklifts, the former for transporting timber from the management area to the sawmill, and the latter for internal handling of timber in various processing stages; (d) other instrumental capital (computers, printers, etc.) supporting administrative and commercial activities; (e) remote emissions resulting from the construction of structures for the storage of instrumental capital and the manufacturing of machinery and equipment used in the processing.

In Table 6, the emissions framework is constructed. Overall, the most emitting actions are those related to the management of raw material in the forest, 2716 kg of CO_2, while the management of timber along the production lines generates emissions of 1041 kg of CO_2. Forest management activities result in emissions of 234 kg of CO_2, and ancillary emissions are less than 100 kg of CO_2. The highest-emitting sources are machinery and equipment, accounting for 2243 kg of CO_2, with transportation and internal handling of timber within the sawmill estimated at around 1025 kg of CO_2. Remote emissions are slightly less than 600 kg of CO_2.

Table 6. Emissions generated by actions and sources (data in kg of CO_2).

			Actions					Total Sources Emissions
			Direct Emissions			Collateral Emissions		
			Forest Management	Raw Material Management	Timber Management	Monitoring and Control	Operation	
Sources	Direct emissions	Forestry tools	234.61				3.52	238.13
		Machines and machinery		874.06	395.03		33.15	1288.13
		Timber-handling vehicles		1453.66	496.89		15.14	1979.81
	Collateral emissions	Other instrumental capital				74.40	1.12	75.52
	Remote emissions	Capitals permanently invested and instrumental capital	39.18	388.73	148.95	12.42	8.84	598.12
Total action emissions			273.79	2716.45	1040.88	86.83	61.77	4179.71

3.2. Badget Balance of CO_2

The functional unit estimates an initial stock of 389,746 kg of CO_2/ha. Atmospheric emissions due to wood processing, between the forest and sawmill, are estimated at 363,625 kg of CO_2, while those due to the use of instrumental capital, whether direct, collateral, or remote, amount to approximately 4180 kg of CO_2. Therefore, the eligible balance for climate change mitigation purposes amounts to 21,940 kg of CO_2 (Table 7).

Table 7. Balance between active and passive (data in kg of CO_2).

Description	Active	Passive	Balance
Accumulated CO_2	389,745.51		
Emissions due to wood loss		363,625.54	
Emissions due to the use of instrumental capital		4179.71	
Balance	389,745.51	367,805.25	21,940.26

4. Discussion

In the pre-Apennine area of Lazio, areas of volcanic origin are the sites where chestnut trees for timber production find particularly favorable conditions for growth. The Tolfa territory is characterized by the presence of a small volcanic area, where there is a chestnut stand whose measurements show a production of approximately 353 m^3/ha at the age of 21 years, with an average increment of 16.8 m^3/ha, excluding standards released and

including biomass. It is primarily a chestnut-dominated stand; however, a significant portion consists of standing dead chestnut trees because of the lack of thinning.

Unfortunately, this traditional approach to the management of chestnut coppices is recurrent in medium and medium–small farms, which are the most numerous but with smaller areas, less than 100 ha, in the Lazio region and also in large parts of Italy.

This is significantly reflected in the coppice's ability to optimize its CO_2 storage capacity. Although starting from a substantial CO_2 endowment, the eligible fraction is live chestnut (48%), while 43% is dead wood, plus 9% of wood of other minor species.

Following the forest operations (gate 1), 38% of the timber that enters the sawmill is classified as workable wood, while timber for energy use constitutes 43%. Finally, 19% is left in the forest for natural decomposition.

Since the chestnut trees are relatively small in size, of the 38% of the incoming volume at the sawmill, a significant portion goes into the production line for timber for poles (25%), while the remainder remains as workable timber (7%). This percentage is further reduced to 6% by the end of processing at the sawmill (gate 2).

The LCA reflects what was highlighted above in terms of CO_2 volume quantities. With an initial allocation of 389,746 kg of CO_2, the emissions resulting from the overall processing of timber amount to 363,625 kg of CO_2, which is 93% of the functional unit. In addition to these, there are the 4180 kg of CO_2 emissions due to the use of instrumental capital, which is approximately 1%. Therefore, the eligible fraction for climate change mitigation amounts to just 6%, approximately 21,940 kg of CO_2/ha. Extending the unit value to the entire forest area (85 ha) results in more than 2000 tons of CO_2.

The forestry management traditionally adopted, while providing a positive budget balance, could certainly do better. A substantial volume is destined for energetic uses due to an excess of plant density and the lack of intercalary maintenance. The implementation of the latter would increase the quantity and quality of timber for long-term use.

A comparative analysis of the environmental performance of chestnut coppices in the Tolfa area and those in the Colli Albani area [20] shows that the latter have better performance. Considering that the ($CO_2/m^{-3} \times ha^{-1}$) of usable wood volume in the compared forests is of the same entity, the differences arise from the high volume of timber discarded during the processing of the Tolfa coppices and the better silvicultural management practices in the Colli Albani forests, which include more intercalary management and a longer rotation period (Table 8).

Table 8. Chestnut coppice forests in comparison.

Chestnut Coppice	CO_2 of the Felled Volume in the Final Cut	CO_2 of Usable Volume	Environmental Performance Index	Rotation	Useful CO_2 Stored Annually	Useful Volume	CO_2 of Useful Volume
	CO_2/ha	CO_2/ha	%	anni	CO_2/anno	m^3	m^3/ha
Tolfa	387,766.38	16,106.81	4.15%	21.00	766.99	18.81	856.31
Colli Albani	547,875.00	107,444.00	19.61%	32.00	3357.63	125.00	859.55

The current study's limitation lies in its company-scale focus, where the "specificities" of the context under investigation generate significant differences. The two parameters are focused on wood density and volume calculation. Nardi Berti [37] attributes a density of 430–580 Kg/m^3 to chestnut wood, while higher values have been recorded at the regional scale, specifically, 613 kg/m^3 for chestnut in the Colli Albani area and 607 kg/m^3 for chestnut in the Tolfa area. The data defined on a national scale would determine an underestimation ranging from 4.7% to 42.56%.

Regarding the amount of the growing stock, the value has been determined using national volume tables [36]. The values obtained refer to the average tree stem shape of chestnut shoots growing in Italian forests under various conditions. Comparing this

method for estimating the volume of stems with the Smalian formula [39], which takes into account their actual shape, statistical parameters indicate that the average volume (shoots and standards) is slightly higher for the Smalian formula, while the standard deviation is greater for the volume tables (Table 9). In other words, according to the Smalian formula, individual stems have a smaller range of volumes. The volumetric data from both methods have also been compared using the Bland–Altman plot (Figure 7). There is a clear and statistically significant agreement between the two methods, as long as shoots and standards are kept separate in the analysis.

Table 9. Comparison of the methods adopted.

	Formula of Smalian	Volume Tables	Differences
Average value	0.115	0.108	6.10%
Standard deviation	0.081	0.115	−29.83%

In terms of volume per unit of surface area, the volume tables estimate 352.80 m^3/ha, while the Smalian formula records a volume of 363.13 m^3/ha, which is 2.93% higher. The differences between the two methods are not particularly significant; however, since this study was conducted at a company scale (microeconomic size), it is appropriate to consider the specific characteristics of the context. Although the variations from this study unit are limited, in terms of absolute values, they could be important. From the perspective of placing on the voluntary carbon credits market, underestimations could lead to significant economic and financial differences.

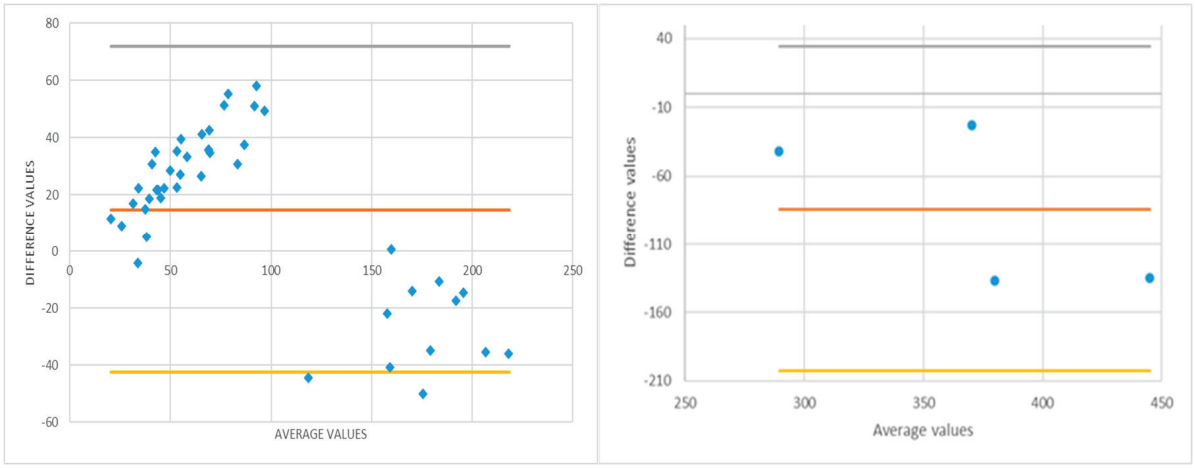

(**a**) (**b**)

Figure 7. Comparative analysis of samples using the Bland-Altman Plot. (**a**) Analysis of shoots; (**b**) Analysis of standards. (Limits calculation: upper limit (grey line, [average value +(2 × 1.96)]); average value (red line); lower limit (orange line, [average value −(2 × 1.96)]).

5. Conclusions

European Union policies for sustainable development converge toward the valorization of forest resources. Chestnut wood possesses qualities that make it suitable for structural uses and capable of providing long-term services. This versatility has generated significant interest in this species. Due to its multi-functionality, chestnut wood could be a competitive substitute for similar fossil-based raw materials [40].

The current study investigated the case of a coppice forest managed with an essential silvicultural model. Although the calculations showed a positive result, it must be emphasized that a large part of the production at the end of rotation, unfortunately, is not eligible for climate change mitigation purposes. Much of the wood production is destined for short to very short-term uses, resulting in a "zero-net" value balance. The emissions

generated by the processing are offset by the preserved stock; however, there is potential to improve the environmental efficiency of these formations so they meet the criteria of the climate-smart forestry approach. Some suggestion are as follows:

- To exceed the current silvicultural model by incorporating thinning during a longer rotation period (up to 30 years) [14];
- To rationalize the current single-compartment layout to introduce a rotational system that allows for scalable management with reduced operational costs;
- To examine whether conditions exist to promote the extension of the rotation period;
- To upgrade the technology level of tools, machines and machineries used in the forest management and in the sawmill.

In terms of forest management practices, it is reiterated to move beyond conventional energy systems and promote the use of biofuels and renewable energy sources. In this regard, the next programming period could provide the necessary resources.

An aspect that deserves attention concerns chestnut pole production. Beyond the standardization of assortment categories [41] it is considered appropriate to develop a methodology for evaluating stored CO_2 so that these productions can also make a contribution to environmental issues.

From a methodological standpoint, the development of this study has highlighted some significant critical issues:

- LCA implementation requires detailed data. Unfortunately, their acquisition is difficult first of all, because operators are generally reluctant to provide data, as well as because Forestry logging companies often also carry out non-forestry activities, so it becomes difficult to obtain data specifically for forestry activities;
- National reference parameters are important for large-scale assessments, but on a micro-scale (forest farm), specific data for the studied context should be used, especially when there are economic objectives involved.

Author Contributions: Conceptualization, F.C.; methodology, F.C. and L.P.; formal analysis, M.R.; investigation, T.G.; resources, F.C.; data curation, T.G.; writing—original draft, T.G.; writing—review & editing, L.P. and F.B.; supervision, M.R.; project administration, F.C. All authors have read and agreed to the published version of the manuscript.

Funding: This research was funded by Administration of Lazio Region. It is part of the project "PSR Lazio 2014–2020. Tipologia di operazione 16.2.1 Bando approvato con Determinazione Dirigenziale n. G11180 del 21/09/2021. Domanda n. 24250029758." Specific code projects F89H2300008009. Project: Innovative Tools for Boosting the Chestnut Ecosystem Services Management.

Data Availability Statement: The data presented in this study are openly available after direct request to the Authors.

Acknowledgments: The authors are grateful to the Tolfa Local Administration and the Chirichilli Forestry Company for their collaboration, which contributed to the success of this study.

Conflicts of Interest: The authors declare no conflicts of interest.

References

1. United Nations Environment Programme. Emissions Gap Report 2022: The Closing Window—Climate Crisis Calls for Rapid Transformation of Societies. *Nairobi*. 2022. Available online: https://www.unep.org/emissions-gap-report-2022 (accessed on 31 January 2024).
2. IPCC. Technical Summary. Climate Change, 2022. Impacts, Adaptation and Vulnerability. 2022. Available online: https://www.ipcc.ch/report/ar6/wg2/downloads/report/IPCC_AR6_WGII_TechnicalSummary.pdf (accessed on 31 January 2024).
3. UNCCS. Climate Action and Support Trends, United Nations Climate Change Secretariat. 2019. Available online: https://unfccc.int/sites/default/files/resource/Climate_Action_Support_Trends2019.pdf (accessed on 31 January 2024).
4. Mathis, W.; Rees, W. *Our Ecological Footprint: Reducing Human Impact on the Earth*; New Society Publishers: Gabriola, BC, Canada, 1998; Volume 9.
5. Dirk, K.; Löhr, D.; O'Regan, B. Valuation of ecological impacts—A regional approach using the ecological footprint concept. *Environ. Impact Assess. Rev.* **2006**, *26*, 156–169. [CrossRef]

6. La Torre, M.A. *La Questione Ambientale: Tra sostenibilità, Responsabilità e Crescita Economica*; Libreriauniversitaria Edizioni: Limena, Italy, 2015.
7. Zhang, L.; Dzakpasu, M.; Chen, R.; Wang, X.C. Validity and utility of ecological footprint accounting: A state-of-the-art review. *Sustain. Cities Soc.* **2017**, *32*, 411–416. [CrossRef]
8. Schulze, E.-D.; Valentini, R.; Sanz, M.-J. The long way from Kyoto to Marrakesh: Implications of the Kyoto Protocol negotiations for global ecology. *Glob. Chang. Biol.* **2002**, *8*, 505–518. [CrossRef]
9. Cienciala, E.; Schelhaas, M.J.; Nabuurs, G.J.; Lindner, M. Expected impact of the Kyoto Protocol on European forestry. *MEACAP WP4 D* **2007**, *12*, 3–11.
10. Fawzy, S.; Osman, A.I.; Doran, J.; Rooney, D.W. Strategies for mitigation of climate change: A review. *Environ. Chem. Lett.* **2020**, *18*, 2069–2094. [CrossRef]
11. AA.VV. The Economics of Ecosystems and Biodiversity: Mainstreaming the Economics of Nature: A Synthesis of the Approach, Conclusions and Recommendations of TEEB. 2010. Available online: https://eclass.hua.gr/modules/document/file.php/GEO200/TEEB%20(2010),%20economics%20of%20nature.pdf (accessed on 31 January 2024).
12. Barbati, A.; Ferrari, B.; Alivernini, A.; Quatrini, A.; Merlini, P.; Puletti, N.; Corona, P. Sistemi forestali e sequestro del carbonio in Italia. *L'Italia Forestale e Montana* **2014**, *69*, 205–212. [CrossRef]
13. Calfapietra, C.; Barbati, A.; Perugini, L.; Ferrari, B.; Guidolotti, G.; Quatrini, A. Carbon mitigation potential of different forest ecosystems under climate change and various managements in Italy. *Ecosyst. Health Sustain.* **2015**, *1*, 11878999. [CrossRef]
14. Prada, M.; Bravo, F.; Berdasco, L.; Canga, E.; Martínez-Alonso, C. Carbon sequestration for different management alternatives in sweet chestnut coppice in northern Spain. *J. Clean. Prod.* **2016**, *135*, 1161–1169. [CrossRef]
15. Wiedmann, T.; Barrett, J. A review of the ecological footprint indicator—Perceptions and methods. *Sustainability* **2010**, *2*, 1645–1693. [CrossRef]
16. *UNI EN ISO 14040*; Environmental Management—Life Cycle Assessment—Principles and Framework. International Organization for Standardization: Geneva, Switzerland, 2021.
17. Limnios EA, M.; Ghadouani, A.; Schilizzi, S.G.; Mazzarol, T. Giving the consumer the choice: A methodology for Product Ecological Footprint calculation. *Ecol. Econ.* **2009**, *68*, 2525–2534. [CrossRef]
18. Lippke, B.; Wilson, J.; Meil, J.; Taylor, A. Characterizing the importance of carbon stored in wood products. *Wood Fiber Sci.* **2010**, *42*, 5–14.
19. Sala, S.; Amadei, A.M.; Beylot, A.; Ardente, F. The evolution of life cycle assessment in European policies over three decades. *Int. J. Life Cycle Assess.* **2021**, *26*, 2295–2314. [CrossRef]
20. Martínez-Alonso, C.; Berdasco, L. Carbon footprint of sawn timber products of *Castanea sativa* Mill. in the north of Spain. *J. Clean. Prod.* **2015**, *102*, 127–135. [CrossRef]
21. Carbone, F.; Corona, P.; Hussain, M.; Barbarese, F. Net-Carbon Dioxide Surplus as an Environmental Indicator for Supporting Timber Markets: A Case Study in Italy. *Forests* **2023**, *14*, 419. [CrossRef]
22. National Forest Services. *National Inventory of Forest and Forest Carbon Pools—INFC2005*, 2nd ed.; Inventory Survey; Consiglio per la Ricerca in Agricoltura e l'Analisi dell'Economia Agraria (CREA); Arma dei Carabinieri: Rome, Italy, 2017.
23. National Forest Services. *National Inventory of Forest and Forest Carbon Pools—INFC2015*, 3rd ed.; Consiglio per la Ricerca in Agricoltura e l'Analisi dell'Economia Agraria (CREA); Arma dei Carabinieri: Rome, Italy, 2022.
24. Venanzi, R.; Picchio, R.; Piovesan, G. Silvicultural and logging impact on soil characteristics in Chestnut (*Castanea sativa* Mill.) Mediterranean coppice. *Ecol. Eng.* **2016**, *92*, 82–89. [CrossRef]
25. Venanzi, R.; Picchio, R.; Grigolato, S.; Latterini, F. Soil and forest regeneration after different extraction methods in coppice forests. *For. Ecol. Manag.* **2019**, *454*, 117666. [CrossRef]
26. Manetti, M.C.; Conedera, M.; Pelleri, F.; Montini, P.; Maltoni, A.; Mariotti, B.; Pividori, M.; Marcolin, E. Optimizing quality wood production in chestnut (*Castanea sativa* Mill.) coppices. *For. Ecol. Manag.* **2022**, *523*, 120490. [CrossRef]
27. Mattioli, W.; Mancini, L.D.; Portoghesi, L.; Corona, P. Biodiversity conservation and forest management: The case of the sweet chestnut coppice stands in Central Italy. *Plant Biosyst.* **2016**, *150*, 592–600. [CrossRef]
28. Manetti, M.C.; Amorini, E.; Becagli, C.; Pelleri, F.; Fratini, R.; Marone, E. Valorizzazione dei cedui di castagno: Modalità di gestione e realtà socio-economica del territorio. *Ann. Silvic. Res.* **2010**, *36*, 97–108.
29. Giannini, R.; Maltoni, A.; Mariotti, B.; Paffetti, D.; Tani, A.; Travaglini, D. Valorizzazione della produzione legnosa dei boschi di castagno. *L'Italia For. E Mont.* **2014**, *69*, 307–317. [CrossRef]
30. Manetti, M.C.; Becagli, C.; Carbone, F.; Corona, P.; Giannini, T.; Romano, R.; Pelleri, F. *Linee Guida per la Selvicoltura dei Cedui di Castagno*; Rete Rurale Nazionale (RRN); Consiglio per la Ricerca in Agricoltura e l'Analisi dell'Economia Agraria (CREA): Rome, Italy, 2017; ISBN 9788899595579.
31. Quatrini, V.; Mattioli, W.; Romano, R.; Corona, P. Caratteristiche produttive e gestione dei cedui in Italia. *L'Italia Forestale e Montana* **2017**, *72*, 273–313. [CrossRef]
32. Carbone, F.; Moroni, S.; Mattioli, W.; Mazzocchi, F.; Romagnoli, M.; Portoghesi, L. Competitiveness and competitive advantages of chestnut timber laminated products. *Ann. For. Sci.* **2020**, *77*, 51. [CrossRef]
33. Conedera, M.; Tinner, W.; Krebs, P.; de Rigo, D.; Caudullo, G. Castanea Sativa in Europe: Distribution, Habitat, Usage and Threats. 2016. Available online: https://boris.unibe.ch/80790/1/Castanea_sativa.pdf (accessed on 31 January 2024).

34. Weatherall, A.; Nabuurs, G.-J.; Velikova, V.; Santopuoli, G.; Neroj, B.; Bowditch, E.; Temperli, C.; Binder, F.; Ditmarová, L.-U.; Jamnická, G.; et al. Defining Climate-Smart Forestry. In *Climate-Smart Forestry in Mountain Regions*; Tognetti, R., Smith, M., Panzacchi, P., Eds.; Springer: Berlin/Heidelberg, Germany, 2022; pp. 34–58.
35. Fattori, C. Aggiornamenti Dataset "Aree Naturali Protette" Geoportale Regione Lazio. 2018. Available online: https://www.cartinegeografiche.eu/cartina_geografica_del_lazio_mappa.htm (accessed on 5 June 2023).
36. Tabacchi, G.; Di Cosmo, L.; Gasparini, P.; Morelli, S. Stima del Volume e Della Fitomassa Delle Principali Specie Forestali Italiane. In *Equazioni di Previsione, Tavole del Volume e Tavole Della Fitomassa Arborea Epigea*; Consiglio per la Ricerca e la sperimentazione in Agricoltura, Unita di Ricerca per il Monitoraggio e la Pianificazione Forestale: Trento, Italy, 2011; 412p, Available online: https://www.inventarioforestale.org/wp-content/uploads/2022/10/tavole_cubatura.pdf (accessed on 31 January 2024).
37. Intergovernmental Panel on Climate Change (IPCC). *Guidelines for National Greenhouse Gas Inventories*; Agriculture, Forestry and Other Land Use; IPCC: Geneva, Switzerland, 2006; Volume 4.
38. Nardi Berti, R.; Fioravanti, M.; Macchioni, N. *La Struttura Anatomica del Legno ed il Riconoscimento dei Legnami Italiani di più Corrente Impiego*; CNR Istituto per la BioEconomia: Sesto Fiorentino, Italy, 2006.
39. La Marca, O. *Elementi di Dendrometria*, 3rd ed.; Pàtron Editore: Bologna, Italy, 2017; pp. 1–530.
40. Cremonini, C.; Zanuttini, R. Legno di castagno: Versatilità e tradizione. In *Note Tecniche e Prospettive per la Castanicoltura da Legno in Piemonte*; Centro Regionale di Castanicoltura del Piemonte—University of Torino: Grugliasco, Italy, 2020; pp. 6–9.
41. Sirna, A.; Carbone, F. Criticità nei processi di valorizzazione del castagno. *Estimo Territorio* **2008**, *7*, 27–33.

Disclaimer/Publisher's Note: The statements, opinions and data contained in all publications are solely those of the individual author(s) and contributor(s) and not of MDPI and/or the editor(s). MDPI and/or the editor(s) disclaim responsibility for any injury to people or property resulting from any ideas, methods, instructions or products referred to in the content.

forests

MDPI

Article

The Effects of Soil Compaction on the Growth and Architecture of the Seedlings of Species Commonly Used for Afforestation in Iran

Meghdad Jourgholami [1,*], Elahe Alsadat Hosseiniala [1], Francesco Latterini [2], Rachele Venanzi [3] and Rodolfo Picchio [3]

[1] Department of Forestry and Forest Economics, Faculty of Natural Resources, University of Tehran, Karaj 999067, Iran; elahe_nademi@ut.ac.ir
[2] Institute of Dendrology, Polish Academy of Sciences, Parkowa 5, 62-035 Kórnik, Poland; latterini@man.poznan.pl
[3] Department of Agriculture and Forest Sciences, Tuscia University, Via San Camillo de Lellis, 01100 Viterbo, Italy; venanzi@unitus.it (R.V.); r.picchio@unitus.it (R.P.)
* Correspondence: mjgholami@ut.ac.ir

Abstract: The aim of the present study was to elucidate the effects of soil compaction on the seedlings of two species of deciduous (*Acer velutinum* and *Alnus subcordata*) and evergreen trees (*Pinus eldarica* and *Pinus nigra*) in terms of above- and below-ground morphology in a greenhouse. Six soil compaction levels were applied: the lowest intensity (control), very low, low, moderate, heavy, and very heavy. The results showed that there were different effects according to the species. These effects were on lateral root length, stem diameter, leaf dry biomass, SSL (specific stem length), SRL (specific root length), LMR (leaf mass ratio), RMR (root mass ratio), SMR (stem mass ratio), and R/S (root-to-shoot ratio). The results showed that soil penetration resistance (SPR) had a significant effect on seedling variables such as lateral root length, stem diameter, leaf dry biomass, and SRL ($p < 0.05$). *A. velutinum* seedlings have the highest values of growth variables compared to three other species, followed by *A. subcordata* seedlings. The two evergreen species, *Pinus eldarica* and *Pinus nigra*, have the lowest values of these growth variables. It is worth noting that we found that deciduous species had enhanced growth up to a moderate compaction level (1.3 MPa), while the growth decreased at an SPR that was higher than this value.

Keywords: soil compaction; morphological response; biomass growth; architectural response; velvet maple; Caucasian alder; eldar pine; black pine

1. Introduction

Soil plays a crucial role in forest ecosystems, and it is a mediator of nutrients, water, and energy flows that guarantee the productivity of the forest ecosystem and maintain biodiversity [1–4]. Logging operations are required to obtain wood for multiple purposes [5–7]. However, it is well known that logging operations can trigger substantial disturbance to the forest soil [3,8–13]. Forest soils after logging are, indeed, in most cases, prone to compaction. Soil compaction is commonly represented by soil bulk density (oven dry mass/volume) or penetration resistance as measured by a penetrometer [14–16]. Soil compaction can cause several changes in soil structure and hydrology, especially separation of soil aggregates, reduced soil porosity, destruction of pore continuity, an increment in shear strength, and a decrease in infiltration capacity [17–22]. Even a minor increment in soil compaction may lead to a change in the growth of young seedlings and inhibit the development of the root system [23]. A set of factors, including soil strength, water and nutrient availability, and aeration, regulate the effects of compaction on root growth [24,25]. If root growth is restrained due to soil compaction, roots have a lesser volume of soil to explore, causing a decrease in the amount of water available for the plant [26]. Previous findings have also

shown that soil compaction can negatively affect shoot growth [19,24,25]. Shoot growth of both *Leptospermum scoparium* and *Cordyline australis* was reduced by augmenting soil strength [27]. In another study, the authors found that shoot diameter and root–shoot ratio were influenced by soil type and degree of compaction [28]. In the bulk of research, soil compaction leads to reduced aboveground biomass to a different degree [24–26,29]. Variables such as height and diameter of seedlings in various species are frequently of lower values due to an increase in soil density [26,27]. For instance, some parameters, including shoot dry weight, leaf area, and dry weight, may be reduced by augmenting soil strength or density [28,30]. The interactions between root and shoot of perennial woody plants in response to increased soil compaction are a complicated topic due to the architecture and growth allocation of woody plants [26,31]. Previous studies have indeed indicated that increased soil strength may alter the growth allocation between the above- and below-ground fractions of seedlings [27,32].

Severe compaction of soil not only shortens and thickens roots but also may alter their branching patterns [18,23,33]. However, the decline in root growth may not lead to a decrease in the total biomass of woody plants in all cases [34,35]. Hence, some factors regulate the plant response to soil compaction, such as soil type and texture, climate, light, water and nutrient availability, species, and the degree and extent of soil compaction [25,32,34]. In general, the growth of plants in compacted soils causes them to have more branched roots [27]. Weak root architecture can be expected due to an increase in soil bulk density, particularly in loamy sand soil, which, in turn, results in a decline in root branches' development and propagation, which consequently can have detrimental influences on water and nutrient uptake [24]. Also, the total length of primary and lateral roots reduces as soil bulk density increases [36]. Woody plant root elongation is generally prohibited at soil strength values higher than 2–2.5 MPa. However, it depends on the soil texture and plant species [37]. However, Skinner et al. (2009) [38] reported that any increase in soil strength may change the root growth of woody plants.

In the Hyrcanian forests in Iran, forest soils are heavily compacted due to logging operations with heavy machines and cattle grazing [39–43]. In this area, four main species have been used for afforestation and ecosystem restoration. These are velvet maple (*Acer velutinum* Boiss.), Caucasian alder (*Alnus subcordata* C.A.M.), *Pinus eldarica* Medw., and *Pinus nigra* Arn. Despite the extensive literature on the topic of the interaction between soil compaction and seedling growth, such information is scarce for these four species used for afforestation in Iran. Therefore, the aim of the present study was to fulfill this knowledge gap by evaluating the effects of soil compaction on the growth of two species of deciduous trees (*Acer velutinum* Boiss. and *Alnus subcordata* C.A.M) and evergreen trees (*Pinus eldarica* Medw. and *Pinus nigra*) in a greenhouse experiment.

In this study, we tried to shed light on the relationship between penetration resistance and various growth variables in deciduous and evergreen seedlings to test the following hypotheses: (1) all the above- and below-ground variables, including seedling sizes (morphology) and biomass (growth), reduced as soil strength increased; (2) soil compaction can cause significant changes in growth allocation patterns (architectural variables) to the above- and below-ground fractions of these deciduous and evergreen tree seedlings.

2. Materials and Methods

2.1. Soil Strength Experiment

Seeds of deciduous (*Acer velutinum* Boiss. and *Alnus subcordata* C.A.M.) and evergreen (*Pinus eldarica* Medw. and *Pinus nigra*) trees were chosen from the seed center of Amol city (north of Iran), then transported to a seed laboratory situated in the Faculty of Natural Resources, Karaj, to investigate the quality and quantity of seeds. The deciduous *Acer velutinum* and *Alnus subcordata* are mainly distributed in the north of Iran in areas with temperate characteristics. The evergreen *Pinus eldarica* (Eldar pine) and *Pinus nigra* (Black pine) are mostly planted in arid and semi-arid areas of Iran.

Undisturbed soil from a depth ranging from 1 to 30 cm from Kheyrud Educational and Research Forest Station (located in the Nowshahr, north of Iran) was collected from the A_0 (litter), A_1, and A_2 horizons and transferred to the greenhouse with a temperature-controlled situation in the Faculty of Natural Resources in Karaj city. Dry air is needed to prevent seeds from decaying because they contain a high amount of moisture. Then, the seeds were preserved in the seed laboratory refrigerator at 4 °C. In February, four types of seeds were planted in loam or clay loam soils in plastic pots (20 × 15 cm) with a constant moisture regime, controllable temperature and humidity (between 18 °C and 24 °C, and a relative humidity level between 50% and 60%, depending on the type of seed) without adding fertilizer to avoid the possible confounding effects of different soil water regimes. Small seeds like *Alnus subcordata*, *Pinus eldarica*, and *Pinus nigra* were potted at a depth of 1–3 mm, and *Acer velutinum* was planted at a depth of 2–3 cm because its seeds are larger than the others. Pots were irrigated every day for 70 days in a greenhouse located in the Faculty of Natural Resources, Karaj.

After 70 days, seedlings began to sprout; thus, in late March, seedlings were transplanted into larger pots (20 × 30 cm) so as to avoid the limitation of space for root growth over the experiment period. Six soil compaction levels with three replicates—including C, the lowest intensity (no compaction or control); VL, very low; L, low; M, moderate; H, high; and VH, very high—were applied with a compaction hammer (4.736 kg weight) from the height of 45.7 cm by manually applying 1, 2, 4, 6, and 8 blows. Water was supplied consistently each day using a sprinkler irrigation system (20 min of irrigation day^{-1}), and greenhouse situations were uniformly adjusted for all seedlings for light, water, humidity, and temperature throughout the entire experiment by changing the pot locations in the greenhouse during the experiment period. Soil penetration resistance (SPR) was determined with a hand-held penetrometer (Eijkelkamp 06.01.SA penetrometer, Wilmington, NC, USA) by measuring every 10 cm along the soil profile. The six values were averaged for each pot. The total number of pots was 72 (4 deciduous and evergreen tree species × 6 levels of soil strength × 3 replicates).

2.2. Seedling Growth Measurements

The seedlings were extracted and harvested from pots after 130 days (starting in late March and ending in late September). After carefully harvesting each seedling from the pots, the roots were washed and lightly dried. Then, the measurements of the fresh weight of the leaves, stems, and roots of each seedling were carried out. Seedling morphology parameters such as collar diameter and seedling height were determined by digital Collis calipers (0.01 mm accuracy, E-Base, MC 02050282-I, Taiwan, China) and scaled rulers (with 0.1 cm accuracy), respectively. After drying all fractions of seedlings at 70 °C, the dry weight of all seedlings was obtained.

Finally, for each seedling, the following parameters were determined or counted: The seedling morphological (or size) variables are as follows: length and diameter of the stem, length of the main root, main root diameter, and lateral root length. The seedling growth or dry biomass variables are as follows: total, shoot, stem, leaf, total root, main root, and lateral root biomass. The seedling's architectural variables are as follows: lateral/main root length ratio; lateral/main root dry biomass ratio; SSL: specific stem length (stem length/stem dry biomass); SRL: specific root length (fine root length/fine root dry biomass); LMR: leaf mass ratio (leaf dry biomass/total dry biomass); RMR: root mass ratio (root dry biomass/total dry biomass); SMR: stem mass ratio (stem dry biomass/total dry biomass); R/S: root-to-shoot ratio (root/shoot dry biomass).

2.3. Statistical Analysis

After checking data normality and homoscedasticity with Kolmogorov–Smirnov and Levene tests, respectively, we selected the statistical model for the analysis. Considering the lack of any nesting structure in our data (date independence), we selected the two-way ANOVA with interaction. Specifically, we considered the effects on all the investigated

variables of two fixed factors: species and experimental treatment (compaction level), as well as their interaction. The SPSS version 15.0 (IBM, New York, NY, USA) statistical package was applied to carry out all the statistical analyses.

3. Results

3.1. Compaction Level

The level of compaction in the pots significantly augmented the value of soil penetration resistance from 0.38 ± 0.03 MPa in the C treatment to 1.93 ± 0.13 MPa in the VH treatment ($p \leq 0.01$). Results showed that the values of soil bulk density were increased from 1.08 ± 0.03 g cm^{-3} in the C treatment to 1.38 ± 0.03 g cm^{-3} in the VH treatment ($p \leq 0.01$; Table 1). Also, the values of total porosity significantly declined from 54.04 ± 1.3% in the C treatment to 41.36 ± 1.2% in the VH treatment ($p \leq 0.01$).

Table 1. Mean (±standard deviation) of soil compaction indexes (i.e., penetration resistance, bulk density, and total porosity) in each of the six levels of compaction treatments measured in this study.

Compaction Treatment	Penetration Resistance (MPa)	Bulk Density (g cm^{-3})	Total Porosity (%)
1 (C, control)	0.38 ± 0.03	1.08 ± 0.03	54.04 ± 1.28
2 (VL, very low)	0.65 ± 0.10	1.14 ± 0.02	51.35 ± 0.89
3 (L, low)	0.95 ± 0.11	1.21 ± 0.03	48.37 ± 1.07
4 (M, moderate)	1.27 ± 0.08	1.26 ± 0.06	46.38 ± 2.66
5 (H, high)	1.51 ± 0.14	1.34 ± 0.04	43.12 ± 1.61
6 (VH, very high)	1.93 ± 0.13	1.38 ± 0.03	41.36 ± 1.15

3.2. Species and Growth Variables

Results showed that the species was a significant variable that statistically affected the seedling variables such as lateral root length, stem diameter, leaf dry biomass, SRL, SSL, SMR, LMR, RMR, R/S, lateral/main root length, and lateral/main root dry biomass ($p < 0.05$) (Figure 1).

The degree of lateral root length statistically differed among species, with Velvet maple (41.93 cm) as the highest and Caucasian alder (29.24 cm) as the lowest lateral root length. The value of stem diameter was statistically significant among species, with Velvet maple (4.32 mm) as the highest and black pine (3.13 mm) as the lowest. Duncan's test showed that species had significant effects on leaf dry biomass, with Velvet maple (11.39 g) as the highest and black pine (1.49 g) as the lowest for leaf dry biomass. Duncan's test showed that species had significant effects on SRL (root length/root dry biomass), with Eldar pine and black pine (39.8 and 37.4 cm g^{-1}) having the highest values and Velvet maple and Caucasian alder (3.3 and 2.7 cm g^{-1}) having the lowest values of SRL.

The same was confirmed for SSL (stem length/stem dry biomass), with Eldar pine (15.54 cm g^{-1}) as the highest and Caucasian alder (1.83 cm g^{-1}) as the lowest SSL. Duncan's test showed that species had significant effects on SMR, with Caucasian alder (0.32) having the highest and Eldar pine (0.17) having the lowest SMR. Duncan's test also showed that species had a significant effect on LMR; for this variable, black pine (0.34) had the highest value, while Velvet maple (0.18) had the lowest. Duncan's test showed that species had significant effects on RMR, with Velvet maple (0.53) as the highest and black pine (0.45) as the lowest. Similar effects were detected for root–shoot ratio; indeed, Velvet maple (1.15) showed the highest value and black pine (0.87) the lowest root–shoot ratio. Duncan's test showed that species had significant effects on lateral/main root length, with Eldar pine (by 3.26) having the highest and Velvet maple (by 1.63) having the lowest. Finally, Duncan's test showed that species had a significant effect on lateral/main root dry biomass; specifically, black pine (1.69) showed the highest values and Caucasian alder (0.71) the lowest one.

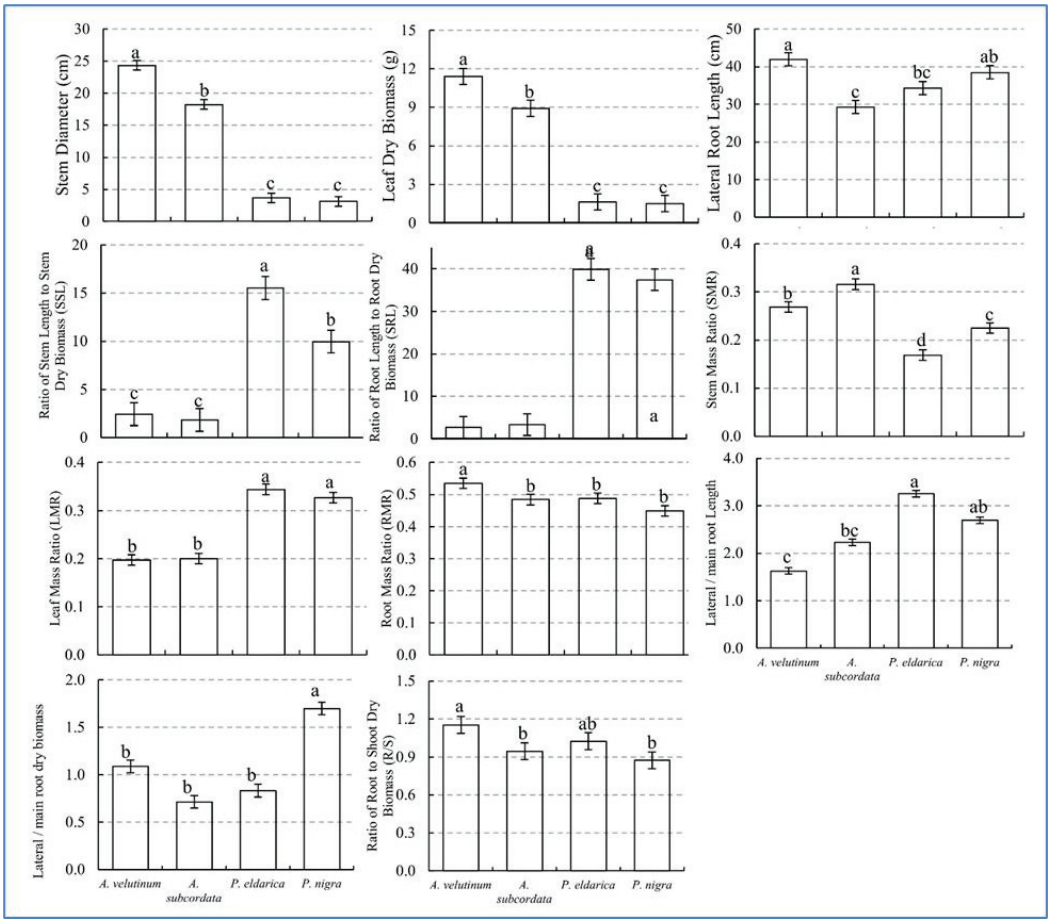

Figure 1. Mean (±standard deviation) of the species effect on seedling growth variables (different letters in a row indicate significant differences among intensities of soil compaction ($p < 0.05$) based on Duncan's tests).

3.3. Soil Penetration Resistance and Growth Variables

Results reported in Figure 2 showed that the experimental treatment was a significant driver of seedling growth, specifically for lateral root length, stem diameter, leaf dry biomass, and SRL ($p < 0.05$). In particular, lateral root length decreased with increasing soil compaction. Stem diameter decreased as well with increasing compaction, even if there were no significant differences in the stem diameter among the very low (VL), low (L) soil compaction, and C treatments. Leaf dry biomass and specific root length (SRL) followed a similar trend, with decreasing values with increasing soil compaction but no significant differences among C, VL, L, and M treatments.

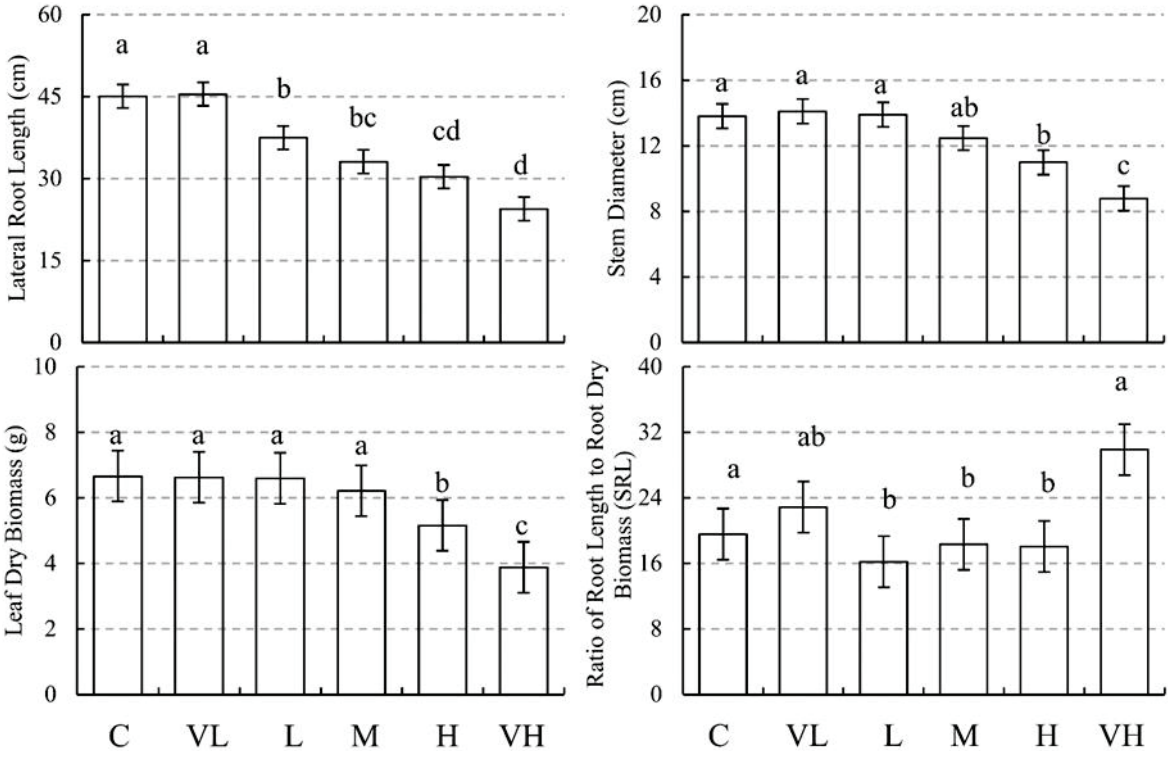

Figure 2. Mean (±standard deviation) of soil penetration resistance (SPR) effect on seedling growth variables (different letters in a row indicate significant differences among intensities of soil compaction ($p < 0.05$) based on Duncan's multiple range tests). Different levels of soil compaction include C: control, VL: very low, L: low, M: moderate, H: high, and VH: very high.

3.4. Interaction Effect between Species and Soil Compaction

Tables 2 and 3 show the analysis of the seedling growth variable data as affected by species and soil penetration resistance (SPR) for deciduous and evergreen species.

Results showed that the interaction effect between species (SP) × experimental treatment was significantly affecting seedling variables such as stem length, main root length, root diameter, dry biomass of total, shoot, root, stem, main root, and lateral root ($p < 0.05$). Contrarily, we did not detect any effect of the interaction between species and experimental treatment: lateral root length, stem diameter, leaf dry biomass, SRL, SSL, SMR, LMR, RMR, R/S, lateral/main root length, and lateral/main root dry biomass.

In the deciduous species, results showed an increase in biomass with increased soil compaction until moderate levels (M treatment—about 1.3 MPa), while at higher compaction values, these variables were reduced. Evergreen species showed decreased growth with increasing compaction.

Table 2. Means of seedling morphology (size), growth (biomass), and architecture (allocation ratios) variables of *Acer velutinum* and *Alnus subcordata* seedlings at different intensities of soil compaction. Different letters in each species column indicate significant differences among intensities of soil compaction ($p < 0.01$) based on Duncan's tests.

Species	Compaction Intensity	Seedling Morphology (Size)					Seedling Growth (Dry Biomass)							Seedling Architecture (Allocation Ratios)						
		Stem Length (cm)	Stem Diameter (mm)	Main Root Length (cm)	Main Root Diameter (mm)	Lateral Root Length (cm)	Total (g)	Shoot (g)	Stem (g)	Leaf (g)	Main Root (g)	Lateral Root (g)	Total Root (g)	Lateral/ Main Root Length	Lateral/ Main Root Dry Biomass	SSL (cmg^{-1})	SRL (cmg^{-1})	SMR	LMR	RMR	R/S
Acer velutinum	control	38.67 ^{a}	26.93 ^{a}	28.5 ^{ab}	18.7 ^{ab}	46.6 ^{a}	64.79 ^{a}	30.43 ^{a}	17.81 ^{a}	12.63 ^{a}	16.5 ^{ab}	17.17 ^{a}	34.36 ^{a}	1.64 ^{a}	1.08 ^{a}	2.17 ^{a}	2.61 ^{a}	0.27 ^{a}	0.19 ^{a}	0.53 ^{a}	1.13 ^{a}
	very low	44.1 ^{a}	28.07 ^{a}	31.2 ^{a}	19.4 ^{ab}	46.7 ^{a}	65.86 ^{a}	29.89 ^{a}	17.58 ^{a}	12.31 ^{a}	18.01 ^{a}	14.71 ^{a}	35.97 ^{a}	1.52 ^{a}	1.0 ^{a}	2.53 ^{a}	2.61 ^{a}	0.27 ^{a}	0.19 ^{a}	0.55 ^{a}	1.21 ^{a}
	low	41.73 ^{a}	27.07 ^{a}	31.6 ^{a}	20.6 ^{a}	43.5 ^{ab}	67.54 ^{a}	32.02 ^{a}	19.44 ^{a}	12.58 ^{a}	16.6 ^{ab}	12.04 ^{a}	35.52 ^{a}	1.39 ^{a}	1.16 ^{a}	2.15 ^{a}	2.29 ^{a}	0.29 ^{a}	0.19 ^{a}	0.53 ^{a}	1.11 ^{a}
	medium	44.1 ^{ab}	24.5 ^{ab}	27.0 ^{ab}	20.9 ^{a}	43.6 ^{ab}	64.87 ^{a}	29.38 ^{a}	16.6 ^{a}	12.78 ^{a}	16.87 ^{a}	10.78 ^{a}	35.49 ^{a}	1.61 ^{a}	1.12 ^{a}	2.67 ^{a}	2.35 ^{a}	0.26 ^{a}	0.2 ^{a}	0.55 ^{a}	1.21 ^{a}
	high	29.6 ^{bc}	21.3 ^{ab}	22.8 ^{bc}	15.7 ^{bc}	37.8 ^{ab}	50.98 ^{b}	22.62 ^{b}	12.27 ^{b}	10.36 ^{a}	13.21 ^{b}	8.62 ^{b}	28.36 ^{b}	1.67 ^{a}	1.15 ^{a}	2.57 ^{a}	2.55 ^{a}	0.24 ^{a}	0.21 ^{a}	0.56 ^{a}	1.25 ^{a}
	very high	26.27 ^{c}	18.03 ^{b}	18.1 ^{c}	12.2 ^{c}	33.2 ^{b}	36.22 ^{c}	18.12 ^{b}	10.39 ^{b}	7.73 ^{b}	9.08 ^{c}	5.88 ^{c}	18.1 ^{c}	1.92 ^{a}	1.0 ^{a}	2.48 ^{a}	3.65 ^{b}	0.29 ^{a}	0.21 ^{a}	0.5 ^{a}	1.01 ^{a}
Alnus subcordata	control	29.13 ^{a}	18.9 ^{ab}	15 ^{a}	13.3 ^{ab}	30.4 ^{a}	46.76 ^{a}	24.31 ^{a}	14.81 ^{a}	9.49 ^{a}	13.46 ^{a}	17.86 ^{a}	22.46 ^{a}	2.05 ^{a}	0.68 ^{a}	1.96 ^{a}	3.39 ^{a}	0.32 ^{a}	0.2 ^{a}	0.48 ^{a}	0.94 ^{a}
	very low	29.03 ^{a}	19.33 ^{ab}	13.4 ^{ab}	14.5 ^{a}	34.5 ^{ab}	49.21 ^{a}	24.89 ^{a}	15.14 ^{a}	9.75 ^{a}	13.92 ^{a}	17.96 ^{a}	24.32 ^{a}	2.61 ^{a}	0.75 ^{a}	1.98 ^{a}	3.33 ^{a}	0.31 ^{a}	0.2 ^{a}	0.49 ^{a}	0.97 ^{a}
	low	27.1 ^{a}	21.33 ^{a}	15.4 ^{a}	15.1 ^{a}	33.3 ^{a}	50.92 ^{a}	26.98 ^{a}	16.7 ^{a}	10.28 ^{a}	14.49 ^{a}	18.95 ^{a}	23.94 ^{a}	2.2 ^{a}	0.65 ^{a}	1.62 ^{a}	3.55 ^{a}	0.33 ^{a}	0.2 ^{a}	0.47 ^{a}	0.88 ^{a}
	medium	28.4 ^{a}	19.43 ^{ab}	13.1 ^{ab}	13.1 ^{ab}	30.4 ^{ab}	48.0 ^{a}	24.31 ^{a}	15.02 ^{a}	9.3 ^{a}	13.81 ^{a}	18.62 ^{a}	23.68 ^{a}	2.37 ^{a}	0.74 ^{a}	1.91 ^{a}	3.18 ^{a}	0.31 ^{a}	0.19 ^{a}	0.49 ^{a}	0.98 ^{a}
	high	23.0 ^{ab}	17.0 ^{ab}	12.9 ^{ab}	10.1 ^{ab}	27.5 ^{ab}	45.37 ^{a}	23.3 ^{a}	14.96 ^{a}	8.34 ^{ab}	12.9 ^{a}	15.15 ^{a}	22.07 ^{a}	2.22 ^{a}	0.71 ^{a}	1.54 ^{a}	3.11 ^{a}	0.33 ^{a}	0.19 ^{a}	0.48 ^{a}	0.95 ^{a}
	very high	17.27 ^{b}	13.4 ^{b}	10.2 ^{b}	8.3 ^{b}	19.2 ^{b}	29.37 ^{b}	15.11 ^{b}	8.76 ^{b}	6.35 ^{b}	8.17 ^{b}	9.02 ^{b}	14.26 ^{b}	1.93 ^{a}	0.76 ^{a}	1.96 ^{a}	3.25 ^{a}	0.3 ^{a}	0.22 ^{a}	0.48 ^{a}	0.94 ^{a}

Table 3. Means of seedling morphology (size), growth (biomass), and architecture (allocation ratios) variables of *Pinus eldarica* and *Pinus nigra* seedlings at different intensities of soil compaction. Different letters in each species column indicate significant differences among intensities of soil compaction ($p < 0.01$) based on Duncan's tests.

Species	Compaction Intensity	Seedling Morphology (Size)					Seedling Growth (Dry Biomass)							Seedling Architecture (Allocation Ratios)						
		Stem Length (cm)	Stem Diameter (mm)	Main Root Length (cm)	Main Root Diameter (mm)	Lateral Root Length (cm)	Total (g)	Shoot (g)	Stem (g)	Leaf (g)	Main Root (g)	Lateral Root (g)	Total Root (g)	Lateral/ Main Root Length	Lateral/ Main Root Dry Biomass	SSL (cmg^{-1})	SRL (cmg^{-1})	SMR	LMR	RMR	R/S
Pinus eldarica	control	12.67 ^{a}	5.24 ^{a}	13.6 ^{a}	3.9 ^{a}	45.4 ^{a}	7.18 ^{a}	3.9 ^{a}	1.37 ^{a}	2.53 ^{a}	1.74 ^{a}	9.0 ^{a}	3.28 ^{a}	3.35 ^{a}	0.91 ^{ab}	9.65 ^{a}	30.0 ^{a}	0.19 ^{a}	0.35 ^{a}	0.46 ^{a}	0.86 ^{a}
	very low	12.06 ^{a}	4.55 ^{ab}	15.0 ^{a}	3.4 ^{ab}	48.3 ^{a}	6.16 ^{ab}	3.66 ^{ab}	1.1 ^{ab}	2.56 ^{a}	1.37 ^{ab}	10.4 ^{ab}	2.5 ^{abc}	3.26 ^{a}	0.85 ^{ab}	12.1 ^{a}	44.2 ^{a}	0.18 ^{a}	0.41 ^{a}	0.42 ^{a}	0.77 ^{a}
	low	12.23 ^{a}	4.02 ^{abc}	11.6 ^{ab}	3.1 ^{abc}	39.4 ^{ab}	5.08 ^{bc}	2.44 ^{bc}	0.79 ^{bc}	1.65 ^{ab}	1.37 ^{ab}	9.45 ^{ab}	2.64 ^{ab}	3.52 ^{a}	0.91 ^{ab}	18.9 ^{a}	35.1 ^{a}	0.15 ^{a}	0.33 ^{a}	0.51 ^{a}	1.09 ^{a}
	medium	8.21 ^{b}	3.27 ^{bcd}	9.03 ^{bc}	2.9 ^{bc}	28.0 ^{bc}	3.74 ^{cd}	2.13 ^{cd}	0.71 ^{bc}	1.42 ^{ab}	0.77 ^{c}	9.88 ^{bc}	1.62 ^{cd}	3.11 ^{a}	1.14 ^{a}	13.1 ^{a}	34.6 ^{a}	0.19 ^{a}	0.37 ^{a}	0.44 ^{a}	0.84 ^{a}
	high	8.45 ^{b}	2.83 ^{cd}	9.2 ^{bc}	2.2 ^{c}	25.1 ^{bc}	3.11 ^{d}	1.34 ^{cd}	0.47 ^{c}	0.87 ^{c}	1.02 ^{bc}	9.15 ^{bc}	1.76 ^{bcd}	3.26 ^{a}	0.73 ^{ab}	19.7 ^{a}	40.5 ^{a}	0.15 ^{a}	0.28 ^{a}	0.57 ^{a}	1.48 ^{a}
	very high	5.54 ^{b}	2.13 ^{d}	6.8 ^{c}	2.4 ^{bc}	19.2 ^{c}	2.12 ^{d}	1.0 ^{d}	0.33 ^{c}	0.68 ^{c}	0.78 ^{c}	6.09 ^{c}	1.12 ^{d}	3.04 ^{a}	0.44 ^{b}	19.7 ^{a}	55.0 ^{a}	0.15 ^{a}	0.32 ^{a}	0.52 ^{a}	1.1 ^{a}
Pinus nigra	control	12.49 ^{a}	4.13 ^{a}	24.1 ^{a}	3.7 ^{a}	57.6 ^{a}	6.18 ^{a}	3.41 ^{a}	1.41 ^{a}	2.0 ^{a}	1.38 ^{a}	1.55 ^{a}	2.77 ^{a}	2.47 ^{a}	1.0 ^{a}	9.49 ^{a}	42.3 ^{ab}	0.23 ^{a}	0.32 ^{a}	0.45 ^{a}	0.82 ^{a}
	very low	10.21 ^{ab}	4.44 ^{ab}	20.5 ^{ab}	2.8 ^{ab}	52.3 ^{ab}	5.55 ^{ab}	3.16 ^{a}	1.28 ^{a}	1.89 ^{ab}	1.06 ^{ab}	1.13 ^{a}	2.39 ^{ab}	2.56 ^{a}	1.39 ^{a}	8.92 ^{a}	41.4 ^{ab}	0.22 ^{a}	0.34 ^{a}	0.44 ^{a}	0.84 ^{a}
	low	9.12 ^{ab}	3.18 ^{abc}	14.8 ^{bc}	2.5 ^{b}	33.6 ^{bc}	5.6 ^{ab}	3.27 ^{a}	1.38 ^{a}	1.89 ^{ab}	0.89 ^{ab}	1.27 ^{a}	2.33 ^{ab}	2.42 ^{a}	1.79 ^{a}	6.82 ^{a}	23.9 ^{b}	0.25 ^{a}	0.34 ^{a}	0.41 ^{a}	0.71 ^{a}
	medium	7.2 ^{bc}	2.65 ^{bc}	13.6 ^{bc}	2.3 ^{bc}	30.2 ^{a}	4.46 ^{bc}	2.74 ^{ab}	1.38 ^{a}	1.37 ^{abc}	0.6 ^{bc}	0.85 ^{a}	1.72 ^{b}	2.23 ^{a}	2.59 ^{a}	6.41 ^{a}	33.3 ^{ab}	0.31 ^{a}	0.31 ^{a}	0.39 ^{a}	0.63 ^{a}
	high	6.78 ^{bc}	2.81 ^{abc}	9.8 ^{c}	1.6 ^{bc}	30.9 ^{c}	3.76 ^{c}	1.79 ^{bc}	0.72 ^{ab}	1.07 ^{bc}	0.75 ^{bc}	0.74 ^{a}	1.97 ^{b}	3.21 ^{a}	1.68 ^{a}	13.1 ^{a}	26.0 ^{ab}	0.18 ^{a}	0.28 ^{a}	0.54 ^{a}	1.29 ^{a}
	very high	4.22 ^{c}	1.57 ^{c}	9.6 ^{c}	1.2 ^{c}	26.0 ^{c}	1.93 ^{d}	1.08 ^{c}	0.31 ^{b}	0.77 ^{c}	0.35 ^{c}	0.34 ^{b}	0.85 ^{c}	3.29 ^{a}	1.73 ^{a}	15.0 ^{a}	57.7 ^{a}	0.16 ^{a}	0.37 ^{a}	0.47 ^{a}	0.95 ^{a}

4. Discussion

Augmenting soil strength vigorously influenced the morphological and growth parameters of four deciduous and evergreen seedlings in the present study and supported the current study's hypotheses that increasing the soil mechanical hindrance could cause decreased seedling growth. All of the morphological and biomass responses in maple and alder seedlings augmented slowly to the moderate (M) treatment (up to 1.3 MPa), then, with further increasing compaction, to the VH treatment, reduced quickly. Concerning the response to soil compaction of the evergreen species *Pinus eldarica* and *Pinus nigra*, all of the size and biomass variables in all these seedlings statistically decreased from the control treatment to the very high treatment with increasing compaction. The alterations in the morphological variables of the root system, such as the lateral root length and the main and lateral root dry biomass, were specifically conspicuous. Smaller primary and lateral roots reported in compaction-induced soils are in agreement with the former literature concluding that increased soil strength leads to a decrease in the growth rate of roots [25,27] and support the statement that increased soil penetration resistance is a crucial element that can unfavorably influence the initial progress of woody species seedling establishment and growth [18].

The reduction in the penetration of plant roots may hamper the approach to and absorption of nutrients and water [34]. This will then lead to insufficient water in the leaf, a reduction in the photosynthetic rate, a decrease in the size and growth of the stem and the total biomass of the seedling, and restricted seedling durability in drought conditions [32].

Contrary to the commonly accepted notion that soil compaction has a negative impact on tree species accomplishment, the results that we obtained in studying deciduous species showed that total dry biomass increased by augmenting soil compaction to M treatment (up to 1.3 MPa). Similarly, Tracy et al. (2012) [33] demonstrated that plants developed on soil with clay loam texture commonly achieved higher growth at the greatest value of soil BD by 1.5–1.6 Mg m^{-3}, whereas plants developed on soil with loamy sand texture reached the greatest growth at the BD of 1.3 Mg m^{-3}. Similarly, Alameda and Villar (2009) [24] concluded that just 53% of the 17 studied woody species (nine from seventeen) revealed a greater total biomass after a slight increase in soil BD, which can be explained by a higher root–soil connection. Additionally, Mosena and Dillenburg (2004) [44] illustrated that the shoot expansion growth and total plant biomass enhanced by a higher degree of soil compaction could be explained by the observation of a closer contact in the root–soil matrix.

According to the results, we can conclude that restraint for seedling growth for the investigated species occurs at values that are lower than the commonly reported threshold of 2.0–2.5 MPa [35,45]. Although the above-mentioned limit may be further pertinent for woody species seedlings being to survive rather than grow [31], the value of SPR < 2.5 MPa found to be effective in reducing the growth variables of *Pinus radiata* [46], even the value of SPR < 0.6 MPa can impede the establishment of seedlings of the cabbage tree (*Cordyline australis*) [27]. Also, Alameda et al. (2012) [47] concluded that the increasing values of soil BD until 1.4 Mg m^{-3} boosted growth variables, but at BD values > 1.4 Mg m^{-3}, the growth variables reduced. Therefore, we can conclude that the species usually used for afforestation in the Hyrcanian forests in Iran are very sensitive to soil compaction, showing decreased growth at values lower than those generally reported as thresholds in the literature. Thus, we strongly recommend the application during the establishment of the skid trails of all those best management practices to decrease soil compaction, such as placing mats or mulches on the skid trails [48–50].

Our hypothesis states that increased soil mechanical hindrance would cause changes in the growth allocation patterns in the various seedling portions, leading to architectural alterations to the woody species seedlings. It is supported by the obtained results. According to the concept of a 'functional equilibrium' for the allocation of seedling biomass, woody species seedlings will devote somewhat greater biomass to the root portions if the restrictive parameter for the growth is below ground (e.g., nutrients and water). Conversely, plants will devote relatively higher biomass to shoots if the restrictive parameter is above

ground (e.g., light and CO_2) [51]. It can, therefore, be said that the woody seedling devotes greater biomass to the organ that is in a situation of restricted resources and, therefore, compensates to obtain the most [51]. Our results revealed higher allocation to roots by enhancing soil strength to moderate treatment (up to 1.3 MPa) in deciduous species, both *A. velutinum* and *A. subcordata*. However, the two deciduous species selected in this study were fast-growing. A high allocation to root mass is typically associated with situations where soil resources, namely water and nutrients, are low [44]. Then, fast-growing tree species have, to some extent, greater LMR [52,53]. Contrarily, decreased architectural features were observed in evergreen species with increasing compaction.

The results revealed that the growth variables showed two trends: first, in deciduous species, the results showed that with enhancing SPR to moderate treatment (up to 1.3 MPa), total dry biomass improved. Second, following augmenting SPR from M to VH treatment, the total dry biomass diminished. In evergreen species, results showed that total dry biomass gradually decreased by enhancing soil compaction levels. However, there was a higher difference in total dry biomass between deciduous and evergreen species, with deciduous species up to 5 times higher in the moderate compaction level and up to 2 times higher in the very high compaction level than evergreen species. These results were consistent with Alameda and Villar (2009) [24], who found that total dry biomass follows two types of answers. Species type I are those in which increased SPR initially fosters higher growth, while further increasing SPR causes a growth decrease.

It is worth highlighting that there may be a study limitation. The results obtained in the greenhouse may be somewhat higher than those obtained in a natural context. This is due to the fact that the pots exert a force on the plant roots due to the rigid structure of the pot. This condition is very different from soil, where a root will move through cracks and fragile parts of the soil [34]. The soil texture was not changed in this study. However, the effects of soil texture on root growth could be primarily interpreted according to the differences in air, water, and strength of soil between textures [46,54–61]. In this study, the seedling pots were irrigated regularly daily and did not experience any water deficit.

For future studies, multivariate statistics can be applied to compare the growth and architecture variables of seedlings in different species and different soil conditions. Also, the functional characteristics of plants, such as the total surface of the roots, the absorption of elements on the roots and the rate of their uptake to the roots, the oxygen content under conditions of soil compaction, and root respiration, can be considered as basic variables.

5. Conclusions

We examined the alterations in seedling morphology, growth, and architecture of four species (two deciduous and two evergreen) usually used for afforestation in the Hyrcanian forests in Iran following experimentally set soil compaction levels in a greenhouse. Augmenting soil compaction heavily impacted the morphological and growth variables of four deciduous and evergreen seedlings and revealed that enhancing soil penetration resistance (SPR) would lead to a reduction in all variables of above- and below-ground seedling sizes and biomass of the total seedling. On the one hand, our results demonstrated that the features of deciduous species even improved with compaction levels up to 1.3 MPa. Above this threshold, the seedling features started to decline quickly. On the other hand, we found that the features of evergreen species decreased with increasing soil compaction in a uniform trend. However, the threshold value of 1.3 MPa is much lower than those reported in the literature for other species, so it is possible to state that the species used for afforestation in the Hyrcanian forests of Iran are very sensitive to soil compaction, and therefore, the application of reduced-impact logging and of best management practices to decrease soil disturbance are particularly recommended. However, extensive studies should be conducted on the sensitivity of selected tree species for afforestation in Hyrcanian forests to soil compaction so that species with less sensitivity to soil compaction may be selected for the restoration program of the Hyrcanian forest in northern Iran.

Author Contributions: Conceptualization, M.J. and E.A.H.; methodology, M.J. and E.A.H.; formal analysis, M.J. and E.A.H.; investigation, M.J. and E.A.H.; writing—original draft preparation, M.J. and E.A.H.; writing—review and editing, F.L., R.V. and R.P. All authors have read and agreed to the published version of the manuscript.

Funding: This research received no external funding.

Data Availability Statement: Data are available from the corresponding author upon reasonable request.

Acknowledgments: This work was supported by the Italian Ministry for Education, University, and Research (MIUR) for financial support (Law 232/2016, Italian University Departments of Excellence 2023–2027) project "Digitali, Intelligenti, Verdi e Sostenibili (D.I.Ver.So)—UNITUS-DAFNE WP3. Also, the authors would like to acknowledge the constructive and valuable comments provided by the editor and two anonymous reviewers, which remarkably helped us to improve the manuscript.

Conflicts of Interest: The authors declare no conflicts of interest.

References

1. Latterini, F.; Dyderski, M.K.; Horodecki, P.; Picchio, R.; Venanzi, R.; Lapin, K.; Jagodziński, A.M. The Effects of Forest Operations and Silvicultural Treatments on Litter Decomposition Rate: A Meta-Analysis. *Curr. For. Rep.* **2023**, *9*, 276–290. [CrossRef]
2. Labelle, E.R.; Hansson, L.; Högbom, L.; Jourgholami, M.; Laschi, A. Strategies to Mitigate the Effects of Soil Physical Disturbances Caused by Forest Machinery: A Comprehensive Review. *Curr. For. Rep.* **2022**, *8*, 20–37. [CrossRef]
3. Nazari, M.; Arthur, E.; Lamandé, M.; Keller, T.; Bilyera, N.; Bickel, S. A Meta-Analysis of Soil Susceptibility to Machinery-Induced Compaction in Forest Ecosystems Across Global Climatic Zones. *Curr. For. Rep.* **2023**, *9*, 370–381. [CrossRef]
4. Ambrosio, E.; Pietras, M.; Feest, A. Biotic and Abiotic Factors Influencing Macrofungal Diversity and Biomass in Mediterranean Forests with a Focus on the Porcini Group. *Dendrobiology* **2024**, *91*, 16–31. [CrossRef]
5. Çiçekler, M.; Tutus, A.; Üzüm, V. The Use of *Eucalyptus Grandis* Bark and Root as Raw Material in Pulp and Paper Production. *Drewno* **2023**, *66*, 1–11. [CrossRef]
6. Tsioras, P.A.; Żak, J.; Karaszewski, Z. RFID Implementations in the Wood Supply Chains: State of the Art and the Way to the Future. *Drewno. Pr. Nauk. Doniesienia Komun.=Wood. Res. Pap. Rep. Announc.* **2022**, *65*, 209. [CrossRef]
7. Łukawski, D.; Hochmańska-Kaniewska, P.; Janiszewska-Latterini, D.; Lekawa-Raus, A. Functional Materials Based on Wood, Carbon Nanotubes, and Graphene: Manufacturing, Applications, and Green Perspectives. *Wood Sci. Technol.* **2023**, *57*, 989–1037. [CrossRef]
8. Grünberg, J.; Ghaffariyan, M.R.; Jourgholami, M.; Labelle, E.R.; Kaakkurivaara, N.; Robert, R.C.G.; Kühmaier, M. Criteria for Assessing the Sustainability of Logging Operations—A Systematic Review. *Curr. For. Rep.* **2023**, *9*, 350–369. [CrossRef]
9. Latterini, F.; Dyderski, M.K.; Horodecki, P.; Rawlik, M.; Stefanoni, W.; Högbom, L.; Venanzi, R.; Picchio, R.; Jagodziński, A.M. A Meta—Analysis of the Effects of Ground—Based Extraction Technologies on Fine Roots in Forest Soils. *Land Degrad. Dev.* **2024**, *35*, 9–21. [CrossRef]
10. Nazari, M.; Lamandé, M.; Weber, P.L.; Sharififar, A.; Iversen, B.V.; Arthur, E. Impact of Spruce Deadwood Logs on Physical Properties of a Loamy Sand Podzol in a Steep Temperate Forest. *Land Degrad. Dev.* **2024**, *35*, 2137–2144. [CrossRef]
11. Labelle, E.R.; Jaeger, D. Quantifying the Use of Brush Mats in Reducing Forwarder Peak Loads and Surface Contact Pressures. *Croat. J. For. Eng.* **2012**, *33*, 249–274.
12. Labelle, E.R.; Jaeger, D. Soil Compaction Caused by Cut-to-Length Forest Operations and Possible Short-Term Natural Rehabilitation of Soil Density. *Soil Sci. Soc. Am. J.* **2011**, *75*, 2314–2329. [CrossRef]
13. Labelle, E.R.; Jaeger, D. Effects of Steel Flexible Tracks on Forwarder Peak Load Distribution: Results from a Prototype Load Test Platform. *Croat. J. For. Eng.* **2019**, *40*, 1–23.
14. Pousse, N.; Bonnaud, P.; Legout, A.; Darboux, F.; Ranger, J. Forest Soil Penetration Resistance Following Heavy Traffic: A 10-Year Field Study. *Soil Use Manag.* **2022**, *38*, 815–835. [CrossRef]
15. Campbell, D.M.H.; White, B.; Arp, P.A. Modeling and Mapping Soil Resistance to Penetration and Rutting Using LiDAR-Derived Digital Elevation Data. *J. Soil Water Conserv.* **2013**, *68*, 460–473. [CrossRef]
16. Mohieddinne, H.; Brasseur, B.; Spicher, F.; Gallet-Moron, E.; Buridant, J.; Kobaissi, A.; Horen, H. Physical Recovery of Forest Soil after Compaction by Heavy Machines, Revealed by Penetration Resistance over Multiple Decades. *For. Ecol. Manag.* **2019**, *449*, 117472. [CrossRef]
17. Grigal, D.F. Effects of Extensive Forest Management on Soil Productivity. *For. Ecol. Manag.* **2000**, *138*, 167–185. [CrossRef]
18. Kozlowski, T.T. Soil Compaction and Growth of Woody Plants. *Scand. J. For. Res.* **1999**, *14*, 596–619. [CrossRef]
19. Ampoorter, E.; Goris, R.; Cornelis, W.M.; Verheyen, K. Impact of Mechanized Logging on Compaction Status of Sandy Forest Soils. *For. Ecol. Manag.* **2007**, *241*, 162–174. [CrossRef]
20. Hansson, L.J.; Koestel, J.; Ring, E.; Gärdenäs, A.I. Impacts of Off-Road Traffic on Soil Physical Properties of Forest Clear-Cuts: X-Ray and Laboratory Analysis. *Scand. J. For. Res.* **2018**, *33*, 166–177. [CrossRef]
21. Hansson, L.; Šimůnek, J.; Ring, E.; Bishop, K.; Gärdenäs, A.I. Soil Compaction Effects on Root—Zone Hydrology and Vegetation in Boreal Forest Clearcuts. *Soil Sci. Soc. Am. J.* **2019**, *83*, S105–S115. [CrossRef]

22. Hansson, L.J.; Ring, E.; Franko, M.A.; Gärdenäs, A.I. Soil Temperature and Water Content Dynamics after Disc Trenching a Sub-Xeric Scots Pine Clearcut in Central Sweden. *Geoderma* **2018**, *327*, 85–96. [CrossRef]
23. Kormanek, M.; Banach, J.; Sowa, P. Effect of Soil Bulk Density on Forest Tree Seedlings. *Int. Agrophys* **2015**, *29*, 67–74. [CrossRef]
24. Alameda, D.; Villar, R. Moderate Soil Compaction: Implications on Growth and Architecture in Seedlings of 17 Woody Plant Species. *Soil Tillage Res.* **2009**, *103*, 325–331. [CrossRef]
25. Bejarano, M.D.; Villar, R.; Murillo, A.M.; Quero, J.L. Effects of Soil Compaction and Light on Growth of *Quercus pyrenaica* Willd.(*Fagaceae*) Seedlings. *Soil Tillage Res.* **2010**, *110*, 108–114. [CrossRef]
26. Siegel-Issem, C.M.; Burger, J.A.; Powers, R.F.; Ponder, F.; Patterson, S.C. Seedling Root Growth as a Function of Soil Density and Water Content. *Soil Sci. Soc. Am. J.* **2005**, *69*, 215–226. [CrossRef]
27. Bassett, I.E.; Simcock, R.C.; Mitchell, N.D. Consequences of Soil Compaction for Seedling Establishment: Implications for Natural Regeneration and Restoration. *Austral Ecol.* **2005**, *30*, 827–833. [CrossRef]
28. Tirado-Corbalá, R.; Slater, B.K. Soil Compaction Effects on the Establishment of Three Tropical Tree Species. *Arboric. Urban. For.* **2010**, *36*, 164–170. [CrossRef]
29. Jourgholami, M.; Khoramizadeh, A.; Zenner, E.K. Effects of Soil Compaction on Seedling Morphology, Growth, and Architecture of Chestnut-Leaved Oak (*Quercus castaneifolia*). *Iforest-Biogeosci. For.* **2016**, *10*, 145. [CrossRef]
30. Jordan, D.; Ponder, F., Jr.; Hubbard, V.C. Effects of Soil Compaction, Forest Leaf Litter and Nitrogen Fertilizer on Two Oak Species and Microbial Activity. *Appl. Soil Ecol.* **2003**, *23*, 33–41. [CrossRef]
31. Bulmer, C.E.; Simpson, D.G. Soil Compaction and Water Content as Factors Affecting the Growth of Lodgepole Pine Seedlings on Sandy Clay Loam Soil. *Can. J. Soil Sci.* **2005**, *85*, 667–679. [CrossRef]
32. Alameda, D.; Villar, R. Linking Root Traits to Plant Physiology and Growth in *Fraxinus angustifolia* Vahl. Seedlings under Soil Compaction Conditions. *Environ. Exp. Bot.* **2012**, *79*, 49–57. [CrossRef]
33. Tracy, S.R.; Black, C.R.; Roberts, J.A.; Sturrock, C.; Mairhofer, S.; Craigon, J.; Mooney, S.J. Quantifying the Impact of Soil Compaction on Root System Architecture in Tomato (*Solanum lycopersicum*) by X-ray Micro-Computed Tomography. *Ann. Bot.* **2012**, *110*, 511–519. [CrossRef] [PubMed]
34. Blouin, V.M.; Schmidt, M.G.; Bulmer, C.E.; Krzic, M. Effects of Compaction and Water Content on Lodgepole Pine Seedling Growth. *For. Ecol. Manag.* **2008**, *255*, 2444–2452. [CrossRef]
35. Tavankar, F.; Nikooy, M.; Ezzati, S.; Jourgholami, M.; Latterini, F.; Venanzi, R.; Picchio, R. Long-Term Assessment of Soil Physicochemical Properties and Seedlings Establishment after Skidding Operations in Mountainous Mixed Hardwoods. *Eur. J. For. Res.* **2022**, *141*, 571–585. [CrossRef]
36. Misra, R.K.; Gibbons, A.K. Growth and Morphology of Eucalypt Seedling-Roots, in Relation to Soil Strength Arising from Compaction. *Plant Soil* **1996**, *182*, 1–11. [CrossRef]
37. Day, S.; Bassuk, N. A Review of the Effects of Soil Compaction and Amelioration Treatments on Landscape Trees. *Arboric. Urban. For.* **1994**, *20*, 9–17. [CrossRef]
38. Skinner, A.K.; Lunt, I.D.; Spooner, P.; Mcintyre, S. The Effect of Soil Compaction on Germination and Early Growth of *Eucalyptus albens* and an Exotic Annual Grass. *Austral Ecol.* **2009**, *34*, 698–704. [CrossRef]
39. Goushehgir, Z.; Feghhi, J.; Innes, J.L. Challenges Facing the Improvement of Forest Management in the Hyrcanian Forests of Iran. *Forests* **2022**, *13*, 2180. [CrossRef]
40. Ezzati, S.; Najafi, A.; Durston, T. Impact of Animal Logging on Soil Physical Properties in Mule Trail in Hyrcanian Forests. *Transp. Res. D Transp. Environ.* **2011**, *16*, 316–320. [CrossRef]
41. Solgi, A.; Naghdi, R.; Marchi, E.; Laschi, A.; Keivan Behjou, F.; Hemmati, V.; Masumian, A. Impact Assessment of Skidding Extraction: Effects on Physical and Chemical Properties of Forest Soils and on Maple Seedling Growing along the Skid Trail. *Forests* **2019**, *10*, 134. [CrossRef]
42. Solgi, A.; Naghdi, R.; Tsioras, P.A.; Ilstedt, U.; Salehi, A.; Nikooy, M. Combined Effects of Skidding Direction, Skid Trail Slope and Traffic Frequency on Soil Disturbance in North Mountainous Forest of Iran. *Croat. J. For. Eng.* **2017**, *38*, 97–106.
43. Naghdi, R.; Solgi, A.; Zenner, E.K.; Tsioras, P.A.; Nikooy, M. Soil Disturbance Caused by Ground-Based Skidding at Different Soil Moisture Conditions in Northern Iran. *Int. J. For. Eng.* **2016**, *27*, 169–178. [CrossRef]
44. Mósena, M.; Dillenburg, L.R. Early Growth of Brazilian Pine (*Araucaria angustifolia* [Bertol.] Kuntze) in Response to Soil Compaction and Drought. *Plant Soil* **2004**, *258*, 293–306. [CrossRef]
45. Jourgholami, M.; Fathi, K.; Labelle, E.R. Effects of Litter and Straw Mulch Amendments on Compacted Soil Properties and Caucasian Alder (*Alnus subcordata*) Growth. *New For.* **2020**, *51*, 349–365. [CrossRef]
46. Zou, C.; Penfold, C.; Sands, R.; Misra, R.K.; Hudson, I. Effects of Soil Air-Filled Porosity, Soil Matric Potential and Soil Strength on Primary Root Growth of Radiata Pine Seedlings. *Plant Soil* **2001**, *236*, 105–115. [CrossRef]
47. Alameda, D.; Anten, N.P.R.; Villar, R. Soil Compaction Effects on Growth and Root Traits of Tobacco Depend on Light, Water Regime and Mechanical Stress. *Soil Tillage Res.* **2012**, *120*, 121–129. [CrossRef]
48. Latterini, F.; Spinelli, R.; Venanzi, R.; Picchio, R. Acorn Review: Focus on Ground-Based Extraction Systems: Is Skidding Really More Impactful than Forwarding? *For. Ecol. Manag.* **2024**, *551*, 121514. [CrossRef]
49. Ilintsev, A.S.; Nakvasina, E.N.; Högbom, L. Methods of Protection Forest Soils during Logging Operations (Review). *Lesn. Zhurnal (For. J.)* **2021**, *5*, 92–116. [CrossRef]

50. Ring, E.; Andersson, M.; Hansson, L.; Jansson, G.; Högbom, L. Logging Mats and Logging Residue as Ground Protection during Forwarder Traffic along till Hillslopes. *Croat. J. For. Eng.* **2021**, *42*, 445–462. [CrossRef]
51. Iwasa, Y.; Roughgarden, J. Shoot/Root Balance of Plants: Optimal Growth of a System with Many Vegetative Organs. *Theor. Popul. Biol.* **1984**, *25*, 78–105. [CrossRef]
52. Freschet, G.T.; Pagès, L.; Iversen, C.M.; Comas, L.H.; Rewald, B.; Roumet, C.; Klimešová, J.; Zadworny, M.; Poorter, H.; Postma, J.A.; et al. A Starting Guide to Root Ecology: Strengthening Ecological Concepts and Standardising Root Classification, Sampling, Processing and Trait Measurements. *New Phytol.* **2021**, *232*, 973–1122. [CrossRef] [PubMed]
53. Poorter, H.; Niklas, K.J.; Reich, P.B.; Oleksyn, J.; Poot, P.; Mommer, L. Biomass Allocation to Leaves, Stems and Roots: Meta—Analyses of Interspecific Variation and Environmental Control. *New Phytol.* **2012**, *193*, 30–50. [CrossRef] [PubMed]
54. Oravec, A.; Ferus, P.; Košútová, D.; Konôpková, J. Screening for Drought Resistance among Ornamental Maples (*Acer* Sp.). A Field Experiment in Juvenile Plants. *Dendrobiology* **2023**, *89*, 35–45. [CrossRef]
55. DeArmond, D.; Ferraz, J.B.S.; Lima, A.J.N.; Higuchi, N. Surface soil recovery occurs within 25 years for skid trails in the Brazilian Amazon. *Catena* **2024**, *234*, 107568. [CrossRef]
56. DeArmond, D.; Emmert, F.; Pinto, A.C.M.; Lima, A.J.N.; Higuchi, N. A Systematic Review of Logging Impacts in the Amazon Biome. *Forests* **2023**, *14*, 81. [CrossRef]
57. Aroca-Fernández, M.J.; Bravo-Fernández, J.A.; García-Viñas, J.I.; Serrada, R. Soil Compaction and Productivity Evolution in a Harvested and Grazed Mediterranean Scots Pine (*Pinus sylvestris* L.). *Forest. For.* **2024**, *15*, 451. [CrossRef]
58. Mariotti, B.; Hoshika, Y.; Cambi, M.; Marra, E.; Feng, Z.; Paoletti, E.; Marchi, E. Vehicle-Induced Compaction of Forest Soil Affects Plant Morphological and Physiological Attributes: A Meta-Analysis. *For. Ecol. Manag.* **2020**, *462*, 118004. [CrossRef]
59. Ampoorter, E.; De Frenne, P.; Hermy, M.; Verheyen, K. Effects of Soil Compaction on Growth and Survival of Tree Saplings: A Meta-Analysis. *Basic Appl. Ecol.* **2011**, *12*, 394–402. [CrossRef]
60. Cambi, M.; Hoshika, Y.; Mariotti, B.; Paoletti, E.; Picchio, R.; Venanzi, R.; Marchi, E. Compaction by a Forest Machine Affects Soil Quality and *Quercus robur* L. Seedling Performance in an Experimental Field. *For. Ecol. Manag.* **2017**, *384*, 406–414. [CrossRef]
61. Sugai, T.; Yokoyama, S.; Tamai, Y.; Mori, H.; Marchi, E.; Watanabe, T.; Satoh, F.; Koike, T. Evaluating Soil–Root Interaction of Hybrid Larch Seedlings Planted under Soil Compaction and Nitrogen Loading. *Forests* **2020**, *11*, 947. [CrossRef]

Disclaimer/Publisher's Note: The statements, opinions and data contained in all publications are solely those of the individual author(s) and contributor(s) and not of MDPI and/or the editor(s). MDPI and/or the editor(s) disclaim responsibility for any injury to people or property resulting from any ideas, methods, instructions or products referred to in the content.

forests

MDPI

Article

The Estimation of Carbon Storage and Volume in Forest Stands: A Model Incorporating Species Composition and Site Quality

Weiping Hua [1,2], Tian Qiu [2], Xidian Jiang [3], Junzhong Pan [4] and Baoyin Li [1,*]

[1] College of Geographic Sciences, Fujian Normal University, Fuzhou 350007, China; hwp@wuyiu.edu.cn
[2] Department of College of Ecology and Resource Engineering, Wuyi University, Wuyishan 354300, China; qiutian@wuyiu.edu.cn
[3] Forestry College, Fujian Agriculture and Forestry University, Fuzhou 350002, China; fujianjxd@163.com
[4] Fujian Forestry Survey and Planning Institute, Fuzhou 350003, China; junzhongpan@163.com
* Correspondence: liby@fjnu.edu.cn; Tel.: +86-599-5136976

Abstract: We developed a model for estimating the carbon storage and volume of entire forest stands at the provincial level, aiming to improve the accuracy of regional productivity assessments. Based on data from the branches, roots, leaves, and trunks of eight dominant tree species (grouped by origin) in Fujian Province, combined with plot-level data, we developed a compatible carbon storage estimation model. This model integrates species composition coefficients and uses stand volume as the independent variable. We estimated the model parameters using a combination of the immune evolutionary algorithm and an improved simplex method, which enhances convergence speed and solution stability compared to the traditional version. The accuracy of the model was validated by cross-model validation and concurrent testing. Applying the model to forest stand data from Wuyishan City, we simulated theoretical logging volumes to demonstrate its practical utility. The results demonstrated that the model exhibited high accuracy in fitting the observed data, with reliable predictions of carbon storage and volume across different forest components. In the case study area, the volume was 21.0521 million cubic meters and the carbon storage was 7.3238 million tons, both of which increased with decreasing interval periods. When logging factors were considered, the increases in carbon storage fluctuated as the interval periods increased and were higher than those when logging factors were not considered. This study confirmed that the developed models were effective for predicting land carbon storage and volume, and the simulation method successfully overcame the challenges associated with model estimation.

Keywords: carbon storage; stand volume; forest modeling; species composition coefficients; simulation calculation method

1. Introduction

Forests are vital natural resource assets, playing a crucial role in both biodiversity conservation and maintaining the global carbon balance. Stand carbon storage is a key indicator for measuring forest carbon sequestration and is essential for assessing forest carbon budgets. Accurate estimations of stand carbon storage are significantly important for addressing global climate issues and promoting sustainable development [1–3]. Stand volume is another critical metric for evaluating carbon storage, which directly reflects the quantity and quality of forest resource assets that can be obtained by field forestry surveys. Unlike stand volume, which can be directly measured through field surveys, stand carbon

storage requires indirect estimation via biomass measurement models adjusted by a fixed carbon content rate (0.45 or 0.50).

Over the past decade, numerous studies at the level of individual trees have been conducted globally [4,5]. However, stand-level measurement models, which could address gaps when individual tree data are lacking, have received less attention. The reliance on fixed carbon content rates in these models often affords biased outcomes and precludes the dynamic monitoring of carbon storage [6]. Therefore, there is an increasing need for developing models that estimate total stand carbon storage and volume as a supplement to forest carbon storage estimation when data are missing. Recently, research on stand-level carbon storage models has gradually increased [7–10], primarily focusing on the northern and northeastern regions of China [11,12]. However, research on the development of stand-level carbon storage estimation models for southern tree species is limited.

Fujian Province, which has the highest forest coverage rate in China at 66.80%, remains a focal point for forestry and ecological research and is pivotal for practical forestry operations. Stand-level theoretical growth equations have been developed for this region, facilitating regional-scale dynamic monitoring and research into carbon sequestration capacities [13–16]. Despite progress in model development, several challenges persist. The diversity of dominant tree species and their mixed composition complicates accurate carbon estimation at the regional scale. Site quality, a critical driver of stand growth, must be integrated into the model, while the difficulty in determining stand age—particularly in uneven-aged forests—can lead to the propagation of estimation errors. Additionally, models relying on diameter and height may not align well with updated forest inventories, and ignoring logging in theoretical productivity equations may hinder the realistic simulation of forest dynamics and sustainable management planning.

Therefore, in response to these challenges, in this study, we developed a carbon storage estimation model that integrates species composition coefficients with volume as the independent variable, using continuous multi-period forest resource inventory data and supplementary plot data from Fujian Province. Employing the Richards growth equation and mathematical derivation, a stand volume estimation model was also established, incorporating species composition coefficients and site quality grades as dummy variables and interval periods as independent variables. These models collectively formed a growth–carbon storage framework, enabling the dynamic monitoring of total stand carbon storage at the regional level and simulating changes in its increments. This approach also included simulation calculations for determining theoretical logging volumes, providing a foundation for more refined carbon sink monitoring and sustainable forest management.

2. Materials

The foundational data for this model were derived from the continuous forest resource inventory of Fujian Province, specifically from class I fixed plots (the national forest resources continuous inventory) collected in 1998, 2003, 2008, 2013, and 2018. These permanent plots are systematically established and revisited at regular intervals to monitor long-term forest dynamics. The primary dataset used in this study was derived from the forest resource inventory of Fujian Province, which is part of China's national continuous forest inventory system, coordinated by the National Forestry and Grassland Administration. The inventory includes class I fixed plots, which are systematically distributed and revisited every five years. The data used in this study were obtained through official collaboration with the Fujian Provincial Forestry Survey and Planning Institute, which holds custodianship over the regional dataset. Access to this database is not currently available to the public due to confidentiality and regional forest management policies. However, external researchers may request access through formal applications submitted

to the Institute. The dataset includes tree species, origin, age, DBH, height, volume, and site quality, and was provided in tabular form. To supplement the dataset, temporary standard plots were additionally established between March 2021 and December 2022. Each standard plot covers 0.067 ha in a square layout and was designed to capture recent forest conditions and expand species and site variability beyond that of the fixed plots.

Henceforth, the plots and standard plots are collectively referred to as "plots". The collected data included species (group), origin, age, diameter at breast height, and volume (Table 1). Utilizing the three-sigma rule, we eliminated outliers, ultimately selecting 2027 plots for modeling. These included 369 plots of *Cunninghamia lanceolata* plantations, 214 plots of natural *Cunninghamia lanceolata*, 239 plots of *Pinus massoniana* plantations, 226 plots of natural *Pinus massoniana* forest, 257 plots of hard broad-leaved tree species (group) plantations, 284 plots of natural hard broad-leaved tree species (group) forests, 221 plots of soft broad-leaved tree species (group) plantations, and 217 plots of natural soft broad-leaved tree species (group) forests. Using carbon conversion factors, biomass was transformed into carbon storage, and the carbon storage per plot was calculated by combining the number of trees per plot. These data were used to analyze the carbon storage of each dominant tree species (group and origin) (Table 2).

Table 1. Characteristics of tree measurement factors in plots for dominant tree species (group and origin).

Dominant Tree Species (Group, Origin)	Symbol	Number of Trees (Trees per ha)			Average Diameter at Breast Height (cm)		
		Maximum Value	Minimum Value	Average Value	Maximum Value	Minimum Value	Average Value
Cunninghamia lanceolata plantation	Cl_pf	7050	195	2157	26.5	6	14.6
Natural *Cunninghamia lanceolata*	Cl_nf	6418	162	1982	28.1	5.5	13.9
Pinus massoniana plantation	Pm_pf	5400	210	1789	24.6	6.5	13.7
Natural *Pinus massoniana* forest	Pm_nf	5400	300	1461	25.9	7.1	13.2
Hard broad-leaved tree species (group) plantation	HBlts_pf	5310	510	1737	21.7	6.7	11.0
Natural hard broad-leaved tree species (group) forest	HBlts_nf	5730	165	1864	36.6	5.9	13.5
Soft broad-leaved tree species (group) plantation	Sblts_pf	3978	397	1922	26.3	5.7	12.2
Natural soft broad-leaved tree species (group) forest	Sblts_nf	3864	386	1901	25.1	5.1	13.1
Dominant Tree Species (Group, Origin)	**Symbol**	**Volume (m^3 per ha)**			**Average Height (m)**		
		Maximum Value	Minimum Value	Average Value	Maximum Value	Minimum Value	Average Value
Cunninghamia lanceolata plantation	Cl_pf	208	40	119	19.1	4.1	10.0
Natural *Cunninghamia lanceolata*	Cl_nf	201	36	105	18.2	4.9	10.7
Pinus massoniana plantation	Pm_pf	166	41	101	17.4	4.5	8.8
Natural *Pinus massoniana* forest	Pm_nf	173	35	103	16.6	5.2	9.0
Hard broad-leaved tree species (group) plantation	HBlts_pf	202	38	110	15.0	5.0	8.9
Natural hard broad-leaved tree species (group) forest	HBlts_nf	156	23	103	15.1	4.9	9.7
Soft broad-leaved tree species (group) plantation	Sblts_pf	201	28	131	14.9	4.1	9.0
Natural soft broad-leaved tree species (group) forest	Sblts_nf	179	29	122	15.7	4.0	8.7

Note: The symbols from the table represent each dominant tree species (group and origin) in the subsequent text.

Table 2. Carbon storage characteristics of dominant tree species (group and origin) across different site quality levels.

Dominant Tree Species (Group, Origin)	Site Quality Level (kg)					
	1			2		
	Maximum Value	Minimum Value	Average Value	Maximum Value	Minimum Value	Average Value
Cl_nf	7589	621	4162	6044	480	3842
Cl_pf	7680	113	2872	6913	102	2975
Pm_nf	9115	75	6497	8354	67	5751
Pm_pf	8188	271	4637	7251	40	4189
Hblts_nf	9326	193	6515	8783	179	6094
Hblts_pf	9121	311	951	7674	269	1608
Sblts_nf	8282	433	6063	4751	372	3889
Sblts_pf	6013	526	1864	6182	396	1224

Table 2. *Cont.*

Dominant Tree Species (Group, Origin)	Site Quality Level (kg)					
	3			4		
	Maximum Value	Minimum Value	Average Value	Maximum Value	Minimum Value	Average Value
Cl_nf	5830	474	3565	3969	241	2881
Cl_pf	5477	86	2308	3434	74	1788
Pm_nf	6669	101	5123	5115	68	4166
Pm_pf	5552	99	3316	3683	21	2229
Hblts_nf	7879	335	5898	7532	159	5687
Hblts_pf	6835	249	1556	4941	191	2171
Sblts_nf	4744	310	2580	1616	216	1616
Sblts_pf	3891	267	926	1654	154	545

The species composition coefficients (K_j) were calculated for each plot based on the species-level basal area data extracted from the forest inventory. Specifically, the basal area of each of the four dominant species groups was divided by the total basal area of the plot and then scaled to ensure a total sum of 10. These standardized coefficients were used directly as the inputs in the modeling framework.

The data were collected from the resource database for each dominant tree species (group and origin) in Wuyishan City, including factors like area, site quality grade, species composition coefficient, and age. The total area of the study region was 171,393 ha. Hblts_nf occupied the largest area (63,778 ha), followed by Cl_pf (43,801 ha) and Pm_nf (43,663 ha). The areas occupied by Hblts_pf, Sblts_pf, and Sblts_nf were smaller, accounting for 1.15%, 0.58%, and 0.03% of the total area, respectively.

3. Methods

3.1. Construction of Stand Carbon Storage Estimation Model

In this study, Equation (1) was used as the standard carbon storage model, denoted as $f(L_i,M,\beta)$. To account for the mixed-species structure of the stands, we introduced species composition coefficients into the model. These coefficients (K_1, K_2, K_3, and K_4) represent the proportional presence of four dominant tree species (or species groups): *Cunninghamia lanceolata* (K_1), *Pinus massoniana* (K_2), hard broad-leaved species (K_3), and soft broad-leaved species (K_4).

The species composition coefficient was incorporated into the model to address the issues associated with the expression of the mixed-species ratios. The general form of the carbon storage model related to the species composition is expressed as $f[L_i(a_{ij},K_j),M,\beta]$. $L_i(a_{ij},K_j)$ is a linear function; specifically, $L_i(a_{ij},K_j) = a_{i1}K_1 + a_{i2}K_2 + a_{i3}K_3 + a_{i4}K_4$, where K_1 represents *Cunninghamia lanceolata*, K_2 represents *Pinus massoniana*, K_3 represents the hard broadleaf species (group), and K_4 represents the soft broadleaf species (group). The values were in the range of [0, 10] and the sum $K_1 + K_2 + K_3 + K_4 = 10$.

$$W = L_1 \times M^{L_2} + \beta \quad (1)$$

where W is the stand carbon storage, M is the stand volume, L_1 and L_2 are the parameters to be determined in the model, and β represents the model estimation error.

There are differences in carbon storage among the different tree organs. If models are established for total carbon storage (W_0), branches (W_1), roots (W_2), leaves (W_3), and trunks (W_4) separately, the total amount (W_0) is not equal to the algebraic sum of the components ($W_1 + W_2 + W_3 + W_4$). To address this problem, a holistic modeling approach was adopted to resolve the incompatibility between the total and components, forming an additive carbon storage model system. The technical approach involves first establishing the total

model and then establishing the component ratio models. The component amounts were calculated proportionally to the total amount.

As forests grow and develop, the proportion of carbon storage distributed among different components constantly changes. The establishment of a joint estimation system for the components aims to solve the incompatibility issue of independent models. It determines the proportions of the carbon storage components at different growth stages of the forest, and the sum of the proportions satisfies the 100% constraint. In this study, a joint estimation method was used for the nonlinear models to address the incompatibility issues between the total and component models. The basic principles of this method are as follows.

Let the general formulas for the carbon storage models of the entire stand (W_0), branches (W_1), roots (W_2), leaves (W_3), and trunks (W_4) be $f_0(L_i,M,\beta)$, $f_1(L_i,M,\beta)$, $f_2(L_i,M,\beta)$, $f_3(L_i,M,\beta)$, and $f_4(L_i,M,\beta)$, respectively. To ensure compatibility between the component models and the total forest carbon storage model, the following formulas were used to control and build a comprehensive carbon storage model:

$$\hat{w}_1 = \frac{1}{1 + f_2/f_1 + f_3/f_1 + f_4/f_1} w_0' \tag{2}$$

$$\hat{w}_2 = \frac{f_2/f_1}{1 + f_2/f_1 + f_3/f_1 + f_4/f_1} w_0' \tag{3}$$

$$\hat{w}_3 = \frac{f_3/f_1}{1 + f_2/f_1 + f_3/f_1 + f_4/f_1} w_0' \tag{4}$$

$$\hat{w}_4 = \frac{f_4/f_1}{1 + f_2/f_1 + f_3/f_1 + f_4/f_1} w_0' \tag{5}$$

where $\hat{w}_0$,$\hat{w}_1$,$\hat{w}_2$,$\hat{w}_3$, and $\hat{w}_4$ represent the comprehensive carbon storage models for the whole tree (total), branches, roots, leaves, and trunks, respectively, and $W^{'}$ is the estimated value for the total model, W_0.

Let $g_1 = f_1/f_1$ and $g_2 = f_2/f_1$, $g_3 = f_3/f_1$. Substituting these expressions into the above formulas, we obtain the following:

$$\hat{w}_0 = f_0 \tag{6}$$

$$\hat{w}_1 = \frac{\hat{w}_0}{1 + g_2 + g_3 + g_4} \tag{7}$$

$$\hat{w}_2 = \frac{g_2 \times \hat{w}_0}{1 + g_2 + g_3 + g_4} \tag{8}$$

$$\hat{w}_3 = \frac{g_3 \times \hat{w}_0}{1 + g_2 + g_3 + g_4} \tag{9}$$

$$\hat{w}_4 = \frac{g_4 \times \hat{w}_0}{1 + g_2 + g_3 + g_4} \tag{10}$$

This section outlines the basic principles of holistic modeling. By constructing a holistic tree carbon storage model, consistency between the estimates of the total and the individual components was achieved.

3.2. Construction of Dynamic Stand Volume Estimation Model

In the stand carbon storage model, an important independent variable (M) exists, where M represents the actual stand volume. Utilizing $f(L_i,M,\beta)$ allows for the measurement of the actual stand carbon storage. To estimate future trends in carbon storage and the forest carbon sequestration potential, it is necessary to establish a dynamic stand volume estimation model.

Constructing a dynamic estimation model for the stand volume requires the selection of an appropriate growth equation, which is a fundamental task. Among the commonly used growth equations, the Richards equation was chosen as the base equation for constructing the dynamic estimation of stand volume and is expressed as follows:

$$M = b \times [1 - \exp(-c \times T)]^z + \beta \tag{11}$$

where M represents the stand volume; T represents the age of the stand; b, c, and z are the parameters to be determined in the model; and β represents the model's estimation error.

To solve the problem associated with determining the age of uneven-aged forests, a dynamic estimation model for the stand volume using the interval periods as the independent variables was derived from Equation (11) as follows:

$$M_2 = b \times \{1 - [1 - (\frac{M_1}{b})]^{\frac{1}{z}} \times \exp(-c \times T_n)\}^z + \beta \tag{12}$$

where M_1 is the current (initial) stand volume, M_2 is the future (final) stand volume, and T_n represents the interval period ($T_n = T_2 - T_1$; T_2 and T_1 are the final and initial ages of the stand, respectively).

The model parameter b, which is estimated as the maximum value, is generally related to the site quality and can be established as a function of the site quality grades, i.e., $b = f(b_i, I_i) = b_1I_1 + b_2I_2 + b_3I_3 + b_4I_4$. Here, I_1, I_2, I_3, and I_4 represent the site quality grades for class 1, class 2, class 3, and class 4, respectively; the values for the site quality grades are either 0 or 1, where, if the site is fertile, I_1 = 1 and I_2, I_3, and I_4 are 0; if the site is moderately fertile, I_2= 1, and I_1, I_3, and I_4 are 0, and so forth. The parameters b_1, b_2, b_3, and b_4 were determined using the model.

The parameter c represents the rate of change in stand volume with age, and z is related to the assimilation process during tree growth, functioning as a function of the species composition coefficients, with the mathematical expressions $c = c_1K_1 + c_2K_2 + c_3K_3 + c_4K_4$ and $z = z_1K_1 + z_2K_2 + z_3K_3 + z_4K_4$. Here, c_1, c_2, c_3, c_4, z_1, z_2, z_3, and z_4 are the parameters to be determined by the model.

In summary, the dynamic estimation model for stand carbon storage constructed in this study is related to site quality and species composition.

$$\begin{aligned} M_2 = {} & (b_1I_1 + b_2I_2 + b_3I_3 + b_4I_4) \times \left\{1 - [1 - (\frac{M_1}{b_1I_1 + b_2I_2 + b_3I_3 + b_4I_4})]^{\frac{1}{z_1K_1 + z_2K_2 + z_3K_3 + z_4K_4}}\right. \\ & \left. \times \exp[-(c_1K_1 + c_2K_2 + c_3K_3 + c_4K_4) \times T_n]\right\}^{z_1K_1 + z_2K_2 + z_3K_3 + z_4K_4} + \beta \end{aligned} \tag{13}$$

3.3. Parameter Estimation and Accuracy Evaluation

To ensure robustness, the parameter estimation and model validation were conducted concurrently. The methods used for the parameter estimation include traditional intelligent algorithms. Traditional algorithms mainly include the conventional least-squares, improved simplex, and golden section methods. Intelligent algorithms include the immune evolutionary algorithm (IEA) and genetic algorithms, among others. In this study, a combination of the IEA and improved simplex method was used to estimate the model parameters.

The IEA, inspired by biological immune mechanisms, identifies optimal solutions by simulating evolutionary processes, where the fittest individuals are typically closest to the global optimum and carry key problem-solving characteristics [17]. The improved simplex method constructs a simplex in an $n + 1$ dimensional space and iteratively replaces the worst-performing point with a reflection point to approach the optimal solution. This

process adapts through reflection, expansion, and contraction strategies to accelerate convergence [18,19].

Compared with traditional optimization approaches, the combined use of the IEA and improved simplex method offers notable advantages. The IEA provides global search capability and maintains diversity in the solution space, effectively avoiding premature convergence. Meanwhile, the improved simplex method enhances local search efficiency through adaptive operations such as reflection, expansion, and contraction. It dynamically adjusts the step sizes to improve the convergence stability and accuracy. The complementary strengths of these two methods enable efficient and robust parameter estimation in the high-dimensional, nonlinear models developed in this study.

Cross-validation divides all the samples into five groups. In each iteration, one group is selected as the validation sample and does not participate in the modeling, whereas the other four groups serve as modeling samples to determine the model parameters. Throughout the modeling process, modeling and testing are conducted concurrently, with five rounds in total, where each sample undergoes one validation and four modeling sessions [20].

The model evaluation metrics included the correlation index (R), residual standard deviation (RSD), total relative error (RS), mean systematic error (MSE), mean absolute relative error (RMA), and prediction accuracy (EA). The metrics calculated from the modeling samples were used as the fitting accuracy indicators, whereas those calculated from the samples that did not participate in the modeling served as the applicability (or usability) accuracy indicators.

3.4. Simulation Calculation Method to Determine Harvesting Volume

To reflect the trends and potential of forest carbon storage more accurately, the forest harvesting volume was determined using a simulation calculation method. This method, combined with the stand volume and carbon storage estimation models, was used to forecast future carbon storage and its changes. The simulation calculation method simulated stand growth by controlling stand area and was based on legal forest theory to calculate the annual harvesting volume of the stands [21,22].

Because the harvesting of natural forests is currently not permitted in China, this simulation was conducted only for plantations, revealing trends in forest carbon storage and increases (carbon sequestration) under reasonable harvesting volumes. The formula for calculating this increase is as follows:

$$\Delta W = \frac{W_{T_2} - W_{T_1}}{T_2 - T_1} \tag{14}$$

where ΔW represents the increase, W_{T_2} is the forest carbon storage at time T_2, and W_{T_1} is the forest carbon storage at time T_1.

3.5. Simplified Overview of the Modeling Framework

To assist readers less familiar with mathematical modeling, a simplified overview of the modeling process is provided here. The overall modeling framework includes three key components: (1) an estimation of the stand volume using site quality and species composition; (2) a calculation of the total carbon storage based on stand volume and species composition coefficients; and (3) the decomposition of total carbon storage into individual components (trunk, branch, root, and leaf) using a compatible, additive modeling structure. These models were calibrated using optimization algorithms to ensure accuracy and applicability across the dominant tree species and site conditions.

4. Results

4.1. Analysis of Stand Carbon Storage Modeling Results

The samples were divided into five groups for the synchronous modeling and testing to obtain cross-modeling and testing accuracy values for each dominant tree species (group and origin), as shown in Figures 1 and 2. For modeling accuracy (Figure 1), the overall *R* value exceeded 0.9860, the RSD values ranged from 40.44 to 225.66, the RS and MSE values were within ±1%, the RMA values remained below 5.5%, and the EA values surpassed 99.50%. Specifically, for the roots, the *R* value exceeded 0.9800, the RSD values were between 9.80 and 45.00, the RS and MSE values were within ±2%, the RMA values stayed below 5%, and the EA values surpassed 99.60%. For the branches, the *R* value was greater than 0.9920, the RSD values ranged from 6.50 to 25.50, the RS and MSE values were within ±1%, the RMA values remained below 4%, and the EA values exceeded 99.70%. For the leaves, the *R* value surpassed 0.9550, the RSD values ranged from 3.90 to 14.70, the RS and MSE values were within ±0.7%, the RMA values stayed below 5%, and the EA values exceeded 99.50%. These results indicate that the cross-modeling fitting accuracy for each dominant tree species (group and origin) was high, particularly for branches.

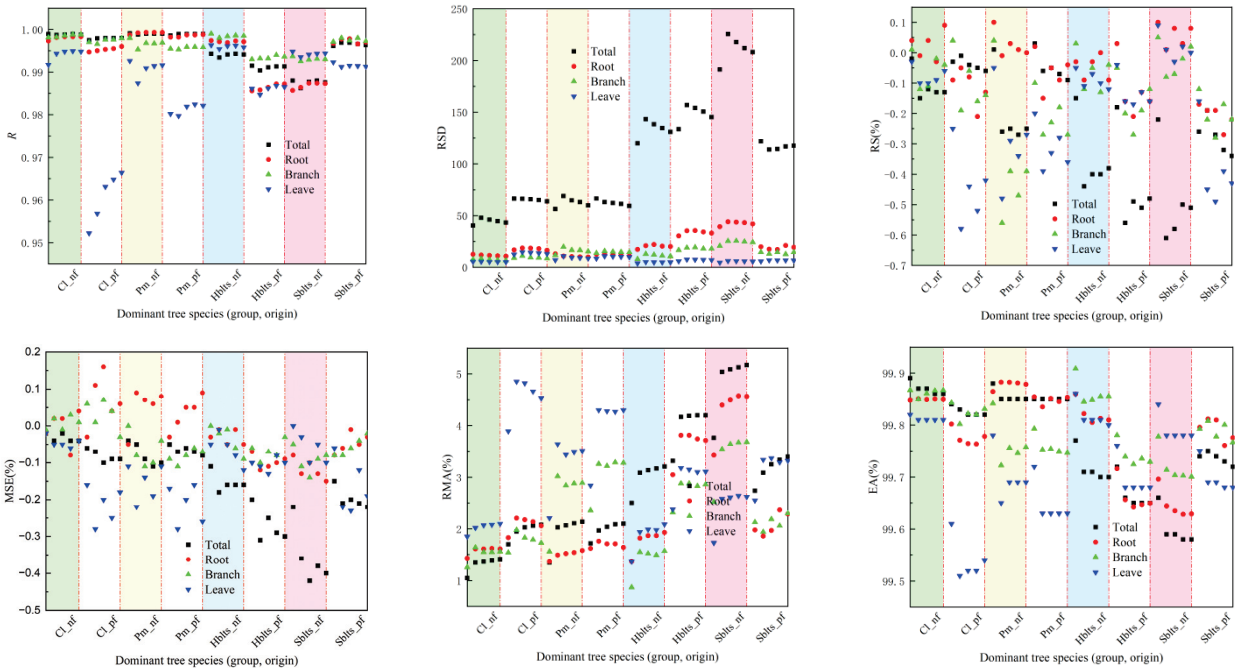

Figure 1. Accuracy indicators for modeling in cross-modeling. The *x*-axis represents the categorical species groups (group and origin); the data points are shown as separate markers without connecting lines to avoid misinterpretation of continuity. The evaluation indicators RS, MSE, RMA, and EA are expressed as a percentage (%), while R and RSD are dimensionless. The species groups include the following: Cl_pf = *Cunninghamia lanceolata* plantation, Cl_nf = *natural Cunninghamia* lanceolata, Pm_pf = *Pinus massoniana* plantation, Pm_nf = natural *Pinus massoniana*, HBlts_pf = hard broad-leaved tree species plantation, HBlts_nf = natural hard broad-leaved tree species, Sblts_pf = soft broad-leaved tree species plantation, and Sblts_nf = natural soft broad-leaved tree species.

Regarding testing accuracy, as depicted in Figure 2, the overall R value exceeded 0.9800, with RSD values ranging between 40.00 and 227.89, RS and MSE values within ±8%, RMA values below 9.2%, and EA values surpassing 98.80%. Specifically for the roots, the R value was greater than 0.9630, the RSD values ranged between 8.90 and 46.53, the RS and MSE values were within ±6%, the RMA values stayed below 7.5%, and the EA values exceeded 99.05%. For the branches, the R value surpassed 0.9810, the RSD values ranged

from 5.65 to 28.33, the RS and MSE values were within ±6%, the RMA values remained below 7%, and the EA values exceeded 99.20%. For the leaves, the R value was above 0.8440, the RSD values ranged from 4.04 to 17.26, the RS and MSE values were within ±8%, the RMA values stayed below 9%, and the EA values exceeded 98.70%. It can be observed that the testing accuracy values are lower than the modeling accuracy values; however, they are still within an acceptable range.

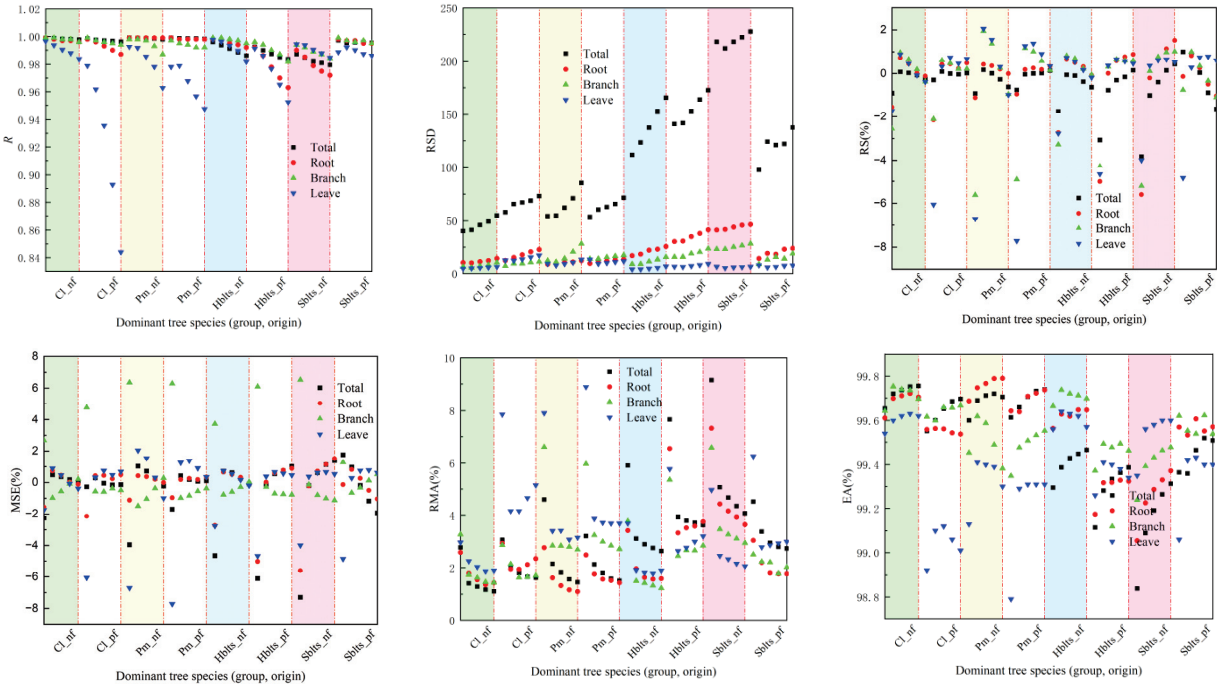

Figure 2. Accuracy indicators for testing in cross-modeling testing.

Using all the samples to fit the stand carbon storage model, comprehensive modeling accuracy values for each indicator were obtained (Figure 3), and the model parameter values for carbon storage in various parts of the stand were determined (Table 3). From the perspective of fitting accuracy, the stand carbon storage models for Cl_nf, Cl_pf, Pm_nf, and Pm_pf showed the highest accuracy, followed by those for Hblts_nf, Hblts_pf, Sblts_pf, and Sblts_nf, which had the lowest fitting accuracy among the eight dominant tree species (group and origin). Overall, the *R* values were greater than 0.9620, the RSD values were within the range of [4.80, 215.39], the RS and MSE values were within ±0.6%, the RMA values were below 5%, and the EA values exceeded 99.50%. The fitting accuracy of the stand carbon storage estimation models for each dominant tree species (group and origin) was high, further improving the cross-modeling and testing accuracy values.

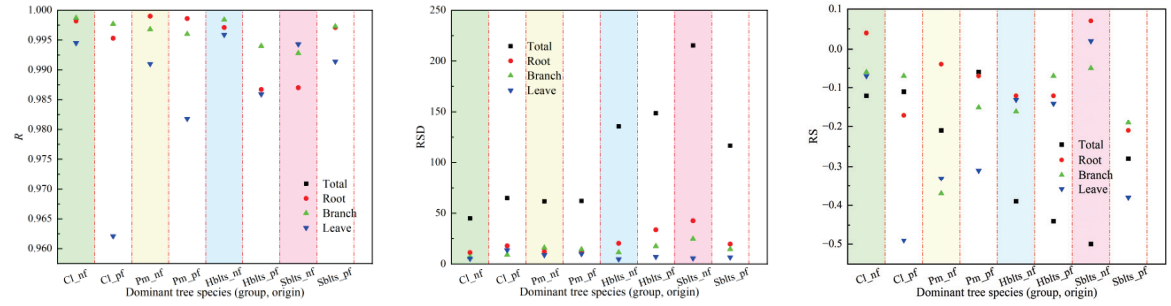

Figure 3. *Cont.*

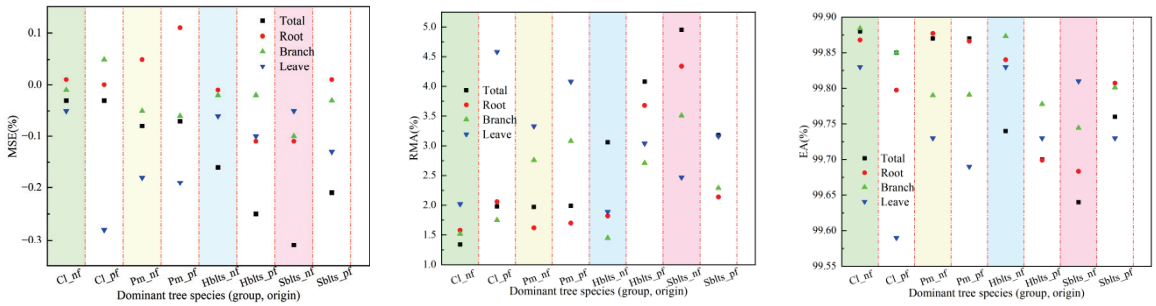

Figure 3. Comprehensive accuracy values for each indicator in the stand carbon storage model.

Table 3. Model parameter values for carbon storage in various parts of the stand for each dominant tree species (group and origin).

Organ	Dominant Tree Species (Group, Origin)	*a*11	*a*12	*a*13	*a*14	*a*21	*a*22	*a*23	*a*24
Total	Cl_nf	44.7356	52.1133	84.5093	94.7353	0.0864	0.0972	0.0857	0.0766
	Cl_pf	36.4470	43.6814	78.8742	57.8114	0.0907	0.0977	0.0765	0.0919
	Pm_nf	37.1275	58.4814	94.7320	101.0136	0.0937	0.0899	0.0777	0.0715
	Pm_pf	29.7181	47.9463	89.4791	69.9471	0.0956	0.0942	0.0726	0.0829
	Hblts_nf	39.6483	65.9525	87.3629	89.7720	0.0886	0.0832	0.0855	0.0801
	Hblts_pf	27.4325	48.6509	89.7190	75.3426	0.0873	0.0895	0.0786	0.0814
	Sblts_nf	42.4085	63.9148	73.9405	97.7149	0.0858	0.0844	0.0918	0.0770
	Sblts_pf	26.3604	50.1866	98.3790	66.5298	0.0943	0.0906	0.0711	0.0879
Root	Cl_nf	0.0643	0.0452	0.0769	0.0760	0.0218	0.0165	0.0227	0.0291
	Cl_pf	0.0714	0.0598	0.0792	0.0543	0.0267	0.0323	0.0299	0.0241
	Pm_nf	0.0561	0.0487	0.0651	0.0720	0.0157	0.0171	0.0122	0.0245
	Pm_pf	0.0699	0.0487	0.0856	0.0536	0.0273	0.0217	0.0380	0.0215
	Hblts_nf	0.0605	0.0497	0.0642	0.0603	0.0164	0.0157	0.0155	0.0177
	Hblts_pf	0.0639	0.0460	0.0723	0.0573	0.0191	0.0187	0.0282	0.0251
	Sblts_nf	0.0658	0.0547	0.0714	0.0690	0.0236	0.0211	0.0230	0.0233
	Sblts_pf	0.0508	0.0417	0.0711	0.0504	0.0102	0.0129	0.0274	0.0189
Leaf	Cl_nf	0.0373	0.0504	0.0427	0.0433	0.0159	0.0290	0.0100	0.0158
	Cl_pf	0.0404	0.0640	0.0450	0.0334	0.0208	0.0463	0.0198	0.0153
	Pm_nf	0.0349	0.0489	0.0314	0.0333	0.0127	0.0262	0.0007	0.0057
	Pm_pf	0.0509	0.0543	0.0420	0.0300	0.0311	0.0358	0.0209	0.0164
	Hblts_nf	0.0377	0.0440	0.0373	0.0353	0.0133	0.0215	0.0058	0.0086
	Hblts_pf	0.0334	0.0462	0.0413	0.0344	0.0090	0.0290	0.0180	0.0160
	Sblts_nf	0.0385	0.0452	0.0422	0.0401	0.0160	0.0221	0.0148	0.0135
	Sblts_pf	0.0265	0.0404	0.0454	0.0303	0.0007	0.0226	0.0256	0.0098
Trunk	Cl_nf	0.0451	0.0390	0.0079	0.0023	0.0455	0.0543	0.0360	0.0338
	Cl_pf	0.0564	0.0543	0.0007	0.0043	0.0533	0.0699	0.0348	0.0439
	Pm_nf	0.0421	0.0364	0.0036	0.0009	0.0463	0.0482	0.0159	0.0153
	Pm_pf	0.0601	0.0467	0.0039	0.0022	0.0584	0.0626	0.0342	0.0347
	Hblts_nf	0.0335	0.0262	0.0142	0.0125	0.0461	0.0369	0.0233	0.0203
	Hblts_pf	0.0363	0.0315	0.0153	0.0127	0.0425	0.0511	0.0327	0.0303
	Sblts_nf	0.0316	0.0255	0.0147	0.0149	0.0436	0.0357	0.0256	0.0283
	Sblts_pf	0.0366	0.0345	0.0139	0.0119	0.0468	0.0616	0.0273	0.0272

Regarding the model parameters, for the total volume, the a_{1j} values for Cl_nf, Pm_nf, Hblts_nf, and Sblts_nf were ordered as $a11 < a12 < a13 < a14$, whereas those for Cl_pf, Pm_pf, Hblts_pf, and Sblts_pf were ordered as $a11 < a12 < a14 < a13$. In terms of the a_{2j} values, Cl_nf and Cl_pf had the highest a_{22} values; Pm_nf, Pm_pf, Hblts_nf, and Sblts_pf had the highest a_{21} values; and Sblts_nf had the highest a_{23} value. However, the effect of the a_{2j} values on the change in the estimated stand carbon storage was greater than that of the a_{1j} values, indicating that *Cunninghamia lanceolata* and *Pinus massoniana* significantly affected the total carbon storage of the stand. The a_{23} and a_{24} values were higher for the

roots of each dominant tree species (group and origin), indicating that the proportion of hard broadleaf and soft broadleaf species significantly affected the carbon storage of the stand roots. Except for the high a_{23} value of the leaves in Sblts_pf, the leaves of the other dominant tree species (group and origin) had higher a_{22} values. The a_{21} and a_{22} values were significant for the trunks of each dominant tree species (group and origin).

4.2. Analysis of Stand Volume Modeling Results

By employing a synchronized approach to cross-modeling and testing, the accuracy values for the stand volume estimation model for each dominant tree species (group and origin) were obtained (Figure 4). Overall, the pattern of changes in the modeling and testing accuracy for stand volume mirrors that of the carbon storage model; that is, modeling accuracy is higher than testing accuracy, and the variation in modeling accuracy among different tree species (group, origin) is relatively small, whereas testing accuracy shows greater fluctuations. The modeling accuracy ($R_1 > 0.9800$, $RSD_1 < 0.7\%$) and testing accuracy ($R_2 > 0.9570$, $RSD_2 < 0.8\%$) indicated robust model performance. The RS_1 and MSE_1 values are within $\pm 1.5\%$, while the RS_2 and MSE_2 values are within $\pm 10.7\%$; the RMA_1 values are all below 7%, and the RMA_2 values are all below 147%; and the EA_1 values are all above 99.30%, and the EA_2 values are all above 98.6%.

Using all the samples to fit the stand volume estimation model, the fitting accuracy and parameter values for each dominant tree species (group and origin) were obtained (Table 4). The R values were greater than 0.9840, the RSD values were in the range of [0.29, 0.57], the RS and MSE values were all within $\pm 1\%$, the RMA values were all below 6%, and the EA values were above 99.40%. The fitting accuracy of the stand volume estimation models for each dominant tree species (group and origin) was high, further improving the cross-modeling and testing accuracy values.

In terms of the model parameters, the bi values were ordered as $b_1 > b_2 > b_3 > b_4$, indicating that the estimated maximum stand volume decreased with decreasing site quality grades, a pattern that aligns with the general relationship between site conditions and tree growth. The ci values generally showed that c_1 and c_2 were higher than c_3 and c_4, indicating that *Cunninghamia lanceolata* and *Pinus massoniana* have higher growth rates than the hard broadleaf and soft broadleaf species (groups). The c_i value is related to the assimilation action power index m during the cumulative process of stand volume, with $m = 1 - 1/c_i$, resulting in m values less than 1; in particular, z_4 has the smallest value, followed by z_3, indicating that the volume growth resistance is more pronounced in hard and soft broadleaf species (groups).

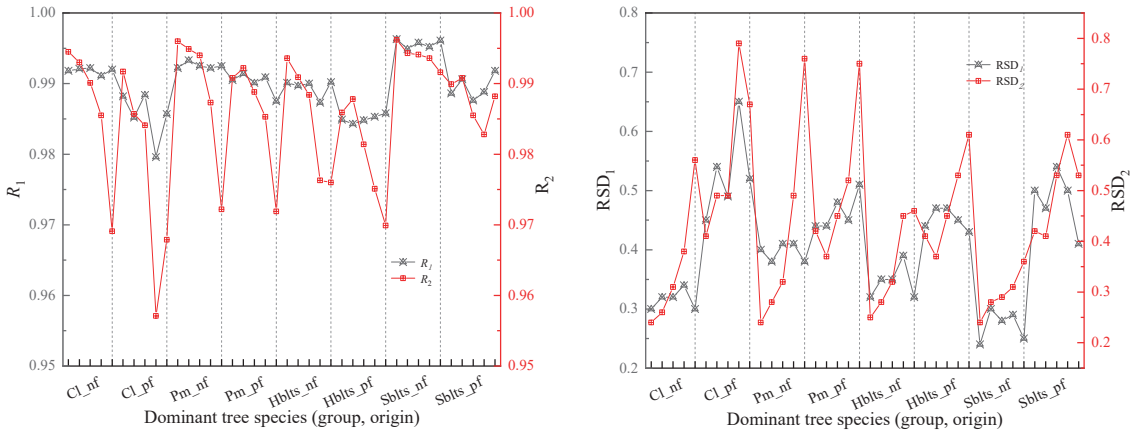

Figure 4. *Cont.*

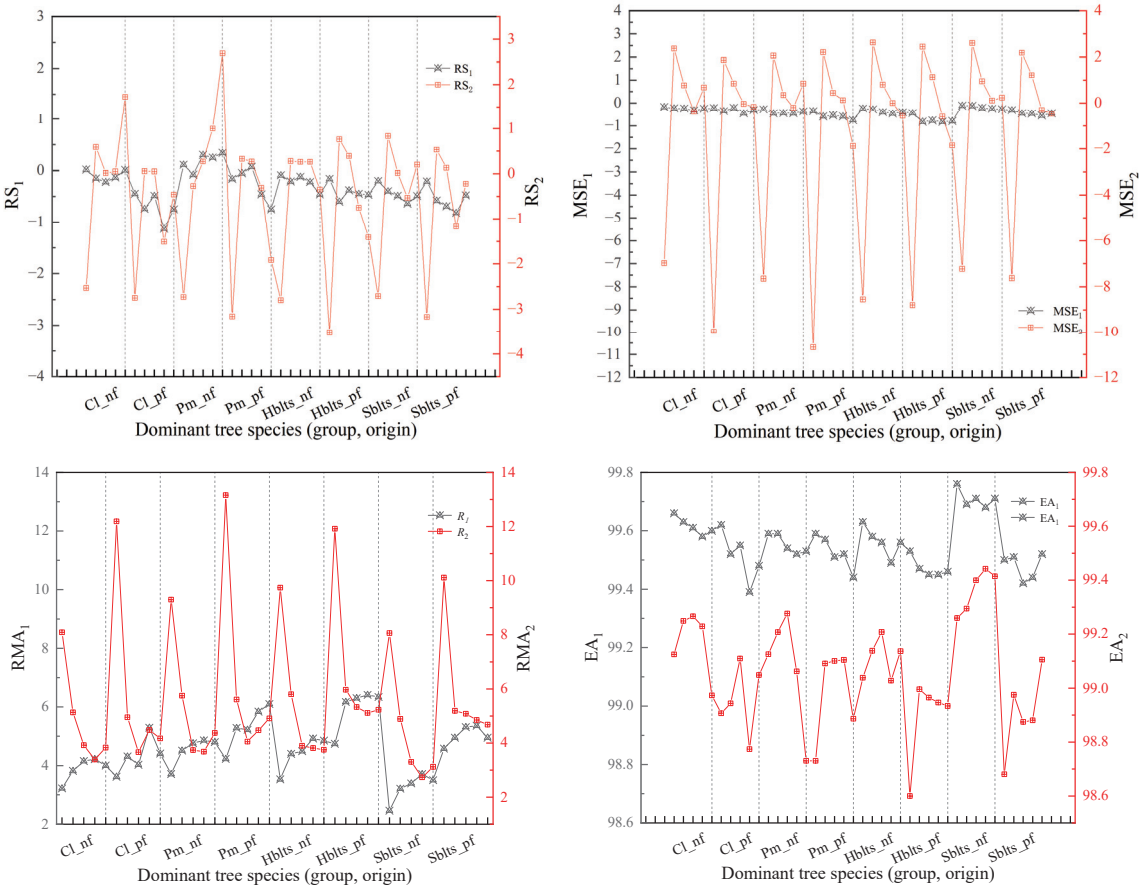

Figure 4. Cross-modeling and testing accuracy values for the stand volume estimation model of each dominant tree species (group and origin). Black indicates modeling accuracy, while red represents validation accuracy.

Table 4. The fitting accuracy and parameter values for the stand volume estimation model of each dominant tree species (group and origin).

Dominant Tree Species (Group, Origin)	*R*	RSD	RS	MSE	RMA	EA
Cl_nf	0.9918	0.32	−0.33	−0.3	4.16	99.66
Cl_pf	0.9903	0.44	−0.48	−0.23	3.68	99.64
Pm_nf	0.9926	0.4	0.24	−0.42	4.55	99.60
Pm_pf	0.9907	0.45	0.09	−0.51	5.24	99.59
Hblts_nf	0.9898	0.34	−0.1	−0.28	4.31	99.62
Hblts_pf	0.9842	0.47	0.07	−0.58	5.67	99.51
Sblts_nf	0.9953	0.29	−0.38	−0.17	3.34	99.73
Sblts_pf	0.9856	0.57	−0.72	−0.54	5.57	99.45
Dominant Tree Species (Group, Origin)	**b_1**	**b_2**	**b_3**	**b_4**	**c_1**	**c_2**
Cl_nf	37.6441	33.0748	28.7237	22.8095	0.00093	0.00173
Cl_pf	22.5935	20.4779	17.2669	11.1085	0.00418	0.00296
Pm_nf	32.8190	28.2997	22.4195	16.4558	0.00099	0.00243
Pm_pf	25.1112	22.3148	17.6255	10.8059	0.00236	0.00311
Hblts_nf	23.9800	21.2664	18.8857	17.1040	0.00171	0.00300
Hblts_pf	21.2793	17.3020	15.2072	10.1491	0.00434	0.00411
Sblts_nf	32.2745	26.0927	20.0831	13.8880	0.00135	0.00208
Sblts_pf	39.2065	29.0603	19.0077	10.3713	0.00259	0.00083

Table 4. *Cont.*

Dominant Tree Species (Group, Origin)	c_3	c_4	z_1	z_2	z_3	z_4
Cl_nf	0.00085	0.00067	0.10133	0.15072	0.10246	0.07431
Cl_pf	0.00076	0.00058	0.14008	0.13940	0.07762	0.06410
Pm_nf	0.00129	0.00128	0.08427	0.17457	0.10713	0.07525
Pm_pf	0.00228	0.00220	0.09064	0.14752	0.11822	0.11118
Hblts_nf	0.00159	0.00208	0.11134	0.17800	0.11504	0.10357
Hblts_pf	0.00193	0.00185	0.13590	0.16166	0.09834	0.09009
Sblts_nf	0.00139	0.00157	0.10262	0.13978	0.10984	0.09668
Sblts_pf	0.00134	0.00113	0.12140	0.07571	0.09959	0.09107

4.3. Analysis of Model Application Results

The calculations indicate that the current volume in the case area is 21.0521 million cubic meters, and the carbon storage is 7.3238 million tons. The carbon storage capacities of the stand branches, roots, leaves, and trunks were 0.1527, 0.2128, 0.12376, and 0.24311 million tons, respectively. Given interval periods of 5, 10, 15, 20, 25, and 30 years, without considering the theoretical logging volume, the calculated volumes and carbon storage, along with their corresponding changes for different interval periods, are shown (Figure 5). It can be observed that both the volume and carbon storage of each part increase with the extension of the interval period, but the magnitude of the increase shows a similar directional change, primarily because of the resistance induced by the stand volume estimation model.

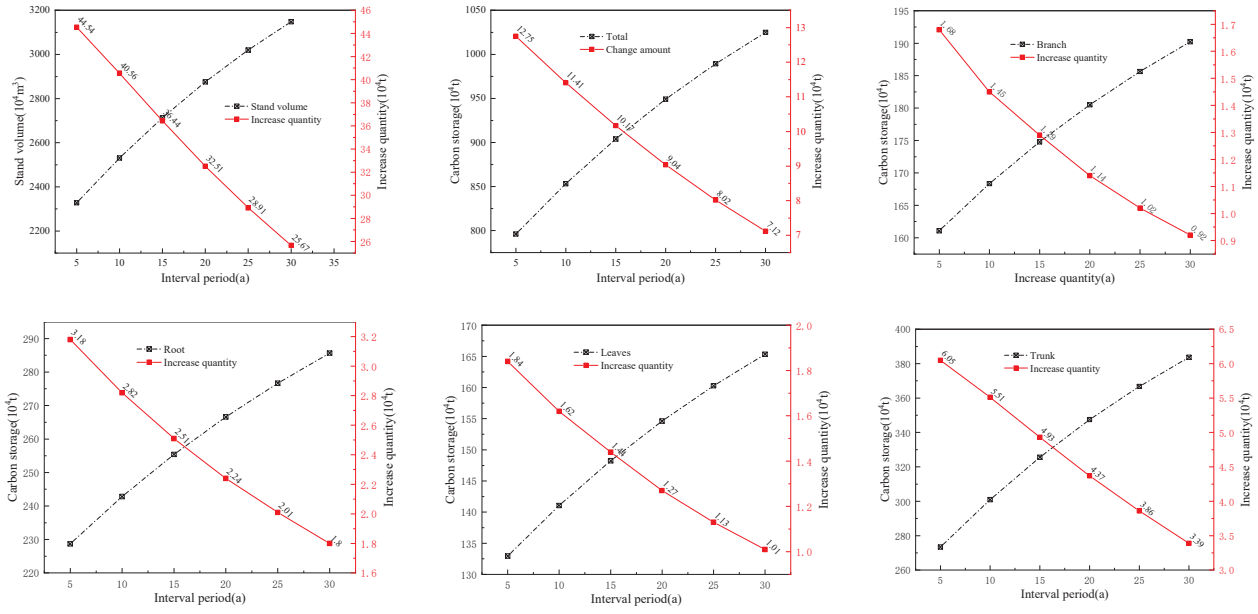

Figure 5. Changes in stand volume and carbon storage over different interval periods.

Using the simulation calculation method, the theoretical logging volumes for each dominant tree species (group and origin) over different interval periods were calculated, and the increases were then determined (Figure 6). It is evident that, without considering the logging volume, the increases (carbon sequestration) for each dominant tree species (group, origin) decrease with the lengthening of the interval period, especially apparent in Cl_pf and Pm_pf. When considering the logging volumes, the increases for each dominant tree species (group and origin) fluctuated with the extension of the interval period, and the increases for all four types of plantations at the time of the main felling were higher than those without logging volume, particularly for Cl_pf, Pm_pf, and Sblts_pf.

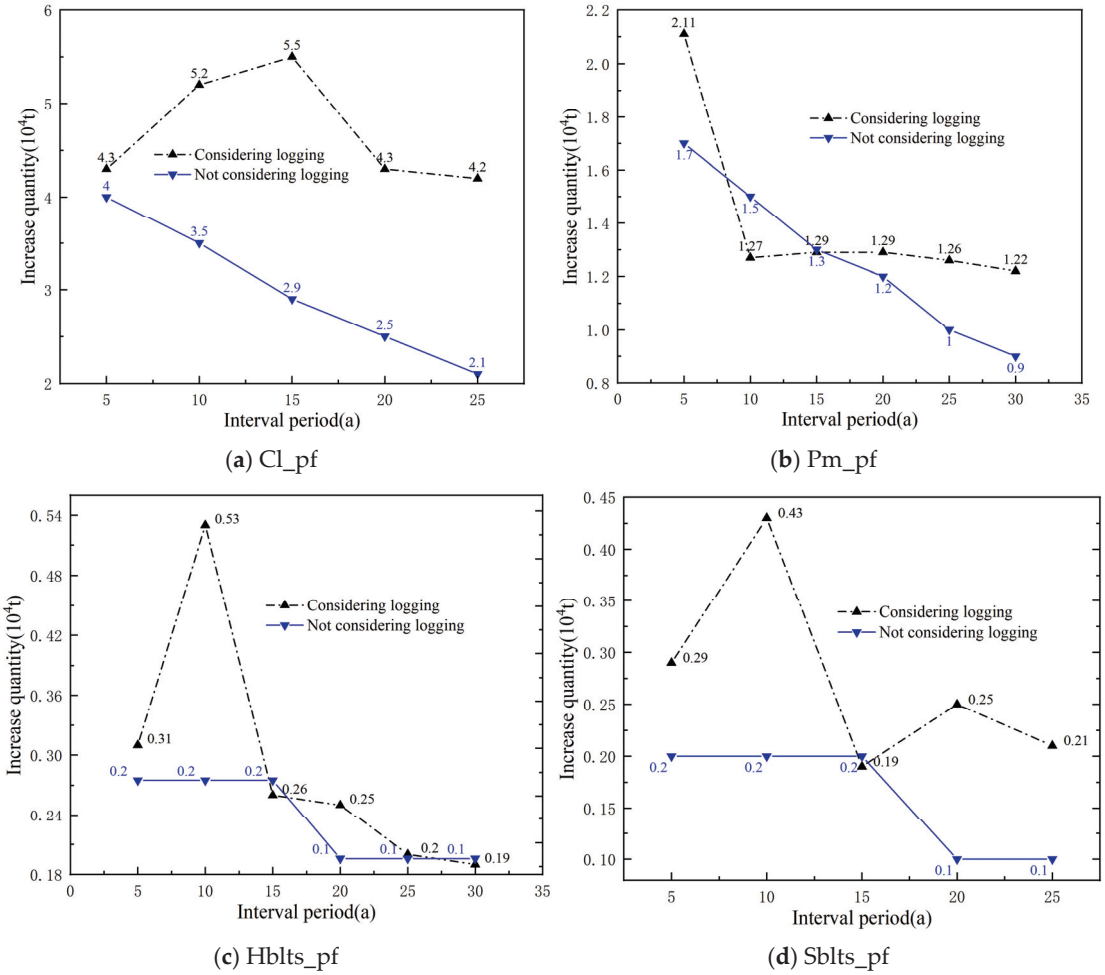

Figure 6. Increases in carbon storage over interval periods with and without considering logging volume.

5. Discussion

Our study demonstrates that the development of a compatible carbon storage model enables the rapid estimation of carbon storage in various parts of a forest stand, saving substantial human, material, and financial resources [23,24]. Furthermore, it achieves compatibility (additivity) between the individual and total organs, thereby addressing the discrepancy between the organ-specific and total carbon storage found in non-additive carbon storage models. This approach effectively mitigates potential errors in practical applications. Cross-modeling and testing demonstrate that the compatible carbon storage model has good fit accuracy and can provide relatively accurate predictions for carbon storage in various parts of the forest. This makes it the optimal choice for model establishment.

By constructing compatible carbon storage models for the total volume, branches, roots, leaves, and trunks and comparing these with carbon storage calculations using a standard carbon content rate (e.g., 0.50), the former exhibits higher predictive accuracy [25]. Other studies have shown that using a fixed carbon content rate to calculate carbon storage in Cunninghamia lanceolata forests can result in errors of up to 5.4% compared with actual measurements [26]. Errors arise because a fixed carbon content obscures variations in carbon content across different species and organs, leading to significant deviations. Widagdo et al. also found significant differences in carbon content among different origins and the organs of larch trees. Therefore, carbon storage models developed separately for different origins, parts, and tree species (groups) to accurately estimate the forest carbon storage.

Conventional modeling processes that typically represent a forest with dominant species to construct yield models and estimate carbon and volume do not address expression issues in mixed forests. Forrester et al. (2016) suggested that forest productivity might decline as the number of species increases [27]. In some forest types, increasing the heterogeneity in tree size can reduce forest productivity by 20% [28]. This is because the negative effect of smaller trees on forest growth outweighs that of larger trees. Estimating forest carbon storage and productivity based on dominant species without distinguishing the species composition can lead to overestimation. Research has also shown that mature, even aged, and mixed coniferous forests do not necessarily have higher productivity than pure stands [29]. Thus, incorporating tree species composition coefficients into the model not only addresses species expression issues in mixed forests but also enhances the accuracy of productivity estimates through ecological complementarity.

Carbon storage in forest stands is influenced by both biotic and abiotic factors [6], and the allocation of carbon storage among different parts is affected by external environmental conditions, species differences, and forest age. In this study, carbon storage in various parts was ranked as trunks > roots > branches > leaves, with trunks accounting for over 33% and leaves accounting for only 16%, similar to the findings of Ma (2023), He et al. (2023), and Guo et al. (2023) [30–32]. This distribution occurs because more carbon is allocated to trunks as trees grow, stabilizing the trees and transporting more water and nutrients to the parts required for photosynthesis [33]. This further demonstrated that the carbon storage estimation model developed in this study was consistent with the distribution of carbon storage across different parts of the stand. Combined with the volume estimation model developed in this study, it provides an accurate and quick prediction method for estimating total forest carbon storage.

6. Conclusions

By incorporating tree species composition coefficients into the model, we developed a carbon storage estimation model using stand volume as the independent variable, and a stand volume prediction model that utilized tree species composition coefficients, site quality grades as dummy variables, and interval periods as independent variables. This approach addresses issues such as the complex expression of tree species and the uncertain determination of age, providing technical support for accurate productivity estimates in mixed forests.

Through synchronized cross-modeling and testing, the compatible carbon storage estimation models for the eight dominant tree species (group and origin) achieved an R value greater than 0.9620, RSD values ranging from 4.80 to 215.39, RS and MSE values within $\pm$0.6%, RMA values below 5%, and EA values above 99.50%. The stand volume prediction models for these species (group and origin) showed an R value greater than 0.9840, RSD values between 0.29 and 0.57, RS and MSE values within $\pm$1%, RMA values below 6%, and EA values above 99.40%. These results also reflect the effectiveness of the parameter estimation approach, where the IEA and improved simplex method contributed to stable convergence and an enhanced model fitting performance compared with traditional optimization routines. These models can be used to predict the total stand carbon storage and volume across Fujian Province.

Using Wuyishan City as a case study, stand carbon storage and volume estimation models were applied to calculate current and future carbon storage and volume over different interval periods. The results showed that the current volume in the area was 21.0521 million cubic meter, and the carbon storage was 7.3238 million tons. However, as the interval period increased, the added amount decreased. After introducing the simulation calculation method and considering the logging volume, the increase in carbon storage

for the four plantation types was significantly higher than in stands where logging was not considered, effectively resolving the resistivity issues encountered during the model estimation.

Author Contributions: Conceptualization, X.J., W.H. and B.L.; methodology, B.L. and W.H.; software, W.H. and T.Q.; validation, X.J., B.L. and J.P.; formal analysis, X.J., W.H. and B.L.; investigation, B.L., W.H., T.Q. and J.P.; resources, W.H., T.Q. and J.P.; data curation, J.P.; writing—original draft preparation, W.H.; writing—review and editing, B.L., W.H. and T.Q.; visualization, X.J., W.H. and B.L.; supervision, X.J., W.H. and B.L.; project administration, W.H. and B.L.; and funding acquisition, W.H. All authors have read and agreed to the published version of the manuscript.

Funding: This research was funded by the Fujian Philosophy and Social Sciences Planning Project (FJ2022X019), Fujian Provincial Department of Finance Project (CR-2304), Fujian Forestry Science and Technology Project (2023FKJ21), Nanping City Resource Chemistry Industry Technology Innovation Joint Project (N2021Z010), and Wuyi University Talent Introduction and Research Start-up Fund Project (YJ202435).

Data Availability Statement: Data are contained within the article.

Acknowledgments: The authors express their gratitude and appreciation to Fujian Provincial Forestry Survey and Planning Institute for the finance, facilities, and opportunity to conduct this research.

Conflicts of Interest: The authors declare that they have no competing interests.

References

1. Wang, X.K.; Feng, Z.W. Potential of plant carbon sequestration in China's forest ecosystems. *J. Ecol.* **2000**, *19*, 72–74.
2. Lü, Z.Q.; Duan, A.G. Biomass and carbon storage models of *Cunninghamia lanceolata* in different production areas. *J. For. Sci.* **2024**, *60*, 1–11.
3. Yang, J.H.; Zhang, H.D.; Li, Y.C.; Liu, S.M. Construction of carbon storage models for *Pinus yunnanensis* and *Pinus armandii* based on additive models. *J. Kunming Univ. Sci. Technol. (Nat. Sci. Ed.)* **2024**, *49*, 140–150.
4. Sileshi, G.W. A critical review of forest biomass estimation models, common mistakes and corrective measures. *For. Ecol. Manag.* **2014**, *329*, 237–254. [CrossRef]
5. Luo, Y.J.; Wang, X.K.; Ouyang, Z.Y.; Lu, F.; Tao, J. A review of biomass equations for China's tree species. *Earth Syst. Sci. Data* **2020**, *12*, 21–40. [CrossRef]
6. Guo, Q.; Zhao, H.B.; Zhou, G.Y.; Long, W.G.; Gan, G.L.; Wu, S.Y.; Meng, M.Y.; Chen, J.L. Biomass and distribution patterns of four tree species plantations in the south subtropics. *For. Res.* **2022**, *35*, 182–189.
7. Khan, N.I.; Shil, M.C.; Azad, M.S.; Sadath, M.N.; Feroz, S.M.; Mollick, A.S. Allometric relationships of stem volume and stand level carbon stocks at varying stand density in *Swietenia macrophylla* King plantations, Bangladesh. *For. Ecol. Manag.* **2018**, *430*, 639–648. [CrossRef]
8. Jagodziński, A.M.; Dyderski, M.K.; Gęsikiewicz, K.; Horodecki, P. Tree and stand level estimations of *Abies alba* Mill. aboveground biomass. *Ann. For. Sci.* **2019**, *76*, 56. [CrossRef]
9. Aguirre, A.; del Río, M.; Ruiz-Peinado, R.; Condés, S. Stand-level biomass models for predicting C stock for the main Spanish pine species. *For. Ecosyst.* **2021**, *8*, 29. [CrossRef]
10. Lin, W.; Bai, Q.S.; Chen, X.M.; Liang, D.C.; Chen, Y.; Xue, K.; He, B.X.; Wen, S.N.; Lian, H.M.; Tang, C.L. Construction of carbon sink capacity evaluation system and selection of superior carbon sink tree species for major afforestation species in South China. *J. Southwest For. Univ. (Nat. Sci.)* **2020**, *40*, 28–37.
11. Zeng, W.S.; Sun, X.N.; Wang, L.R.; Wang, W.; Pu, Y. Development of volume, biomass, and carbon storage models for 10 major forest types in the northeast forest region. *J. Beijing For. Univ.* **2021**, *43*, 1–8.
12. Yue, C.Y. Estimation of Forest Carbon Storage and Carbon Sequestration Potential in Shaanxi Province. Master's Thesis, Northwest A&F University, Xianyang, China, 2023.
13. Wang, Z.; Lu, L.L.; Zhang, X.Q.; Zhang, J.G.; Jiang, L.; Duan, A.G. Construction of a Stand Volume Growth Model for *Cunninghamia lanceolata* Based on Bayesian Model Averaging. *For. Res.* **2021**, *34*, 64–71.
14. Wu, H.W.; Zhang, W.Z.; Tian, Y.; Yan, M.H.; Zhuang, C.Y.; Jiang, X.D. Stand basal area growth model for *Pinus elliottii* based on dummy variables. *J. Cent. South Univ. For. Technol.* **2021**, *41*, 117–123+150.
15. Wan, M.; Sun, Y.J.; Sun, Z.; Pang, R.R. Application of the 3-PG model to predict biomass and stand volume of *Cunninghamia lanceolata* plantations. *J. Northeast For. Univ.* **2023**, *51*, 74–79+94.

16. Hua, W.P.; Wu, J.W.; Yu, L.Y.; Wang, Y.N.; Wu, C.Z.; Zhuang, C.Y.; Chi, S.P.; Jiang, X.D. Classification and application of forest land based on forest potential productivity evaluation model. *For. Resour. Manag.* **2023**, *51*, 29–37. [CrossRef]
17. Li, X.J. Analysis of Wood Structure and Growth Yield Estimation Model of Natural Broadleaf Forests in Northern Fujian. Ph.D Thesis, Fujian Agriculture and Forestry University, Fuzhou, China, 2013.
18. Mirjalili, S.; Lewis, A. The whale optimization algorithm. *Adv. Eng. Softw.* **2016**, *95*, 51–67. [CrossRef]
19. Abdelaziz, M.; Eweesc, A.A.; Hassanien, A.E. Whale optimization algorithm and moth-flame optimization for multilevel thresholding image segmentation. *Expert Syst. Appl.* **2017**, *83*, 242–256.
20. Hua, W.P.; Qiu, T.; Gai, X.M.; Huang, Y.Z.; Xu, M.Z.; Jiang, X.D. Modeling techniques for the binary volume model of *Pinus hwangshanensis* based on cross-modeling validation. *J. Wuyi Univ.* **2015**, *34*, 13–17.
21. Gao, X.L. Application of the simulation calculation method in determining the reasonable annual logging volume during the eleventh five-year plan period. *For. Resour. Manag.* **2006**, *1*, 38–42.
22. Hua, W.P.; Jiang, X.D.; Qiu, T.; Li, P.; Jiang, H.; Huang, S.Y. Determining logging volume using the simulation calculation method and its impact on value. *J. Northwest AF Univ. (Nat. Sci. Ed.)* **2016**, *44*, 79–84+92.
23. Sierra, C.A.; del Valle, J.I.; Orrego, S.A. Total carbon stocks in a tropical forest landscape of the Porce region, Colombia. *For. Ecol. Manag.* **2007**, *243*, 299–309. [CrossRef]
24. Bi, H.; Murphy, S.; Volkova, L. Additive biomass equations based on complete weighing of sample trees for open eucalypt forest species in south-eastern Australia. *For. Ecol. Manag.* **2015**, *349*, 106–121. [CrossRef]
25. Dong, L.H.; Liu, Y.S.; Song, B.; Zhou, Y.F.; Li, F.R. Comparison of methods for estimating carbon content in standing trees. *J. For. Sci.* **2020**, *56*, 46–54.
26. Zeng, W.S.; Chen, X.Y.; Pu, Y.; Yang, X.Y. Comparative analysis of different methods for estimating biomass and carbon storage based on national forest inventory data. *For. Res.* **2018**, *31*, 66–71.
27. Forrester, D.I.; Bauhus, J. A review of processesbehind diversity-productivity relationships in forests. *Curr. For. Rep.* **2016**, *2*, 45–61. [CrossRef]
28. Soares, A.A.V.; Leite, H.G.; Souza, A.L.; Silva Sérgio, R.; Lourenço, H.M.; Forrester, D.I. Increasing stand structuralheterogeneity reduces productivity in Brazilian *Eucalyptus* monoclonal stands. *For. Ecol. Manag.* **2016**, *373*, 26–32. [CrossRef]
29. Chen, H.Y.; Klinka, K.; Mathey, A.H.; Wang, X.; Varga, P.; Chourmouzis, C. Are mixed-species stands more productive thansingle-species stands: An empirical test of threeforest types in British Columbia and Alberta. *Can. J. For. Res.* **2003**, *33*, 1227–1237. [CrossRef]
30. Ma, Y. Characteristics and Distribution of Biomass and Plant Carbon Storage in *Cunninghamia lanceolata* Plantations in Hubei Province. Master's Thesis, Central South University of Forestry and Technology, Changsha, China, 2023.
31. He, L.; Yan, J.X.; Duan, L.L.; Liu, J.; Wang, Y. Allometric growth models of biomass for major forest types in the Shanxi plateau. *Sci. Soil Water Conserv. (Chin. Engl.)* **2023**, *21*, 102–111.
32. Guo, Z.X.; Hu, Z.Y.; Cao, C.; Liu, P. Development of biomass and carbon storage models for major forest types in guangdong. *J. For. Sci.* **2023**, *59*, 37–50.
33. Altanzagas, B.; Luoy Altansukh, B.; Dorjsuren, C.; Fang, J.; Hu, H. Alometric equations for estimating the above-ground biomass of five forest tree species in Khangai, Mongolia. *Forests* **2019**, *10*, 661. [CrossRef]

Disclaimer/Publisher's Note: The statements, opinions and data contained in all publications are solely those of the individual author(s) and contributor(s) and not of MDPI and/or the editor(s). MDPI and/or the editor(s) disclaim responsibility for any injury to people or property resulting from any ideas, methods, instructions or products referred to in the content.

forests

MDPI

Article

Maintaining Fertilization Supports Productivity in Second Rotation Eucalypt Plantations

Nivaldo S. Martins [1], Bruno O. Lafetá [2,*], Marcio L. R. Oliveira [3] and Reynaldo C. Santana [3]

[1] Aperam BioEnergy, Itamarandiba 39670-000, Brazil; nivaldo.martins@aperam.com
[2] Department of Forest Engineering, Federal Institute of Education, Science and Technology of Minas Gerais, São João Evangelista 39705-000, Brazil
[3] Department of Forest Engineering, Federal University of the Jequitinhonha and Mucuri Valleys, Diamantina 39100-000, Brazil; marcioromarco@ufvjm.edu.br (M.L.R.O.); reynaldo.santana@ufvjm.edu.br (R.C.S.)
* Correspondence: bruno.lafeta@ifmg.edu.br

Abstract

Eucalypt plantations form the basis of Brazilian forestry; however, successive rotations under coppice systems often experience productivity declines. This study presents an original long-term investigation over a 13-year cultivation cycle (2005–2018) with *Eucalyptus grandis* W. Hill ex Maiden × *E. urophylla* S. T. Blake, assessing whether the full maintenance of nine phosphate fertilization packages could sustain productivity from the first to the second rotation in a commercial plantation in Itamarandiba, Minas Gerais. Continuous forest inventories and rotation-specific growth modeling were used. Productivity in the second rotation declined by 33%–46% in packages TP1 to TP6, which included various phosphorus sources, highlighting the recurring challenges of coppice systems. Conversely, the highest and most consistent yields (~305 m^3 ha^{-1} $rotation^{-1}$) were obtained with package TP9, which consisted of 280 kg ha^{-1} of triple superphosphate (TSP) applied at the beginning of each rotation and 600 kg ha^{-1} of ammonium sulfate (SA) in split topdressing applications. These findings demonstrate that the full maintenance of fertilization, specifically with highly soluble phosphorus sources combined with balanced nitrogen and sulfur supplementation, is an effective strategy to secure productivity and ensure the economic viability of coppice systems. This offers a new paradigm for managing successive rotations, where nutritional synergy, rather than single-nutrient fertilization, is key to enhancing the resilience of clonal eucalypt plantations.

Keywords: coppice system; cultivation cycle; phosphorus sources; seedling system

1. Introduction

The Brazilian forest sector is rapidly expanding in the global market, with more than 8 million hectares planted with eucalypts [1]. Its national relevance derives from rapid growth, high biomass accumulation, and broad adaptability to diverse edaphic and climatic conditions. Such characteristics have made eucalypts a strategic resource for the pulp, paper, bioenergy, and sawn timber industries, while contributing to carbon sequestration and environmental restoration initiatives. These plantations typically occur on soils with low natural fertility, where limited phosphorus (P) availability is a major constraint to productivity [2–5]. Under such conditions, balanced phosphate fertilization using soluble or moderately soluble P sources is recommended [3,6].

Achieving high productivity in forest plantations relies on efficient management of growth-regulating resources, particularly nutrients [7–9]. Phosphate fertilization is commonly applied during stand establishment to support a single rotation and alleviate nutrient depletion caused by stem removal at harvest [10]. The benefits of P fertilization in first-rotation eucalypt plantations are well documented [3,6,11–14]. When managing successive rotations, nonetheless, the challenge extends beyond selecting an appropriate P source; the fertilisation rate plays a central role because it influences both plant physiological performance and soil chemical dynamics. Adequate P inputs promote rapid root establishment, canopy development, and sustained biomass accumulation [3], whereas insufficient or excessive applications may lead to nutritional imbalances, economic inefficiencies, or increased soil P fixation [6].

Nutrient dynamics in successive rotations are also not fully understood. The prevailing assumption is that nutrient cycling from harvest residues, together with nutrients retained in roots and stumps, would partially meet the demand of following rotations [15–18]. As a result, even when supplemental fertilization is applied, second-rotation stands rarely receive the same dose or nutrient balance used during stand establishment. Therefore, systematic evaluation of full fertilization maintenance across rotations remains an experimental gap. Our study directly addresses this gap by providing an original, long-term assessment of whether full maintenance of initial fertilization packages can sustain productivity throughout a complete cultivation cycle in a clonal eucalypt plantation.

Forest managers require reliable guidance for input allocation in each rotation [8]. The appropriate source and amount of fertilizer enhance rapid root system establishment and promote crown development and stem biomass accumulation [3]. Commonly used P sources range widely in reactivity, from rock phosphates to superphosphates. Accelerated growth resulting from adequate P supply can shorten rotation lengths and, in some cases, enable successive cultivation on the same site [14].

Nutrient uptake by eucalypts depends on the spatial extent of the root system and its capacity to explore larger soil volumes [6,11]. Clones may reach depths greater than 10 m [19], partially compensating for low nutrient availability in surface layers; benefit enhanced in coppice systems due to pre-existing roots [20]. However, fertilization in successive rotations should not merely replicate the previous scheme; it must also replenish nutrients exported at harvest based on nutrient budget principles. Such replenishment sustains productivity and ensures sufficient wood supply for industrial processing and economic returns throughout the cultivation cycle.

Eucalypt plantations in Brazil are predominantly managed under seedling systems, in which the cycle ends after harvest and the stand is fully replanted. Although coppicing system, which relies on stump sprouting for new rotations, offers decisive operational advantages such as lower costs and no need for replanting [12,21,22], its adoption is often limited by recurring productivity declines in subsequent rotations. This contrast between systems generates uncertainty about fertilization recommendations specific to each rotation.

Scientific investigations that directly test fertilization strategies across successive rotations are essential to develop sustainable management protocols and counteract recurring yield declines in coppice systems. To address this gap, we conducted a novel 13-year field assessment to evaluate whether maintaining the initial fertilization regime across successive rotations sustains productivity in *Eucalyptus grandis* W. Hill ex Maiden × *E. urophylla* S. T. Blake stands over two complete rotations. The work tested two central hypotheses: (1) that full maintenance of the fertilization regime across rotations sustains second-rotation productivity at levels comparable to the first; and (2) that P-source solubility influences growth dynamics but does not alter final stand productivity at maturity.

https://doi.org/10.3390/f17010013

2. Materials and Methods

2.1. Study Site

This study was conducted in an area belonging to Aperam BioEnergy, in the municipality of Itamarandiba, Minas Gerais, Brazil, at coordinates 17°39′58.09″ S and 42°50′30.23″ W (WGS84 Datum). Regional climate is classified as Cwa (Köppen), characterized by rainy summers and dry winters. According to 30-year (1991–2020) climate normals from the National Institute of Meteorology (https://portal.inmet.gov.br/; accessed on 12 July 2024), the mean annual temperature is 20.5 °C, ranging from 17.6 °C (July) to 22.4 °C (February), and mean annual precipitation is 921 mm, with monthly values varying from 11 mm (June–August) to 195 mm (December).

The 50.5-ha experimental stand is located on a very clayey Red–Yellow Latosol, on flat terrain at 889 m elevation. The latossolic B horizon (Bw) exhibits a predominantly granular structure (>80%), is plastic and sticky when wet and firm when moist, and has a particle density of 2.47 g cm^{-3} and a bulk density of 0.95 g cm^{-3}. Chemical characterization of the 0–40 cm soil layer is presented in Table 1. Phosphorus (P), potassium (K), calcium (Ca), and magnesium (Mg) contents were determined using the ion-exchange resin method; sulfur (S) as SO_4^{2-} was quantified by turbidimetry after extraction with $Ca(H_2PO_4)_2$; and organic matter (OM) was assessed by colorimetry. Soil pH was measured in $CaCl_2$. Among micronutrients, boron (B) was extracted with hot water, whereas copper (Cu), iron (Fe), manganese (Mn) e zinc (Zn) were extracted using diethylenetriaminepentaacetic acid (DTPA).

Table 1. Chemical analysis of the soil in the experimental site across different rotations within the same cultivation cycle.

Rotations	Soil Chemical Attributes					
	pH	OM (g dm^{-3})	$P_{(resin)}$ (mg dm^{-3})	K (mg dm^{-3})	Ca ($cmol_c$ dm^3)	Mg ($cmol_c$ dm^3)
1st	4.1	39.5	3.7	15.6	0.22	0.08
2nd	4.3	40.4	4.1	15.6	0.24	0.08
	S-SO_4 (mg dm^{-3})	B (mg dm^{-3})	Cu (mg dm^{-3})	Fe (mg dm^{-3})	Mn (mg dm^{-3})	Zn (mg dm^{-3})
1st	7.2	0.6	0.2	109.0	0.9	0.4
2nd	7.6	0.6	0.2	117.0	1.2	0.6

The durations of the first and second rotations were 84 and 72 months, respectively. OM = organic matter; P = phosphorus; K = potassium; Ca = calcium; Mg = magnesium; S-SO_4 = sulfur as sulfate; B = boron; Cu = copper; Fe = iron; Mn = manganese; and Zn = zinc. Soil texture consisted of 12.14% sand, 3.38% silt, and 84.48% clay.

The available phosphorus content (3.7–4.1 mg dm^{-3}; Table 1) was classified as low according to Brazilian technical standards (e.g., Cantarutti et al. [23] and the Agronomic Institute of Campinas, https://www.iac.sp.gov.br; accessed on 12 July 2024), indicating a strong limitation to early stand development and reinforcing the relevance of assessing phosphate-fertilization strategies. The remaining attributes corroborate a low-fertility environment, with intermediate organic matter, S-SO_4 and B levels; low Ca, Mg, Cu, Mn and Zn; very low K; and high Fe. Altogether, these indicators characterize a chemically impoverished soil, particularly deficient in phosphorus and basic cations. This context justifies the fertilizer rates adopted and underscores the study's focus on the efficiency of phosphate fertilization under conditions of low nutrient availability.

2.2. Experimental Design

The experiment was established in June 2005 with clone AEC 1528® of *E. grandis* × *E. urophylla*. This clone was selected as it is a benchmark genotype for scientific studies in the region, developed by Aperam BioEnergy for the Jequitinhonha Valley in Minas Gerais. It is

widely adopted in Brazil for combining the fast growth of *E. grandis* with the resilience of *E. urophylla*, showing good drought tolerance and phenotypic plasticity.

Planting followed a minimum-tillage system with subsoiling (40 cm depth) and a 3.0 × 2.8 m spacing (8.4 m^2). A randomized block design with four replicates was used to evaluate the effect of nine technological packages emphasizing phosphate fertilization (Table 2). These packages were formulated using commercially available fertilizers that are widely employed in regional silviculture practices. The doses were initially determined following technical guidelines established for low-fertility soils [23,24] and were subsequently adjusted based on the extensive operational experience of the partner company (active since 1974), through systematic field observations of growth responses and nutrient-use efficiency. Each experimental unit consisted of six planting rows, with 90 trees measured in the two central rows (double border).

Table 2. Technological packages with emphasis on phosphate fertilization applied in both rotations of the eucalypt cultivation cycle, with basal fertilization corresponding to planting fertilization in the first rotation and to post-sprout fertilization in the second rotation.

Packages	Basal Fertilization			Topdressing Fertilization	
	(kg ha^{-1})	(g $plant^{-1}$)	(Mg ha^{-1})	(kg ha^{-1})	(kg ha^{-1})
TP1	500 ANP	130 NPK	2 AG	210 KCl	210 KCl
TP2	600 SSP	130 NPK	2 AG	210 KCl	210 KCl
TP3	280 TSP	130 NPK	2 AG	210 KCl	210 KCl
TP4	860 RP	130 NPK	2 AG	210 KCl	210 KCl
TP5	400 NRP	130 NPK	2 AG	210 KCl	210 KCl
TP6	500 ANP	130 NPK	2 AG	210 KCl + 200 SA	210 KCl + 400 SA
TP7	280 TSP	130 NPK	2 AG	210 KCl + 200 SA	210 KCl + 400 SA
TP8	500 ANP	130 NPK	1 AG	210 KCl	210 KCl
TP9	280 TSP	130 NPK	1 AG	210 KCl + 200 SA	210 KCl + 400 SA

Operations schedule: First rotation (84 months)—planting and basal fertilization (June 2005), topdressing (January 2006 and December 2006), and clear-cutting (July 2012). Second rotation (72 months)—initiated after clearcutting with primary sprout thinning (January 2013), followed by basal fertilization (April 2013), secondary sprout thinning (July 2013), topdressing (October 2013 and October 2014), and final clearcutting (July 2018). ANP = Araxá natural phosphate (24% P_2O_5 + 28% Ca). SSP = Single superphosphate (18% P_2O_5 + 16% Ca + ~10%–12% S). TSP = Triple superphosphate (41% P_2O_5 + 13% Ca). RP = Residual phosphate (RLT2; 21% P_2O_5 + 27% Ca). NRP = Natural reactive phosphate (30% P_2O_5 + 28% Ca). NPK = 04:26:16 + 0.5% Cu + 1.0% Zn. AG = Agrosilicon (19% Ca + 4.2% Mg). KCl = Potassium chloride (56% K + 0.5% B). SA = Ammonium sulfate (20% N + 22% S).

Cultivation cycle included two rotations, following the operational schedule of the forest company. The first rotation lasted 84 months, with clearcutting performed in July 2012, and wood removed two months later. Coppice system comprised a primary sprout selection six months after harvest, consisting of selecting one sprout per stump (or two sprouts in the subsequent plant in the event of failure), based on physiological vigor, size, and attachment quality. A secondary sprout thinning was applied at 12 months, eliminating competing sprouts that developed after the primary intervention. The second rotation was harvested in July 2018, lasting 72 months.

All fertilizations applied in the first rotation were repeated in the second (Table 2), differing only in their application method. In the first rotation, fertilizers were applied in planting furrow and NPK in a lateral pit; in the second rotation, both were applied as a continuous band under the crown projection, at 20 cm depth and after sprout thinning. Agrosilicon was broadcast over the entire area in each rotation without incorporation. Topdressing fertilizations were also applied uniformly as a continuous band under the crown projection throughout the cycle.

https://doi.org/10.3390/f17010013

2.3. Data Collection

A continuous forest inventory was conducted annually beginning at 12 months of age in each rotation. Circumference at 1.30 m height (*CBH*, cm) was measured using a metric tape, and total tree height (*H*, m) was determined with a Haglöf hypsometer. Diameter at breast height (*DBH*) corresponding to *CBH* was calculated by dividing circumference by π (3.1415927). Individual stem volume with bark (V_i, m^3) was estimated using rotation-specific allometric equations provided by the company.

First rotation:

$$Ln(V_i) = -11.090325 + 1.766661\ Ln(DBH) + 1.471862\ Ln(H);\ R^2 = 98.62\% \quad (1)$$

Second rotation:

$$Ln(V_i) = -10.488624 + 1.794069\ Ln(DBH) + 1.292210\ Ln(H);\ R^2 = 99.23\% \quad (2)$$

2.4. Statistical Analysis

Volume with bark was quantified for each experimental unit and inventory age (V, $m^3\ ha^{-1}$). Functional relationship between volume and age (A, months) was established using nonlinear regression, fitted with the Gauss–Newton iterative algorithm for the three-parameter logistic model. The logistic model was selected due to its biological foundation, interpretable parameters, and proven efficacy in modeling sigmoidal growth in even-aged stands.

$$V = \frac{\alpha}{1 + \beta\ e^{-\gamma A}} + \varepsilon \quad (3)$$

where α, β, and γ are the logistic model parameters; e is Euler's constant; and ε is the random error.

Technical cutting age (*TCA*, months) was estimated for each technological package as the age at which the mean annual increment (*MAI*) is maximized, defined as point on the production curve where the line from the origin has the greatest slope. *TCA* was obtained analytically by differentiation:

$$TCA = -\frac{Ln\left(\frac{(2-\sqrt{3})}{\beta}\right)}{\gamma} \quad (4)$$

Goodness-of-fit was evaluated using the mean absolute error (MAE), root mean squared error (RMSE), and Pearson correlation coefficient between observed and estimated values ($r_{Y\hat{Y}}$). Lower MAE and RMSE values indicate higher predictive quality. Nonlinear model identity test [25] was applied to assess whether production curves differed significantly between rotations and technological packages. Graphical inspection was performed using production curves for each rotation and package, along with their respective confidence bands.

All analyses were conducted in R statistical computing environment (version 4.5.2) [26], adopting a significance level of 1%.

3. Results

3.1. Model Fitting and Volume Estimation

Production modeling based on the logistic model allowed establishing functional relationships for estimating over-bark volume across all technological packages emphasizing phosphate fertilization and both rotations (Table 3). On average, the MAE and RMSE accounted for only 4.1% and 4.8% of the volume estimated at *TCA* in the first rotation, and

https://doi.org/10.3390/f17010013

5.6% and 7.2% in the second rotation, respectively, denoting high volumetric estimation accuracy across rotations. Equations generated for the first and second rotations exhibited minimal deviations, with low MAE and RMSE values. Correlation coefficients were high and statistically significant ($r_{Y\hat{Y}} \geq 0.98$, $p \leq 0.01$). Asymptotic volume estimates, represented by the parameter "α," were higher in the first rotation compared to the second.

Table 3. Coefficients and goodness-of-fit statistics of the logistic model for estimating over-bark volume (m^3 ha^{-1}) in eucalypt stands managed under different technological packages, with emphasis on phosphate fertilization.

Package	α	β	γ	MAE	RMSE	$r_{Y\hat{Y}}$
		---------- 1st Rotation ----------				
TP1	434.3286	49.4904	0.0580	16.04	19.92	0.98 **
TP2	408.9646	50.5419	0.0694	12.81	15.37	0.99 **
TP3	418.6802	46.6026	0.0646	15.26	18.01	0.99 **
TP4	448.7831	54.6627	0.0634	11.72	13.39	0.99 **
TP5	443.5112	43.5550	0.0587	18.63	21.34	0.99 **
TP6	384.7184	67.7944	0.0780	8.21	9.80	1.00 **
TP7	404.2187	55.5387	0.0726	13.51	16.11	0.99 **
TP8	360.2595	61.4684	0.0729	12.53	15.75	0.99 **
TP9	395.1711	59.0284	0.0747	10.55	11.82	1.00 **
		---------- 2nd Rotation ----------				
TP1	232.5159	126.5257	0.1109	10.67	13.65	0.99 **
TP2	238.1158	158.9645	0.1293	12.63	16.31	0.98 **
TP3	242.7047	187.5699	0.1261	9.15	12.78	0.99 **
TP4	300.6563	57.5854	0.0838	13.77	17.53	0.98 **
TP5	263.3778	103.7745	0.1038	12.00	15.85	0.99 **
TP6	250.5299	228.5574	0.1342	7.37	10.85	0.99 **
TP7	335.9723	55.0127	0.0831	13.89	16.59	0.99 **
TP8	317.5659	56.5937	0.0772	15.89	19.05	0.98 **
TP9	377.8788	40.6167	0.0693	19.08	22.71	0.98 **

** Significant at the 1% level according to the t-test. α, β and γ are parameters of the logistic model. MAE = mean absolute error. RMSE = root mean square error. $r_{Y\hat{Y}}$ = correlation coefficient.

TCA analysis revealed that cultivation cycle duration and volumetric productivity were influenced by the technological package (Table 4). Cycle duration estimates (months; m^3 ha^{-1}) were 146 (526) for TP1, 125 (510.72) for TP2, 132 (522) for TP3, 148 (591) for TP4, 144 (558) for TP5, 121 (501) for TP6, 138 (584) for TP7, 144 (535) for TP8, and 145 (610) for TP9. The descending order of mean end-of-cycle wood production estimates was: TP9 > TP4 > TP7 > TP5 > TP8 > TP1 > TP3 > TP2 > TP6. Among these, packages TP7 to TP9 stood out for higher productivity consistency (relative similarity above 85%) and lower *TCA* variation (relative similarity above 80%) between rotations. This similarity indicates that the fertilization strategy in these packages effectively replenished nutrients exported during the first rotation, supporting consistent stand growth in the following rotation. Cross-referencing these results with the fertilization design (Table 2) reveals a clear association: the packages achieving the highest second-rotation consistency (TP7 and TP9) were precisely those that received highly soluble phosphate sources (triple superphosphate) combined with nitrogen and sulfur supplementation (ammonium sulfate).

https://doi.org/10.3390/f17010013

Table 4. Technical cutting age (TCA), over-bark volume, and percentage difference of the second rotation relative to the first in eucalypt managed under different technological packages, with emphasis on phosphate fertilization.

Packages	1st Rotation		2nd Rotation	
	TCA (Months)	Volume (Months)	TCA (Months)	Volume (m^3 ha^{-1})
TP1	89.98	342.55	55.52 (61.70%)	183.37 (53.53%)
TP2	75.50	322.54	49.39 (65.42%)	187.82 (58.23%)
TP3	79.85	330.18	51.95 (65.06%)	191.41 (57.97%)
TP4	83.88	353.93	64.08 (76.39%)	237.10 (66.99%)
TP5	86.73	349.79	57.41 (66.19%)	207.72 (59.38%)
TP6	70.94	303.41	50.29 (70.89%)	197.59 (65.12%)
TP7	73.47	318.79	64.07 (87.21%)	264.96 (83.11%)
TP8	74.56	284.12	69.34 (93.00%)	250.47 (88.15%)
TP9	72.22	311.65	72.46 (100.33%)	298.05 (95.63%)

Values in parentheses represent the percentage similarity of the second rotation relative to the first. TCA = Technical Cutting Age.

3.2. Statistical and Graphical Comparison of Production Patterns

Nonlinear model identity tests indicated that the different fertilization regimes had a significant effect ($p \leq 0.01$) on over-bark volume production patterns throughout the eucalypt cultivation cycle (Table 5). In the first rotation, two distinct groups with similar growth patterns were formed: the first comprised TP3, TP7, and TP9, which used highly soluble P sources, and the second involved TP1, TP4, and TP5, which used less soluble P sources.

Table 5. Summary of the nonlinear model identity test for volume production equation of eucalypt managed under different technological packages, with emphasis on phosphate fertilization.

Groups	*p*-Value	Groups	*p*-Value	Groups	*p*-Value
1st Rotation		2nd Rotation		Combined rotations	
TP1 a TP9	≤0.01	TP1 a TP9	≤0.01	TP7 a TP9	≤0.01
TP1-TP6-TP8	≤0.01	TP1-TP6-TP8	≤0.01	TP7-TP8	≤0.01
TP3-TP7-TP9	0.71	TP3-TP7-TP9	≤0.01	TP7-TP9	0.40
TP7 a TP9	≤0.01	TP7 a TP9	≤0.01	TP8-TP9	≤0.01
TP1 a TP6	≤0.01	TP1 a TP6	0.02	-	-
TP1-TP4-TP5	0.03	-	-	-	-

p-value = probability value.

Production curves displayed a sigmoidal growth pattern in both rotations, with clear differences among technological packages (Figure 1). Visual analysis of the confidence bands ($1 - \alpha = 0.99$) revealed that volume estimates in the first rotation tended to exceed those of the second in most packages (TP1 to TP6), particularly after 72 months, with the largest difference at 84 months. This divergence resulted from accelerated growth after 36 months relative to the previous rotation, followed by a decline around 60 months and subsequent stabilization at a lower volume plateau than the first rotation (Figure 1). Consequently, the *TCA* of these packages was anticipated, from 81.15 ± 7.31 months in the first rotation to 54.77 ± 5.50 months in the second (Table 4). Finally, the growth pattern of this group, which was distinct in the first rotation, became homogeneous in the subsequent rotation, forming a single similarity group (Table 5; $p > 0.01$).

The most productive technological packages (Table 4) that also maintained similar growth patterns between rotations ($p > 0.01$) were TP7 and TP9 (Table 5; Figure 1). Maintaining these technological packages across successive rotations demonstrated productivity consistency throughout the cultivation cycle. Regarding the average *TCA* estimate, TP7 showed an advancement of approximately 9 months in the second rotation, indicating an

https://doi.org/10.3390/f17010013

accelerated production cycle, while TP9 maintained nearly stable values across rotations, evidencing regularity and predictability in silvicultural performance.

Comparison of the nutrient formulation between TP7 and TP9 (Table 2) showed that halving the agrosilicon dose did not limit clone productivity (Table 5; Figure 1). TP9 achieved similar yields with only half the TP7 dose, representing savings of up to 226 t of Ca and 42 t of Mg per 1000 ha rotation^{-1}. Thus, 1 t ha^{-1} of agrosilicon was considered the most suitable for both rotations, demonstrating the feasibility of maintaining a consistent nutritional balance throughout the entire crop cycle.

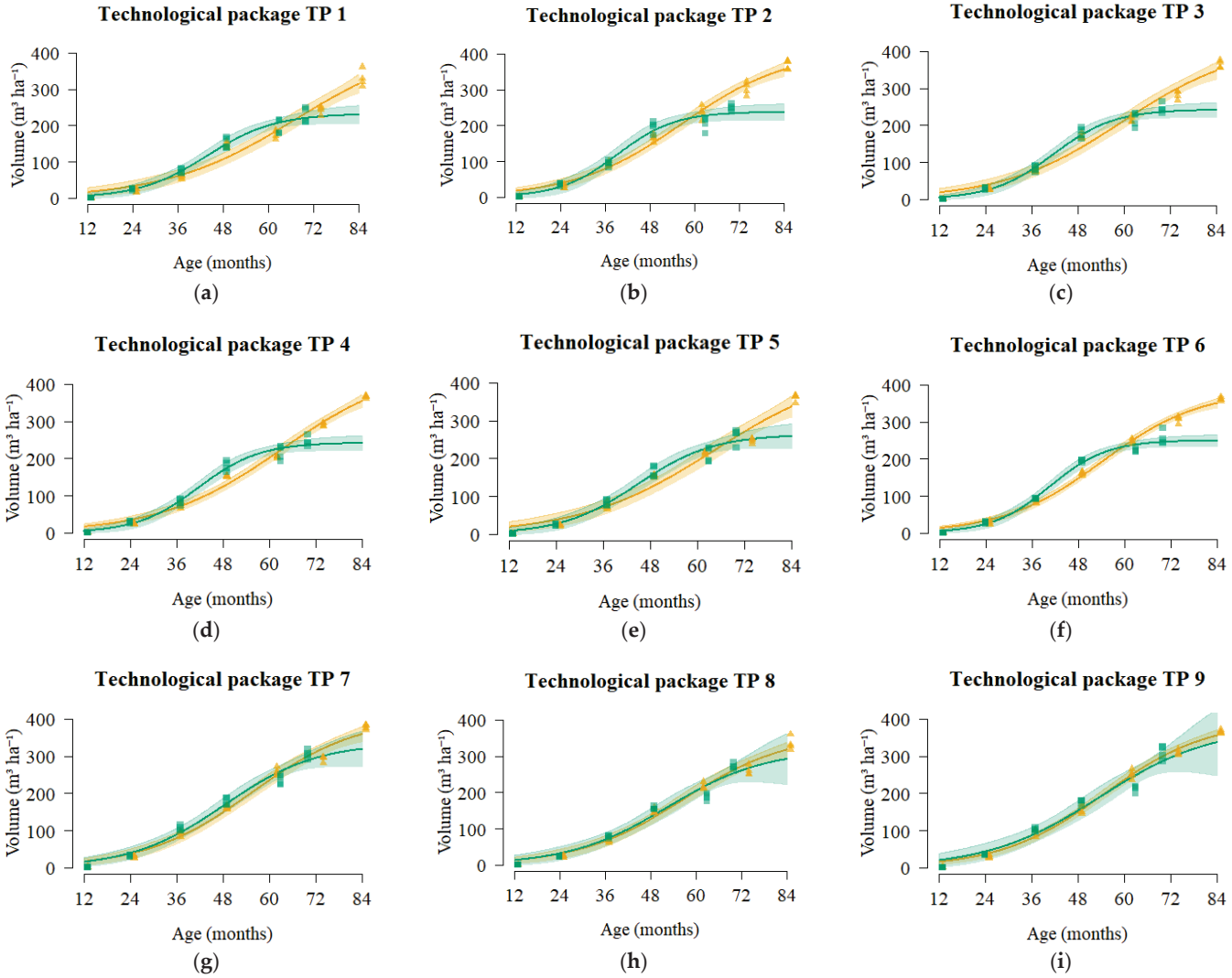

Figure 1. Graphical representations of volume production curves with bark (m^3 ha^{-1}) in the first (orange) and second (green) rotations under different technological packages, with emphasis on phosphate fertilization. Shaded areas represent confidence interval ($1 - \alpha = 0.99$).

3.3. Contextual Analysis Based on Site Conditions

Divergent rotational performance patterns occurred within a specific environmental context. Soil monitoring data (Table 1) showed minimal variation in key chemical attributes between rotation cycles, with pH increasing slightly from 4.1 to 4.3, organic matter from 39.5 to 40.4 g dm^{-3}, and resin-extractable phosphorus from 3.7 to 4.1 mg dm^{-3}. This stability suggests that drastic soil fertility degradation was not the primary driver of the generalized second-rotation decline observed in TP1–TP6.

Climatic stress, especially severe water deficits, likely contributed to differences in the nutritional performance of some technological packages. The first rotation experienced

a severe drought in its second year (2007: 581.7 mm), while the second rotation faced cumulative stress, with critical water deficits recorded both in the establishment phase (2014: 590.0 mm) and mid-rotation growth period (2017: 650.7 mm), compared with the regional average of 921 mm. This more frequent and intense water stress in the second rotation coincided with a marked decline in productivity relative to the first rotation, most evident in packages relying on less soluble phosphate sources (TP1, TP3–TP6).

Packages TP7–TP9, applying the synergistic TSP + SA fertilization strategy at planting and topdressing, exhibited greater resilience under these water deficits, maintaining both productivity and cycle stability. Conversely, TP1–TP6 showed marked reductions in volume and shorter cycles under the same conditions. These results indicate that climatic variability acted as a conditioning factor, accentuating inherent differences in the effectiveness of the fertilization packages rather than being the primary cause of observed performance differences.

4. Discussion

Over-bark volume production of the eucalypt clone was modeled for two successive rotations within the same cultivation cycle, evaluated under nine technological packages with emphasis on phosphate fertilization. The logistic model exhibited satisfactory predictive performance, establishing 18 single-input (age) functional relationships for volume estimation (Table 3), which demonstrates flexibility in describing growth dynamics under different nutrient regimes.

Detailed biometric information is necessary for adequate forest management. However, the asymptote should not be considered in isolation, as it only represents the estimated maximum growth potential without reflecting increment dynamics throughout the cultivation cycle. Accuracy of management decisions depends on a thorough analysis of the sigmoidal growth pattern, plant response to interventions, and the technical cutting age. This integrated approach supports the definition of silvicultural and regulatory prescriptions aimed at maintaining high productivity and plantation sustainability.

All phosphate fertilization packages promoted gains in volumetric productivity, regardless of P source solubility, with clone 1528 exceeding the production of commercial stands adjacent to the experiment (averages of 228 and 180 m^3 ha^{-1} at 84 months in the first and second rotations, respectively; unpublished data). Nevertheless, this did not prevent productivity decline in the second rotation for most packages (TP1 to TP6), a phenomenon widely documented in the literature [16,22,27]. The volume difference relative to the first rotation ranged from 33.01 to 46.47% (TP1 to TP6; Table 4) at corresponding *TCA*s, confirming the challenge posed by resource depletion in successive rotations. This decline aligns with findings by Silva et al. [28], who reported that fifteen eucalypt clones, cultivated at spacings of 4.9 to 9.5 m^2 per plant in different regions of Minas Gerais, showed an average productivity decline of approximately 33.6% between the first and second rotations at seven years of age. In another study in the state, Lafetá et al. [22] observed volumetric declines of 61.7% and 58.7% for a spacing of 3.0 × 2.8 m in three eucalypt clones at 72 and 84 months, in a total evaluated area of 20,317 ha.

The high productivity achieved across all technological packages directly reflected the nutritional balance provided by fertilization. The strong P-fixation capacity in highly weathered tropical soils requires the combined application of soluble and slow-release sources, a well-established practice in Brazilian eucalypt cultivation [6]. This approach contributed to maintaining nutrient availability throughout the cultivation cycle, partially sustaining growth and enabling higher productive increments. It is emphasized that replenishing nutrients exported through harvest is indispensable for forest production sustainability [17], supporting consistent yields from stand establishment through multiple cultivation cycles.

https://doi.org/10.3390/f17010013

This pronounced response to phosphorus, however, is context-dependent, varying with site conditions and genetic material. This principle is illustrated by the contrasting results of Brinkhoff et al. [29], who found no growth response to P fertilization in mid-rotation *E. nitens* plantations where nitrogen was identified as the limiting nutrient.

Average soil P concentration between rotations was 3.9 mg dm^{-3} (Table 1), considered insufficient for establishing eucalypt plantations [23]. The referenced study recommends applying at least 10.5 g $plant^{-1}$ of soluble P at planting; for soils with less than 15 mg dm^{-3} P (resin extractable), an additional 62.8 kg ha^{-1} of slightly soluble P in a continuous band is indicated. To meet these requirements, all packages supplied 130 g $plant^{-1}$ of P via NPK (Table 2), exceeding the minimum recommendation. Packages TP2, TP3, TP7, and TP9 received an additional 54.5 kg ha^{-1} of soluble P on average, whereas the remaining packages were supplemented with 62.7 kg ha^{-1} of low-solubility P sources.

The range of mean annual increment corresponding to *TCA* (46–52 m^3 ha^{-1} yr^{-1} in the first rotation and 40–50 m^3 ha^{-1} yr^{-1} in the second) indicated that clone productivity is sensitive to silvicultural strategies (Table 4; Figure 1). This demonstrates the need to adjust nutrient doses and sources according to specific site conditions and the genetic potential of the plants. Such productive variability among packages underscores that careful selection of management practices is critical for achieving high increments and successful forest systems.

In the first rotation, P-source solubility organized the technological packages into two distinct growth patterns (Table 5): one associated with highly soluble sources (TP3, TP7, TP9) and the other with less soluble sources (TP1, TP4, TP5). Despite these initial differences influenced *TCA* (Table 4), production converged to similar volumes at 84 months in this rotation, with overlapping confidence intervals (Figure 1; $p > 0.01$). This convergence may reflect intrinsic physiological growth limitations of the genotype or a saturation of the fertilization response, consistent with Mitscherlich's Law of diminishing returns, where additional inputs do not necessarily result in proportional volume increments [6].

Package TP6 exhibited higher productivity than TP1 in the first rotation, matching it in the second (Figure 1), although both used Araxá natural phosphate (Table 1). This initial gain in TP6 may be attributed to ammonium sulfate supplementation, highlighting the importance of N and S supply to enhance low-solubility P efficiency. One plausible hypothesis is that the availability of P and S promoted a synergistic interaction, improving nutrient uptake and conversion into biomass [6,11,30]. This corroborates Novais et al. [6], who noted that low S concentrations suffice to maintain adequate N and P balance for plant growth. Consequently, the use of different P sources, even low-solubility ones, provides technical alternatives for achieving productivity without compromising fertilizer efficiency.

Evidence from packages TP7 and TP9 confirmed that coppice system can sustain high initial productivity and reach production levels equivalent to seedling system (Table 5 and Figure 1). This performance relies on maintaining appropriate fertilization balance, favorable climatic conditions, and rational management of other silvicultural and harvesting practices [22]. It is relevant to mention that both packages employed triple superphosphate with ammonium sulfate topdressing, generally marketed in granular form, which reduces compaction or caking risks and facilitates storage, transport, and application [31].

Alternating P sources between rotations is a promising strategy to enhance operational flexibility aligned with practical silvicultural conditions. In cases of financial constraints or limited fertilizer availability, less soluble natural sources or more accessible soluble sources may be used. Some P sources lack S, potentially limiting productivity and sustainability; in such cases, supplemental S from other sources or practices should be technically reviewed to maintain nutrient balance throughout the cycle.

https://doi.org/10.3390/f17010013

The obtained results provide support for the development of future research to define the optimal quantity and ideal source of nutrients for the establishment and management of multiple forest rotations. The selection and recommendation of nutritional sources requires considerable caution to achieve higher productivity at a reduced cost, considering technical, economic, and practical field applicability aspects.

5. Conclusions

Based on 13 years of experimental data, this study demonstrates that the productive potential of second-rotation eucalypt stands can match that of the first rotation, but only under specific, fully maintained fertilization regimes. For most technological packages (TP1 to TP6), which included various phosphorus sources, productivity in the second rotation declined by 33%–46%, highlighting the recurring challenges of coppice systems.

The most effective strategy to sustain high and consistent productivity across successive rotations was the full maintenance of fertilization using package TP9. This package is defined by a balanced nutritional regimen centered on the application of 280 kg ha^{-1} of triple superphosphate (TSP) at the beginning of each rotation and topdressing applications of ammonium sulfate (SA) totaling 600 kg ha^{-1} (split into 200 and 400 kg ha^{-1}). Package TP7 produced equivalent results but required a higher dose of soil correctives, pointing to a clear opportunity for input optimization by reducing this dose.

Proper selection of fertilizer sources and doses, together with maintenance of nutritional balance, is decisive for sustaining productivity and provides foresters with technical alternatives to optimize yield and economic efficiency. Soluble and partially soluble phosphorus sources are suitable for successive rotations, although less soluble sources delayed the achievement of first-rotation volumes until 84 months.

Finally, these results support future research to define the optimal quantity and ideal source of nutrients for the establishment and management of multiple forest rotations. The selection and recommendation of nutritional sources requires considerable caution to achieve higher productivity at a reduced cost, considering technical, economic, and practical field applicability aspects.

Author Contributions: N.S.M.: conceptualization, data curation, methodology, and Writing—original draft visualization; B.O.L.: methodology, formal analysis, Investigation, and Writing—original draft; M.L.R.O.: formal analysis, supervision, and visualization; R.C.S.: conceptualization, Project administration, and writing—review and editing. All authors have read and agreed to the published version of the manuscript.

Funding: This study was supported by the Coordination for the Improvement of Higher Education Personnel—CAPES (Finance Code 001).

Data Availability Statement: The data that has been used is confidential.

Acknowledgments: This work was possible due to the support of the Federal University of the Jequitinhonha and Mucuri Valleys, Federal Institute of Minas Gerais, and Aperam BioEnergy.

Conflicts of Interest: Author Nivaldo S. Martins was employed by the company Aperam BioEnergy. The remaining authors declare that the research was conducted in the absence of any commercial or financial relationships that could be construed as a potential conflict of interest.

Abbreviations

The following abbreviations are used in this manuscript:

AG	Agrosilicon
ANP	Araxá Natural Phosphate
Bw	Latossolic B Horizon
Ca	Calcium
CBH	Circumference at Breast Height
DBH	Diameter at Breast Height
DTPA	Diethylenetriaminepentaacetic Acid
H	Total Height
K	Potassium
KCl	Potassium Chloride
MAE	Mean Absolute Error
MAI	Mean Annual Increment
Mg	Magnesium
N	Nitrogen
NPK	NPK Fertilizer
NRP	Natural Reactive Phosphate
P	Phosphorus
RMSE	Root Mean Square Error
RP	Residual Phosphate
$r_{Y\hat{Y}}$	Pearson correlation coefficient
S	Sulfur
SA	Ammonium Sulfate
SSP	Single Superphosphate
TCA	Technical Cutting Age
TSP	Triple Superphosphate
V	Volume with Bark per hectare
V_i	Individual Volume with Bark

References

1. Indústria Brasileira de Árvores (IBÁ). *Relatório Anual 2025: Ano Base 2024*; IBÁ: São Paulo, Brazil, 2025.
2. Gonçalves, J.L.M.; Stape, J.L.; Laclau, J.P.; Gava, J.L. Silvicultural effects on the productivity and wood quality of eucalypt plantations. *For. Ecol. Manag.* **2004**, *193*, 45–61. [CrossRef]
3. Crous, K.Y.; Ósvaldsson, A.; Ellsworth, D.S. Is phosphorus limiting in a mature *Eucalyptus* woodland? Phosphorus fertilization stimulates stem growth. *Plant Soil* **2015**, *391*, 293–295. [CrossRef]
4. Garay, M.; Amiotti, N.; Zalba, P. Response of phosphorus pools in Mollisols to afforestation with *Pinus radiata* D. Don in the Argentinean Pampa. *For. Ecol. Manag.* **2018**, *422*, 33–40. [CrossRef]
5. Viana, T.O.; Gama-Rodrigues, A.C.; Gama-Rodrigues, E.F.; Aleixo, S.; Moreira, R.V.S.; Sales, M.V.S.; Marques, J.R.B. Phosphorus transformations in Alfisols and Ultisols under different land uses in the Atlantic Forest region of Brazil. *Geoderma Reg.* **2018**, *14*, e00184. [CrossRef]
6. Novais, R.F.; Smyth, T.J.; Nunes, F.N. Phosphorus. In *Fertilidade do Solo*; Novais, R.F., Alvarez, V.H., Barros, N.F., Fontes, R.L.F., Cantarutti, R.B., Neves, J.C.L., Eds.; SBCS: Viçosa, Brazil, 2007; pp. 471–550.
7. Melo, E.A.S.C.; Moraes, G.J.L.; Tertulino, J.H.; Hakamada, R.E.; Bazani, J.H.; Wenzel, A.V.A.; Arthur, J.C., Jr.; Borges, J.S.; Malheiros, R.; Lemos, C.C.Z.L.; et al. Responses of clonal eucalypt plantations to N, P and K fertilizer application in different edaphoclimatic conditions. *Forests* **2016**, *7*, 2. [CrossRef]
8. Albaugh, T.; Rubilar, R.A.; Maier, C.A.; Acuña, E.A.; Cook, R.L. Biomass and nutrient mass of *Acacia dealbata* and *Eucalyptus globulus* bioenergy plantations. *Biomass Bioenergy* **2017**, *97*, 162–171. [CrossRef]
9. Carrero, O.; Stape, J.L.; Allen, L.; Arrevillaga, M.C.; Ladeira, M. Productivity gains from weed control and fertilization of short-rotation *Eucalyptus* plantations in the Venezuelan Western Llanos. *For. Ecol. Manag.* **2018**, *430*, 566–575. [CrossRef]
10. Bender, M.A.; Santos, D.R.; Tiecher, T.; Minella, J.P.G.; Barros, C.A.P.; Ramon, R. Phosphorus dynamics during storm events in a subtropical rural catchment in southern Brazil. *Agric. Ecosyst. Environ.* **2018**, *261*, 93–102. [CrossRef]
11. Graciano, C.; Goya, J.F.; Frangi, J.L.; Guiamet, J.J. Fertilization with phosphorus increases soil nitrogen absorption in young plants of *Eucalyptus grandis*. *Forest Ecol. Manag.* **2006**, *36*, 202–210. [CrossRef]

12. Stape, J.L.; Binkley, D.; Ryan, M.G.; Fonseca, S.; Loos, R.A.; Takahashi, E.N.; Silva, C.R.; Silva, S.R.; Hakamada, E.; Ferreira, J.M.A.; et al. The Brazil *Eucalyptus* potential productivity project: Influence of water, nutrients and stand uniformity on wood production. *For. Ecol. Manag.* **2010**, *259*, 1684–1694. [CrossRef]
13. Costa, M.G.; Gama-Rodrigues, A.C.; Gonçalves, J.L.M.; Gama-Rodrigues, E.F.; Sales, M.V.S.; Aleixo, S. Labile and non-labile fractions of phosphorus and its transformations in soil under *Eucalyptus* plantations, Brazil. *Forests* **2016**, *7*, 15. [CrossRef]
14. Bassaco, M.V.M.; Motta, A.C.V.; Pauletti, V.; Prior, S.A.; Nisgoski, S.; Ferreira, C.F. Nitrogen, phosphorus, and potassium requirements for *Eucalyptus urograndis* plantations in Southern Brazil. *New For.* **2018**, *49*, 681–697. [CrossRef]
15. Mendham, D.S.; O'Connell, A.M.; Grove, T.S.; Rance, S.J. Residue management effects on soil carbon and nutrient contents and growth of second rotation eucalypts. *For. Ecol. Manag.* **2003**, *181*, 357–372. [CrossRef]
16. Walmsley, J.D.; Jones, D.L.; Reynolds, B.; Price, M.H.; Healey, J.R. Whole tree harvesting can reduce second rotation forest productivity. *For. Ecol. Manag.* **2009**, *257*, 1104–1111. [CrossRef]
17. Laclau, J.P.; Ranger, J.; Gonçalves, J.L.M.; Maquere, V.; Krusche, A.V.; M'Bou, A.T.; Nouvellon, Y.; Saint-André, L.; Bouillet, J.P.; Piccolo, M.; et al. Biogeochemical cycles of nutrients in tropical *Eucalyptus* plantations: Main features shown by intensive monitoring in Congo and Brazil. *For. Ecol. Manag.* **2010**, *259*, 1771–1785. [CrossRef]
18. Oliveira, G.G.; Queiroz, T.B.; Kupper, A.P.; Masullo, L.; Hakamada, R.; Guerrini, I.A. Optimizing forest residue management after harvesting: Nutrient export scenarios in *Eucalyptus* plantations across high forest and coppice systems. *Forestry* **2025**, cpaf044. [CrossRef]
19. Pinheiro, R.C.; Deus, J.C., Jr.; Nouvellon, Y.; Campoe, O.C.; Stape, J.L.; Aló, L.L.; Guerrini, I.A.; Jourdan, C.; Laclau, J. A fast exploration of very deep soil layers by *Eucalyptus* seedlings and clones in Brazil. *For. Ecol. Manag.* **2016**, *366*, 143–152. [CrossRef]
20. Lima, A.S.; Gonçalves, J.L.M.; Gonçalves, A.N. Effect of nutrients omission in the *Eucalyptus* shoots. *Nucleus* **2017**, *14*, 147–160. [CrossRef]
21. Gonçalves, J.L.M.; Alvares, C.A.; Behling, M.; Alves, J.M.; Pizzi, G.T.; Angeli, A. Productivity of eucalypt plantations managed under high forest and coppice systems, depending on edaphoclimatic factors. *Sci. For.* **2014**, *42*, 411–419.
22. Lafetá, B.O.; Santana, R.C.; Oliveira, M.L.R.; Leite, H.G.; Soares, L.C.S.; Vieira, D.S. Eucalypt production in different rotations, sites and spatial arrangements. *For. Ecol. Manag.* **2024**, *571*, 122222. [CrossRef]
23. Cantarutti, R.B.; Barros, N.F.; Prieto, H.E.; Novais, R.F. Avaliação da fertilidade do solo e recomendação de fertilizantes. In *Fertilidade do Solo*; Novais, R.F., Alvarez, V.H., Barros, N.F., Fontes, R.L.F., Cantarutti, R.B., Neves, J.C.L., Eds.; SBCS: Viçosa, Brazil, 2007; pp. 471–550.
24. Barros, N.F.d.; Novais, R.F.; Teixeira, J.L.; Fernandes Filho, E.I. NUTRICALC 2.0—Sistema para cálculo del balance nutricional y recomendación de fertilizantes para el cultivo de eucalipto. *Bosque* **1995**, *16*, 129–131. [CrossRef]
25. Bates, D.M.; Watts, D.G. *Nonlinear Regression Analysis and Its Applications*; John Wiley & Sons: New York, NY, USA, 1988. [CrossRef]
26. R Core Team. *R: A Language and Environment for Statistical Computing*; R Foundation for Statistical Computing: Vienna, Austria, 2024.
27. Miranda, I.; Gominho, J.; Pereira, H. Heartwood, sapwood and bark variation in coppiced *Eucalyptus globulus* trees in 2nd rotation and comparison with the single-stem 1st rotation. *Silva Fenn.* **2015**, *49*, 1141. [CrossRef]
28. Silva, L.G.; Santana, R.C.; Oliveira, M.L.R.; Gomes, F.S. Evaluation of different silvicultural management techniques and water seasonality on eucalyptus yield. *Sci. Agric.* **2022**, *79*, e20200064. [CrossRef]
29. Brinkhoff, R.E.; Mendham, D.; Hunt, M.A.; Britton, T.G.; Hovenden, M.J. The response of mid-rotation *Eucalyptus nitens* to nitrogen fertiliser is non-linear and not influenced by phosphorus application. *For. Ecol. Manag.* **2024**, *561*, 121897. [CrossRef]
30. Taiz, L.; Møller, I.M.; Murphy, A.; Zeiger, E. *Plant Physiology and Development*, 7th ed.; Oxford University Press: New York, NY, USA, 2022.
31. Rodrigues, R.F.; Leite, S.R.; Santos, D.A.; Barrozo, M.A.S. Drum granulation of single super phosphate fertilizer: Effect of process variables and optimization. *Powder Technol.* **2017**, *321*, 251–258. [CrossRef]

Disclaimer/Publisher's Note: The statements, opinions and data contained in all publications are solely those of the individual author(s) and contributor(s) and not of MDPI and/or the editor(s). MDPI and/or the editor(s) disclaim responsibility for any injury to people or property resulting from any ideas, methods, instructions or products referred to in the content.

MDPI AG
Grosspeteranlage 5
4052 Basel
Switzerland
Tel.: +41 61 683 77 34

Forests Editorial Office
E-mail: forests@mdpi.com
www.mdpi.com/journal/forests



Disclaimer/Publisher's Note: The title and front matter of this reprint are at the discretion of the Guest Editors. The publisher is not responsible for their content or any associated concerns. The statements, opinions and data contained in all individual articles are solely those of the individual Editors and contributors and not of MDPI. MDPI disclaims responsibility for any injury to people or property resulting from any ideas, methods, instructions or products referred to in the content.

MDPI

Academic Open
Access Publishing

mdpi.com

ISBN 978-3-7258-8892-4